JOURNAL OF NEW ENERGY

presents the

PROCEEDINGS OF THE LOW ENERGY NUCLEAR REACTIONS CONFERENCE

Notice: This meeting was organized by J.O'M. Bockris and G.H. Lin as scientists and searchers of truth. This meeting was not advertised in any of the technical journals. Participation in the meeting was by invitation. Although the meeting was held in a conference room at Texas A&M, College Station, Texas on June 19, 1995, the meeting was not a part of college-supported activities. No public press was invited nor present.

These proceedings have been prepared from contributions of papers prepared for this meeting. We are grateful to Dr. Guang H. Lin for his help in arranging for the details of the conference, the pictures of participants, and for getting the papers submitted for publication.

PUBLISHER'S COMMENTS

On March 23, 1989, Pons and Fleischmann made a public announcement (at the request of the administration of the University of Utah) of the discovery of cold nuclear fusion. In July, 1989 this editor began the publication of *Fusion Facts*, a monthly newsletter which has reported monthly on the national and international progress of cold nuclear fusion. New discoveries made during the past six years have led to an expanded interest in low-energy nuclear reactions both in cold fusion cells and in other experiments. Over six hundred cold fusion papers (of the 2500 papers reviewed) have reported on measuring nuclear byproducts from cold fusion experiments. In addition to cold fusion, there have been other experimental findings, often not explained by traditional scientific models, of low-energy nuclear reactions. In the opinion of this editor, progress in science is made by discovery, by the pursuit of anomalies, and not by the dogmatic acceptance of previous models. Many of the participants in the conference have been actively involved in either cold fusion theory or experiments. Having participated in the international exchange of information on cold fusion and having seen the growth of a new science from pathologic skepticism to the verge of commercialization, it is a pleasure to volunteer to publish the proceedings of this historic conference.

ACKNOWLEDGMENTS

The publisher wishes to thank those responsible for this conference, especially Dr. J. O'M. Bockris and Guang H. Lin for the invitations and the meeting arrangements. All participants are congratulated for their experimental, theoretical, and informational contributions. Robyn Harris, Dinch Torres and Dee Winter have been diligent in effectively using their time (between preparing and publishing two monthly newsletters) to produce this document. We especially acknowledge and congratulate all of those true scientists and experimenters who have been responsible for forging ahead with investigations of new anomalies when assured by lesser lights that what they were trying to do was scientifically impossible. This is the same professional category of pioneers to which Faraday, the Wright Brothers, the Curies, Goddard, Steinmetz, Tesla, Kervran, and (more recently) Pons and Fleischmann belong. More important than the winners of Nobel prizes, amidst the acclaims of their peers, are those, who against the "better judgement" of their peers, persevere in the discoveries of new truths and change both scientific knowledge and the way in which we more abundantly live, work, and play.

Note: Some editorial privilege was invoked in making changes to papers that had been translated from foreign languages. Any lack of clarity can be attributed to the lack of suitable knowledge of the editor/publishers.

Hal Fox, Salt Lake City, Utah, January, 1996

Attendees at the
Low Energy Nuclear Reactions Conference

Front Row: Thomas Claytor, Toby Grotz, David Hudson, Ronald J. Kovac, Tadayoshi Ohmori, Jerry W. Decker, Conrad S. Hopman.
Middle Row: Roberto Monti, Harold Puthoff, Anna Polyak, John O'M. Bockris, Reiko Notoya, Yeong E. Kim, Georgiy Stepanovich Rabzi, R. Cox, Ernst Bauer, Guang H. Lin.
Back Row: Thomas Ward, Hal Fox, Charles Becker, John Dash, Robert Bush, Tadahiko Mizuno, Timothy A. Binder, Gregory Goulas, Tom Passell, Randy Davis, Peter Hagelstein, Yan Kucherov.

JOURNAL OF NEW ENERGY

DOES LOW TEMPERATURE NUCLEAR CHANGE OCCUR IN SOLIDS?

Proceedings Contents:

THEORETICAL MODELS

Chairman Guang H. Lin

INNOVATIVE APPROACHES

Chairman Guang H. Lin

OTHER PAPERS NOT FROM PROCEEDINGS:

DO NUCLEAR REACTIONS TAKE PLACE UNDER CHEMICAL STIMULATION?

J. O'M. Bockris
Department of Chemistry
Texas A&M Univ., College Station, TX

R.T. Bush
Physics Department
Cal-Polytechnic Univ., Pomona, CA

G.H. Lin
Department of Chemistry
Texas A&M Univ., College Station, TX
and

R.A. Monti
Instituto TESRE, CNR Bologna, Italy

INTRODUCTION

In the first years of this century it was thought that atoms were indivisible entities, but Rutherford found that a great deal of an atom was free space although it contained at its center a particle, the nucleus making up the majority of the mass of the atom. He attempted to see what was inside this tiny particle by striking it with an energetic stream of energetic particles and produced, in his first "atom splitting" reaction, O^{17} from N^{14} [1].

This seminal achievement founded the field of high energy physics, but it also created a mindset that breaking into nuclei needed colossal energy, about a million times more energy than is given out in a chemical reaction. Large machines (cyclotrons) and nuclear reactors have been thought to be necessary to cause nuclear reactions to occur. A remarkable change appears to be coming across nuclear physics. It was suggested by Fleischmann and Pons [2] in 1989 that palladium heavily loaded with deuterium was the site of a nuclear reaction and Bockris et al. [3] found that deuterium evolved from D_2O-LiOD in aqueous electrolysis contained up to 10^{-9} mole fraction of a tritium-containing species, i.e., a neutron had been introduced into a nucleus "in the cold."

It now appears that there are situations in which nuclei split open at the stimulus only chemical energies. This paper is a very brief presentation of the evidence for this seminal idea.

THE DEUTERIUM PALLADIUM SYSTEM

This system has been examined widely since 1989 and there are some 1,000 reports and papers concerning it already published. However, the system is awkward to use since it needs several weeks of electrolysis to "turn on" and even then nuclear products are formed only if the palladium has a sufficiently small number of cracks so that the D/Pd ratio exceeds 0.9.

On the way to that ratio, but at D/Pd > 0.7, tritium begins to form at very low yield [2]. The tritium formation is not sufficient in amount to explain the anomalous heat [4] evolved. Miles and Bush [5] have

found that He^4 is contained in the D_2 gas stream from the electrolysis as well. The amount produced with the observed heat if the heat producing reaction is

$$D + D \rightarrow He^4 + \gamma$$

There are other ways in which the occurrence of nuclear reactions inside palladium are manifest. Bush and Eagleton found more than a kilowatt per cc of heat from D-Pd in thin layers [6]. A low level evolution of neutrons (10^8 less than expected) accompanies the heat [7].

TRANSMUTATION IN SOLID LATTICES

One of us (RM) pointed out in 1990 that a "cold nuclear reaction" had already been claimed by Borghi [8]. The most well known name in pre 1989 work is that of Kevran [9]. Strong evidence of nuclear reactions in Pd in gaseous D_2 has been presented by Karabut et al [10]. An example of a reaction supported by the finding of micro quantities (10^{10} atoms/cc) of new nuclei is:

$$^{46}Pd + D \rightarrow {}^{42}Mo^{95} + {}^{5}B^{11}$$

Many other reactions involving the nuclear formation of, e.g., selenium, zinc, chromium, zirconium, germanium, and ruthenium from D-Pd have been reported by the same authors.

Bush and Eagleton [11] have found the formation of Sr from Rb, with the Sr showing an isotopic abundance frequency which differs from that of solar-derived Sr.

Dash [12] has reported the formation of silver and gold from palladium electrodes during electrolysis of light water. Ohmori and Enyo [13] have found that iron is formed in gold electrodes during electrolysis. Stringham and George [14] found helium and cadmium in a palladium electrode under sono-illumination. Iron has been found from carbon by arcing two carbon electrodes under very pure water. Precautions taken here by Sundaresan and Bockris [15] to avoid contamination were extreme.

THE GUN POWDER METHOD

A remarkable, if uncertain, method was introduced into the author's laboratory by J. Champion [16] in 1992, the experimental study being carried out by Guang Lin and Ramesh Bhardwaj [17]. A mixture of carbon potassium nitrate, sulfur, silica, cadmium, lead chloride and cadmium oxide was utilized and after ignition of the mixture the noble metal content after 2-3 days was up to 300 ppm. Some radioactivity (emission) was heard from the mixture. Success in this method appears to need a sufficiently rapid explosion.

NUCLEAR CHANGES IN BIOLOGICAL ORGANISMS?

Evidence that nuclear reactions occur in the cold in some biological reaction was first described in detail by Kevran [9]. Among modern workers are Komaki [18] who has worked with microorganisms grown in media which lack one of several nutrients needed. He finds that the needed nutrient atoms arise in the organisms although not present in the nutrient fluid.

Work giving some support to earlier claims includes that of Alper [19]. Here, a microorganism called pedomitropiom appears to produce metallic gold.

THEORETICAL COMMENTS

All these happenings are anomalous in terms of ideas of the structure of nuclei given in present textbooks. The production of tritium in palladium at room temperatures from deuterium is regarded as not feasible because of the difficulty of penetrating the coulomb barrier between two D^+ ions. However, although only the palladium deuterium system that has been subject to extensive confirmatory work worldwide, it appears time to put forward the more tentative proposition that nuclear change in lattices at room temperature is a widespread phenomenon.

Theories of the production of heat in palladium can be divided into three classes of which an example can be given in each one.

In the first, screening [20] of the nuclear charge by electrons of the metal is the center of attention. A metal contains around one mobile electron per atom. This does not seem to give a screening charge but to produce 1 kilowatt per cc of heat. Only one collision in 10^{21} need be nuclear so that a fluctuation in which, say, several electrons exist momentarily between two ions (hence greatly reducing the Coulomb barrier) is more easy to accept.

Hagelstein [21] has suggested that the virtual neutrons which must persist in a metal system exist for $\tau > 10^{-21}$ sec (Uncertainty Principle). If they existed for, say, 10^{-17} seconds then they would have a roaming radius of up to 100Å around the metal and could enter nuclei.

It was first shown by Bohm [22], but when the internuclear distance between two atoms and lattice attains a certain value there, the reflected amplitude of the deBroglie waves interfere destructively with the incident wave whereupon the barrier becomes transparent to charged particles Turner [23], Bush [24].

Concepts forming in the effort to interpret new facts have been forming in a parallel way in some physics laboratories where the stability associated with the model of Rutherford has been subject to some reservation since about 1980. The evolution of thought has been described by Greiner and Sandalescu [25]. The key is to understand that the nucleus is a small, stable sphere only in the ground state. Some atoms appear to transfer to an excited state, whereupon the nucleus becomes elliptical in shape. Nuclear protons are normally held together against their coulomb repulsions by the strong nuclear force at differences of ~ 1 Fermi. In the elliptical excited state the protons are apart by ~ 10 Fermi. Then, the short range strong force is greatly decreased and the nuclear repulsion becomes dominant, the nucleus unstable. In fact, the above article mentions "cold fission" experiments described in the recent nuclear literature which parallel the concepts which form the basis of the present chemical approach.

SUMMARY

According to classical nuclear physics, nuclei can only be split apart by forces corresponding to energy changes of an order of 10^6 ev. For about five years now it has been shown that it is possible to observe nuclear reactions within the stimulating energies in order of 5 ev so long as the particles are in a solid lattice. Thus, assisted nuclear transformations, occurring near room temperatures, have been widely observed. Interpretations may involve transmission resonance screening of nuclear charge, long lived virtual neutrons or activated nuclei elliptical in shape, which readily decompose.

REFERENCES

[1] E. Rutherford .and J. Checkwich, *Nature*, 107 (1921) 41.
[2] M. Fleischmann, S. Pons and M. Hawkins, "Electrochemically Induced Nuclear Fusion of Deuterium," *J. Electroanalyt. Chem.*, 261 (1989) 301.
[3] J. O'M. Bockris, N.J.C. Packham, K.L. Wolf, J.C. Wass, and R.C. Kainthla, "Production of Tritium from D_2O Electrolysis at a Palladium Cathode," *J. Electroanalyt. Chem.*, 270 (1989); F.G. Will, K. Cedzynska, and D.C. Linton, "Production of Tritium from D_2O Electrolysis at a Palladium Cathode," *J. Electroanalyt. Chem.*, 360 (1993) 161.
[4] G.H. Lin, R.C. Kainthla, N.J.C. Packham, O. Velev, and J. O'M. Bockris, "On Electrochemical Tritium Production," *Int. J. H. Energy*, 15 (1990) 537.
[5] M. Miles and R. Bush. (No title furnished)
[6] R.T. Bush and R.D. Eagleton, "Experimental Studies Supporting the Transmission Resonance Model for Cold Fusion Light Water: II Correlation of X-ray Emission with Excess Power," ICCF3, 1993, 409.
[7] H. Menlove. (No title furnished)
[8] D.C. Borghi, *Nuovo Cimento*, Savie Nova, 1, (1943) 1. (No title furnished)
[9] C.L. Kevran, Biological Transmutation, Beckman, NY, 1971. (No title furnished)
[10] A.R. Karabut, Y. Kucherov and I.B. Savvatimova, "Possible Nuclear Reactions Mechanism at Glow Discharge in Deuterium," ICCF3 (1993) 54.
[11] R. Bush and R.D. Eagleton, "Calorimetric Studies for Several Light Water Electrolytic Cells with Nickel Fibrex Cathodes & Electrolytes with Alkali Salts of Potassium, Rubidium & Cesium," ICCF4, 2 (1993) 13.
[12] J. Dash, G. Noble and D. Diman, "Surface Morphology & Microcomposition of Palladium Cathodes after Electrolysis is Acidified Light & heavy Water: Correlation with Excess Hear," ICCF4, 2 (1993) 25.
[13] T. Ohmori and M. Enyo, "Detection of Iron Atoms on Gold Electrodes used in Electrolysis of H_2O and P_2O in Natural & Alkaline Media," ICCF4 (1993) 52.
[14] J. Stringham and R. George, "Cavitation Induced Micro-Fusion," ICCF4 (1993).
[15] R. Sundaresan and J. O'M. Bockris, "Anomalous Reactions During Arcing Between Carbon Rods in Water," *Fusion Technology*, 26 (1994) 261.
[16] J. Champion, Twentieth Century Alchemy, Discovery Publishing, 1992. (No title furnished)
[17] G. Lin and R. Bhardwaj, Texas A&M University, 1993. (No title furnished)
[18] Komaki, *Revue de Pathologie Comparee*, 67 (1967), 213. (No title furnished)
[19] J. Alper, *A.S.M. News*, Jan 22, 1993, 650. (No title furnished)
[20] J. Kim, Y.E. Zubarev and M. Robinowitz, "Reaction Barrier Transparency for Cold Fusion with Deuterium," ICCF4, 4 (1993) 3.
[21] P.L. Hagelstein, "The Three Miracles: An Update on Neutron Transfer Reactions," ICCF5 Book of Abstracts (1995) 411.
[22] D. Bohm, Quantum Theory, Prentice Hall, New York, 1951. (No title furnished)
[23] C. Turner, *Physics Today*, Sept. 1989, 140. (No title furnished)
[24] R.T. Bush, "A Unifying Model for Cold Fusion," ICCF4, 4 (1993) 15-1.
[25] W. Greiner and A. Sandalescu, *Sci. American*, March 1990, 59. (No title furnished)

EPRI/NPD

SIGNIFICANCE OF TEXAS A& M FINDINGS IN OCT. 1992

THOMAS O. PASSELL

Electric Power Research Institute

June 19, 1995

June 1995

EPRI/NPD

THE FINDINGS BY KEVIN WOLF

- 3 Cells Electrolyzed in Series at Constant Low Current 42 days near a Neutron Detector of Low Background (40 Counts/Hr) using a Protocol of Adding Boron and Aluminum at 0.001 Molar to the 0.1 Molar LiOD Electrolyte at ~18th Day
- Cathodes Were Loaded With Deuterium Slowly at a Few 10's of milliamps/cm2 With a 12-Hour Cryogenic Treatment @ Day 17 and Were Sanded and Replaced in the Cell Every 7 Days
- On the ~21st & 22nd DaysTwo Successive Fast Neutron Episodes Were Observed at About 2 Times Background. The Neutron Detector is Minimally Sensitive to Gamma Rays but Gammas Were Observed Near the End of the 20-Hour Neutron Episode
- Upon Dismantling the Cells ~ 9-30-92 all three Cathodes (6 mm Diameter x 60 mm Long) Were Observed to be Mildly Radioactive.
- Analysis by Germanium Gamma Detectors Revealed Presence of 100 Billion Atoms of Ag, Pd, Rh, and (one)Ru Isotopes Having Ratios Unlike Those From Bombardment by High Energy Deuteron or Proton Beams

June 1995

EPRI/NPD

Wolf's Findings

- Isotopes Observed in The Most Active One of Three Cathodes ~9-7-92 at Texas A&M

ISOTOPE	NO. of ATOMS (Billions)	NO./Ag110m
Silver-105	26	32
Rhodium-101m	22	28
Rhodium-102	12	15
Rhodium-101	12	15
Rhodium-102m	6.3	8
Silver-106m	4.5	5.6
Ruthenium-103	3.7	4.6
Rhodium-99	2.7	3.4
Silver-110m	0.8	1

June 1995

EPRI/NPD

Postulated Reactions to Produce The Observed Isotopes

PRODUCT	REACTION
Silver-110m	Pd-108 (d,Gamma) (Q=+10.9 Mev) or on Impurity Silver -Ag-109 (d,p) (Q=+4.5 Mev)
Rhodium-99	Pd-102(p,Alpha) (Q=+3.2 Mev)
Ruthenium-103	Pd-106(d,pAlpha) (Q=+1.2 Mev) or Ru-102(d,p)Ru-103 (Q=4.14 Mev) on Impurity Ru
Silver-106m	Pd-105(d,n) (Q=+3.5 Mev) or Pd-105(p,gamma) (Q= +5.8 Mev)
Rhodium-102	Pd-104(d,Alpha) (Q=+8.1 Mev) or Pd-105(p,alpha) Q= +3.6 Mev
Rhodium-101	Pd-104(p,Alpha) (Q=+3.2 Mev)
Silver-105	Pd-104(d,n) (Q=+2.0 Mev) or Pd-104(p, gamma) (Q= +4.2 Mev)

June 1995

EPRI/NPD

Tentative Conclusions if Wolf's Findings are Confirmed

- Neutron Capture is Precluded as the Primary Mechanism Because These Isotopes Lie on the Neutron Deficient Side of Isotope Stability
- Deuterons or Protons Must Have Somehow Entered Palladium Nuclei with the Subsequent Emission of Alpha (He-4) Particles and Neutrons
- The Protocol for Achieving this Phenomena Has Some Similarities to that Found at SRI for Enhancing Production of Excess Heat (XSH)
- Wolf's Cells Were Not Instrumented to Observe XSH
- All 3 Cathodes Were Activated to Degrees Varying by no more than a Factor of 3
- Replication Attempts Have So Far Failed to Show the Effect

June 1995

EPRI/NPD

Tentative Conclusions if Wolf's Findings are Confirmed

- Reactions Postulated to Produce The Observed Isotopes Indicate PROTONS as Well as Deuterons Are Apparently Entering Pd Nuclei
- If Protons Can Enter a Pd Nucleus (Z=46), Then the Light Water XSH Reported on Nickel (28), Silver (47), Tin (50) and Gold (79) May Show Similar Nuclear Signatures Also.
- The Low-Z Electrolyte or Impurity Atoms that Diffuse into or Exist in Cathodes May Similarly Activate to give Both Heat and Nuclear Reaction Products
- If these Pd +D and Pd+P Reactions are Confirmed, then Other Nuclear Reactions Leading to **STABLE** Nuclei Should be Produced - but not Easily Observed
- Since the Activation Levels in Pd are 2 or 3 Orders of Magnitude Above Detector Background, this Phenomenon Provides a Unequivocal Nuclear Signature Observable Outside the Cells Because of the High Penetrating Power of Gamma Rays

June 1995

EPRI/NPD

Pd Impurity Light Element Reactions Capable of Making Helium-4, Heat, and Tritium

B-10(d,α)Be-8-->2α	Q=17.8 Mev (He-4=α)
B-11(d,α)Be-9	Q=8.02 Mev
B-11(p,α)Be-8 --->2α	Q=8.58 Mev
Be-9(d,α)Li-7	Q=7.15 Mev
Be-9(p,α)Li-6	Q=2.13 Mev
Be-9(d,T)Be-8 --->2α	Q=4.59 Mev (T=Tritium)
C-13(d,T)C-12	Q=1.31 Mev
O-17(d,T)O-16	Q=2.11 Mev

- All Reaction Products Listed Above (Except Tritium) are STABLE Nuclei

June 1995

EPRI/NPD

Unequivocal Ways to Measure Isotope Shifts in Palladium Cathodes

- Thermal Neutron Capture (Prompt) Gamma Rays
  - Sensitive to All Isotopes With Reasonably High Thermal Neutron Cross Section (>0.1 Barns)
  - Each Isotope Gives Many Well-Known Gamma Rays Previously Tabulated by Lone, Leavitt and Harrison to 3 figure accuracy
  - Interferences Should be Managable Using High Resolution Germanium Gamma Detection Since Each Isotope Produces More than One Gamma
  - Cathodes Could be Analyzed Before and After Heat Production in a Neutron Beam to get Accurate RATIO Changes - Method is Non-Destructive and can view the entire Sample
- Various Surface Analysis Techniques
  - The Best of these, Mass Spectroscopy of Stripped (Single Atom) Ions Still Samples Only a Small Portion of the Sample Which May or May Not Have Been Active

June 1995

EPRI/NPD

Palladium Neutron Capture Gammas

Pd-102 **0.4% - No Gammas fit Pd-103 levels

Pd-104 **11% - 3 Gammas * Fit Pd-105 levels, namely 325.8 (7.33) 415.0 (0.28), & 560.9 (0.24)

Pd-105 **67% - 7 Gammas Fit Pd-106 levels, namely 615.9 (8.4), 1048.1 (6.77), 1127.8 (2.83), 5404.3 (0.04), 8331.2 (0.11), 8002.6 (0.05) and 7996.3 (0.05)

Pd-106 **1% - 3 Gammas Fit Pd-107 lev els, namely 804.7 (0.62), 1348.7 (0.46), and 1572.6 (1.71)

Pd-108 **18% - 4 Gammas fit Pd-109 levels, namely, 265.9 (0.45), 291 (1.49), 325.6 (7.33) and 338 (6.71)

Pd-110 **0.9% - 2 gammas fit Pd-111 levels, namely 559.4 (0.24), and 1618.6 (1.49)

*Gamma Energies in keV followed by parentheses . with the number of those gammas emitted per 100 thermal neutron captures in Pd

**This is the % of all Pd neutron capture events that involve capture in this particular isotope.

June 1995

EPRI/NPD

Detailed Data from Wolf Electrolysis Experiment of September, 1992

June 1995

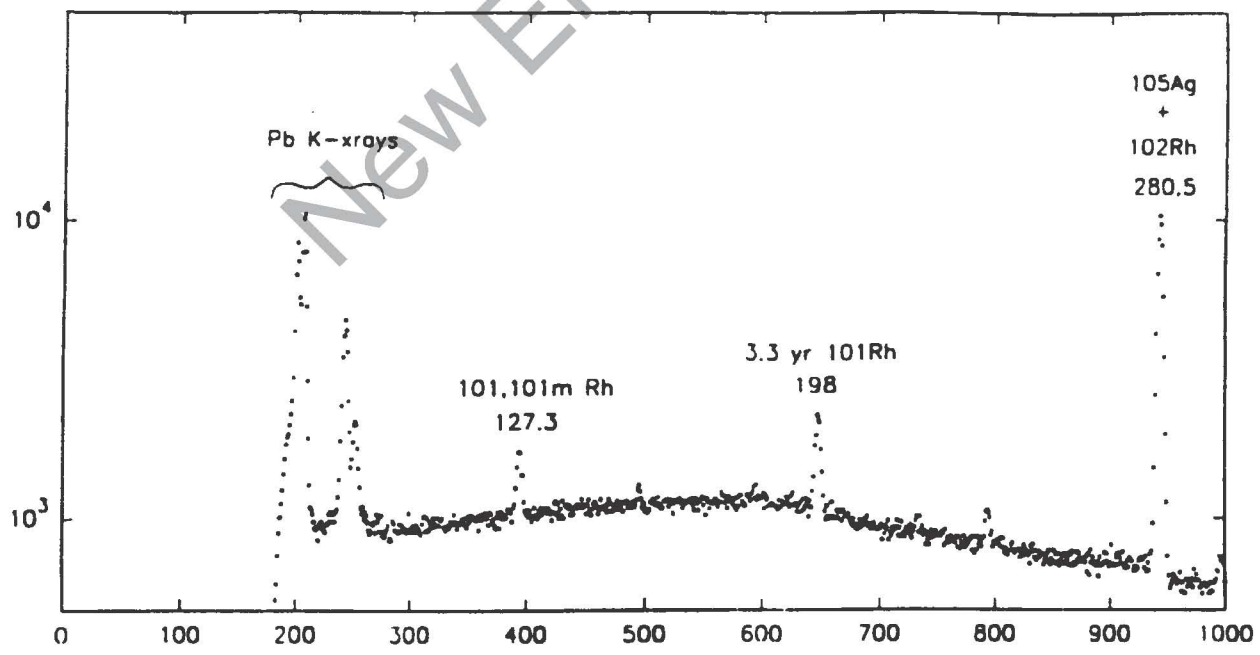

Fig. 6. Gamma Spectrum over the Energy Range 0-295 keV from a Palladium Cathode of dimensions 0.6 cm diameter by 6 cm length loaded with Deuterium in a cell having a Nickel mesh anode and using an electrolyte containing 0.1 M LiOD and ~100 PPM of Boron and Aluminum.

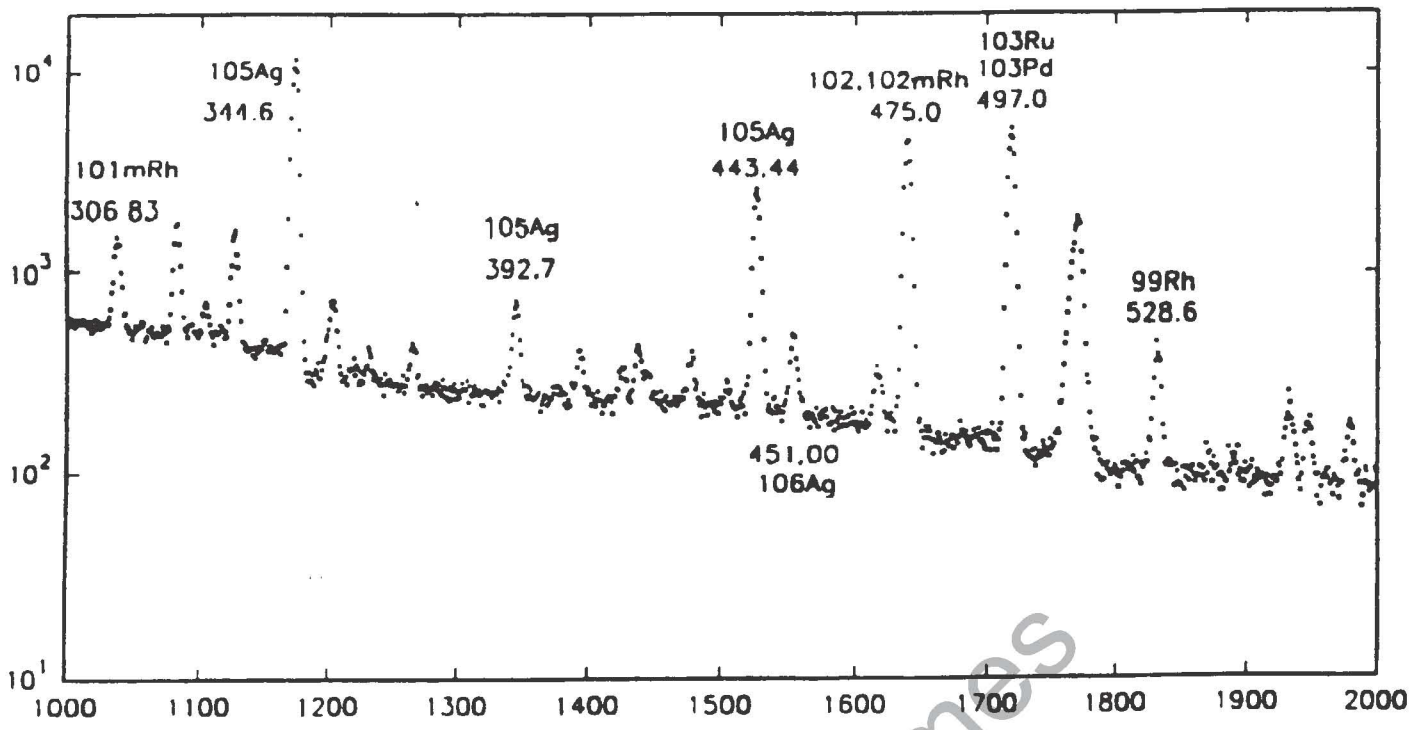

Fig. 7. Gamma Spectrum from 295 keV to 574 keV for the same cathode as in Fig. 6.

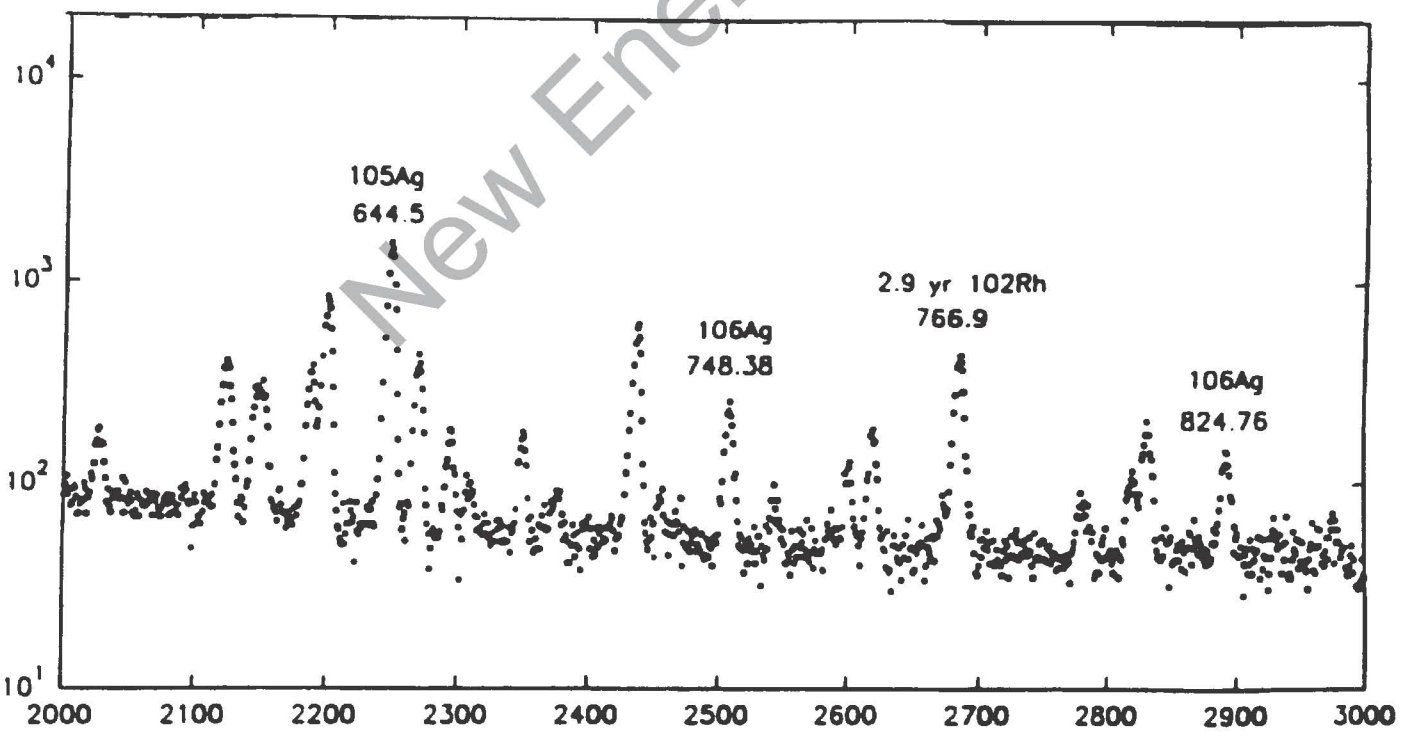

Fig. 8 Gamma Spectrum from 574 keV to 855 keV for the same cathode as in Fig 6.

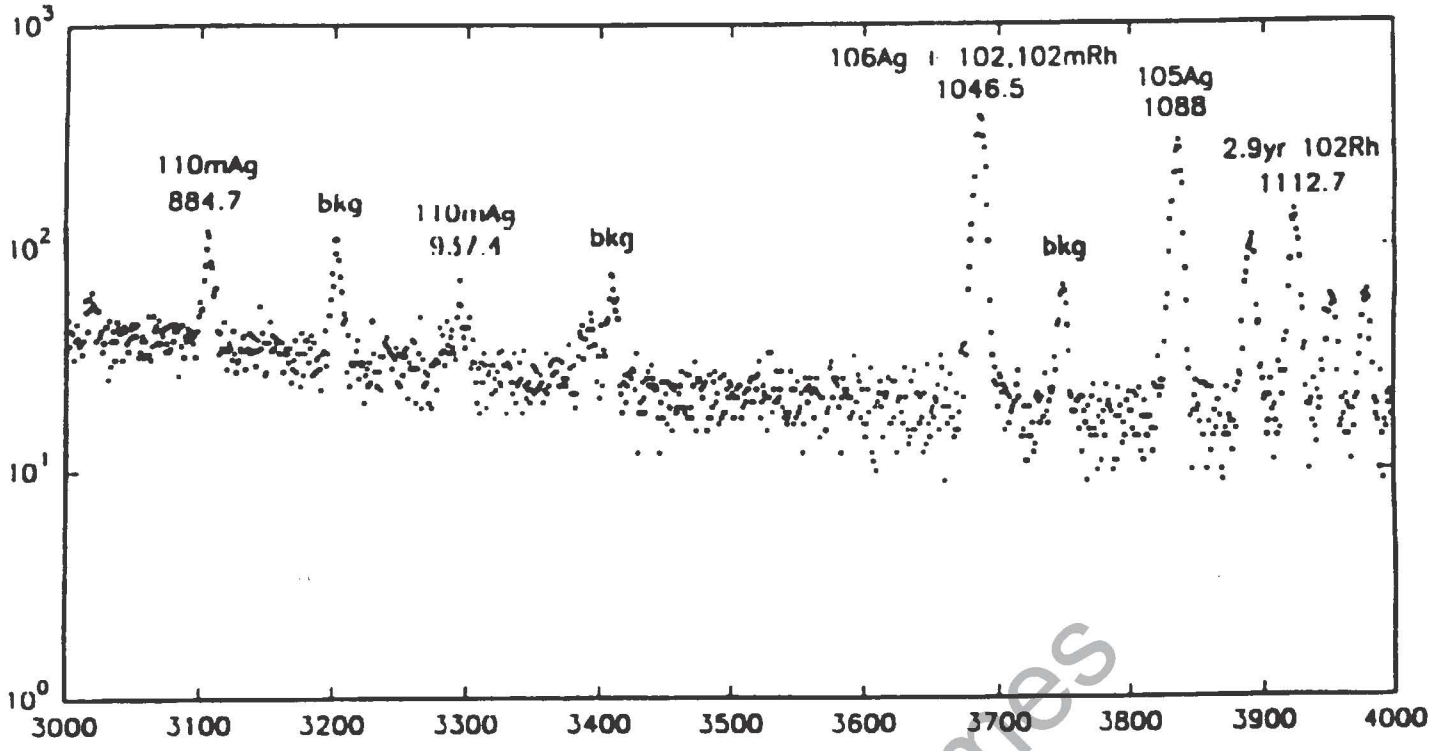

Fig. 9. Gamma Spectrum from 855 keV to 1133 keV for the same cathode as in Fig. 6.

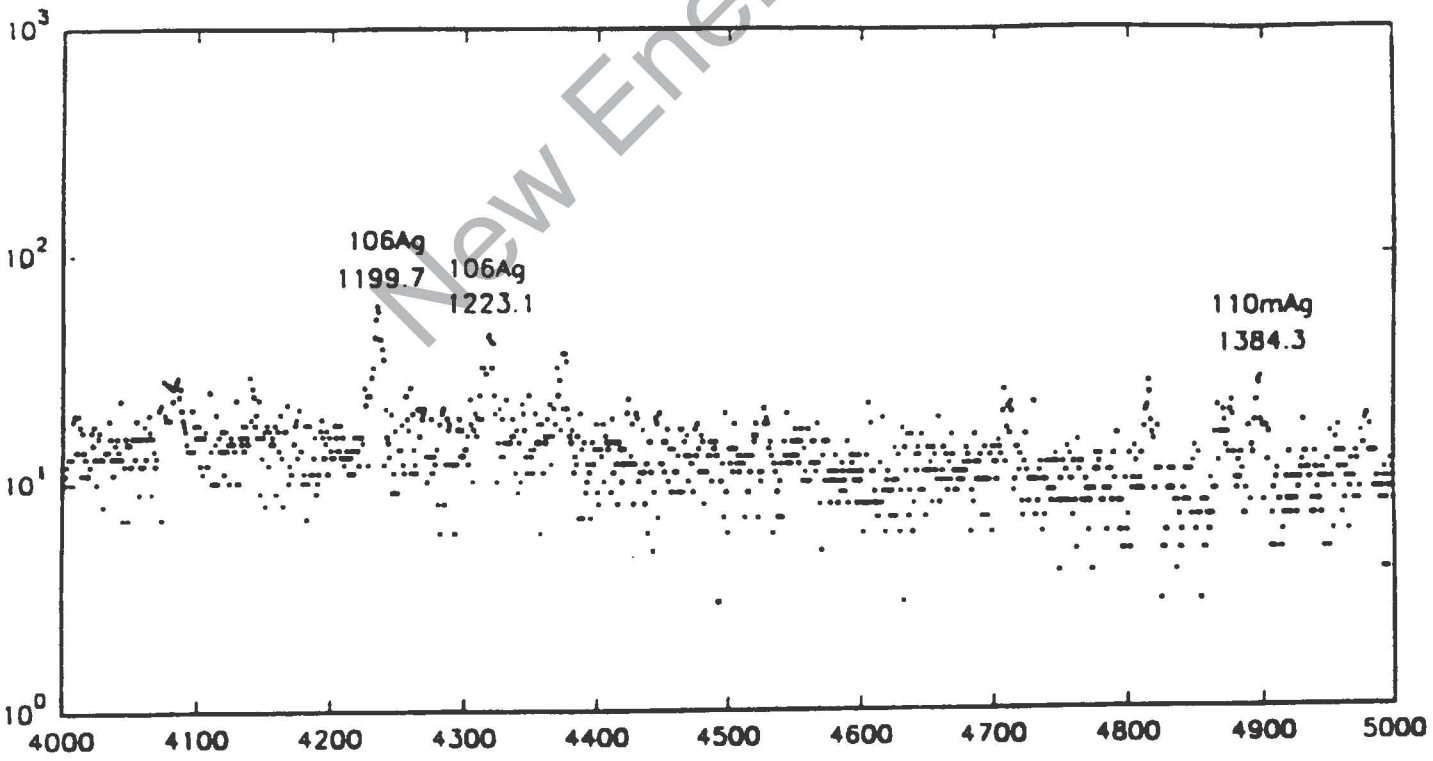

Fig 10. Gamma Spectrum from 1133 keV to 1412 keV for the same cathode as in Fig. 6

				Ag-105	Ag-106 m	Ag-107 stable		Ag-109 stable	Ag-110 m	
		Pd-102 stable		Pd-104 stable	Pd-105 stable	Pd-106 stable		Pd-108 stable		Pd-110 stable
Rh-99		Rh-101 and Rh-101m	Rh-102 and Rh-102m	Rh-103 stable						
					Ru-103					

Fig. 11 Portion of the Isotopes Table for Palladium, Silver, Rhodium, and Ruthenium showing Isotopes consistent with the Gamma Spectra in Figs. 6-10.

IRON FORMATION IN GOLD AND PALLADIUM CATHODES

T. Ohmori
Catalysis Research Center, Hokkaido Univ.
Kitaku, Sapporo, 060 Japan

M. Enyo
Hakodate National College of Technology
Tokura-cho, Hakodate, 042 Japan

ABSTRACT

Investigation of some reaction products possibly produced by electrolyzing with Au and Pd electrodes in Na_2SO_4, K_2CO_3, and KOH light water solutions was made. The electrolysis was performed for 7 days with a constant current of 1 A. After the electrolysis the elements accumulated in the electrode were analyzed by means of AES. In every case a notable amount of Fe atoms were detected together with a certain amount of excess energy evolution, being in the range of 9×10^{15} to 1.8×10^{16} atoms/cm^2 for Au and of 1.2×10^{15} to 4.0×10^{16} atoms/cm^2 for Pd. The isotopic abundance of these Fe atoms was measured by means of SIMS, which was 6.5, 77.5, and 14.5% for ^{54}Fe, ^{56}Fe and ^{57}Fe, respectively, at the top surface of Au electrode, obviously different from the natural values. For Pd electrode, a considerable increase in the contents of ^{54}Fe and ^{57}Fe was observed.

INTRODUCTION

We recently observed the production of Fe atoms reaching about 10^{16} atoms/cm^2 (true area) together with the excess heat evolution of several hundred mW at Au cathode [1,2]. In order to verify that such a Fe atom production is responsible for some nuclear transmutation, it is absolutely necessary to investigate the isotopic abundance of these Fe atoms.

For this reason we made the determination of the isotopic abundance of Fe product together with its quantification with Au and Pd electrodes after the electrolysis in light water electrolyte solutions. In this work, we also measured the excess heat and checked its correlation with the amount of Fe atoms produced.

EXPERIMENTAL

Five quartz (Fe<0.3 ppm) electrolytic cells were used. These electrolytic cells were in the form of flat bottomed cylinder (about 20 cm^2 x 15 cm) with a 5 cm thick silicone rubber stopper holding a test electrode, a counter electrode, a thermocouple and a quartz glass inlet tube for H_2 gas, which were cleaned carefully with hot mixed acid (1:1 H_2SO_4, HNO_3), rinsed with MQ water ultrasonically. The test electrode was suspended by an Au lead wire (0.03 cm diam.) for Au electrode or by a Pd lead wire (0.03 cm diam.) for Pd electrode, which was sealed with a thin teflon film without the extremity. The cells were placed in the air thermostat whose temperature was regulated at around 21 ± 1°C. The working electrodes used were cold worked Au plates (5 cm^2 app. area, 0.1 mm thick, 99.99% purity, Fe< 1 ppm), or cold worked Pd plates (5cm^2 app. area, 0.1 mm thick, 99.95% purity, Fe< 5 ppm), whose surfaces were scraped with a cleaned glass fragment edge and then washed with methyl alcohol and MQ water. The roughness factor of the electrode determined from the measurement of double layer capacitance by the galvanostatic

transient method [3] was 2.0. The counter electrode was 1 x 7 cm, 80-mesh platinum net (99.98% purity, Fe< 16 ppm). The electrolyte solutions used were 0.5 M Na_2SO_4, K_2CO_3 and KOH which were prepared from Merck sprapur grade chemicals. The volume of the electrolyte solution used was 100 ml. The electrolysis was conducted galvanostatically for 7 days by a constant current of 1 A. Before the electrolysis the Au electrode was kept at RHE by passage of H_2 into the cell. During the electrolysis MQ water was added to make up for the solution loss every 24 hours.

In order to identify the elements present in Au electrodes after the electrolysis and determine these atomic abundances, AES and SIMS measurements were carried out. For the AES measurement the electrode sample after washing with MQ water was placed on a Ni plate holder in a chamber in a vacuum of 2.0 x 10^{-8} Torr. Argon ion bombardment was performed under 99.9995% argon atmosphere of 2.5 x 10^{-5} Torr. The SIMS measurement was made in a vacuum of 5 x 10^{-9} Torr. by the O_2^+ irradiation.

RESULTS

Fig. 1 shows typical AES spectra from the top to the several 10 layers of Au electrode after the electrolysis in Na_2SO_4 solution. In the spectrum of the top surface (no A^+ bombardment treatment), Fe and O signals were observed in addition to Au spectral signals.

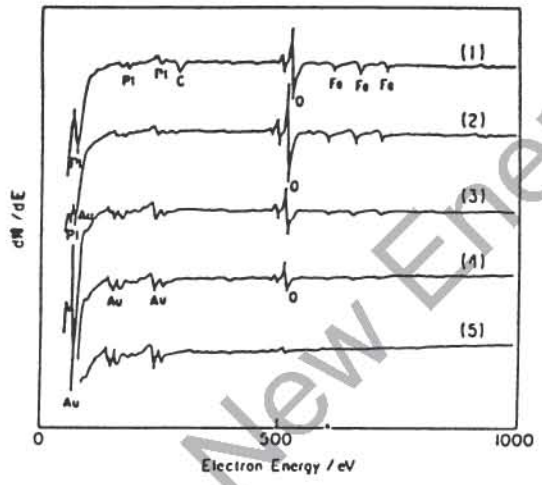

Fig. 1. AES spectra of Au electrode after electrolysis in Na_2SO_4 solution; bombardment time: 0 sec. (1), 30 sec. (2), 120 sec. (3), 180 sec. (4), & 600 sec. (5).

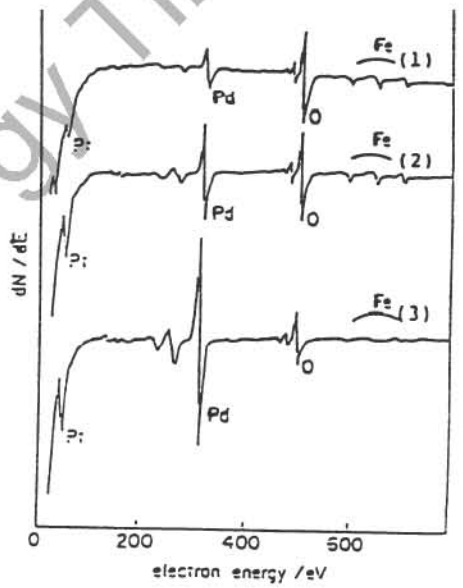

Fig. 2. AES spectra of Pd electrode after electrolysis in Na_2SO_4 solution; bombardment time: 0 sec. (1), 60 sec. (2), & 180 sec. (3).

On carrying out A^+ bombardment, the Fe and O signals decline and disappear after several minutes of the bombardment. Fig. 2 shows typical AES spectra for Pd electrodes after the electrolysis in Na_2SO_4 solution. In this case Fe, O and Pt signals were observed, the strength of Pt signal tending to increase with bombardment time in this time region. The Fe and O signals were observed for every Au and Pd electrodes independent of the nature of the electrolyte. The O signal always appears together with the Fe signals and the intensity ratio of Fe to O is nearly the same as that of the spectrum obtained on a pure Fe plate. Perhaps, traces of O_{2+} contained in the AES chamber bind with Fe atoms during the A^+ bombardment. We considered that the number of O atoms estimated from O signal is equal to the number of Fe atoms covered with O atoms, assuming that each O atom binds for each Fe atom, and added the number of O atoms to the number of Fe atoms estimated from the Fe signal itself, when estimating the total amount of Fe atoms from the AES spectra.

The distribution of Fe atoms from the top surface to the inner layers of the electrode estimated from the results in Fig. 1 and Fig. 2 is shown in Fig. 3 and Fig. 4, respectively. For Au electrode the content of Fe atoms on the top surface amounts to 44%. The amount of Fe atoms, in this case, becomes maximum (about 60%) at several mono-layers from the surface and the distribution extends down to about 80 mono-layers (corresponding to about 5 min. of the bombardment time). Whereas for Pd electrode the maximum content of Fe is about 45% (top surface) and its distribution extends down to 150 mono-layers. It is noticeable that a large amount of Pt is also accumulated in the bulk of Pd electrode. The amounts of Fe atoms produced in Au and Pd electrodes in every electrolyte solutions range between 1.0×10^{15} and 1.8×10^{16} atom/cm^2 for Au electrode and between 1.2×10^{15} and 4.0×10^{16} atom/cm^2 for Pd electrode.

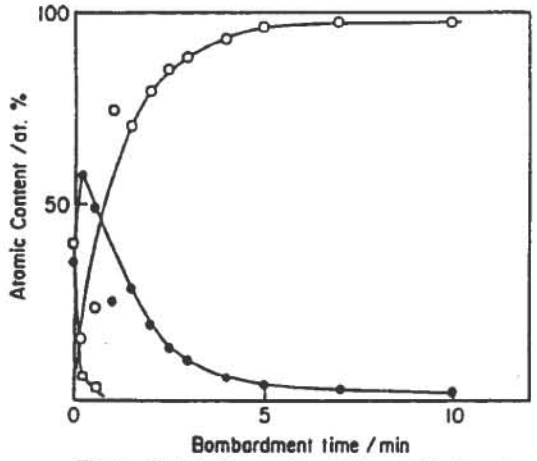

Fig. 3. Distribution profile of Fe and Pt atoms in Au electrode after electrolysis in Na_2SO_4 solution: Fe (●), Pt (□), & Au (O).

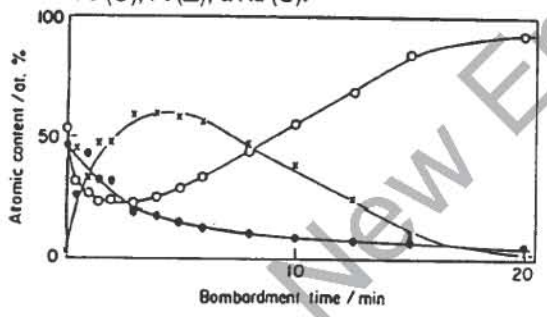

Fig. 4. Distribution profile of Fe and Pt atoms in Pd electrode after electrolysis in Na_2SO_4 solution: Fe (●), Pt (x), & Pd (O).

Thus, the maximum total amounts of Fe present in Au and Pd electrodes yield about 17 μg and 38 μg, respectively. However, in the case of Au electrode without any mechanical treatment, the amount of Fe atoms produced at the same electrolysis condition is smaller by one - two orders of magnitude. This result suggests that the production of Fe atoms is strongly influenced by the stress of the surface crystal lattice.

Fig. 5 shows the relationship between the amounts of Fe atoms and the mean excess energies obtained for Au electrodes in every electrolyte solutions. Although the data are rather scattered, there is a proportionality between these two terms. This supports strongly that the production of Fe atoms is related to the excess heat evolution observed.

SIMS spectrum was measured for each scan (up to 15 scans) for Au and Pd electrodes after the electrolysis in Na_2SO_4 solution. Fig. 6 and Fig. 7 show the profiles of the isotopic abundance of Fe atoms in Au and Pd electrodes, respectively. The Fe atoms detected at 15 scans correspond to those existing in the depth around 180 mono-layers from the top surface. For Au electrode, the contents of the particles with mass numbers 54, 56, 57, and 58 corresponding to Fe isotopes obtained from the spectrum of first scan are 6.5, 77.5, 14.5, and 1.5%, respectively, clearly different from the natural isotopic abundance of Fe atom.

In particular, the difference is remarkable for the particles with mass number 57, whose content is about 6.6 times the natural ^{57}Fe content. On the contrary, the content of the particles with mass number 56 is decreased by 15.5% from the natural ^{56}Fe content. Whereas, for Pd electrode, the rates of the particles with mass numbers 54, 56, 57, and 58 are 7.8, 85.4, 6.2 and 0.6%, respectively, different from these natural value to some extent. Such a departure becomes significant with the particles present in more inner layers of the electrode. Eventually, for Au electrode the content of the particles of mass number 57 after 10 scans reaches about 25%, being about 11 times the natural ^{57}Fe content.

Similar results should be obtained also from the analysis of the signals of mass numbers of 70, 72, and 73 corresponding to FeO, if all the particles with mass numbers 54, 56, and 57, are of Fe atoms. The signal intensity ratios of 57 to 56 and of 73 to 72 obtained are plotted against every scan numbers for Au electrode in Fig. 8. Although the plots are rather scattered, we can see that these ratios are, on the whole, in agreement with each other. Therefore, the change of the content of mass numbers 54, 56, and 57 from the natural value, shown in Fig. 6 is not due to FeH formation but probably due to some nuclear transmutation to produce Fe atoms.

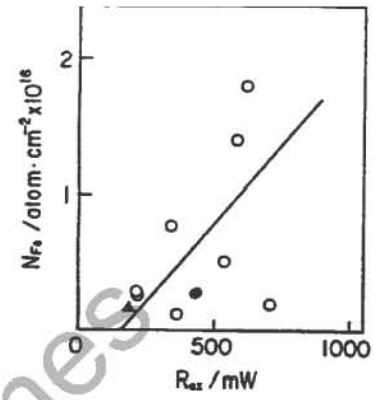

Fig. 5. Plots of the total amount of Fe atoms against the mean excess energy for Au electrode: Na_2SO_4 (O), K_2CO_3 (●), & KOH (▲).

As can be seen from Fig. 6 and Fig. 7, there is unambiguous difference in the isotopic abundance change between Au and Pd electrodes. In the former case, the increase of ^{57}Fe is significant, while, in the latter case, the increase of ^{54}Fe is noticeable. This suggests that the nuclear transmutation proceeds through somewhat different processes for different metals.

The possibility of the formation of Fe atoms from the impurities of chemical reagents or of the cell materials would be negligible because of the following reasons; (i) the number of Fe atoms from the electrolyte reagent should be at most 7 x 10^{14} atoms, e.g., in 100 ml of 0.5 M Na_2SO_4 (Merck spurapur grade reagent, Fe< 0.01 ppm,) solution, and (ii) the number of Fe atoms coming from the impurities in Au cathode and Pt anode materials would be negligible judging from the purity of these materials as have already mentioned. Hence, the amount of Fe atoms produced in Au electrodes in this experiment is at least 1 - 2 orders of magnitude larger than the values estimated above. Even if all impurity Fe atoms are accumulated in an Au electrode they could not give such clear Fe AES signals as those shown in Fig 1. From this point of view, most of the ^{56}Fe atoms, which being still the major isotopic component, are considered to be the product of nuclear transmutation together with ^{54}Fe and ^{57}Fe atoms.

The isotopic abundances of Mg, Si, K and Ti, obtained from the SIMS spectrum of first scan are shown to Table 1. As seen, the isotopic abundances of these elements are in agreement with these natural ones. Therefore, these atoms can be regarded as the impurities from the electrolyte reagents. The isotopic abundance of Pt atoms accumulated in Pd electrode was close to

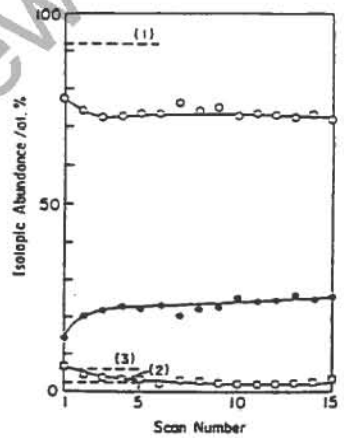

Fig. 6. Profile of the isotopic abundance of Fe atoms in the Au electrode. Solid line: the content of the particles on mass number 56 (O), 57 (●), & 54 (□). Dotted line: natural isotopic abundance levels of ^{56}Fe (1), ^{57}Fe (2), & ^{54}Fe (3).

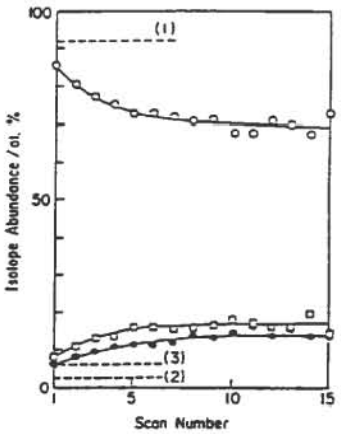

Fig. 7. Profile of the isotopic abundance of Fe atoms in the Pd electrode. Solid line: the content of the particles on mass number 56 (O), 57 (●), & 54 (□). Dotted line: natural isotopic abundance levels of ^{56}Fe (1), ^{57}Fe (2), & ^{54}Fe (3).

the natural isotopic abundance. Accordingly, we can not connect this Pt formation with nuclear transmutation, however, it is a very curious phenomenon that a considerable amount of Pt atoms are formed and the content becomes maximum at around 100 layers below the Pd electrode.

From these facts, it may be concluded that iron with a different isotope composition was produced by the light water electrolysis and its production is attributed to some nuclear transmutation.

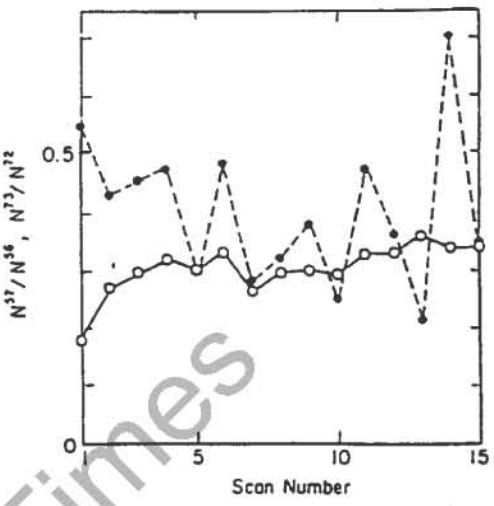

Fig. 8. Signal intensity ratio of mass number 57 to mass number 56 (O) and of mass number 73 to mass number 72 (●).

REFERENCES

[1] T. Ohmori and M. Enyo, ICCF-4 Abstract N 2.2, Lahaina (1993)

[2] T. Ohmori and M Enyo, *Fusion Technology*, 24, 293, (1993)

[3] T. Ohmori, *J. Electroanal. Chem.*, 157, 159, (1983)

TABLE I

Isotopic Abundance of Mg, Si, K and Ti Atoms

Elements	Isotopes	Isotope content (%)	Natural isotope content (%)
Mg	^{24}Mg	77.07	78.70
	^{25}Mg	12.19	10.13
	^{26}Mg	10.74	11.17
Si	^{28}Si	90.75	92.21
	^{29}Si	5.62	4.70
	^{30}Si	3.62	3.09
K	^{39}K	93.93	93.10
	^{41}K	6.06	6.88
Ti	^{46}Ti	8.68	7.93
	^{47}Ti	7.19	7.28
	^{48}Ti	74.37	73.94
	^{49}Ti	5.15	5.51
	^{50}Ti	4.59	5.34

POSSIBLE NUCLEAR REACTIONS MECHANISMS AT GLOW DISCHARGE IN DEUTERIUM

A.B. Karabut, Y.R. Kucherov, I.B. Savvatimova
Scientific Industrial Association "Luch"
Zhelesnodorozhnaya str.,24, Podolsk
Moscow Region, Russian Federation 142100

ABSTRACT

Experimental results of impurity concentration measurements in palladium cathode by different methods before and after glow discharge in deuterium experiments are presented. Some very strange elements which we could not find in discharge environment can be seen. An attempt to understand this situation on the basis of fission and fusion in Pd-d system is presented.

1. INTRODUCTION

One of the main problems of the "cold nuclear fusion" is the discrepancy between experimentally obtained amount of heat and amount of nuclear products. Let us summarize some known experimental facts [1,2]:

1. Excessive heat is generated with the output a few times larger than input.
2. Weak neutron signals with intensity 10-10^7 s^{-1}
3. Weak gamma-radiation with intensity $<10^5$ s^{-1}
4. Characteristic X-rays with intensity $<10^9$ s^{-1}
5. Tritium formation.
6. Helium isotopes, mostly ^4He with intensity $<10^8$ s^{-1}
7. Charged particles have high energy, up to 10 MeV and more.

As we noted in [2], to explain excessive heat we must assume that either charged particles have small energy (E < 1 MeV), or they are heavy (heavier than ^4He). This situation cannot be explained in terms of "hot" or "micro hot" fusion, because in this case cross-sections of nuclear reactions are well known and branching of nuclear reactions - neutrons to tritium and 14 MeV neutron group to 2.45 MeV group does not correspond to thermal d-d reaction.

An interesting data appears with material science results. Earlier we considered only helium and tritium aspects of cold fusion, though we could see anomalies with other impurities for some time.

2. INITIAL MATERIAL

We used pure 99.99 grade palladium as a cathode material. The bulk impurities content was defined by spark mass-spectrometry for all the elements of the Periodic Table. The analyses were made in the mass-spectrometry laboratory of GIREDMET analytical center. The method resolution was 10^{-8} atomic %, with standard deviation 0.15 -0.30 for different elements.

3. THE INVESTIGATION OF CATHODE MATERIAL COMPOSITION

For cathode material element and isotopic composition investigation X-ray microprobe (SEM "Hitachi S-800" with Link Analytical "LZ-5" detector) was used (A.D. Senchukov's group, SIA "Luch"), and secondary ion mass-spectrometry (SIMS) in I.P. Chernov's group (Tomsk Polytechnical Institute) and in A.G. Lototski's group (GIREDMET). Impurities in discharge environment (Mo, SiO^2, Al_2O_3) which could be transported to the cathode in the discharge were also investigated.

As a result such elements as Na; Mg; Al; Si; S; Ca; Ti; Cr; Fe; Ni; Zn; Ge; Br; Sr; Mo can be seen in the Pd after glow discharge experiments, sometimes up to 0.1% in the upper 1 micron layer of the cathode. Especially large is the contents of Na; Mg; Br; Zn; S; Mo; Si. The last two elements can appear due to sputtering. The appearance of other elements we can't explain. Wholly unexpected is the presence of germanium. The distribution of the impurities over the cathode surface was measured by the microprobe. The comparison of the distribution with SEM photos shows that most of the impurities are localized along the palladium crystalline boundaries. We must note that this method resolution is about 10^{-2}% and it doesn't show any impurities in the initial material. Adjacent to palladium Mo-cap only silicon can be seen.

The data on isotopic composition obtained in different groups varies and we will discuss it in our next paper.

4. DISCUSSION

Let us look at a possible nuclear reactions which can lead to heavy charged particles (A>4) formation. We can extract reactions that do not contradict known data. Reactions can be written as follows:

$$A_1 + A_2 + A3 + ... + A_n \rightarrow B_1 + B_2 + ... + B_n \quad (1)$$

in the left side are the reacting particles and reaction products are in the right side. As sharp peaks can be seen on charged particles spectrum, the pulse of reaction products must be fixed and there are no more than two reaction products in each act. It means that (1) can be written as:

$$A_1 + A_2 + ... + A_n \rightarrow B_1 + B_2 \quad (2)$$

For the discharge in deuterium with palladium cathode left side can look like: d+d; d+d+d; nd; Pd; d+Pd; 2d+Pd; 3d+Pd etc. Variant d+d in form of $d(d,^3He)n$ and d(d,t)p, judging from neutron and c.p. spectra is not the main reaction.

For nuclear reaction to take place conservation laws must take place: energy, pulse, charge, barion charge, spin, isotopic spin, evenness. The deviation from these laws usually asks for too much energy and in case of "cold" reaction can be put aside. If we put aside Coulomb barrier problem, which is the main problem for "cold fusion," it appears that there are a rather limited number of nuclear reactions for which

conservation laws are fulfilled. The amount of possible reactions goes down dramatically it we assume that only stable isotopes are formed. This statement must be true because palladium sample's radioactivity is very weak after the experiment. Than the list of possible reactions will look like:

$$_{46}Pd \rightarrow (_{36}Kr + _{10}Ne);\quad (_{35}Br + _{11}Na);\quad (_{34}Se + _{12}Mg);$$

$$(_{32}Ge + _{14}Si);\quad (_{30}Zn + _{16}S);\quad (_{28}Ni + _{18}Ar); \tag{3}$$

$$(_{26}Fe + _{20}Ca);\quad (_{24}Cr + _{22}Ti)$$

$$_{46}Pd + d \text{ - all forbidden.} \tag{4}$$

$$_{46}Pd + 2d \rightarrow (^{87}Sr + ^{22}Ne);\quad (^{73}Ge + ^{36}S) \tag{5}$$

$$_{46}Pd + 3d \rightarrow (^{95,\ 97}Mo + ^{19}F);\quad (^{98\text{-}104}Ru + ^{10}B) \tag{6}$$

$$\rightarrow (_{46}Pd + ^{6}Li) \tag{7}$$

It should be noted that the only allowed "catalytic" reaction is with ^{6}Li formation. From this point of view the following elements can be expected in palladium: ^{6}Li; ^{10}B; F; Ne; Na; Mg; Si; S; Ar; Ca; Ti; Cr; Fe; Ni; Zn; Ge; Se; Br; Sr; Mo; Ru.

The order of the energy in these reactions ~1 MeV for group (3) - fission, ~20 MeV for group (5) and ~30-40 MeV for groups (6) and (7) - "fusion-fission." For excessive heat release in our experiments (~10kJ) this corresponds to $\sim 10^{16}$ reactions in one experiment for the sample with the volume 10^{-3} cm^3, or 10^{-4} - 10^{-3} atomic %, which is higher than resolution threshold for the most analytical methods. If the reaction takes place in a thin layer this only increases the local impurities concentration. If this layer is about 1 micron thick, reaction product concentration can reach ~0.1%.

CONCLUSION

In the assumption that mechanisms exist allowing to overcome nuclear barriers, fusion and fission reactions for which conservation laws are fulfilled are taken into account. The analyses of the impurities, appeared in pure palladium after glow discharge experiments, give suspicious correlation with predicted elements. The given results are still difficult to call final, but if they will be confirmed on the basis of larger statistics they will suggest a new approach to the problem. The unique role of the deuterium will be questioned because the same thing can be constructed for other gases and metals. It will also initiate the search for long-living resonances of nuclear shell of Pd, excited by inelastic scattering of discharge ions (of the type of the laser effect).

REFERENCES

[1.] E. Storms, "Review of Experimental Observations About the Cold Fusion Effect," 1991, Fusion Technology, 20, 433.

[2.] A. Karabut, Ya Kucherov, I. Savvatimova, "Nuclear Product Ratio for Glow Discharge in Deuterium," 1992, Physics Letters A, 170, 265.

MICROANALYSIS OF PALLADIUM AFTER ELECTROLYSIS IN HEAVY WATER

Sylvie Miguet and John Dash
Physics Department, Portland State University
PO Box 751
Portland, OR 97207-0751

ABSTRACT

The morphology and microcomposition of palladium after electrolysis in heavy water were studied. Fibers which appeared on the surface were observed to change with time. Evidence which supports the possibility of transmutation is presented.

INTRODUCTION

Previously we reported finding concentrations of unexpected elements on palladium cathodes after electrolysis in an electrolyte containing H_2SO_4 and D_2O (1,2). We report here the results of analysis of palladium 0.315 mm thick used as a cathode for 25 hours and then inadvertently as an anode for 170 minutes.

EXPERIMENTAL METHODS AND RESULTS

The electrolysis experiments have been carried out, first, for about 5 hours during summer 1993, and then for about 23 hours during summer 1994.

For the first 5 hours of operation, the experimental setup consisted of two cells in series, one (light water control cell) containing 0.06 mol fraction H_2SO_4 (analytical reagent) in deionized H_2O, the other (heavy water cell) contained 0.06 mol fraction H_2SO_4 in D_2O (99% D_2) and both containing a cold-rolled Pd cathode and a Pt anode. The anodes were made from 99.9% platinum and the cathodes were made from 99.9% palladium. Chemical analyses of the palladium and platinum were provided by the supplier. The palladium foils were produced by cold rolling from the initial 0.5 mm thickness to 0.315 mm.

For the next 20 hours of operation, a new setup was used. Two cells were connected in series but, this time, the control cell contained two Pt electrodes, and the experimental cell contained the previous Pd cathode and Pt anode of the heavy water cell. Both contained acidified heavy water (0.06 mol fraction H_2SO_4).

In the last experiment, the palladium was used inadvertently as an anode. After electrolysis for 170 minutes, the cell current rapidly dropped to zero. When the cell was opened, we found that the lower part of the palladium had dissolved. The electrolyte, originally a clear liquid, was now a black powdery solid. Some of this black solid was attached to the platinum anode but the platinum was not damaged.

In this series of experiments, a recombination catalyst consisting of a substrate coated with platinum black (Los Alamos type electrode, 20% Pt on carbon) was utilized to recombine the off-gases in a closed system. Electrolysis was performed at current densities ranging from 0.75 to 1.5 A per cm^2.

Excess heat compared with the control was observed during both the 1993 and the 1994 experiments.

Surface chemical analyses of the palladium cathode were performed with a LINK AN10,000 Energy Dispersive Spectrometer (EDS) attached to an ISI-SS40 Scanning Electron Microscope (SEM). The thin window of the EDS detector was in place, thus allowing detection of atomic number six and above. The cathode was titled 45 degrees along the longitudinal axis for efficient X-ray detection and enhancement of the surface relief.

We report here the results of analyses of the concave side and the edges of the palladium cathode.

Fig. 1 shows the lower part of the concave side of the palladium cathode after the last electrolysis experiment during which anodic dissolution occurred. The smooth, rounded features near the bottom are believed to be the result of electropolishing; although localized melting might also produce similar features. Comparison of the crystal size in the upper and lower parts of this electrode may be helpful in deciding this question. This has not yet been done.

Microchemical analyses were obtained from the bottom of the electrode and from the areas indicated by the letters **k** and **s** in Fig. 1. Unexpected elements observed on the bottom edge include aluminum and titanium.

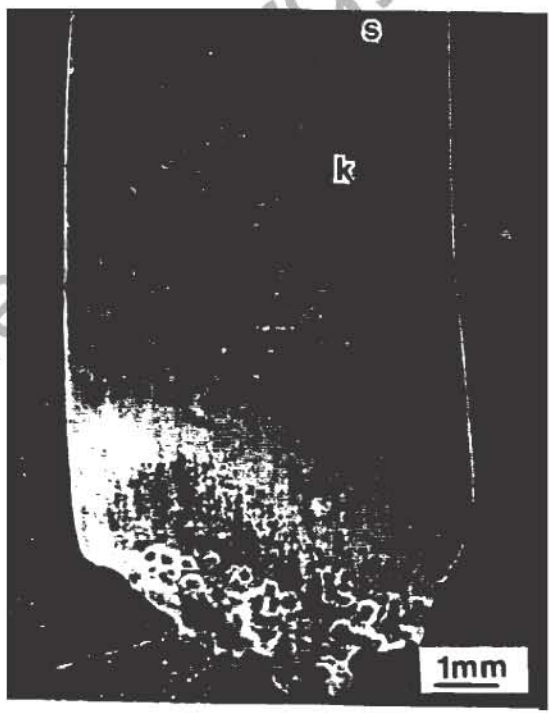

Fig. 1 Lower part of the concave side of the palladium cathode. This side faced the counter electrode during all of the electrolysis experiments. The region indicated by the letter **k** is approximately at the electrolyte level.

An example of the location of titanium is shown by the region labeled j in Fig. 2a, which is enlarged in Fig. 2b. The spot labeled **J1** has no titanium (Fig. 3a), whereas the spot labeled **J2** contains about 25% titanium (Fig. 3b).

a. b.

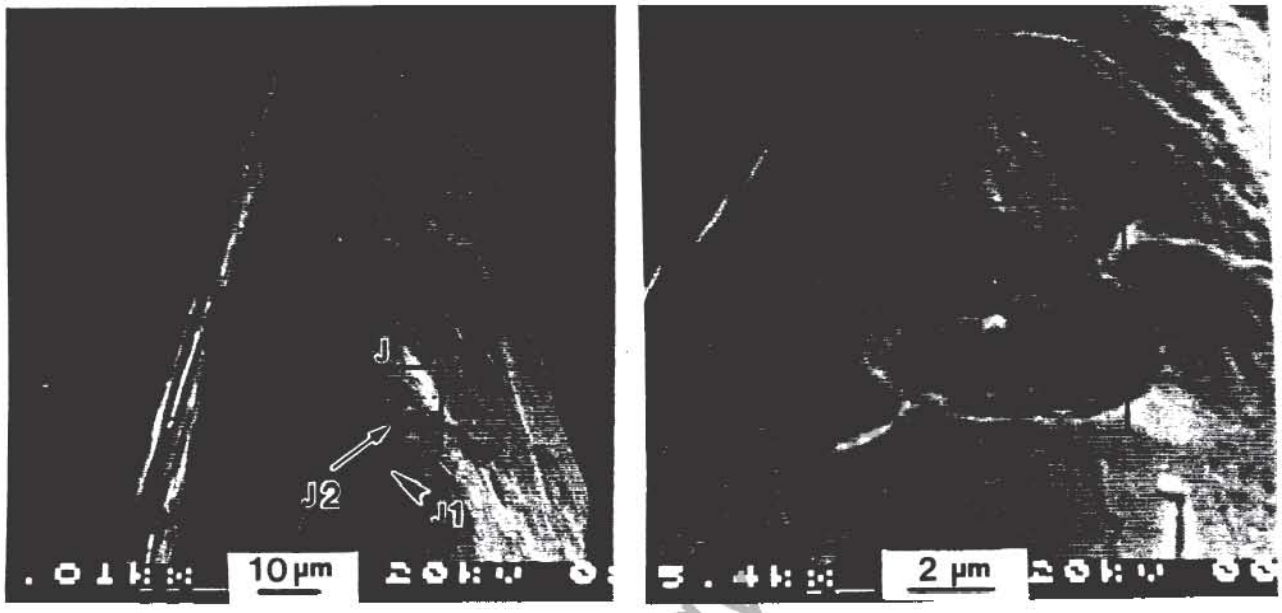

Fig. 2(a) Portion of the lower edge of the palladium electrode. **(b)** Enlargement of the region **J** in Fig. 2a.

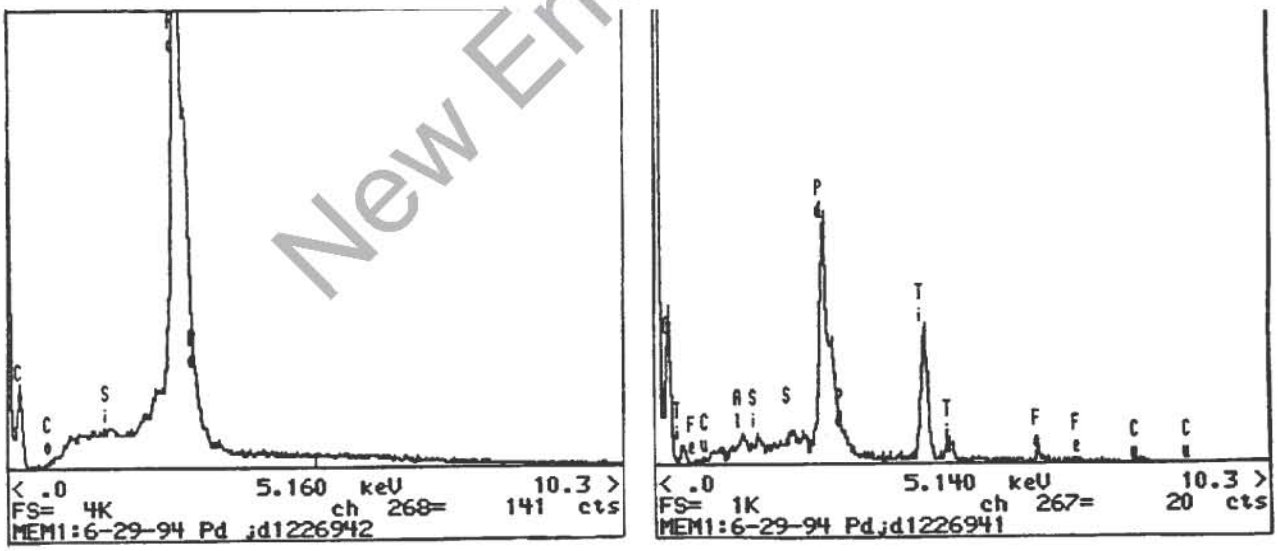

Fig. 3a EDS spectrum of spot **J1** in Fig. 2a

Fig. 3b EDS spectrum of spot **J2** in Fig. 2a.

A black blob appeared on the palladium electrode, near the electrolyte level, after 10 hours of electrolysis, in June 1994. This persisted for 15 more hours of electrolysis and through numerous washings with deionized water. The portion of the blob in region **k** of Fig.1 is shown in Fig. 4a as it appeared on Dec.

1, 1994. Here it is obvious that fibers protrude from the blob. Apparently, changes occurred in both the blob and the fibers, either while the lower part of the electrode was being examined in the SEM or during storage between successive SEM examinations. For example, Fig. 4b shows that bulges occurred along the fibers.

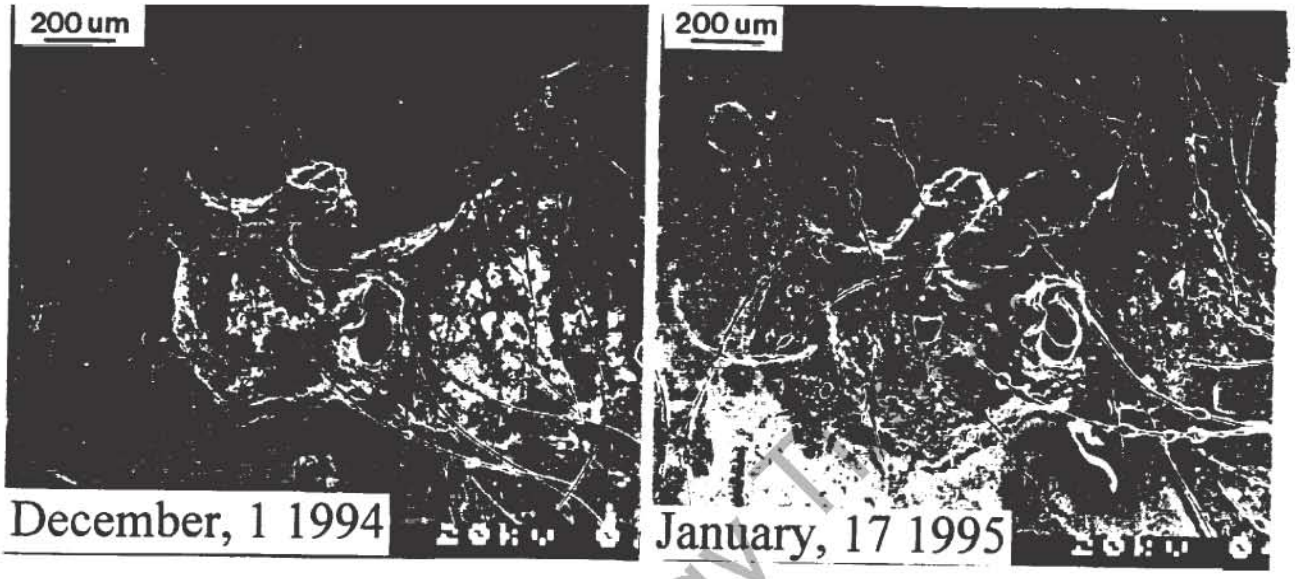

Fig. 4 Enlarged view of region **k** in Fig. 1 (a) 12-1-94. (b)1-17-95

The fibers are composed mainly of palladium, sulfur, carbon, and oxygen, but the proportions of these elements are quite variable. The bulges also have variable composition, which appears to change with time. This can be seen in Fig. 5. The bulge labeled **E1** in Fig. 5b gave the spectrum shown in Fig. 5d, in which peaks for silver **L**α and silver **L**β are labeled. The ratio of the intensities of these two peaks is 0.57. About one month later, the bulge changed in appearance (point $\mathbf{E_2}$ in Fig. 5c), and the ratio of the two silver peaks increased to 0.82 (Fig. 5e). Because the silver **L**β peak coincides with the cadmium **L**α peak, a possible explanation for the change in peak ratio is that silver has been slowly changing to cadmium. This is consistent with our observation on another palladium cathode which had been electrolyzed in heavy water. Silver was observed in high, localized concentrations shortly after electrolysis. Examination 15 months later showed the presence of cadmium in addition to silver.

DISCUSSION OF RESULTS

The results presented here for a palladium cathode after electrolysis in heavy water are consistent with those presented previously in that localized concentrations of elements not expected from impurities in the system have been observed. Whereas we previously found gold and silver on the surface, we here report aluminum and titanium concentrated inside the palladium, in addition to silver on the surface. A new finding is the appearance of fibers on the surface, whose composition appears to change with time. Similar fibers have been observed by others after electrolysis of palladium in heavy water (3).

ACKNOWLEDGEMENT

The electrolysis experiments were performed by Daniel Fredrickson, Grant Noble, Maureen Breiling, and Elizabeth McNasser.

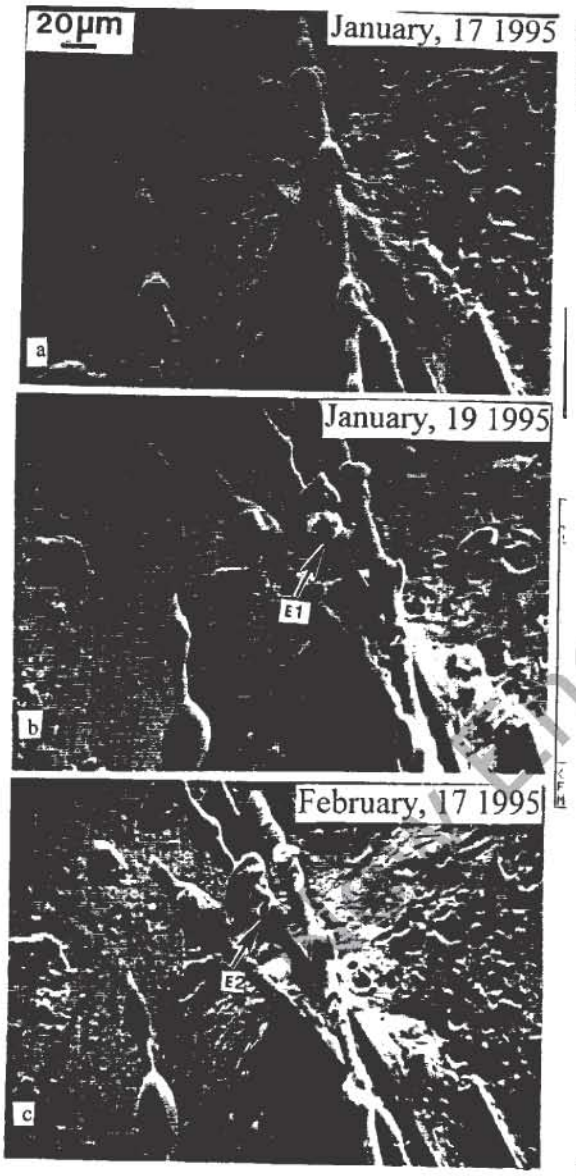

Fig. 5 Changes in morphology and EDS spectra of the features in the square shown in Fig. 4a. These changes occurred during storage at room temperature with no further electrolysis.

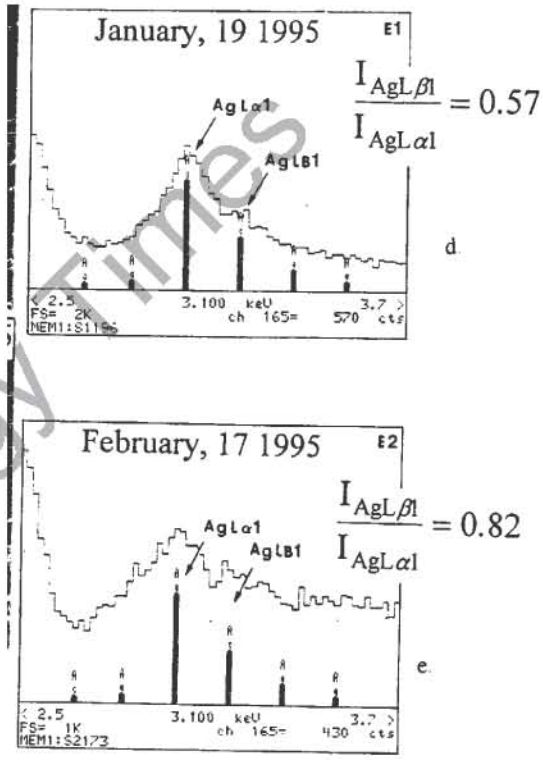

REFERENCES

1. D.S. Silver, J. Dash, and P.S. Keefe, "Surface Topography of a Palladium Cathode After Electrolysis in Heavy Water", *Fusion Technology*, vol 24, 423 (1993).

2. J. Dash, G. Noble, and D. Diman, "Surface Morphology and Microcomposition of Palladium Cathodes after Electrolysis in Acidified Light and Heavy Water: Correlation with Excess Heat", Trans. *Fusion Technology*, vol 26, # 4T, 299 (1994).

3. T. Okmori, Hokkaido Univ., Private Communication (1995).

ELECTROLYTICALLY STIMULATED COLD NUCLEAR SYNTHESIS OF STRONTIUM FROM RUBIDIUM

by
Robert T. Bush
Physics Department, California State Polytechnic University
3801 West Temple Avenue, CA 91768
&
ENECO, Inc., 540 Arapeen Dr., # 205, Salt Lake City, Utah 84108
& Proteus Processes & Technology, Inc., 3801 West Temple Avenue, Pomona, CA 91768

ABSTRACT

Two separate mass spectrometric analyses, SIMS and ICPMS of 1.0 amu discrimination with the latter preceded by an ion-exchange column separation of strontium and rubidium, performed by two independent laboratories on the pre-run and post-run cathode material from a light water based rubidium carbonate cell and a rubidium hydroxide cell provide strong evidence for the electrolytically induced transmutation of rubidium to strontium originally hypothesized by the author in connection with his CAF hypothesis ("Cold Alkali Fusion").

INTRODUCTION

Analyses of the pre-run electrode material and post-run electrodes from two light water based rubidium salt electrolytic cells, cell 53 (rubidium carbonate) and cell 56 (rubidium hydroxide) having nickel mesh cathodes by two independent laboratories provide strong initial evidence in support of Bush's CAF Hypothesis [1,6] ("Cold Alkali Fusion") that strontium is being produced from rubidium via a cold nuclear reaction in which a proton is being added to Rb^{85} (Rb^{87}) to produce Sr^{86}(Sr^{88}). The post-run cathode material of cell 53 was analyzed via SIMS, while that for cell 53 and cell 56 was analyzed via Inductively Coupled Mass Spectrometry (1 amu discrimination) following an ion exchange column enhancement of the strontium relative to the rubidium [1,2,6] at WCAS ("West Coast Analytical Service, Inc.") of Santa Fe Springs, CA. This result combined with the earlier mass spectrometric evidence and its correlation with the excess heats measured via calorimetry also provides support for the author's LANT ("Lattice Assisted Nuclear Transmutation") hypothesis [3] according to which a cold nucleosynthetic chain extending beyond strontium is generated.

CELL DESIGN AND CALORIMETRY

The cell and calorimeter design employed for the present series of experiments were of two types: (1) Cells 53 and 56 were essentially the same as that reported in Ref. 2. which was a modified Fleishmann-Pons electrolytic cell (Ref. 4) with the following principal modifications: (a) the use of a *platinum black recombiner* in the cell to allow for *closed-cell operation*, (b) a *magnetic stirrer* that provided for more uniform electrolyte mixing, and (c) *Teflon* coating of all nonelectrode materials to reduce electrolyte contamination. Additional details regarding the experimental setup provided in ref. 7.

Fig. 1 Cathode post-run mass spectrogram.

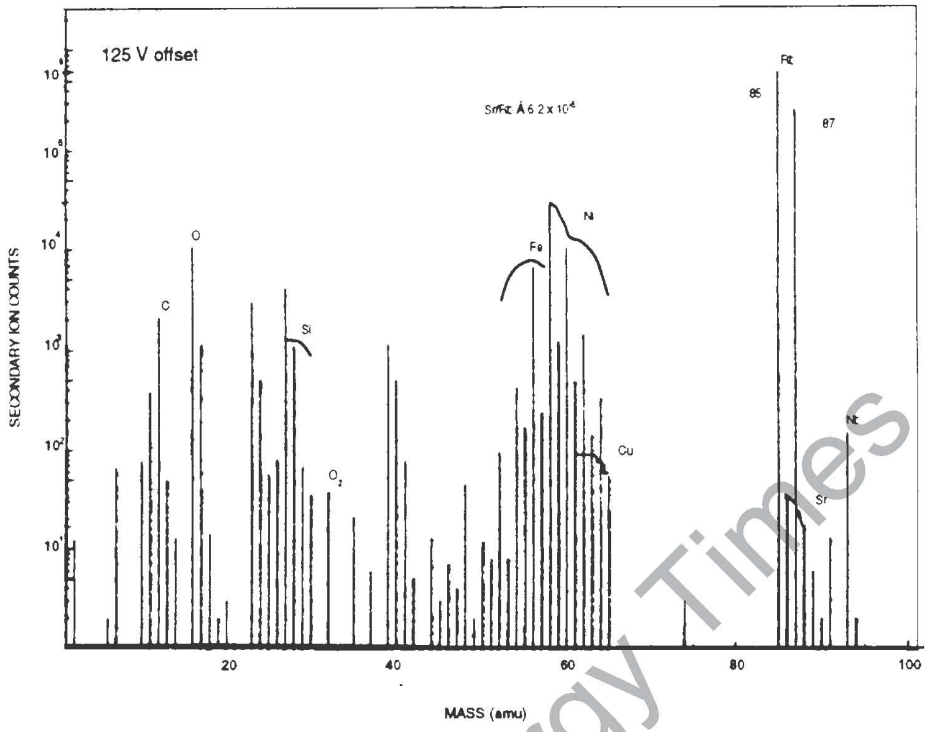

Fig. 2 Cathode pre-run mass spectrogram.

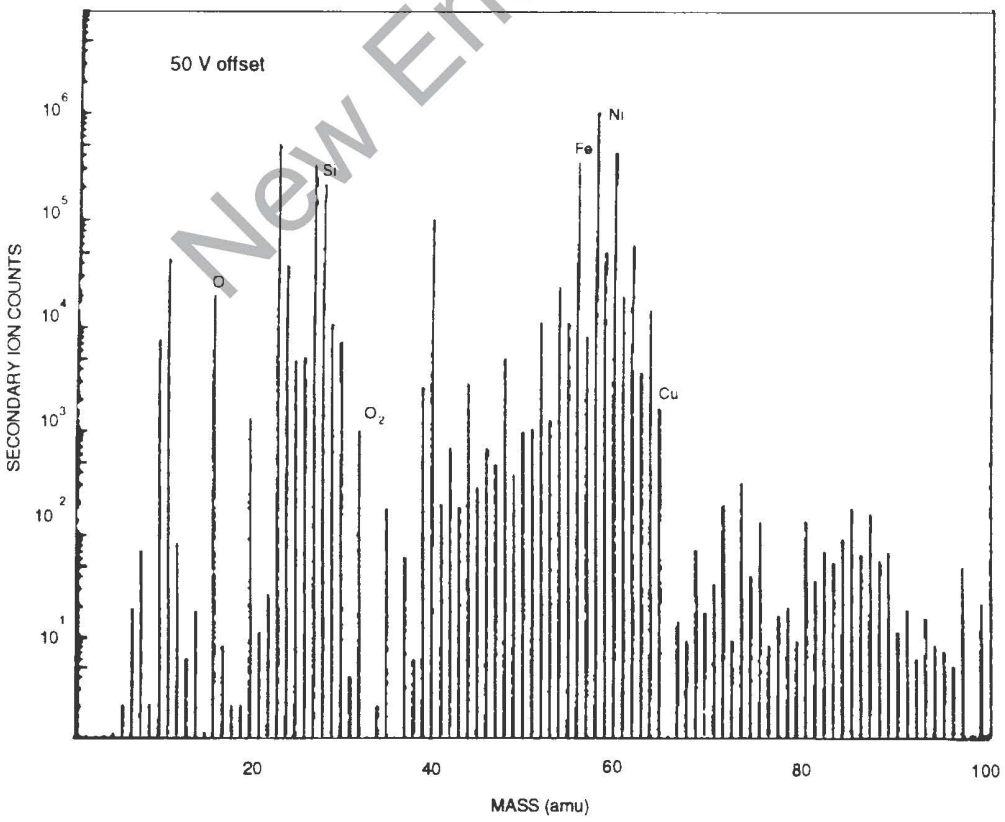

Fig. 3 Cathode post-run mass spectrogram.

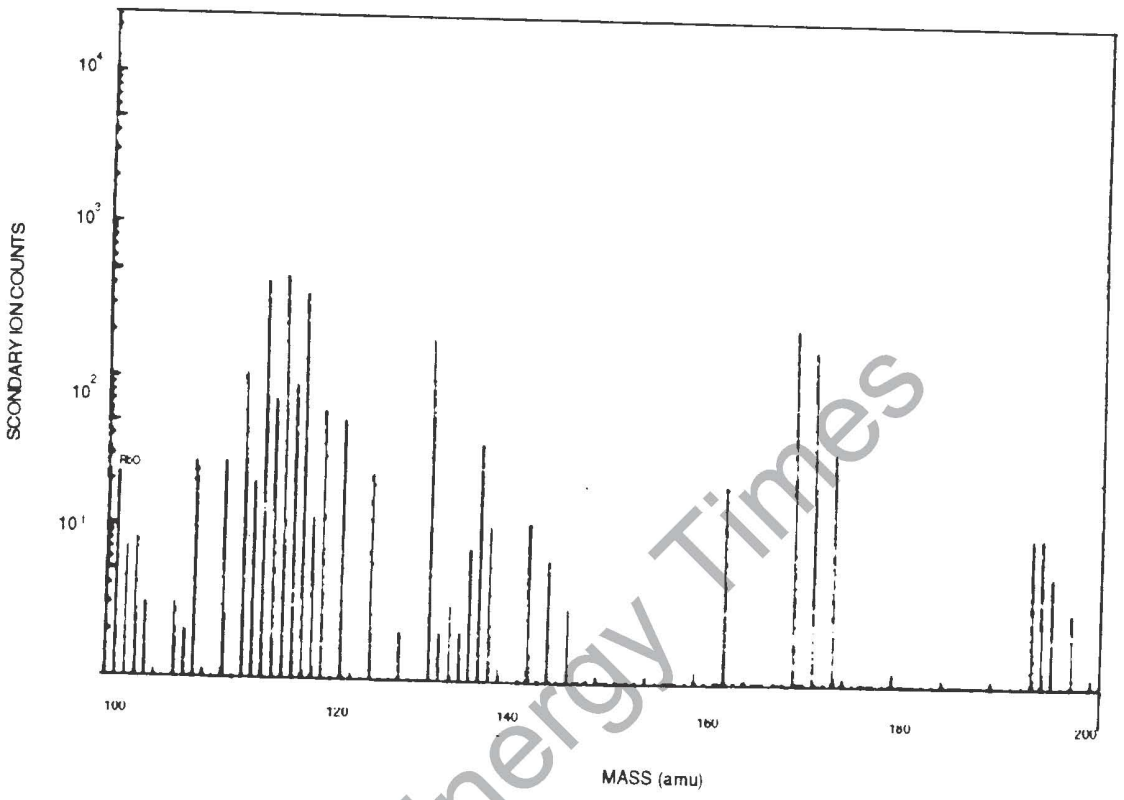

Fig. 4 Cathode pre-run mass spectrogram.

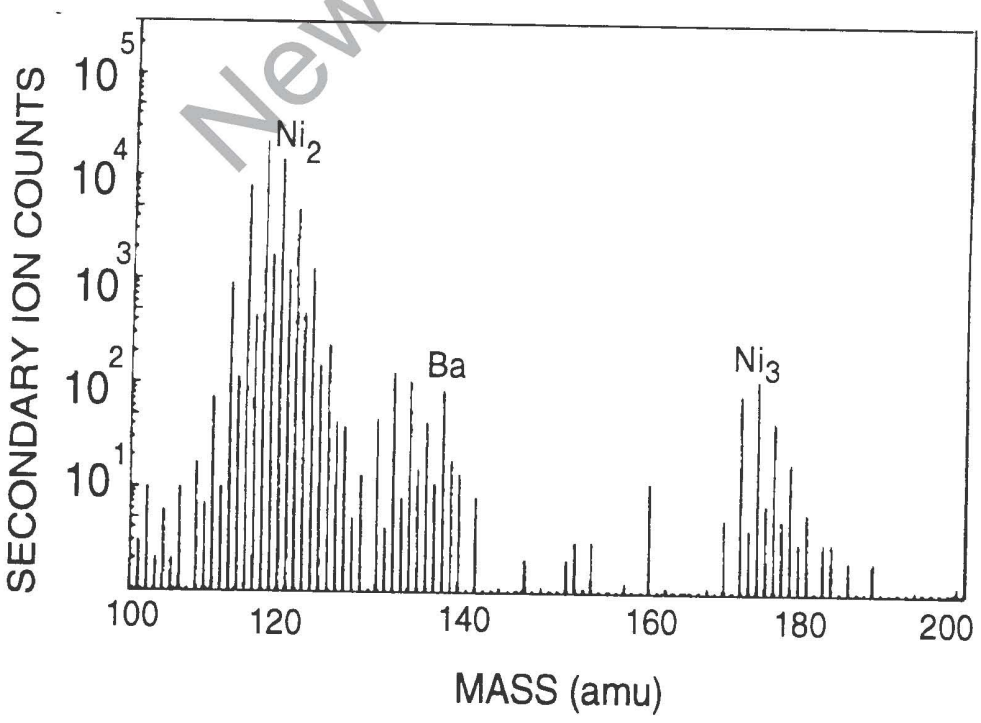

SIMS RESULTS FOR POST-RUN CATHODE OF CELL 53

A SIMS analysis for the pre- and post-run cathode material of cell #53 showed strong signals at mass numbers 86 and 88 that were not present in the pre-run spectrum [1,2,6]. Fig. 1, Fig. 2, Fig. 3, and Fig. 4 portray the four mass spectrograms, respectively: Post-run cathode material: 0-100 amu, Pre-run: 0-100 amu, Post-run: 100-200 amu, and Pre-run: 0-100 amu. Appendix A provides an interpretation of these from the standpoint of hypothetical strontium production. An interesting finding from the standpoint of the CAF Hypothesis [1,3,6] is the fact that, within experimental error, the ratio of the line height for mass number 86 to that for 88 was the same as that for the ratio of the rubidium signals at masses 85 and 87. (The SIMS tests were performed under the auspices of a well known U.S. National Laboratory, which because of the present political atmosphere for cold fusion work, prefers not to have their name revealed at this time.)

A disadvantage of these SIMS tests was that the mass spectrometer employed was unable to discriminate between rubidium hydride and strontium; i.e. $Rb^{85}H$ would be indistinguishable from Sr^{86}. So, even though there was strong evidence pointing to the noninvolvement of rubidium hydride, such as the relative instability of that compound and the fact that the rubidium oxide line, which should have been higher than those for RbH because of the greater stability of RbO, were shorter than those for the putative RbH, it was decided to pursue additional tests in which a chemical separation of the rubidium and strontium would be performed prior to the mass spectrometric analysis. These analyses were carried out by West Coast Analytical Services, Inc., of Santa Fe Springs, CA.

Ion Column Exchange Separation of the Rubidium and Strontium Followed by ICPMS ("Inductively-Coupled Plasma Mass Spectroscopy") (Cells 53, 56)

Since, at least in principle, criticism could be levelled at the SIMS results by suggesting the formation of RbH to account for an apparent strong enhancement of Sr^{86} to Sr^{88} it was decided to have an ICPMS ("Inductively Coupled Plasma Mass Spectrometry") analysis performed at an independent laboratory, West Coast Analytical Service, Inc. [1,2] (Hereafter: WCAS) of Santa Fe Springs, CA. Two pages of their final report are included as Appendix B. Because the mass discrimination of the spectrometer was limited to one amu, an ion-exchange column separation was first performed to concentrate the divalent strontium relative to the monovalent rubidium, which was washed selectively out of the column.

A summary of the WCAS results is included in the Table of Fig. 5. Previously WCAS had found that the virgin cathode material gave readings for the relative percentages of the two strontium isotopes of interest essentially the same as that of the Strontium Standard average given in the data table of Fig. 5 as follows: Sr 86: (10.51 ± 0.04)% and Sr 88: (89.49 ± 0.04)%. This gives a ratio of Sr 88 to Sr 86 for the standard (and virgin cathode material) of (8.515 ± 0.004) to which the ratios for the post-run cathode material will next be compared. From the data summary in Fig. 5, the following results are seen for the post-run cathode material of cell 53 (Sample A#53) for the test date of (4/9/93): Sr 86: (22.20 ± 0.05)% and Sr 88 (77.80 ± 0.05)%. The ratio of Sr 88 to Sr 86 is thus (3.504 ± 0.002), which is lower than the ratio for the virgin material by about 716 standard deviations as seen by the following: (8.515 - 3.504)/ (0.007) = 715.8. Since the ratio was reduced significantly from that of the standard (pre-run cathode material), this provides good evidence for an enhancement of Sr 86 relative to Sr 88 for the post-run cathode of cell 53, a light water based rubidium carbonate cell.

Fig. 5 WEST COAST ANALYTICAL SERVICE, INC.

C.S.P.U. Job # 23653
Dr. Robert T. Bush April 22, 1993

LABORATORY REPORT

Table 1

Date	Sample ID	Total Sr 86	Sr 88	Strontium
4-8-93	0.01ppm Sr Std	10.48	89.52	10ppb
4-9-93	0.01ppm Sr Std	10.48	89.52	10ppb
4-13-93	0.01ppm Sr Std	10.56	89.44	10ppb
4-14-93	0.01ppm Sr Std	10.53	89.47	10ppb
		10.51±0.04	89.49±0.04	
Date	Sample ID	Sr 86	Sr 88	
4-13-93	100ppm Rb/0.01ppm Sr.	10.47	89.53	10ppb
4-15-93	100ppm Rb/0.01ppm Sr.	10.55	89.45	10ppb
		10.51±0.06	89.49±0.06	
Date	Sample ID	Sr 86	Sr 88	
4-8-93	A#53	ND	ND	ND
4-9-93	A#53	22.2	77.8	1400ppb
4-15-93	A#53	12.05	87.95	NC
Date	Sample ID	Sr 86	Sr 88	
4-8-93	#56PR	22.3	77.7	NC
4-9-93	#56PR	26.8	73.2	1500ppb

NC - not calculated

For cell 56 (light water based rubidium hydroxide), which had evidenced about five times as much excess heat as cell 53 based upon calorimetry, the data table of Fig. 5 gives results for the analysis of sample #56PR on (4/9/93) as follows: Sr 86: (26.80 ± 0.05)% and Sr 88 (73.20 ± 0.05)%. The following ratio of Sr 88 to Sr 86 for these numbers implies an even greater electrolytically induced enhancement of Sr 86 relative to Sr 88, which could be anticipated based upon the greater excess heat exhibited by cell 56: (2.731 ± 0.003) Again, as dramatic evidence for this enhancement of Sr 86 relative to Sr 88 this ratio is less than the standard by about 826 standard deviations as seen by the following: (8.515 - 2.731)/(0.007) = 826.3. Thus these ICPMS results of WCAS obtained by first achieving a chromatographic concentration of the strontium relative to the rubidium provide strong independent support for the SIMS results.

SUPPORT FOR THE LANT HYPOTHESIS

According to the author's LANT hypothesis [3] ("Lattice Assisted Nuclear Transmutation") strontium production would not necessarily be the end of the transmutation line. Rather, the Sr atoms formed in the lattice would themselves now become targets for the lattice assisted addition of a proton. This would produce an entire cold nucleosynthetic series, the Rubidium Series [3], shown in Fig. 6 taken from reference 3. A comparison of the SIMS spectrographs of the cathode material of Cell 53 (rubidium carbonate) before and after running provides evidence for the synthesis of such nuclides as shown in the Table of Fig. 7 entitled "Isotope Production via Cold Nucleosynthesis: Rubidium Series [3]." In this respect it is interesting to note from the Table in Fig. 7 that the total excess heat (based upon Q values) produced in connection with this synthesis should be (3.8 + 0.4) x 10^{19} MeV, whereas the actual excess heat for cell 53 as determined from calorimetry [3] was approximately (4.0 + 0.8) x 10^{19} MeV. This is rather good agreement and provides initial support for the LANT hypothesis.

Fig. 6

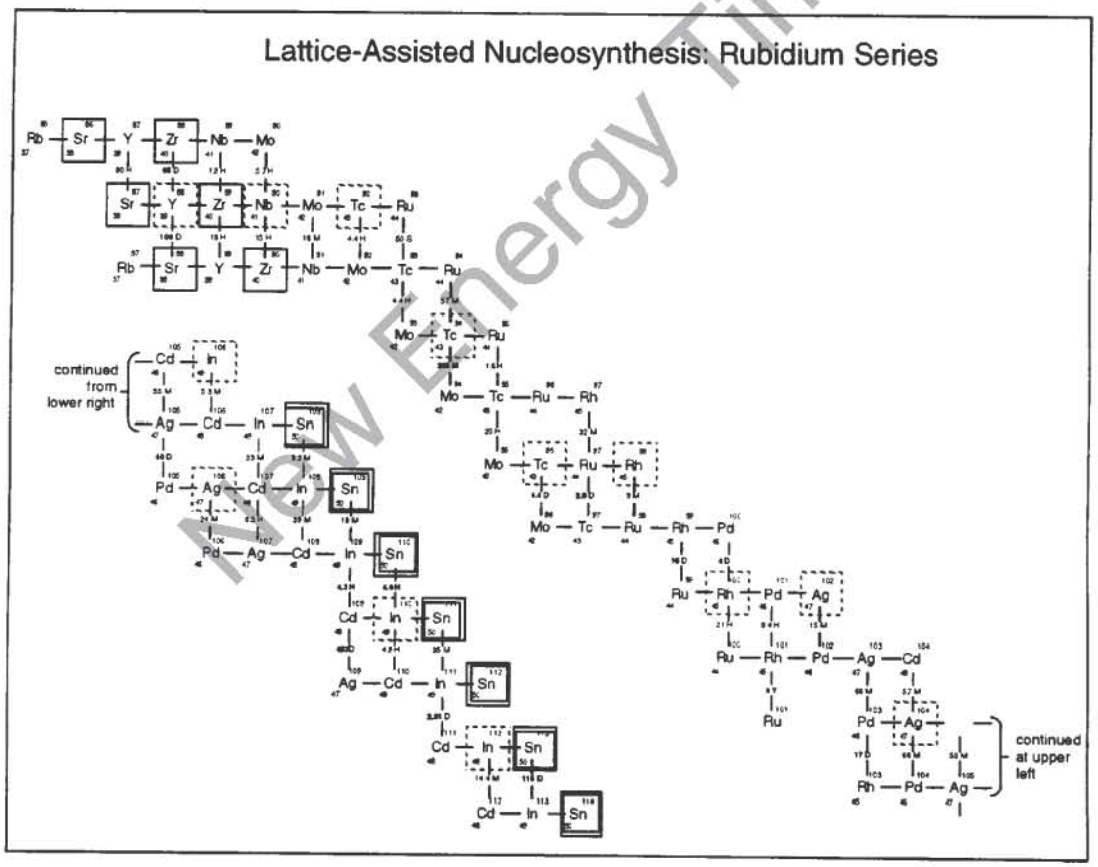

Fig. 7

Isotope Production via Cold Nucleosynthesis: Rubidium Series
(Cell 53)

Mass Number (A)	Nuclides Synthesized	Net number of Nuclei Synthesized x 10^{16}	Total Energy Released (MeV x 10^{17})
86	$_{38}Sr^{86}$	1.34	1.29
87	$_{38}Sr^{87}$	19.25	33.30
88	$_{38}Sr^{88}$, $_{39}Y^{88}{}_{(108D)}$, $_{40}Zr^{88}{}_{(88D)}$	0.52	0.55
89	$_{39}Y^{89}$	1.66	4.6
90	$_{40}Zr^{90}$	0.28	1.1
91	$_{41}Nb^{91}$	3.00	12.1
92	$_{42}Mo^{92}$	(small)	(small)
93	$_{42}Mo^{93}$	27.03	148.10
94	$_{42}Mo^{94}$	0.23	1.43
95	$_{42}Mo^{95}$	(small)	(small)
96	$_{44}Ru^{96}$, $_{43}Tc^{96}{}_{(4.35D)}$	(small)	(small)
97	$_{43}Tc^{97}$, $_{44}Ru^{97}{}_{(2.9D)}$	(small)	(small)
98	$_{44}Ru^{98}$	(small)	(small)
99	$_{44}Ru^{99}$, $_{45}Rh^{99}{}_{(16.1D)}$	(small)	(small)
100	$_{45}Rh^{100}$, $_{46}Pd^{100}{}_{(4D)}$	0.30	3.90
101	$_{44}Ru^{101}$, $_{45}Rh^{101}{}_{(3y)}$	3.70	41.30
102	$_{45}Rh^{102}$, $_{46}Pd^{102}$	1.21	14.50
103	$_{45}Rh^{103}$, $_{46}Pd^{103}{}_{(17D)}$	1.40	17.80
104	$_{46}Pd^{104}$	0.54	7.30
105	$_{46}Pd^{105}$, $_{47}Ag^{105}{}_{(40D)}$	(small)	(small)
106	$_{46}Pd^{106}$, $_{48}Cd^{106}$	(small)	(small)
107	$_{47}Ag^{107}$	0.54	7.30
108	$_{48}Cd^{108}$	0.23	3.90
109	$_{47}Ag^{109}$, $_{48}Cd^{109}{}_{(453D)}$	2.25	39.70
110	$_{48}Cd^{110}$	(small)	(small)
111	$_{48}Cd^{111}$, $_{49}In^{111}{}_{(2.8D)}$	(small)	(small)
112	$_{50}Sn^{112}$	2.25	44.60
	Sums:	65.73 x 10^{16}	384.17 x 10^{16} MeV

Estimating a ten percent error, then, the total energy to produce the above based upon the LANT Model is approximately **(3.8 ± 0.4) x 10^{19} MeV** versus the total excess heat determined from calorimetry for Cell 53 of **(4.0 ± 0.8) x 10^{19} MeV**.

CONCLUSIONS

With the corroborative independent mass spectrographic results of the two separate laboratories the evidence supporting the electrolytically induced transmutation of rubidium to strontium, as evidenced by the shift in the abundance ratio of Sr-86 to Sr-88, must be considered to be significant These results add support to the author's CAF and LANT hypotheses. Note that any strontium contamination would only tend to shift this ratio back to the natural abundance ratio for the two strontium isotopes.

ACKNOWLEDGMENTS

H. Fox, head of the F.I.C. and Editor of Fusion Facts, is thanked for his considerable encouragement of my work. He is thanked for his encouragement and for financial support in connection with my participation in the Texas A&M Conference organized by him and G. Lin. T. Passell (EPRI) is thanked for his encouragement and for his interest in the Cal Poly project. ENECO, formerly FEAT, is thanked for its financial support and encouragement. M. Hovance of West Coast Analytical Service, Inc. (Santa Fe Springs, CA) is greatly appreciated for the independent, and first rate, ICPMS mass spectroscopy. Finally, thanks go to Bunny Gilbert of the Cal Poly (Pomona) Instructional Support Center for her help in preparing the manuscript. I am grateful to Cal Poly, Pomona, for partially financing my participation in the Texas A&M Conference. Finally, it is a pleasure to acknowledge my colleague in the Cal Poly cold fusion project, R. Eagleton, who constructed and calibrated the cells employed in this work. In addition, he has always willingly served as a sounding board for my ideas.

REFERENCES

1. R. Bush, "A Light Water Excess Heat Reaction Suggests that 'Cold Fusion' May Be 'Alkali-Hydrogen Fusion' ", *Fusion Technol.*, 22, 301 (1992).
2. R. Bush and R. Eagleton, "The Transmission Resonance Model for Cold Fusion in Light Water: I. Correlation of Isotopic and Elemental Evidence with Excess Power", Proc. 3-ICCF, 409,(1993).
3. R. Bush, "Towards a Nuclear Physics of Condensed Matter", accepted for *Fusion Technol.*, under revision, est. issue: March '94.
4. R. Bush and R. Eagleton, "Calorimetric Studies For Several Light Water Electrolytic Cells With Nickel Fibrex Cathodes and Electrolytes With Alkali Salts of Potassium, Rubidium, and Cesium", submitted to Proc.4-ICCF (1994).
5. R. Bush and R. Eagleton, "Experimental Studies Supporting the Transmission Resonance Model for Cold Fusion in Light Water: II. Correlation of X-Ray Emission with Excess Power", Proc. 3-ICCF, 409 (1993).
6. R. Bush, "Will the Light Water excess Heat Effect Lead to a Unification with Cold Fusion?", *Twenty First Century Science and Technology*, Fall 1993, p. 75.
7. R. Bush and R. Eagleton. "Evidence for Electrolytically Induced Transmutation and Radioactivity Correlated with Excess Heat in Electrolytic Cells With Light Water Rubidium Salt Electrolytes" , *Transactions of Fusion Technology*, 26, 344 (1994).

APPENDIX A: Interpretation of the SIMS Mass Spectrograms

The mass spectrograms of Fig. 2 and Fig. 3 were carried out by SIMS analysis, respectively, for the post-run cathode material and for the pre-run cathode. (Earlier mass spectrometry established an upper limit on the strontium in the post-run solution from cell 53 of 5 ppb.) Note the following from Fig. 3 (Pre-run):

Fig. 3 (Pre-run): Mass 86: The height of this signal is about 3.6 cm corresponding on the log-scale to an ordinate of 190 counts.

3.5 cm signal height: 150 counts

Nickel 58: 10.0 cm signal height: 1,250,000 counts

Fig. 2 (Post-run): Note that the signal height discrimination for this spectrogram is greater than that for the one of Fig. 3. Thus, the spectrogram of Fig. 3 is associated with only a 50 V offset, whereas that of Fig. 2 is associated with a 125 V offset. Thus, in comparing signal heights from Fig. 2 to those on Fig. 3 we must multiply the numbers of counts in Fig. 2 by the ratio of the Nickel 58 signal in Fig. 3 to that in Fig. 2:

Mass 86: 3.25 signal height: 36 counts

Mass 88: 2.6 cm signal height: 16 counts

Nickel 58: 9.5 cm signal height: 31,000 counts

Ratio of Nickel 58 signal in Fig.3 to that in Fig.2: (1,250,000/ 31,000)= 40.32.

Corrected counts from Fig. 2 to compare with those in Fig. 3:

Mass 86: 36 x 40.32 = 1, 452 counts

Mass 88: 16 x 40.32 = 645

Ratio of Sr-86 to Sr-88: (Corrected for background in Fig. 3):

(1,452 - 190)/ (645 - 150) = 2.55. (1)

Note that the ratio of the natural abundances of Sr-86 and Sr-88 is approximately:

0.12 (2)

Thus, we have an isotopic abundance ratio shift by a factor of

2.55/ 0.12 = 21. (3)

Note, also, that the ratio of the natural abundances of Rb-85 and Rb-86 is about

2.59. (4)

The fact that the ratio in (1) so closely matches that in (4) is strong support for Bush's hypothesis that the strontium arises from the rubidium via the addition of a proton at the surface of the nickel.

Finally, how do we know that masses 86 amd 88 in B correspond to strontium and not, say, to rubidium hydride. Quite aside from the well-known instability of rubidium hydride is the fact that a second mass spectrometric study in which the rubidium and strontium are first chemically separated via an ion exchange column shows a strong enhancement of Sr-86 over Sr-88 both for the post-run cathode material of cell 53 and for a new light water rubidium hydroxide (0.57 M) cell (cell 56).

APPENDIX B **(WCAS)**

WEST COAST ANALYTICAL SERVICE, INC.

C.S.P.U. Job # 23653
Dr. Robert T. Bush April 22, 1993

LABORATORY REPORT

STRONTIUM ISOTOPE RATIO DETERMINATION

SUMMARY

The results obtained and listed in Table 1 (Fig. 6) show that the method works as designed, using single and mixed standards. For sample A#53, some enhancement was determined, particularly on 4-9-93 when sequence 2 was performed, Sr86 = 22.2 ± 0.05. Sequence 2 has been producing the most consistent results. Sample #56PR demonstrated verifiable enhancement, Sr86 =26.8 ± 0.05.

On 4-14-93, we decided to run A#53W1 from the first sequence just to have similar batch results as obtained for #56PR. The strontium standard looks great; not much strontium detected in the sample. (Pages 50 and 9)

The next experiment was designed to improve the chromatography. The amount of rubidium in solution exceeds the capacity of one column, so two columns were hooked together and a series of solutions run through them. The results for the standard are very consistent with single column values; however, for a real sample such as A#53, the strontium is still coming out early in W1 instead of DP-2 where we would like it to. (See pages 51 and 52, also results pages 10 and 11, 4-15-93.)

To demonstrate adequate resolution of the mass spectrometer, an experiment was devised on 4-16-93 (page 53). The idea is to use the scanning mode on the ICPMS instead of the peak jumping mode used when measuring isotope ratios. In the scanning mode, the resolution between peaks would be more obvious because many more data points are taken as the mass spec scans through the mass ranges. This test was run twice because the detector tripped off due to the high rubidium counts. For the second scan, the autotrip function was overridden. Page 12 shows the trip results while page 13 shows the scan with the trip switched off. The results are most vividly shown in the two mass spectra, page 14 and 15. Page 14 shows excellent base-line resolution and demonstrates the difference in magnitude of the rubidium/strontium concentrations.

Page 15 shows what would happen to the spectrum and the results if no chromatography was used on the samples to reduce the rubidium levels. Notice peak saturation for both rubidium isotopes as indicated by pitch-fork shaped peaks. Also notice the peak widths and how they spread out into the mass 84 and 87 to some extent.

Page 16 is a mass spectrum of the peak jumping mode, and it shows the resolution, peak width also.

EXPERIMENTAL

Rubidium carbonate impregnated nickel matte electrodes from WCAS Job number 22542 were subjected to ultrasonic cleaning and acid etching to solubilize any strontium isotopes present so isotope ratio measurements using ICPMS could be made. Results are summarized in Table 1. Total Strontium levels were calculated and are reported in Table 1.

Ion Chromatography/cation exchange was used to separate the nonovalent rubidium from the divalent strontium. Ten milliliter fractions were collected from the end of the column and analyzed in batches by ICPMS.

A two-step sample preparation scheme was used. The first step was eight hours of sonication in 2mH HCl. The second step was 24 hours of sonication in 10% HCl, followed by 4 days of room temperature etching with the end point being a light green color from the nickel matrix. Each of the two samples was then washed with DI water three times and set aside to dry. The solutions of 10% HCl were then brought to approximately thirty milliliters (see page 43).

The first analytical sequence (Ion Chromatography, fraction collection, Isotope ratio ICPMS) of the two samples and a strontium only standard is recorded on pages 44 & 45. The actual instrument printouts are on unruled paper, pages 1-3. The results indicate possible enhancement for A#53 and substantial enhancement for #56, data Table 1, 4-8-93.

The second analytical sequence (pages 46 & 47, results pages 4-6) is from sending the fractions collected in sequence one, back through the column to try to get better separation between the rubidium and strontium. The results indicate enhancement for both samples. See results Table 1 data for 4-9-93.

The third sequence came out of our concern for demonstrating that the rubidium levels in the samples were not artificially enhancing the strontium isotopes, resulting in false ratios. (Pages 48 & 49 on 4-13-93 and pages 7 & 8 from printouts contain test information.) The conclusion is that the chromatography is providing enough separation and the resolution of the mass spectrometer is such that no artificial ratio enhancement is being induced by the high rubidium levels. Isotope ratio values are listed in Table 1 for 4-13-93.

LOW TEMPERATURE NUCLEAR CHANGE OF ALKALI METALLIC IONS CAUSED BY ELECTROLYSIS

R. Notoya
Hokkaido University, Catalysis Research Center
Kita-11, Nishi-10, Kita-ku Sapporo, 060, Japan

ABSTRACT

It was found that the hydrogen evolution reaction on platinized platinum and porous nickel in various alkaline solutions was causative of the nuclear reactions. 0.5 mol/l potassium and sodium carbonate, and 0.1 mol/l cesium sulfate solutions of light and heavy water were used for electrolysis in thermally open cells. Analysis of the electrolytes by use of ICP-MS, a flame photospectrometer, a liquid scintillation spectrometer and a γ-ray spectrometer, revealed that the some nuclear products were generated during electrolysis, for example, from potassium and proton to calcium, from cesium-133 and neutron, proton and so forth to some species of mass numbers of 132 to 140 amu, from sodium-23 and neutron to sodium-24, as well as tritium, which were accompanied by an extraordinary large heat evolution. The reaction mechanism for the cold fusion caused by electrolysis is proposed, in which the intermetallic compounds between alkali metals and cathode materials play an important role in making the solid reaction possible.

INTRODUCTION

In order for low temperature nuclear reactions to occur in solid, the reactants must be present in solid. The cold fusion in heavy water was observed on palladium electrode on which hydrogen electrode reaction was occurring. In such a system, a deuterium which has been regarded as the reactant is absorbed in palladium metal very well [1]. Accordingly the reactant seems to be present in solid in this case. On the other hand in the case of light water cold fusion, there are few works to make a mention of this point of view [2]. But, people do not propose of the low temperature nuclear reactions of alkali metallic species until they show the possibility of these species being present in solid. The author has dealt with this possibility, on the basis of the mechanism for the hydrogen evolution reaction (HER) [3].

The mechanism for HER in alkaline solutions on the so-called low overvoltage metals, namely, platinum group metals, nickel, silver, titanium and so forth has been established by A. Matsuda and his coworkers by use of the galvanostatic transient method (GSTM), as follows [4]:

$$M^{x+} + xe^- \rightarrow M(I), \quad (1)$$

$$M(I) + xH_2O \rightarrow xH(a) + xOH^- + M^{x+}, \quad (2)$$

$$H(a) + H(a) \Rightarrow H_2, \quad (3)$$

where M^{x+}, M(I) and H(a) denoted an alkali or an other metallic ion with the valence x+, the intermetallic compound between alkali or other metal and the cathode material and an adsorbed or absorbed hydrogen atom on or in the electrode, and ⇒ the rate determining. On the contrary, almost of the electrochemists in the world believe that the electron transfer step of HER in alkaline solutions consists in the discharge of water molecule. It can be denied on the basis of the following experimental result.

The exchange current density i_{10} of the electron transfer step (1) determined by GST-analysis of the most initial change of overvoltage shows a linear relationship with that of the concentration of alkali metallic ion but not pH with the slope of 0.5 for mono-valent or 0.8 [5] for di-valent discharge. That is consistent with the kinetic equation (4) of a cation discharge:

$$i_{10} = \text{const. x } [M^{x+}]^{0.5 \text{ or } 0.8, \text{ etc.}} \quad . \qquad (4)$$

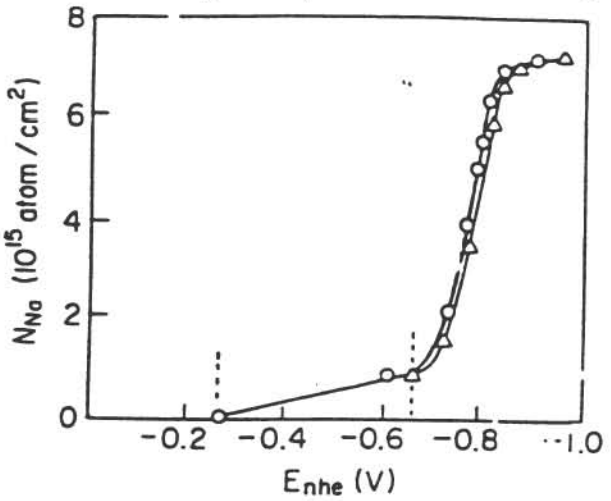

Fig. 1 Relationship between Na atoms/cm^2 of true surface area of Pt and E_{nhe} in 1mol/l Na_2SO_4 solutions, pH=4.7(○) and pH=11.38(Δ).

The another result of GST-analysis of the decay process of overvoltage from a steady state to the equilibrium, indicated that the accumulated alkali atoms of M(I) amounted to about 10^{16} atoms/cm^2 of true surface area of a Pt electrode, as shown in Fig.1 [6]. Consequently, alkali atoms have to penetrate into the depth of ≥ 1,000 monolayers from the surface, in view of the composition of M(I) and the presence of its diffusion layer.

Hence, taking account of the mechanism of HER as shown above, you can expect the following nuclear reaction to occur easily [3]:

$$ {}^{A}_{Z}m + n \text{ or } {}^{1}_{1}p \rightarrow {}^{A+1}_{Z}m' \text{ or } {}^{A+1}_{Z+1}m'' \qquad (5)$$

where $ {}^{A}_{Z}m$, $ {}^{A+1}_{Z}m'$, and $ {}^{A+1}_{Z+1}m''$, and $ {}^{1}_{1}p$ denote the nuclei of M(I), of the products of reaction (5) and of an adsorbed or absorbed hydrogen atom H(a), respectively. In general, reaction (5) produces some nuclear particles as the byproducts and then it is thought that some reactions take place among **m, m'** and these particles in the vicinity in the surface layer of the electrode, as follows:

$$\textbf{m, m' or m" + n, p, d, t, or } \alpha \rightarrow \textbf{m', m" or m" ' etc. + n, p, d, t, or } \alpha, \qquad (6)$$

and m, m',m" and m", etc. should become the reactants of the next step. We found a certain amount of tritium simultaneously in the same light water's electrolytes as used for the analysis of nuclear products. At least, the reaction between deuterium atoms, **d+d** and/or **d+d+d** appeared to be occurring in parallel with reaction (6) [1,7]. Consequently, the mechanism for the nuclear reactions seem to be expressed as a chain reaction which is initiated by the formation of the intermetallic compound M(I).

This paper is concerned with heat evolution and the nuclear products as well as tritium, which were observed in simultaneous or individual experiments.

EXPERIMENTAL RESULTS

The electrolytic cells used for a series of the experiments were the same as in the previous work. All procedures of the experiments and the accuracies of the measurements were also nearly the same as described previously [8,9].

1. Excess Heat Measurement

The excess heat which was due to electrolysis in K_2CO_3 light water solution on porous nickel, was found to be in the range from 200 to 400%, in regard to more than 150 observations. In Cs_2SO_4 also light water solution, excess heat of 200 to 300% was observed on platinized platinum. Excess heat on porous nickel in Cs_2SO_4 light water solution might be considerably large as found to be 6,000% estimated by comparison with the foregoing value on platinum, but not reproducible, because porous nickel was often dispersed violently in Cs_2SO_4 solution.

2. Tritium Measurement

All experiments concerning the tritium production during electrolysis were carried out in the second basement of a building in order to keep the background value of radiation low and constant. A series of the experiments for the measurement of tritium generated by electrolysis simultaneously with the γ-ray measurements were carried out for 6 hours to 3 days in a dark chamber made of a lead wall of 10 cm thickness equipped with a germanium γ-ray detector, which was settled in an air-conditioned room at 20 + 1°C. In this room we couldn't use airflow for cooling the cells, accordingly the observed values of excess heat were slightly small [10]. After electrolysis, the amount of tritium in the electrolyte was measured as described in the previous paper [9].

Typical energy spectra of the radioactivity measurements of the samples prepared by the test electrolyte and control one are shown in Fig. 2. The background value of this scintillation analyzer was found to be 4.4 + 0.4 cpm in the energy region of emission ray, 0 to 18.6 keV, by use of 1 ml distilled water instead of the subject solution. The background value, which was usually kept very stable, was checked before each measurement.

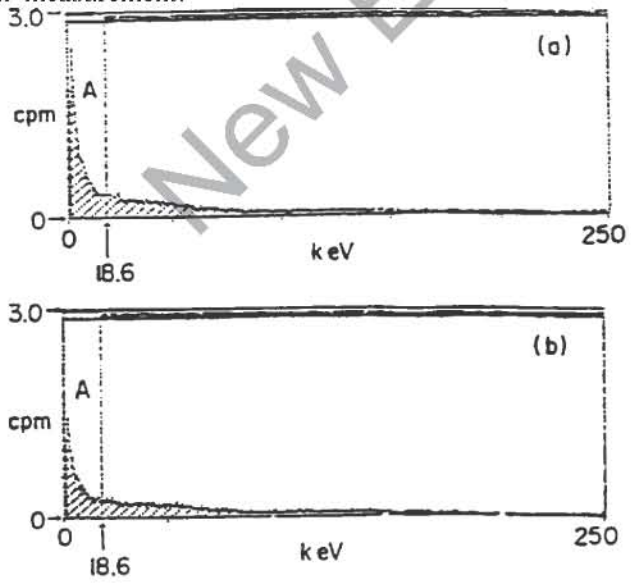

	LL	UL	CPM
A:	0.0	18.6	15.36
B:	18.6	2000	26.41
C:	0.0	2000	41.76

	LL	UL	CPM
A:	0.0	18.6	10.58
B:	18.6	2000	27.17
C:	0.0	2000	37.75

Fig. 2 Energy spectrum of radioactivity measurements by a liquid scintillation spectrometer: (a) test electrolyte of 0.5 mol/l K_2CO_3 of light water after electrolysis in $cell_{Ni}$ and (b) control one, region A is due to ^3t with tables of the counts (cpm) in each energy region of interest.

It is apparent from the experimental result observed in K_2CO_3 solutions of light and heavy water [10] that the ^3t amount generated is proportional only to the value of the excess heat, but not the duration of electrolysis and the other factors. If ^3t is the final product of the nuclear reaction, all of the produced ^3t must be accumulated in the electrolyte according to the mechanism shown by Eqs. 1-3, because step (3) is rate determining. Therefore, the above result suggests that ^3t may be one of the intermediates of the nuclear reaction.

3. Analysis of Other Products of Cold Fusion

It was confirmed that some nuclear products were generated during electrolysis by use of platinized platinum and porous nickel electrodes, in light water solutions of all alkali metallic ions investigated. For example, calcium of 4 ppm was detected in K_2CO_3 light water solutions by a flame spectrometer [8]. The γ- ray measurement revealed the formation of ^{24}Na during electrolysis in Na_2CO_3 solution. ICP-mass spectra of the electrolytes of Cs_2SO_4 light water showed several peaks of various nuclear products in the region from 132 to 140 amu.

The detection of calcium was described in detail in [8], therefore the present paper is concerned chiefly with the result of the electrolysis of Cs_2SO_4 solution in cells equipped with platinum and nickel electrodes (hereafter, expressed by $cell_{Pt}$ and $cell_{Ni}$) [11]. Cesium is one of the most appropriate species as a reactant among alkali metals to determine the nuclear products owing to 100% of the natural abundance of ^{133}Cs, as well as ^{23}Na. The above experiment was carried out simultaneously with excess heat measurement. During electrolysis, cells settled in the thermostat box were cooled by airflow, as described in the section of excess heat measurement. After electrolysis, the electrolyte in $cell_{Pt}$ and $cell_{Ni}$ as well as the control electrolyte was analyzed by means of ICP-MS (SQR-6500, Seiko Instruments). As the sample for ICP-mass spectrometer, the test electrolyte was diluted quantitatively with pure water 4,000 or 10,000-fold. On the other hand, the control electrolyte was diluted merely 100-fold. Therefore strong contamination with the control electrolyte remained at 133 amu and some others on mass spectra. The shape of the mass spectrum of the residual contamination in the range of mass number from 130 to 140 was not varying during the measurements of the test samples. Fig. 3 shows the typical mass spectrum of test sample of 0.1 mol/l Cs_2SO_4 electrolytes in $cell_{Pt}$, which was electrolysed 18.2 hours. The total electricity spent during electrolysis amounted to 18,000 ± 200 coulomb.

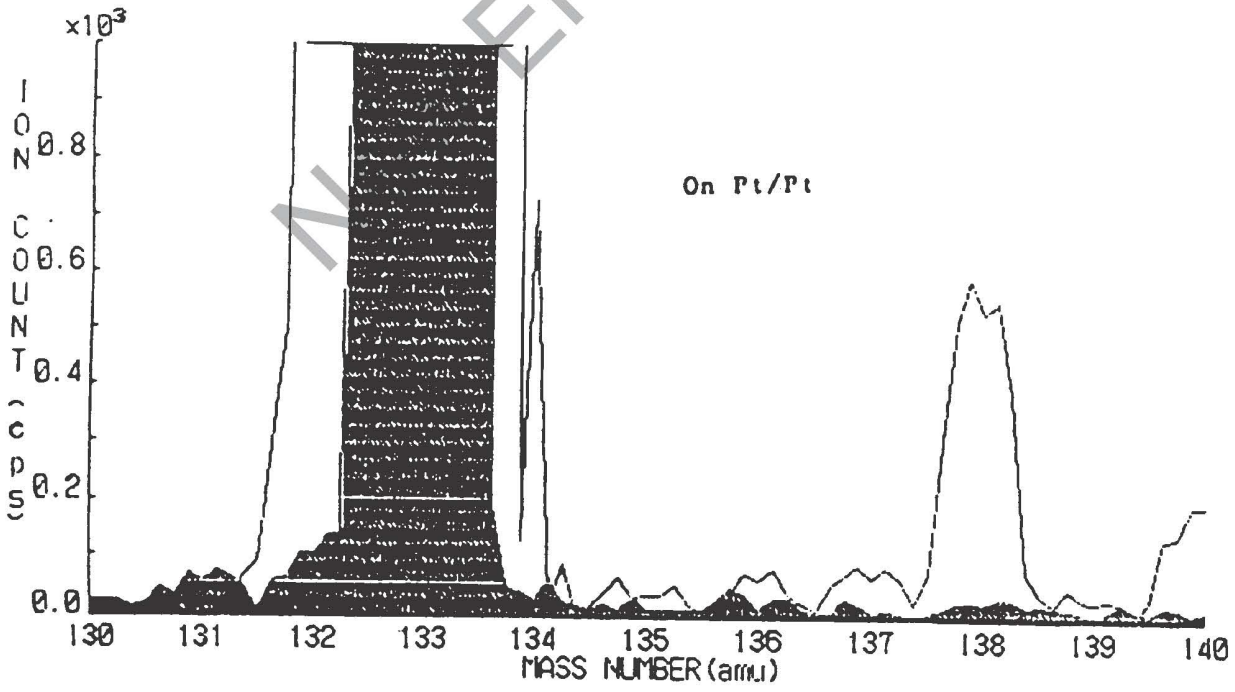

Fig. 3 Mass spectrum of 0.1 mol/l Cs_2SO_4 electrolyte in $cell_{Pt}$: duration of electrolysis = 18.2 hours, spent electricity = 18,000 ± 200 coulomb, black shadow indicates residual contamination by the counter electrolyte measurements of the test samples. Fig. 3 shows the typical mass spectrum of the test.

On the other hand, the mass spectrum of the control electrolyte showed only one peak at 138 amu which was found to be 0.4 ppm, except for 133 amu. The amount of the 138 amu species consisted well with the total amount of barium species determined to be 0.6 ppm by a flame spectrometer, in view of the natural abundance of ^{138}Ba equal to 71.7%.

The amount of the nuclear product of each mass number in the region from 132 to 140 amu was calculated from the area of the peak of mass spectrum of the test electrolyte and compared with that of the control electrolyte, respectively. Thus, the increases of the mass number's species are summarized in Table 1. Concerning the mass numbers 132 and 134 amu the amounts as denoted by + couldn't be determined quantitatively because the resolution of spectra for them was insufficient owing to too large ion counts of 133 amu species, but these amounts seemed to be almost the same as that of 138 amu.

Table 1 Amount of cold fusion products caused by electrolysis of 0.1mol/l Cs_2SO_4 light water solution on platinized platinum.

Mass No.(amu) :	132	134	135	136	137	138	139	140
Δ amount(ppm) :	+	+	0.4	0.3	0.5	4.7	0.2	1.8
Expected Species:	Cs Ba	Xe La	Cs Xe	Ba La	Xe Ba	La Cs	Cs La	Ba La	Cs Ce	Ba	Ba La	Ce Pr	La	Ce

The well-known reactions for nuclear production and activation occurring in a nuclear reactor, were quoted from the literature [12] in the range from 130 to 140 amu and summarized in a diagram (Fig. 4). Moreover, some possible reactions for the changes of nuclei are added in the diagram on the basis of the assumption that the spins I in the reactions must be less than 2, taking into consideration of the parities and Q-values. Fig. 4 shows a few possible products of the nuclear reactions at each mass number, which are listed in Table 1.

It was found that cathodic polarization of porous nickel in Cs_2SO_4 solution caused its violent dispersion. Such a violent dispersion occurred often, especially when you use a worn electrode.

During fifty hours electrolysis in Na_2CO_3 solution of 20 ml by use of a porous nickel cathode, a measurement of γ-ray spectrum was carried out in parallel with that of the excess heat as described at section "excess heat measurement". It was found that there was the peak attributed to the emission of the specific γ-ray from ^{24}Na at 1368.63 keV in the spectrum and this amount was calculated to be 1.35×10^{-3} Bq from the area of that peak. The spent electricity was 45,000 coulomb. It can be suggest that the reaction $^{23}Na(n, \gamma)\ ^{24}Na$ is occurring in the surface layer of the cathode by analogy with the radiation reaction occurring in a nuclear reactor.

CONCLUSION

It was shown by an experimental study that some low temperature nuclear reactions of the intermetallic compounds of alkali metals with neutrons, protons and so forth are occurring in the surface layer of porous nickel and platinized platinum cathodes, during electrolysis in all alkaline solutions investigated as well as d+d and/or d+d+d reactions, but the former is predominant.

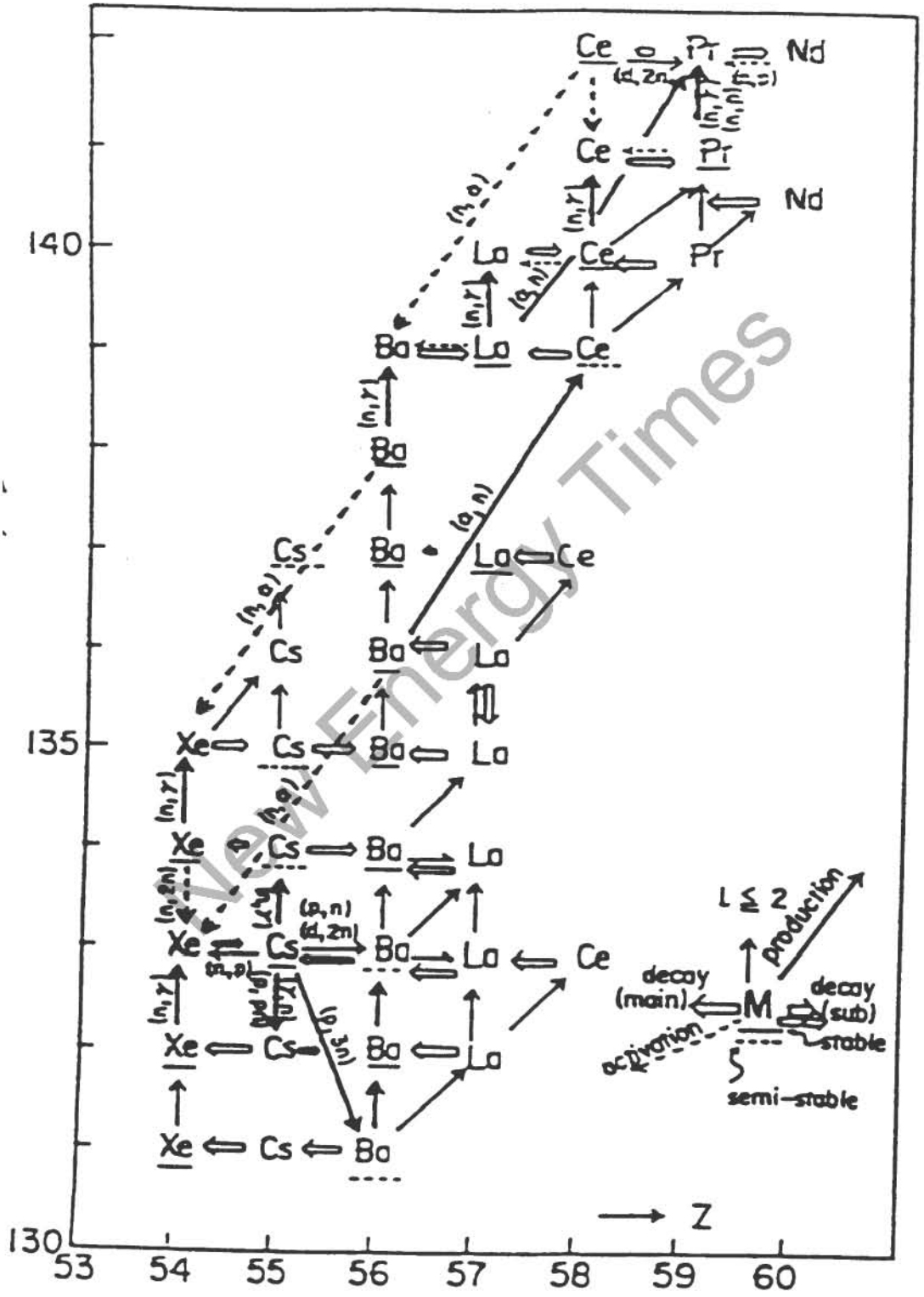

Fig. 4 Diagram composed with reactions for nuclear production (bold line), activation (broken one), decay (short or long arrow means slow or rapid) and possible reaction (thin line) as described in the text: Underline (dotted or solid) expresses a stability of each nucleus (half life, $\tau_{1/2} \geq 10$ days or $\geq 10^4$ years).

REFERENCES

[1] M.Fleischmann and S.Pons, *J. Electroanal. Chem*., vol 261, p 301 (1989).
[2] R.T.Bush, *Fusion Technol*., vol 22, p 301 (1992).
[3] R.Notoya, Abs. 18th Mtg. Hokkaido Electrochem. Soc., Sapporo, Jan.18 (1990).
[4] A.Matsuda, R.Notoya, T.Ohmori, K.Kunimatsu and T.Kushimoto, *J. Res. Inst*., Catal. Hokkaido Univ. vol 24, p 187 (1976).
[5] R.Notoya, *Elektrokhimiya*, vol 29, p 53 (1993) and R.Notoya and A.Matsuda, Extended Abs. 34th Mtg. Int. Soc. Electrochem., no 515, Erlangen, Sept.(1983).
[6] A.Matsuda and R.Notoya, *Denkikagaku* (Electrochemistry in Japan), vol 34, p 619 (1966).
[7] A.Takahashi et al., *Int. J. Appl. Electromagnet. Mat*., vol 3, p 221 (1992).
[8] R.Notoya, *Fusion Technol*., vol 24, p 202 (1993).
[9] R.Notoya, Y. Noya and T. Ohnishi, *Fusion Technol*., vol 26, p 179 (1994).
[10] R.Notoya, Proceedings of the 4th Int. Conf. Cold Fusion, p 205 (1994).
[11] R.Notoya, Reported in Inter. Sympo. Cold Fusion and Advanced Energy Sources, Minsk, May 24-26, 1994.
[12] Jap. Isotope Asso., Isotope Handbook, Chaps.4, 5, 7 -10, Maruzen, Tokyo (1992).

MECHANISMS OF LOW-TEMPERATURE TRANSMUTATION

G.S. Rabzi
Ukrainian International Academy of Original Ideas. Southern Branch. Odessa, Ukraine

I feel it my first and foremost duty to express my sincere gratitude to the Distinguished Professor Bockris who spared no effort in providing for my visit here. It is largely because of the enthusiasts like him that science can progress.

All relevant literature on cold fusion available to date is basically a mere record of the results obtained from electrochemical cells. Everybody agrees that time is apt for an unorthodox theory capable of accounting for uncommon phenomena. I will try to patch this flaw by proceeding to theory from our experimental results.

[Samples of before and after materials here passed to the audience.]

A glimpse of the available samples persuades a viewer that something rather peculiar has occurred to the samples. And it has. An ordinary steel nut acquired the color of copper and diminished in size; magnetic stainless steel turned antimagnetic; asbestos became a ceramic-like material. What you can see is the outcome of low-temperature transmutation. Our experimental scheme is conceptually the same as many use for cold fusion. Those cold fusion cells are not unlike, featuring varied arrangements neglectful of the specific media therein entailing varied field patterns with respective varied interaction forces. The randomized fields thereof can be blamed for the divergence in the results. Our electrolyte-free device was constructed to allow for the specified control of the effect of those fields that provoke certain forces to trigger the transmutation process. We utilized the combined effect of both geoelectric, artificial fields, and temperature field. The latter can be described by a vector of temperature field gradient misaligned with vectors of the electric fields. We started our experiments in an attempt rather to observe transmutations in solids and liquids directly than to investigate, for example, particular behavior of hydrogen in metals. Resemblance between our schematic concepts inspires me to assume that similar phenomena produced by both cold fusion and our experiments must be likewise grounded in the same common laws.

But experimental results must be examined first. The history of our device dates as far back as 1958 when its first embodiment was developed with my colleague Arnold Fabrikant, a mechanical engineer. In our device, the following materials were processed: zinc, carbon, graphite, lead, table salt, silica sand, fuel oil; and different liquids (wine, alcohol, sunflower oil, etc.). Materials of the field-inducing electrodes varied for different experiments: copper, aluminum, titanium, or stainless steel. Now is as good a time as any to applaud Dr. Michael McKubre from SRI International who does not hesitate to confront the orthodox cold-fusionists with the physical, as opposed to chemical, nature of the processes involved in transmutation [1]. We support him with our results and theory.

1. Zinc has transmuted into copper (see sample). I brought here to show you the parent zinc sample; zinc in the process of transmuting into copper; the vessel where transmutation occurred with the residue of zinc pellets; the resulting copper product. In addition, here I have samples from zinc processing that were not lucky to be analyzed. The copper electrode plates with the implanted zinc are surprising with their overlayer of relative density 9.59 g/cm^3, while copper is known to have 8.89 g/cm^3 and zinc 7.1 g/cm^3.

Other attributes of the composition still wait to be decoded. A slide shows the drastic difference between the parent and the processed Zn samples. The samples were investigated and micrographed by my colleague Dr. Kostenko whose does work on α-irradiation.

2. Copper was implanted into a steel nut (see sample). No such composition is known to exist on Earth. The processed sample underwent qualitative spectral analysis. Fe appeared substituted by (Cu). The processed sample displayed mere traces of Fe. The reference nut after soaking for 6 hours in sulfuric acid lost 11.6% of its weight, while the processed one only 0.4%. It became corrosion-resistant and antimagnetic. Corrosion is 29 times weaker. Relative density of steel is 7.78 g/cm^3, density of copper is 8.89 g/cm^3. While density of the obtained composition is 6.41 g/cm^3. Other characteristics were left undetermined.

3. A stainless steel plate turned antimagnetic following implantation of the accelerated lead particles. After a number of years the sample still features antimagnetic behavior. I want to draw your attention to the stem. Though a part of the steel plate body, it was not affected by field and thus still is magnetic. Let me please remind you that lead is the finite product of uranium and thorium decay, therefore its transmutation is of special interest to us. Analysis suggests actual transmutation of lead into a group of elements (gold, cadmium, silver, germanium, palladium, osmium, platinum, etc.) absent in the parent sample and placed in the Periodic System ahead of lead (Fig. 1). This observation supports the claimed transmutation in our device.

Fig. 1

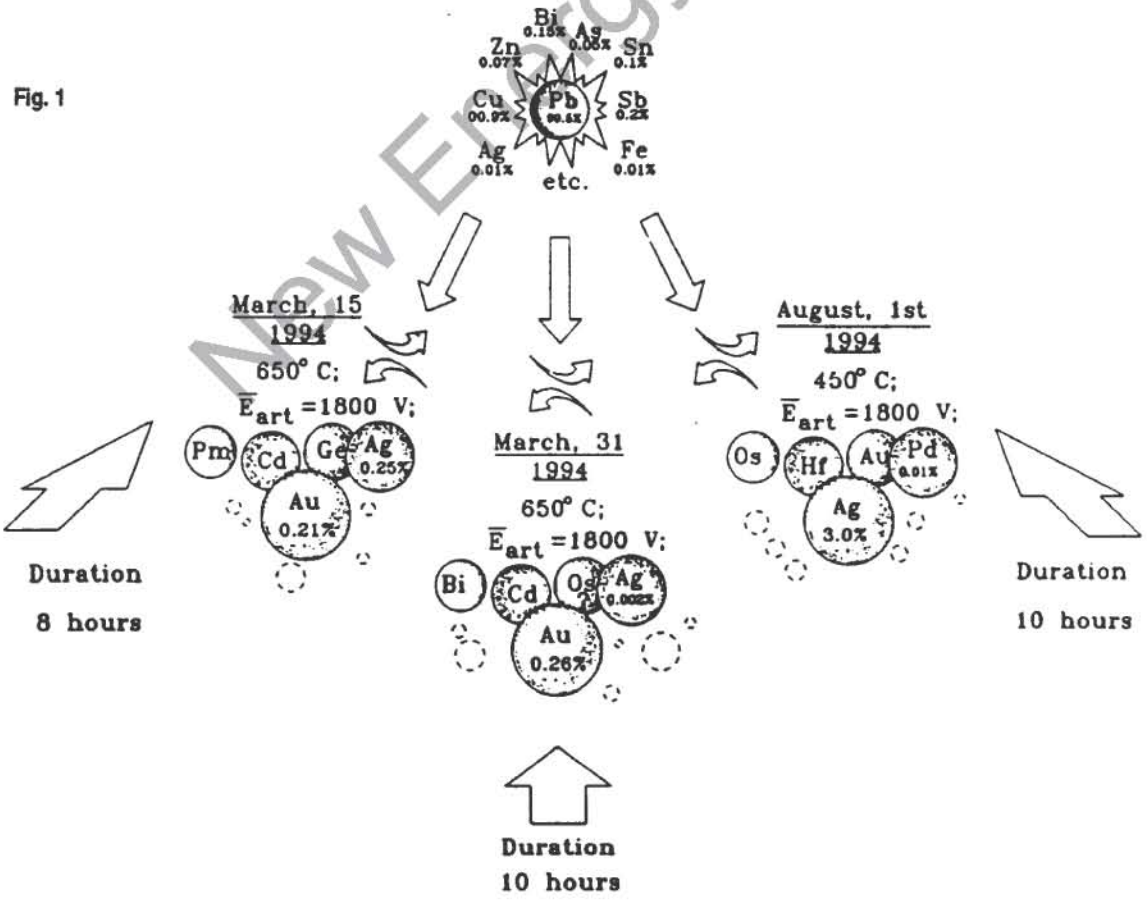

SOME EXPERIMENTAL RESULTS ON LEAD TRANSMUTATION

4. Transmutation of asbestos, high heat resistant sealing material, into a hard and light-weight mass took place under temperatures 750-800°C (see sample).

Electric field and energy utilized in our device made us persist in disclosing unambiguous mechanisms of their impact on material bodies and digging out the roots of transmutation and its stages. The available results furnished by both cold fusion cells and our device indicate inexplicability of their phenomena due to the absence of clear understanding of the processes involved. Studies by Louis Kevran in biologic field of knowledge corroborate the universalism of transmutation [2].

So far we have heard nothing about the excess heat liberation reported for the so-called cold fusion process. Such excess heat can result from certain inner forces liberated as energy that manifests itself, whether as an excess heat, or transmutational process, or both, depending on experimental conditions. Thus, energy is a manifestation of a certain process. To make my arguments more obvious, I invite you to have a look at this Ni-Cr coil with the implanted heavy particles of lead -- which fact, as we were taught, has no right to exist. Spectrochemical analysis of the processed coil revealed 0.05 – 0.08 percentage of lead. Such results cannot be achieved today except in very expensive and sophisticated reactors, while our device involves not only transmutations proper but also self-acceleration of the fission particles up to high energies at temperatures not exceeding 750-800°C. No radioactivity was observed in any of our experiments. I do not specify experimental conditions and arrangement of the device because these are things to be protected by patent (in process). **Our device also claims to transfer radioactive atomic waste into non-radioactive waste.**

It was not our prime goal, however, to well-instrument and protocol our experiments against possible fraud accusations, the sole purpose was getting the brief insight into the origin of the processes involved, be they transmutation or cold fusion.

The clue to this problem is a terrestrial charge that forms a vector of the geoelectric field in our device. It is widely recognized, but never substantiated, that the Earth is charged negatively. Should the terrestrial charge be "-", grounding would be impossible due to the electrons of current that ought to be repelled by the like charge. Lightning is known to strike earth, and what is lightning if not an electron beam? Should the terrestrial charge be negative, then ionization of atoms without heat input never would occur. But an atom is known to be environmentally-ionized. If the terrestrial charge is negative, atoms with orbital electrons would be ousted far upward -- which is never observed. It is simply another of the misleading shibboleths. In order to verify the positive terrestrial charge it is necessary to ascertain the processes in the Earth's core that generates the charge.

Radioactive processes in the Earth's core are accompanied by the stripping of the electron shells of disintegrating atoms with simultaneous liberation of huge energy. In this manner more heavy elements transmute into the lighter ones and are transferred to the upper part of the Periodic System. With their electron shells empty, the newly formed light elements expose the positive charges of their nuclei to produce the "+" charge of the Earth. Thus we know that ^{238}U decays under the neutron exposure to engender Ba, La, Ce. Their atomic weights are lighter than uranium. Uranium nucleus with its 238-82=146 neutrons loses, while Ba, La, Ce are formed, respectively: 146-81=65 neutrons, 146-82=64 neutrons, 146-82=64 neutrons. These 65, 64 and 64 neutrons undergo fission accompanied by beta-particle emission and proton formation. Such a decay of uranium provokes a rise in the "+" charge of the nuclei, which is responsible for the Earth's positive charge. One example more. Ionizing the hydrogen atom by removing its electron makes the heavy proton escape into the protonsphere [sic] as high as 2,400 km from the Earth's surface, while light-weight electrons adhere to the Earth. It is only possible if the Earth is charged positively.

All material bodies in the near-Earth space are polarized in the manner of dipoles with positively charged upper parts which further supports the positive charge of the Earth. The number of the examples to prove the above statement are numerous.

The arguments were backed up by a 21-hour run where a glass disc 50 mm in diameter and 2 mm thick was continuously weighted by ordinary analytical balance in the artificial electric field. The disc was preserved between the electrodes throughout the experiment. When the anode "+" electrode was under the disc its weight increased, while switching the anode "+" sign to "-" brought a loss in its weight. With no artificial field present the weight of the disc was unaffected. Thus, I state that coupling of the positively charged geoelectric field E_E (that never in the past history was included into calculations), with the E_{art} artificial one involves a gain in weight of the disc, and removal of the field results in the loss in weight. [Can this be related to the Townsend bifield effect?]

Another proof, though indirect in favor of our reasoning: voltage reduces from 130 V/m near the Earth surface to 2.5 V/m at the height of 12 mm, which also supports the "+" charge hypothesis because the field intensity is widely known to be maximum around the charge.

The more orbits and electrons which the nucleus has, the better it is shielded from the direct interaction with the external geoelectric field. It is a well-known fact that shielding of the nuclear charge is included into the so-called effective charge $Z_{eff} = \Sigma_{eff}e^{+}$. Effective charge is a fraction of the net nuclear charge that "shines" through the shield of orbital electrons. Out of 10 units of neon charge only 2.52 units manage to "shine through", while the remaining part is shielded by 10 electrons (Table 1).

Table 1 Effective charges of the atomic nuclei.

Atom	$Z_{eff} = \Sigma_{eff}e^{+}$	Atom	$Z_{eff} = \Sigma_{eff}e^{+}$
H	1.0	C	1.82
He	1.345	N	2.07
Li	1.26	O	2.0
Be	1.66	F	2.8
B	1.56	Ne	2.52

Hence $\Sigma_{eff}e^{-} > \Sigma_{eff}e^{+}$.

The difference between the net and effective charges is suggested to be called the acting charge $\Sigma_{act}e^{-}$ which increases with the order number of an element [3,4]. The acting charge is expressed in terms of a number of orbital electrons. Their interaction with the geoelectric field involves formation of the effective electric charges in atoms throughout the near-Earth space, across the Earth, in its depths, and in the cosmos. The charge value $\Sigma_{eff}e^{-}$ exceeds the effective nuclear charge $\Sigma_{eff}e^{+}$. Hence, the acting charge will be $\Sigma_{act}e^{-} = \Sigma_{eff}e^{-} - \Sigma_{eff}e^{+}$.

Interaction of $\Sigma_{act}e^{-}$, acting atomic charge, of any element or individual body with the terrestrial charge is governed by force

$$F = \sum_{act} e^{-} \cdot E_E = \sum_{act} e^{-} \cdot \frac{e_E^{+}}{R_E^2}$$

where E_E is the intensity of geoelectric field $E_E = \frac{e_E^+}{R_E^2}$; where e_E^+ - terrestrial charge in Coulombs, and R_E - radius of the Earth in meters.

Then $$F = \sum_{act} e^- \cdot \frac{570000}{(6370000)^2} = 1{,}405 \cdot 10^{-8} \cdot \sum_{act} e^- \text{ , N} \qquad (1)$$

Equation (1) shows that the $\Sigma_{act}e^-$ value introduced here to describe the acting charge of orbital electrons is the principal factor that controls all sorts of atomic transmutations, radioactivity included.

The atomic charge is constant for every element and increases continuously from the lowest in hydrogen, to the highest in uranium with its poor decay resistance. Thus, $\Sigma_{act}e^-$, the acting charge, is a measure of the atomic radioactivity. $\Sigma_{act}e^- > 0$ for all elements. So we conclude that atoms of the elements are not neutral with regard to the external field but negatively charged.

An atom and its nucleus can be destroyed or brought to decay by stripping electron orbits. We can induce nuclear decay and obtain a less radioactive element. For this purpose radioactivity of the parent element $\Sigma_{act}e^-$ is achieved by removing a sufficient number of electron's atomic orbits to obtain for a new element the expected decay byproducts.

This virgin-fresh equation is introduced here for the first time. It enabled us to also estimate absolute atomic weights of all the elements in the Periodic System and to place the zero, initial group. Following this equation hydrogen was placed firmly in the rear of a non-atomic product, namely neutrino (Table 3). With regard to hydrogen it is necessary to obtain an insight into the origin of the fantastic coincidence of proton and electron absolute charge values, as opposed to differences in their masses and properties. The proton absolute charge e_p^+ cannot equal that of an electron e_e^- because specific charge of the electron $\frac{e^-}{m_{e^+}}$ is 1837 times higher than that of proton $\frac{e_p^+}{m_{p^+}}$.

Masses of proton m_{p^+} and electron m_{e^-} differ. The proton mass m_{p^+} is 1837 times higher than that of electron m_{e^-}. Therefore, a single particle with specific charge $\frac{e^+}{m_{e^+}} = \frac{e^-}{m_{e^-}}$ is able to equilibrate with the specific charge of an electron. Only the positron meets this requirement. A positron can be anchored in a proton only by an electron, thus producing an electron-positron pair (Fig. 2). Nuclear charges of atoms are generated by the terminal positrons in protons. **The fact is beyond all doubt because the identity both of masses and the largest opposite specific charges of electrons and positrons cannot but couple them constantly into the electron-positron pairs**. Mutual attraction between electrons and positrons gives birth to a new particle. The particle is oblate because the attraction force is directed along the geoelectric field. But what size is this oblate particle? As a proton consists of 1837 e^- or 1837 e^+, then proceeding from the classic radius of r_0 = 281.7938 · 10^{-17}cm, the radius of the oblate pair will be $r_{obl} = \frac{2.817938 \cdot 10^{-15}}{1827} = 0.15 \cdot 10^{-17} cm.$ The force to oblate electron with positron is equal

$$F_{e^+ + e^-} = \left(\frac{e^-}{m_{e^-}} \cdot \frac{e^+}{m_{e^+}} \right) \cdot \frac{1}{r_{obl}^2} = \frac{(1.602 \cdot 10^{-19})^2}{(0.15 \cdot 10^{-17})^2 \cdot (0.91 \cdot 10^{-27})^2} = 1.373 \cdot 10^{52}, N \text{ [Newtons]}$$

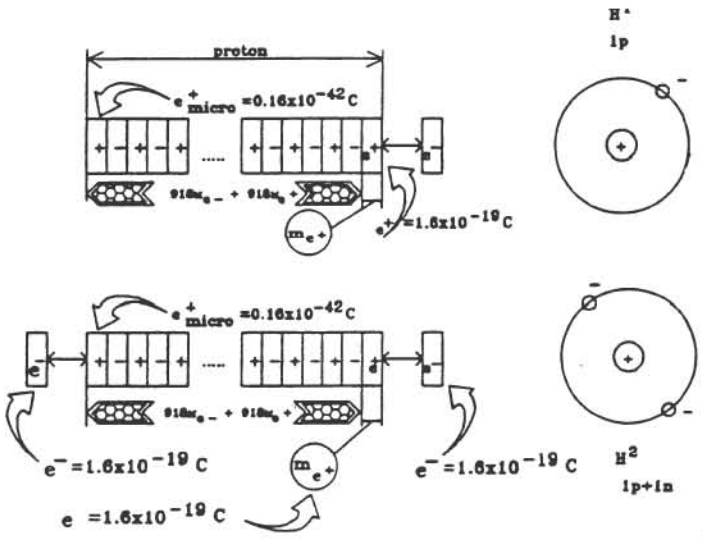

Fig. 2 Electron-positron pairs that constitute proton and neutron are essentially matter, eternal and non-exterminable -- the basis of the Universe. Radius of the oblate electron-positron pair of 0.15 · 10^{-17}cm allows for constructing the nucleus with r_{nucl} = 10^{-13}cm from a large number of these pairs. The recognized mass of a proton m_p = 1837 m_e, mass of a neutron m_n = 1837 m_e. But since the masses of both electron and positron are equal, as well as their specific charges (though opposite in sign), we can represent the mass of a proton as consisting of 918 electron-positron pairs plus a terminal positron m_{e^+}, that is $m_p = 918\, m_{e^-} + 918\, m_{e^+} + m_{e^+}$, while a neutron consists of $918\, m_{e^-} + 918\, m_{e^+}$.

Attraction between the spatial electrons and positrons produces couples with underequilibrated non-exterminable charges that do not annihilate. External noncontiguous surfaces of both charges preserve their stability in the couple as surface microcharges "+" and "-", that is neutrino. Thus, neutrino is an electron-positron pair. The value of neutrino microcharges can be derived using the mass of the neutrino. At the Institute of Theoretical and Experimental Physics in Moscow, the neutrino mass was found about 20,000 times lighter than that of electron [5].

From the above, mass may be defined as the product of the active negative charge of bodies and geoelectric field intensity. Hence, neutrino mass is $m_\nu = \frac{m_{e^-}}{20000} = \frac{9.105 \cdot 10^{-31}}{20000} = 4.5 \cdot 10^{-35}\, kg.$

To verify the introduced notion of mass, let us disclose the dimensional units of both the right-hand and left-hand sides of the Einstein's equation

$$\mathbf{W = mc^2\ ;}$$

$$W = [\ \Sigma_{act}\, e^- \cdot E_E\ ] \cdot c^2\ ;$$

$$[J] = [Newton] \cdot c^2\ ;$$

$$[\frac{kg \cdot m^2}{sec^2}] = [\frac{kg \cdot m}{sec}] \cdot [\frac{m^2}{sec^2}] \quad \text{[sic]}$$

$$[\frac{kg \cdot m^2}{sec^2}] = [0.102\, kg] \cdot \frac{m^2}{sec^2} \Rightarrow 1\, Newton = 0.102\, kg$$

[kg] = [kg]

Identity of both sides is achieved, but in the case of mass it is as a measure of acting charge $\Sigma_{act}e^-$ interaction with a geoelectric field. Originally Einstein's equation lacked equality of left-hand and right-hand sides which made him assume that mass and energy are equivalent. While I showed to you that there is no such necessity if we accept my definition of mass. **Thus we define mass in the only possible way as a measure of interaction between the acting electric charge of a material body and**

the geoelectric field. I must stress here that no similar approach has ever been suggested in the available literature.

Taking the neutrino-to-electron mass ratio as an interaction measure with the geoelectric field let us proceed to the neutrino surface microcharge. Note that neutrino is an electron-positron pair.

$$m_\nu = e_{micro}^{+-} \cdot E_E = (e_{micro}^{+} \cdot E_E) + (e_{micro}^{-} \cdot E_E) = e_{micro}^{+-} \cdot 2\frac{e_E^+}{R_E^2}$$

$$e_{micro}^{+-} = \frac{m_\nu}{E_E} = 0.16 \cdot 10^{-42}, C \text{ [Coulombs]}$$

"+" and "-" microcharges of a neutrino interact both with another neutrino microcharge and the geoelectric field, thus producing in the first place neutrons and then, after coupling with a positron, protons. The attraction force between the coupled neutrinos that brings them together to form a neutron is equal:

$$F_{el.-pos.pair} = \left(\frac{e_{micro}^-}{m_\nu} \cdot \frac{e^+}{m_\nu}\right) \cdot \frac{1}{r_{obl}^2} = 5.6 \cdot 10^{18}, N$$

Neutron is attracted to positron to form proton. Attraction force between them is

$$F_{n+e} = \left(\frac{e_n}{m_n} \cdot \frac{e^+}{m_{e^+}}\right) \cdot \frac{1}{r_{obl}^2} = 7.5 \cdot 10^{27}, N$$

The geoelectric field should be expelling protons into the protonsphere. But it is not what happens during the formation of an atom. The terminal positron of a proton attracts only the electron that is decelerated by geoelectric field, thus preventing its adherence to the proton's positron. Attraction force between an orbital electron and proton's positron is $F_{orbit} = \left(\frac{e^-}{m_{e^-}} \cdot \frac{e^+}{m_{e^+}}\right) \cdot \frac{1}{r_{at}^2} = 3.1 \cdot 10^{32}, N$

Attraction force between proton/neutron pairs (p-n):

$$F_{p\text{-}n} = F_{el.\text{-}pos.pair} \cdot 2 \cdot 918 = 5.6 \cdot 10^{18} \cdot 2 \cdot 918 = 1.028 \cdot 10^{22}, N$$

Evaluation of forces participating in nuclear formation in an atom evidences that their nature is common -- electric. An electronic coat covers the nucleus according to the charge conservation law [6]. It protects the nucleus from the direct interaction with the geoelectric field. A stable atom is born. The atom is electrically neutral but its nuclear charge and that of orbital electrons interact with geoelectric field in unlike fashion.

Following the removal of orbital electrons, the fields between the positrons of the nuclear protons and orbital electrons collapse. Emerged are the balanced, open-for-field effect, positrons of the nuclear protons. Driven by the geoelectric field, positrons escape from the protons that are coupled to neutrons (p-n). A proton without a positron decays together with its twin neutron. This is the native nuclear decay of every elemental atom. Nature-born native radioactive decay stems from weakly bound terminal electrons in atoms that need nothing more than the geoelectric field to be stripped off their orbits. It follows from Eqn. (1) that natural radioactivity is more a causal process than a spontaneous one. It is controlled by the continuous constant geoelectric field with strict correspondence of its nature to the physical essence of matter.

The radioactive nuclear decay described by Eqn. (1) is the specific case of the universal mechanism of transmutation of all material bodies in the Universe. By superposing an artificial E_{art} (V/m) field onto a geoelectric E_E one with simultaneous heating, we can control and accelerate nuclear decay of any element from the Periodic System by simply varying both values (E_{art} and E_E) and the quantity of the supplied heat.

$$F = \Sigma_{act} e^{-} (E_E + E_{art}) \qquad (2)$$

Reproducible results of the experiments in a device constructed according to Eqn. (2) verified its validity. A variety of elements underwent decay, lead included, while being the finite product of thorium and uranium decay. New elements were detected that are placed to the left of lead in the Periodic System. We can suppose that the transmutation processes in our device are identical to the radioactive decay processes in the Earth's core.

Now let us model low-temperature nuclear decay, or transmutation (Fig. 3). The directional field $\mathbf{E}_{dir} = \mathbf{E}_E + \mathbf{E}_{art}$ and heat exposures start ionization of an atom; electron $\mathbf{e}^-_{orbit}$ escapes from its orbit, thus provoking collapse of the field between $\mathbf{e}^+$ positron of $\mathbf{p}_1$ proton and an orbital electron. Field-free positron $\mathbf{e}^+$ of proton $\mathbf{p}_1$ is separated from the nuclear proton due to $\mathbf{E}_{dir}$ force. The proton positron $\mathbf{e}^+$ couples with an orbital electron, and the proton that has lost its positron transmutes into an antiproton $\tilde{p}_1$. The directional field $\mathbf{E}_{dir}$ induces further decay of antiproton $\tilde{p}_1$ to produce $\mathbf{e}^-$ electron and an electron-positron pair, that is neutrino ν. The above antiproton transmutes further into a $\mathbf{p}_2$ proton open for interactions with $\mathbf{E}_{dir}$ field. Neutron $\mathbf{n}_1$ and proton $\mathbf{p}_1$ in the nucleus form a couple **(p-n)**. Therefore, $\tilde{p}_1$ antiproton decay involves $\mathbf{n}_1$ neutron decay accompanied by isolating both $\mathbf{e}^+$ positron as a twin to $\mathbf{e}^-$ electron from $\tilde{p}_1$ antiproton and $\nu\downarrow$ neutrino as a twin to $\nu\uparrow$ antineutrino. Neutron $\mathbf{n}_1$ transmutes into $\tilde{n}_1$ antineutron, and antiproton $\tilde{p}_1$ -- into $\mathbf{p}_2$ proton. Transmutation proceeds further on in like manner: antineutron $\tilde{n}_1$ transmutes into $\mathbf{n}_2$ neutron, and proton $\mathbf{p}_2$ - into antiproton $\tilde{p}_2$. Thus, the nuclear decay results in the following couples: antiproton-proton ($\tilde{p}_1$-$\mathbf{p}_1$), antineutron-neutron ($\tilde{n}_1$-$\mathbf{n}_1$), antineutrino neutrino ($\nu\uparrow$ - $\nu\downarrow$), and an electron $\mathbf{e}^-$ [7-10].

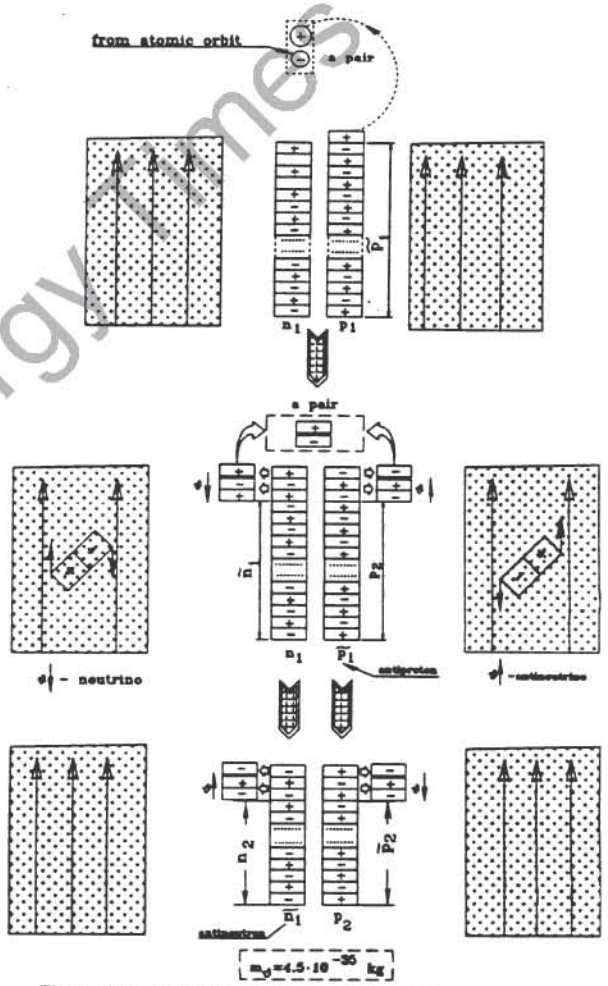

Fig. 3 MODEL OF PROTON AND NEUTRON TRANSMUTATION

Obtained speculative sequence of the nucleons' decay into antinucleons is valid and can be verified by the results from sophisticated hot-fusion accelerators in the U.S. as far back as 1955 and 1956 when antiprotons and antineutrons were received [7]. Antinucleons are of principal interest for us due to their interaction with nucleons. When antinucleons $\tilde{p}_j, \tilde{n}_j$ and nucleons p_i, n_i meet, huge energy is liberated

$$W = 2m_N \cdot c^2 = 2\Sigma_{act}\, e^- \cdot E_E \cdot c^2 = 2.81 \cdot 10^{-8} \cdot \Sigma_{act}\, e^- \cdot c^2 = 1900,\ MeV.$$

Irreproducible or scarcely reproducible experiments with cold fusion cells evidence at least two facts: first, continuously active natural forces are not taken into account; second, electrolytes and cell elements react to these forces.

Both electric fields and energy induce transmutation that expands (or becomes more advanced) when the artificial electric field E_{art} is backed by the geoelectric field E_E. Transmutation slows down when they are uncoupled. Change of polarity sign in the cold fusion cells entails the related change in the direction of acting forces. [sic - We are not aware of what is meant by change of polarity. We assume it means "if one changes the polarity." --Ed.]

The above concepts enable us to suggest that all phenomena in the electrochemical cells associated with Pons and Fleischmann, and in the wide range of their diverse constructions, are nothing else than the outcome of low-temperature transmutation. Neutrino, nucleus, atom - these are three inseparable constituents of a single whole, the Holy Trinity that is God Himself.

I hope to have introduced by my theoretical study a fresh understanding of cold fusion as an essentially natural cold fission, a mere stage in the universal transmutation.

Thank you.

LAST MINUTE CONSIDERATIONS

In the isolated system, the net electric charge, i.e. algebraic sum of the positive and negative charges, stays constant. An isolated system is a system whose boundaries are impenetrable for any other substance. The net charge of the isolated system (atom) is a quantity that never changes.

The charge conservation law would be violated if a positively charged particle is created without simultaneous creation of a negatively charged one. The event is never observed. The charged particles are born in pairs, with equal and opposite charges. This absolute equality of charges, as well as equality of masses, displays some universal symmetry of nature inherent in particle and antiparticle [6].

It appears that conservation of charge results from some more general conservation law that governs the emergence and decay of particles.

It must be more probable, that conservation of the net charge in the isolated system is the primary requirement which all other laws obey. Here is a valid substantiation: the transmutation mechanism in the Earth's core gives birth to all the elements of the Periodic System - this is the basis of the universe having all the forces to support transmutation. Its mechanism is actuated into continuous operation by the never-violated conservation law: the net charge of an isolated system being the primary requirement that transmutation obeys. Hence, transmutation is the all-embracing process in the universe that proceeds eternally, differing in time and in objects.

Transmutation is present in the cold fusion cells too, but as a low temperature transmutation and not fusion. Artificial violation ionization, stripping of orbital electrons of the net electric charge in the isolated system results in the immediate, accelerated and controllable nucleus transmutation. It leads to restoring the conservation law by the compulsory formation of a new element that is placed in the Periodic System higher than the decaying one. Continuous transmutation of all materials proceeds in the universe with different rates. These rates can be controlled by artificial means.

REFERENCES

1. E.F. Mallove and J. Rothwell, *Cold Fusion*, May 1994, vol 1, no 1, p 51.
2. L. Kervran, Transformation l'Energie du Faibles, Paris: Malon, 1975, 150 pp.
   L. Kervran, Prenvens en Biologie de Transmutation a Faibles Energies, Paris: Malon, 1975, 210 pp.
3. A.K. Barnard, Theoretical Basis of Inorganic Chemistry, Moscow: Mir Pub., 1968, in Russian.
4. K.V. Ovchinnikov, S.A. Shchukarev, Electrons in Atoms, Moscow: Khimia Pub., 1970, in Russian.
5. E.N. Velikhov, *Science and Life*, 1987, no 11, in Russian.
6. E.M. Purcell, Berkely Physics Course. V.2. Electricity and Magnetism, Moscow: Nauka Pub., 1967, in Russian.
   Max Jammer, Concepts of Mass in Classical and Modern Physics, Moscow: Progress Pub., 1967, in Russian.
7. Jay Orear, Physics. V.2, Moscow: Mir Pub., 1981, in Russian.
8. Isaac Asimov, The Neutrino - Ghost Particle of the Atom, Moscow: Atomizdat Pub., 1969, in Russian.
9. W. Greiner, A. Sandulescu, *Sci. Amer.*, 1990, nol 262, no 3.
10. K. Mukhin, Introduction to Nuclear Physics, Moscow: Atomizdat Pub., 1965, in Russian.

Groups of Elements							
Period	Row	0	I	VII	VIII		
1	I	ν 45.696 · 10^{-30}	H 1 14.03 · 10^{-26}	H 2 27.57 · 10^{-26}			
2	II	He 2 32.503 · 10^{-26}	Li 3 39.0 · 10^{-26}	F 9 148.986 · 10^{-26}			
3	III	Ne 10 170.136 · 10^{-26}	Na 11 210.487 · 10^{-26}	Cl 17 324.751 · 10^{-26}			
4	IV	Ar 18 342.252 · 10^{-26}	K 19 382.488 · 10^{-26}	Mn 25 509.313 · 10^{-26}	Fe 26 523.445 · 10^{-26}	Co 27 546.86 · 10^{-26}	Ni 28 574.16 · 10^{-26}
	V		Cu 29 587.47 · 10^{-26}	Br 35 707.017 · 10^{-26}			
5	VI	Kr 36 733.897 · 10^{-26}	Rb 37 839.08 · 10^{-26}	Tc 43 979.6 · 10^{-26}	Ru 44 1006.5 · 10^{-26}	Rh 45 1028.5 · 10^{-26}	Pd 46 1050.0 · 10^{-26}
	VII		Ag 47 1074.8 · 10^{-26}	I 53 1191.2 · 10^{-26}			
6	VIII	Xe 54 1210.65 · 10^{-26}	Cs 55 1218.7 · 10^{-26}	Re 75 1645.23 · 10^{-26}	Os 76 1664.71 · 10^{-26}	Ir 77 1680.5 · 10^{-26}	Pt 78 1690.0 · 10^{-26}
	IX		Au 79 1734.65 · 10^{-26}	At 85 1785.1 · 10^{-26}	Rn 86 1793.15 · 10^{-26}		
7	X		Fr 87 1840.21 · 10^{-26}				

SOME RESULTS OF EXPERIMENTAL INVESTIGATIONS IN LOW-TEMPERATURE METALS TRANSMUTATIONS

A. Fabrikant, M. Meyerovich
Ukrainian International Academy of Original Ideas, South Branch
Ukraine, 270011, Odessa-11, P.O. Box 3
Phone: (0482) 45-39-74, 23-71-23 Fax: (0482) 22-67-35
Presented by Dr. G. Rabzi, as they were not able to attend.

It is interesting to note that in the well-known reports concerning observed transmutations (see references 1, 2, 3, as well as the works by Nagaoki. J. Bockris, J. Champion, and others) the process of transmutation has been observed under various physical effects which have been, however, always principally different from nuclear fusion processes in reactors of particle accelerators.

In 1966 G.S. Rabzi and A.E. Fabrikant started investigations into the properties of some chemical elements and their compounds under the effect of electric and thermal fields. The obtained results could be interpreted only through transmutation process, since not only principal changes of elements' physical properties took place but also their direct transmutation into other elements that were absent both in the source material and in substances involved in the experiments.

As source material the following were used: chemically pure lead and zinc as well as bidistillate (H_2O). table salt (NaCl), quartz sand (SiO_2), nepheline concentrate $(NaK)_2O\cdot Al_2O_3\cdot 2SiO_2$), fuel oil, and some liquid food products.

There were electrotechnical copper, titanium, aluminum, steels Ст3 (0.3% C) and CT45 (0.45% C), and stainless steel 12X18H10T (1.2% Cr; 1.8% Ni; 1.0% Ti) that interacted with the source substances as electrodes.

The following observed phenomena were common for all the experiments:

1. Formation of new elements both in the source materials and in the electrodes. Thus, at treating steel electrodes with lead, there appeared hafnium, europium, and zinc: at treating stainless steel 12X18H10T with lead--cadmium, bismuth, gold, and silver appeared: and at treating copper with zinc--cobalt, boron, hafnium, and selenium. (Unfortunately, we have had no opportunity to verify the results throughout the whole range of possible combinations.) The control of the results was carried out by using an atomic absorption spectrophotometer and chemical methods; in addition, only those results were taken into account that exceeded resolving power of the appliances by one or two orders of magnitude.

2. Changes observed in physical properties of the source materials and electrodes:
--changes in density and hardness of electrodes;
--changes in magnetic properties, e.g., appearance of magnetic properties in non-magnetic stainless steel;
--change in electrodes' f-potential, which testifies to changes of free electrons quantity in them;
--emergence of radioactivity in lead;
--changes in the structure and phase composition of the elements and their saturation with other materials, for example, that of steel with copper or lead;
--formation of intermetallides, such as. e.g., $TiZn_2$ and $TiZn_3$ at the interaction of stainless steel with zinc;

--escape of some elements from a source element, for instance, thallium and antimony from lead;
--appearance of nucleopores.

The attempt to explain these results led to the formation of a hypothesis (G. Rabzi, A. Fabrikant) to the effect that the cause of elements' radioactivity was the combined action of thermal and electrical fields on atoms, and gave rise to the theory of nucleons and atomic nucleus structure.

As of 1993 E. Gromovoy (theoretical part) and M. Meyerovich (practical one) have joined the investigation. On the basis of UIAOI SB a laboratory was established where a new experimental plant was assembled. The objective of experiments was to prove the fact of transmutation using chemically pure lead as the source material at ordinary atmospheric conditions. (Two experiments were also carried out using nepheline in order to make effect upon the radioactivity of potassium 40; after the experiment, up to 1% change in radio background has been observed.)

The experiments with lead were performed to investigate the effect of different plant's elements and working parameters upon the course of the process.

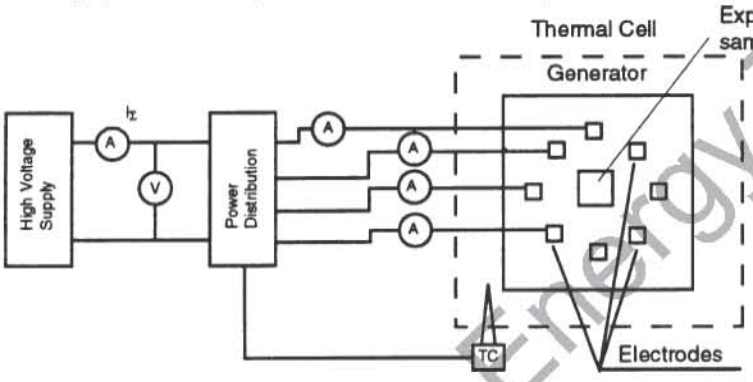

Fig. 1. Schematic layout of the experimental unit.

The scheme of the plant is represented in Fig. 1. It consists of high-voltage rectifier (BB) with a mode switch (PK) attached to its outlet. To the mode switch electrodes are attached, partly to its positive and partly to its negative poles. Between groups of the electrodes arranged in a certain order, the source material (Pb) was placed, and then the whole package was put in a certain position into a muffle furnace serving as a heating chamber. The temperature in the furnace was balanced automatically with a thermocouple signal received by the mode switch.

During the experiment the following parameters were changed:

--quantity of electrodes, their arrangement, shape, and material;
--voltage supplied to the electrodes and its polarity;
--disposition of the material processed relatively to the electrodes;
--amount, shape, and size of the processed material;
--insulation materials;
--duration of processing and holding at different modes;
--temperature;
--rate of permanent current change, and others.

During the experiments there were under control the temperature in the furnace, the DC output voltage, the electrodes' current, the total rectifier current, and the duration of effect.

The results were verified with an atom absorption spectrophotometer and at the same time with X-ray phase control method to reveal the presence of elements in the processed material in the amount that was known to be absent in the source material as well as in the materials used in the experiment.

Of most interest appears to be the series of experiments the averaged characteristics of which are presented in Fig. 2.

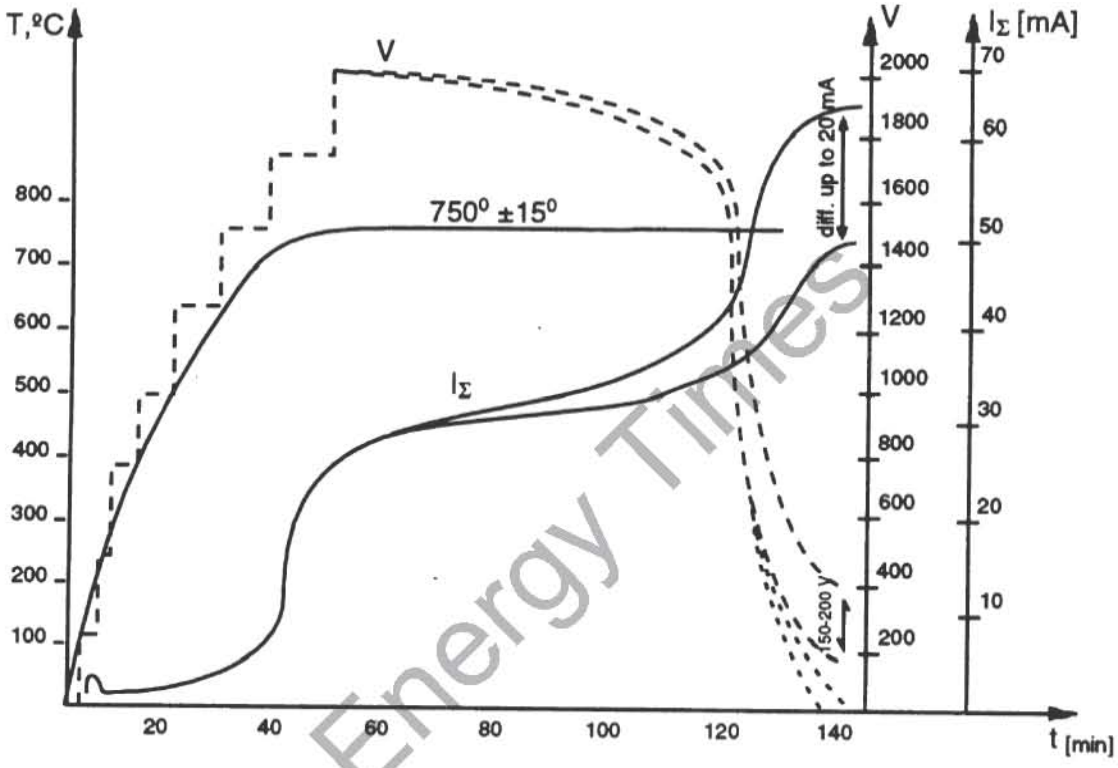

Fig. 2. The graphs of working parameters of the process.

As a sample was heated, the voltage was abruptly raised each 100-200°C so that at the designated working temperature, the voltage would reach 2000 V. The electric current values were registered with such a frequency that allowed to notice each significant change starting from microamperes.

The first abnormal current overswing was observed at 150-160°C, and, in relation to voltage value, reached some milliamperes (an increase by three orders). It is noteworthy that with the sample being cooled and the mode repeated, this overswing was not observed. To explain the causes of the voltage overswing, two versions are offered which are to be verified:

--electrode spark-over because of moisture;

--stripping of free and valence electrons and rearrangement of crystalline structure.

The further current increase was rather proportional to that of temperature and voltage. In the working mode (750°C and 2000 V), holding for a specified time span was carried out. The authors reckon that the characteristic beginning of the transmutation process is the voltage fluctuation which commences from small deviations of +10 V and gradually increases to 60-80 V. The electric current fluctuations at that phase were insignificant. The voltage abruptly dropped, from the experimental voltage to 350-400 V, and remained within a range of 250-450 V, constantly fluctuating. In addition, the current value sharply increased (sometimes nearly by an order), while current fluctuations reached 20-25% of the measured value.

A complete drop in voltage (down to 0) was registered twice, in one occasion the outer voltage being turned off by the authors from the rectifier (brought to zero) without opening the rectifier circuit. However, the current value did not change, which affords grounds to suggest that the process was supported with its inner energy.

The formation of new elements (within the range of atomic numbers 82 through 40) was observed in almost every experiment, but the quantitative and qualitative variations even for one element were too broad ranging from 10^{-1} to 10^{-5}% (see Table 1). Likewise, rare-earth elements (Eu, Ce, Pr, Sm, La) occasionally appeared in the amount of up to 0.01%.

It is also characteristic that the new elements were disposed predominantly in the upper layer of the processed lead.

However, due to vagueness of the factors influencing the process and impossibility to provide absolutely identical conditions while conducting experiments, reproducibility of results has not been achieved at the moment.

The formation of new elements runs contrary to the existing theories of the atomic nucleus structure and running of nuclear reactions, which requires further investigation and interpretation.

The attempt to explain the observed phenomena, most elaborated and accepted as a basic one by the group of members, was set forth in the paper by G.S. Rabzi and E.P. Gromovoy "Nuclei Transmutations as the Basis for Natural Substances Transformations." There are several possible interpretations in respect of separate issues and stages of that phenomenon.

1. The drop in voltage with simultaneous increase of current (see Fig. 2) evidences that the question is in the electric spark and electric are processes characterized by discharges producing local heating up to 3,000 ... 5,000°C. Such an increase in temperature results in high ionization of lead atoms and can be the cause of changes in their properties (Fabrikant).

2. Combined effect of strong electrostatic and thermal fields drives ALL the atom particles into excited condition. At the first stage (the first current overswing) there is the stripping of valence electrons and uncovering of electron shells. Thermal electron emission generated in the inter-electrode space and the electrons bombarding processed material yield in its surface some local zones with very high temperature (up to the boiling temperature), which, in its turn, activates thermal electron emission (current increase at constant temperature and voltage) and causes a counter flow of positive ions to the cathodes.

The increased combined action of fields upon the course of process results in that interaction of electrons (probably in the resonance mode) with excited processed material atomic nuclei, which are already poorly protected by their electron shell and have the positive charge not balanced by the shell, causes the splitting of protons and neutrons (occurrence and growth of fluctuations in horizontal stretches of current and voltage characteristics). The splitting fragments, charged both positively and negatively, are immediately drawn by strong electrodes fields and prevent them from recombining inside a single atom, which produces changes in nucleons' quantity inside the atom nucleus and thus provokes formation of new elements. The amount of released energy is sufficient to sustain the process without any external energy source (the zone of voltage drop and current increase) (M.I. Meyerovich).

REFERENCES

1. *Progress of Physics*, vol 5, no 4-5, 1925, p 104.
2. Proceedings of the International Symposium on Cold Nuclear Synthesis, Minsk, may 24-26, 1994.
3. B.V. Bolotov, Save Yourself, Moscow, 1992, p 7.
4. B.M. Javorski, A.A. Detlaf, Physics Handbook, Moscow, Science Pub. House, 1964, p 375.
5. L.A. Artzimovich, Elementary Physics of Plasma, Moscow, Pub. House of Lit. & At. Scil, 1966, p 6.

Work Parameters of the Experiments on Lead Treatment and their Results

Date of Experiments	Duration of exper., hrs	Working Temp. deg. C	Voltage K - A (V)	Synthesized elements and their mass content in the sample, %
14.01.80	6	500	950	Tl, Sb, Hf, Eu (litharge formation)
12.03.82	6	450	1000	Co, Sc, Ge, Hf
18.05.84	12	650	1200	Au, Eu, Sc, Os
10.03.94	6	450	800	In–0.003%, Bi–0.0006%, Cd–0.0004% (increased content of forcing matter)
15.03.94	8	650	1800	Au–0.21%, Cd–0.001%, Ag–0.25%, Ge–0.0001%, Pm–0.00002%
31.03.94	10	650	1800	Au–0.26%, Cd–0.0008%, Bi–0.0015%, Ag–0.002%
04.07.94	8	600	1800	Au–0.00014%, Os–0.0034% Pd–0.00008%, W–0.003%
06.07.94	8	600	1800	Au–0.00011%, Os–0.0004%
29.07.94	12	750	1400	Au–0.082%, Eu–0.0001%, Os–0.004%, Pd–0.0001%, Pt–0.00003%
01.08.94	10	450	1800	Au–0.004%, Os–0.004%, Hf–0.002%, Pd–0.01%, Ag–3.0%

NOTES:

1. The results of experiments carried out before 1984 were not quantitatively analyzed.
2. For quantitative analysis of the elements' content atomic absorption spectrophotometers "SATURN" and "SPECORD" M-400 (GDR) and spectrograph xxx-30 were used.
3. As an analytical chemical laboratory was not available the presence of some elements in the samples was not determined.

FORMULATION OF LOW-ENERGY NUCLEAR INTERACTION BASED ON OPTICAL THEOREM

Presented by Yeong E. Kim
Department of Physics, Purdue University
West Lafayette, IN 47907-1396, U.S.A.

Dr. Kim's presentation was based on two papers that have been accepted for publication. The following are the titles and abstracts of these two papers:

Title: Uncertainties of Conventional Theories and New Improved Formulations of Low-Energy Nuclear Fusion Reactions. By Yeong E. Kim and Alexander L. Zubarev, Department of Physics, Purdue University. This paper will be printed in the proceedings of the Fifth International Conference on Cold Fusion.

Abstract: We examine uncertainties of conventional theoretical estimates for low-energy nuclear fusion cross-section $\sigma(E)$ and fusion rate $\langle\sigma v\rangle$. Using new formulations based on the optical theorem and the radial distribution function, we derive new improved formulae for $\sigma(E)$ and $\langle\sigma v\rangle$. Our results of the optical theorem formulation for $\sigma(E)$ indicate that a near cancellation of the Gamow factor can occur if the imaginary part of the effective nuclear interaction in the elastic scattering channel has a very weak component with a long finite interaction range. Uncertainties of conventional estimates of the electron screening effect for $\sigma(E)$ are also examined and a new alternative formulation is proposed. Finally, based on a solution of three-body Schrödinger equation and the optical theorem formulation, we derive a new formula for three-body fusion cross-section and rate and compare its predictions with conventional estimates and also with the recent experimental data for three-deuteron fusion reaction.

Title: Optical Theorem and Effective Finite-Range Nuclear Interaction for Low-Energy Nuclear Fusion Reactions. By Yeong E. Kim and Alexander L. Zubarev, Department of Physics, Purdue University. Paper accepted for publication in *Nuovo Cimento.*

Abstract: We describe a new improved formulation of low-energy nuclear fusion reactions based on the optical theorem. Our formulation is much less model-dependent than previous theoretical approaches. We obtain an analytic formula for the cross-section, $\sigma(E)$, which exhibits explicitly the energy and charge dependence of $\sigma(E)$. The formula indicates that some of the anomalous effects observed in deuterated metals may be justified theoretically if the imaginary part of the effective nuclear interaction in the elastic channel has a very weak component with a long finite interaction range.

EDITOR'S SUMMARY AND COMMENTS:

Since 1989, there have been reported numerous examples of low-energy nuclear reactions in electrochemical cells using palladium [1] and titanium [2]. While these experiments are not always 100% reproducible, there have been persistent claims of the observation of low-energy nuclear reactions. Many theoretical models have been presented to explain the observed results but almost none of the theories explain the observed phenomena. Kim presented the basic results of a new alternative theoretical formulation of low-energy nuclear fusion reactions based on the optical theorem. The optical theorem is much less model dependent than previous theoretical approaches and show that some of the cold fusion

phenomena may be justified theoretically **if the imaginary part of the effective nuclear interaction in the elastic channel has a very weak component with a long finite interaction range.**

Kim and Zubarev explain how the Gamow penetration factor (Coulomb barrier transparency) may be essentially removed under certain conditions. Using the formulations developed in their paper, Kim and Zubarev state, "Another interesting aspect of d + Pd and p + Pd reactions is that the final fusion product can be unstable with a finite lifetime, which may help to explain **heat after death** phenomenon reported by Pons and Fleischmann [3]."

Pons and Fleischmann apparently predicted that if fusion could occur within a palladium lattice, it would be fusion of deuterium. It has long been believed that fusion between a deuteron and a light element was much more probable than fusion with a higher mass element. Kim presented the following information (quoted from the first paper): [If the fusion byproducts are not consistent with low-mass fusion] "...Other possibilities are now numerous, since our results with the electron screening effect ... show a surprising result that the fusion cross-section for nuclei with larger values of Z can be comparable or much greater than that for nuclei with small Z, **contrary to the commonly accepted belief.**"

Dr. Kim, in his presentation in Monaco at the Fifth International Conference on Cold Fusion, illustrated that under certain conditions (or assumptions) the new formulation equations indicated that some high mass elements could be expected to fuse with deuterons or protons fifty orders of magnitude more readily than with lower mass elements. This editor suggests that the anomalies discovered by Bush and Eagleton in their experimental work with light-water nickel-cathodes reactors where a rubidium salt is used in the electrolyte may be explained by the work of Kim et al. [Bush and Eagleton found evidence for the production of elements up through tin by suspected **proton capture**.]

The experimental work (especially the elegant experiments by Bush and Eagleton) coupled with this important mathematical formulation present by Professor Kim must certainly be considered as one of the most important findings in low-energy nuclear reactions. It may be comforting to the reader to understand that the highly unexpected phenomenon of cold fusion is now being coupled with the learned discoveries of Kim et al. that are also unexpected (contrary to popular belief.)

REFERENCES

[1] M. Fleischmann, S. Pons, and M. Hawkins, "Electrochemically induced nuclear fusion of deuterium." *J. Electroanal. Chem.*, 261, pp 301-308, and erratum, 263, p187 (1989).

[2] C. Sanchez, J. Sevilla, B. Escarpizo, F.J. Fernandez, and J. Canizares, "Nuclear Products Detection during Electrolysis of Heavy Water with Ti and Pt Electrodes.", *Solid State Communications*, Vol. 71, No. 12, pp 1039-1043, 1989.

[3] S. Pons & M. Fleischmann, "Heat After Death," *Transactions of Fusion Technology*, Vol 26, no 4T, part 2, Dec, 1994, pp 87-95, 11 refs.

THE ELECTRON CATALYZED FUSION MODEL (ECFM) RECONSIDERED WITH SPECIAL EMPHASIS UPON THE PRODUCTION OF TRITIUM AND NEUTRONS*

R.T. Bush
Physics Department, California State Polytechnic University
3801 W. Temple Avenue, Pomona, CA 91768, USA
ENECO, Inc., Salt Lake City, Utah
Proteus Processes and Technology, Inc., Denver, Colorado

ABSTRACT

The author's ECFM ("Electron Catalyzed Fusion Model") first presented at the ICCF-4 is re-examined with special reference to the production of tritium and neutrons. The model is of some interest in that it is the first model to fit excess power-vs-loading fraction data of McKubre et al. (SRI International/EPRI) and, independently, that of Kunimatsu et al. (IMRA). Of special note is that the peak of the theoretical curve of tritium production versus loading fraction, which is related to that for neutrons by a branching ratio scaling factor, is found to be at a fractional D/Pd loading of approximately 0.825, which is in good agreement with the empirical value of 0.83 announced at the ICCF-5 by Iwamura et al. (Mitsubishi) for both tritium and neutrons. It is of interest then that this theoretical ECFM tritium production curve arises essentially from purely statistical mechanical considerations involving the deuteron occupation of the three-dimensional interstitial lattice, rather than arising from the details of a specific nuclear mechanism. The model shows why tritium is ordinarily not observed when excess heat is being observed. For the neutron-to-triton branching ratio a theoretical lower limit $(r/R)^{12}$ results (r is the protonic charge radius and R is the deuteronic charge radius) yielding a value of 2×10^{-9} in agreement with the empirical value of 2×10^{-9} for the neutron-to-triton branching ratio.

INTRODUCTION: REVIEW OF THE ECFM

The author's ECFM [6] ("Electron Catalyzed Fusion Model") employs collapsed electron orbits catalyzing genuine cold fusion reactions between deuterons within the Pd. The orbital collapse is hypothesized to be the result of the weakening of the zero point field induced by the cathodic environment, as explained in reference [6]. It is based upon work of Boyer [1,2] and Puthoff [3] according to which, on the basis of "stochastic electrodynamics" (SED), the electronic ground state of an electron in an atom is a dynamic state in which the energy radiated away by the accelerating electron is compensated for by stimulated absorption from the zero point electromagnetic field. The ECFM has been highly successful at fitting data on excess power versus loading fraction, S, for the data of McKubre et al. [4], (SRI International/EPRI)] as shown in Fig. 1, and for the data of Kunimatsu et al. [5] (IMRA)].

STATISTICAL MECHANICAL PICTURE: TRITIUM /NEUTRON PRODUCTION VS. HEAT PRODUCTION

Much of the dependence in the ECFM of the formulas for power or particle production upon S (fractional loading) arise from strictly statistical features of the deuteron occupation of the interstitial lattice. To that extent the S-functionality is independent of a specific nuclear mechanism and therefore exploitable. Thus,

the experimental corroboration of such nuclear mechanism nonspecific behavior would provide additional proof that the phenomenon is genuine.

Fig. 1 Comparison of ECF Model with Data of McKubre et al. (SRI-EPRI)

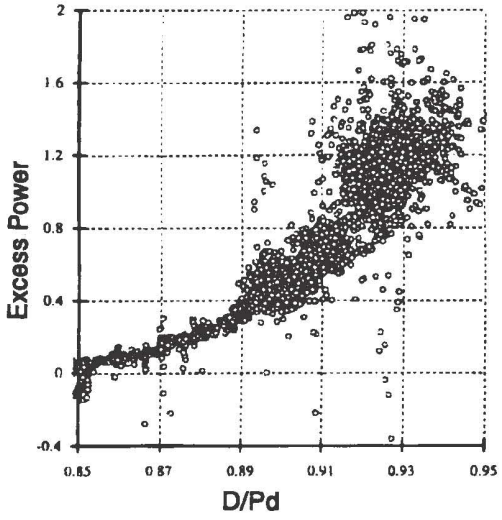

Fig. 2 Relative Tritium Produciton Rate vs. Loading (ECFM)

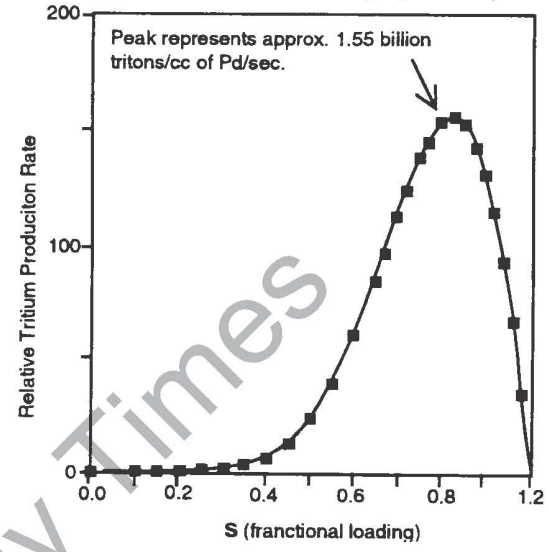

Consider a 1-dimensional interstitial lattice configuration:
(Key: • represents an interstitial D, o represents an empty interstitial site.)

o • o • o • o • o • o . . . . etc.

(1) represents a hypothetical one dimensional lattice configuration for which no cold fusion occurs due to a lack of nearest-neighbor D's.

Clearly, then, any expression for excess power will contain a factor that is a function of loading fraction, S, and arises strictly from the statistical mechanical picture accounting for the different possible interstitial lattice configurations that can contribute to cold fusion. Quoting from ref. [6], we make the distinction in the context of the model between the situation for heat production and that of triton production. (At this stage we merely note that neutron production is linked to triton production in the ECFM via a branching ratio.) We hypothesize that the cold fusion reaction D + D → He^4 + 24 MeV occurs for lattice configurations with nearest-neighbors on either side to produce a "sideways charge polarization" of the D's with protons directly opposite neutrons so that collisions are highly "guided" (lattice assisted anti-Tokamak regime):

o • • • o + o • • • • o + o • • • • • o + ... etc (2)
(S^3) (S^4) (2^5)

Thus, each D near the center of these configurations sees a nearest-neighbor D on either side. It is further hypothesized that tritium and neutrons result from the opposite situation; viz. the oscillatory collision of two nearest-neighbor D's isolated from their neighbors for which charge polarization favors neutronic components of the D's facing each other, thus heavily favoring tritium production via D + D → T + p + 4.03 Mev as an Oppenheimer-Phillips type nuclear reaction:

o • • o + o • • o • • o + o • • o • • o • • o +. . . .etc (3)
$(1 - S)^2 S^2$ $(1 - S)^3 S^4$ $(1 - S)^4 S^6$

For He^4 production the configurations in (2) yield a sum of probabilities (dependent upon fractional occupation, S):

$$p = S^3 + S^4 + S^5 + \ldots \quad \text{etc.} \tag{4}$$

that, when combined with other considerations, leads to an expression for excess power production given by

$$P_{exc} = (26.07) \bullet \{[(2 - S)/(1 - S)]^3 S\} \bullet (e^{\theta/T} - 1)^{-1} \bullet 10^{[23.6 - (24.774)S \exp -1/12]} \tag{5}$$

TRITIUM PRODUCTION ON THE BASIS OF THE ECFM

From (3) the sum of the probabilities is

$$p = (1-S)^2S^2 + (1-S)^3S^4 + (1-S)^4S^6 + \ldots \text{ etc.} \tag{6}$$

Ref. [6] shows that this leads to the following

$$N(S,T) = (6.789 \times 10^{12}) \bullet S(1-S)[1 - (1-S)S^2]^{-3} \bullet (e^{\theta/T} - 1)^{-1} \bullet 10^{[23.6 - (24.774)S \exp -1/12]} \tag{7}$$
(Tritons/cm^3/sec)

Fig. 2 shows a graph of triton production rate (tritons/cm^3 of Pd.sec) based upon (7) for a temperature of 60°C showing a peak value of about 1.6 x 10^9 tritons/(cm^3 of Pd.sec.). A computer study of the S-dependent part of (7) shows that the peak of the production curve is located at about S=0.825. This is of some interest since it was reported by Iwamura et al. [7] (Mitsubishi) at the ICCF-5 that tritium production was maximized at about S=0.83. (Presumably the uncertainty in their experimental result would put this in reasonable agreement with S=0.825). In a second ICCF-5 paper Iwamura et al. [8] reported that neutron emission was also maximized at about S=0.83. This feature is of special interest here since the ECFM simply relates neutron production to triton production via a branching ratio; i.e., the theoretical neutron production curve is simply a uniformly scaled down version for that of tritium.

In their abstract, Iwamura et al. [7] note that they had "previously reported that neutron emissions and tritium production were observed even with low deuterated palladium metals (D/Pd = 0.66). It is expected that the yield of nuclear products will increase using highly deuterated palladium metals (D/Pd = 0.8), since it has been widely recognized that anomalous nuclear effects are related to the D/Pd ratio." In this regard, note from Fig. 2 that the theoretical tritium (or neutron) production rate at S=0.66 would be about half of what it is at the peak of about S=0.83. Additionally, we note from Fig. 2 that the curve plunges more steeply with S to the right of the peak than to the left. It is this latter feature that accounts for two general observations: (1) Tritium production is rarely observed simultaneously with excess heat production [Recall that excess power grows with increasing values of S above about 0.8.] (2) Neutron emission decreases as excess power increases. With regard to (2) note that Takahashi et al.[9] (Osaka University) in their ICCF-5 abstract state that "the neutron emission rate was about 2n/s at most and appeared to decrease when the excess heat rates increased, as was the case for our 1922 experiments." The present author [10] has reported observing a decrease in the emission rate of thermal neutrons as excess heat increases. Finally the neutron emission rate reported by Takahashi et al. [9] of about 2n/s is apparently in reasonable agreement with the prediction of the ECFM, which is now shown: Note from Fig. 2 the value of 1.55 billion tritons/ cc of Pd.sec. Multiplying this by the theoretical branching ratio

of 1.64 x 10^{-9} given in the next section yields a neutron production rate of about 2.54 neutrons/cc of Pd.sec. [In reference [6], Fig. 8 shows the theoretical tritium production vs S (ECF Model) for three different temperatures (100°C, 600°C, and 1200°C) and emphasizes that the production peak does not shift with temperature, but remains fixed at about S=0.825.]

NEUTRON PRODUCTION

Based upon the ECFM [6], neutron production is given by N in (7) multiplied by an appropriate branching ratio highly favoring (T,p)-production over (He^3,n)-production. The author [11] has derived an extreme limiting branching ratio based upon charge polarization considerations, which reduces to a good approximation to

$$BR = (r/R)^{12} \tag{8}$$

where r is the protonic charge radius, and R is the deuteronic charge radius. Substituting r = 0.8x10^{-13}cm, and R = 4.31x10^{-13}cm, from DeBenedetti [12], yields

$$BR = 2 \times 10^{-9}, \tag{9}$$

which compares well with the best experimental value [13] for the smallest branching ratio given by about

$$(BR)exp = 2 \times 10^{-9}. \tag{10}$$

ACKNOWLEDGMENTS

H. Fox, Head of the F.I.C. and Editor of Fusion Facts, is thanked for his considerable encouragement of my work. **J. Bockris** is thanked for his encouragement and for financial support in connection with my participation in the Texas A&M Conference organized by **Bockris** and **G. Lin. T. Passell (EPRI)** is thanked for his encouragement and for his interest in the Cal Poly project. **ENECO, Inc**. (Salt Lake City, UT), and especially **Fred Jaeger** (CEO) is greatly appreciated for its encouragement and support of the Cal Poly cold fusion program. **Proteus Processes and Technology, Inc**. (Denver, CO) are thanked for their encouragement and support of my research. In particular, **Joe Ignat** (CEO) and **Ron Flores** are especially thanked in this regard. **Tim Shoemaker (Head)** and **Jeanne O'Neill** of the Cal Poly (Pomona) College of Science Instructional Support Center are appreciated for their help with the preparation of the two manuscripts. **James Djunaedy**, Cal Poly undergraduate electrical engineering major from Semarang, Indonesia, is thanked for some number crunching. Finally, Cal Poly (Pomona), and especially the Physics Department and the College of Science is appreciated for their support.

REFERENCES

1. Boyer, Phys. Rev. D., **11**, 790 (1975).
2. Boyer, Phys. Rev. D, **11**, 809 (1975).
3. Puthoff, "Ground State of Hydrogen as a Zero-Point-Fluctuation Determined State", Phys. Rev. D, **35**, 3266 (1987).
4. McKubre, Crouch-Baker, Riley, Smedley, and Tanzella, "Excess Power Observations in Electrochemical Studies of the D/Pd System; the Influence of Loading, Proc. ICCF-3, Universal Academy Press, Inc. (Tokyo), 5 (1993).
5. Kunimatsu, Hasegawa, Kubota, Imai, Ishikawa, Akita, and Tsuchida (IMRA), "Deuterium Loading Ratio and Excess Heat Generation during Electrolysis of Heavy Water by a Palladium Cathode

in a Closed Cell Using a Partially Immersed Fuel Cell Anode", Proc. 3-ICCF, 31 (1993).
6. Bush, "A Unifying Model for Cold Fusion," Transactions of Fusion Technol., December 1994, **26**, No. 4T, p. 431.
7. Itoh, Iwamura, Gotoh, and Toyoda, "Observation of Nuclear Products Under Vacuum Condition from Deuterated Palladium with High Loading Ratio, Proc. ICCF-5, Monte Carlo, April 9-13, 1995.
8. Iwamura, Gotoh, Itoh, and Toyoda, "Characteristic X-ray and Neutron Emissions from Electrochemically Deuterated Palladium", Proc. ICCF-5, Monte Carlo, April 9-13, 1995.
9. Takahashi, Miyamaru, Inokuchi, Chimi, Ikegawa, Kaji, Nitta, Kobayashi, and Taniguchi, "Experimental Correlation Between Excess Heat and Nuclear Products," **Proc. ICCF-5**, Monte Carlo, April 9-13, 1995.
10. Bush and Eagleton, "Neutron Emission from Electrolytic Cells: Correlation With Current Density," Poster at ICCF-2, Como, Italy, June 31-July 4, 1991.
11. Bush, " 'Cold Fusion': The Transmission Resonance Model Fits Data on Excess Heat, Predicts Optimal Trigger Points, and Suggests Nuclear Reaction Scenarios," Fusion Technol., **19**, 313 (1991).
12. DeBenedetti, Nuclear Interactions, John Wiley & Sons, New York (1966).
13. Storms, Los Alamos National Laboratory, Personal communication, June, 1990.

* This paper constitutes the major source for the author's talk at the T.A.M. Conference, "Can the ECFM ("Electron Catalyzed Fusion Model") Account for Light Water Cold Fusion?")

APPLICATION OF THE NUCLEON CLUSTER MODEL TO EXPERIMENTAL RESULTS

R.A. Brightsen (Author of Concept)
Clustron Sciences Corporation
1917 Upper Lake Drive Reston, VA 22091
Phone: 703-476-8731 FAX; 703-827-4066
Presented by Randy Davis

ABSTRACT

According to the Nucleon Cluster Model and the Periodic Table of Beta-Stable Nuclides, the proton **must** contain antimatter clusters as well as positive matter clusters. Within palladium cathodes, antimatter clusters are strongly attracted to matter clusters of the same type, **avoiding** the so--called "coulomb barrier." The resulting reactions produce the many different radioactive species recently reported for cold fusion experiments. The **^{104}Pd (p,α) ^{101}Rh** reaction is discussed as an example.

The Nucleon Cluster Model (NCM) provides a pathway for experimentalists to understand the results that they obtain in the laboratory in the study of low temperature transmutations/low energy reactions. In the future, it may permit experiments to be tailored to obtain particular results desired. This briefing (Slide 1) describes one of the ways that the NCM can be applied, by considering the results reported earlier by Dr. Tom Passell in the lead-off presentation of today's meeting on Low Energy Nuclear Reactions. The species that were observed by Dr. Wolf are explained by the Nucleon Cluster Model as having been produced by matter-antimatter reactions. The attached paper, "General Explanation of Radioactivities Reported by Dr. Wolf as Described by Dr. Passell (EPRI) at Monaco," provides supporting detail. The paper was written by Ron Brightsen of Clustron Sciences, who is the developer of the Nucleon Cluster Model.

Before discussing the physics involved, I would like to say that Ron Brightsen can be called upon to assist you in applying the NCM to your experimental results. As this field of investigation becomes a mature technology, we will also be available in the Washington. D.C. area to assist in developing proposals and programs for federal funding. Mr. Brightsen can be contacted through the telephone and address given, or through my email address (rhame@aol.com).

The NCM was developed (Slide 2) over many years of investigation by Mr. Brightsen, who lives in Reston, Virginia. While at MIT, beginning in the late 1940s, he became interested in the structure of nuclei due to the theory of Maria Mayer which indicated that nuclei with certain numbers of protons or neutrons are more stable than other nuclei. The "magic numbers" that indicated greater stability included, for example: 20, 50, 82 and 126. To him, this was a clear indication that nuclei must have some type of structure, rather than simply consisting of neutrons and protons without any particular order. He was also concerned that no beta-stable nuclear species exist for atomic numbers (Z) of 43 and 61, or for neutron numbers (N) of 19, 21, 35, 39, 45, 61, 71, 89, 115, 123, and 147. Shouldn't stable isotopes with all numbers of protons and neutrons be possible if protons and neutrons truly are the basic building blocks of nuclei?

By studying the entire range of approximately 340 beta-stable nuclei, Mr. Brightsen discovered that all stable nuclear species are arranged in a systematic manner around particular nuclear species, having certain

mass and charge numbers, which he has identified as "centers of symmetry." Furthermore, the nuclei are arranged in symmetric patterns around these particular centers of symmetry. Importantly, these symmetric patterns indicate that one nucleus may be related to another nucleus by the addition of a neutron-proton (NP) cluster, or an NPN cluster, or a PNP cluster. This is an important observation. It is not possible to draw this conclusion unless all three relationships are considered. Thus, beta-stable nuclei must consist of NP, NPN, and PNP clusters.

Through further research, Mr. Brightsen was able to describe all of the 340 beta-stable nuclei in a completely systematic, periodic and symmetric manner. He developed a detailed table depicting the centers of symmetry and the numbers of each of the types of clusters (NP, NPN, and PNP) for each nuclide. The results of this effort are described in a paper, "The Nucleon Cluster Model and the Periodic Table of Beta-Stable Nuclides," which is available from Clustron Sciences Corporation ($5 is requested to cover copying and postage). The Periodic Table of Beta-Stable Nuclides in Figure 21 of that paper is analogous to the Periodic Table of Elements discovered by the Russian Scientist Mendeleev in 1869. It is believed that this NCM description is correct due to the symmetry of nature that it is able to demonstrate. The model is also able to show that "missing" proton and neutron numbers, mentioned above, are only an artifact of the way that isotopes have been described in the past (reference the DOE/GE/Knolls Atomic Power Laboratory Chart of the Nuclides) [1].

Based on this understanding, Clustron Sciences Corporation has filed patent applications on several processes that may be developed through application of the Nucleon Cluster Model. These include: methods for converting radioactive nuclear wastes to short-lived or stable isotopes; methods for converting Pu-239 to U-235 and/or non-fissionable heavy nuclides; and, methods for improving the performance of silicon-based semiconductors. Further work with the model is being pursued to explain the origin of the elements and missing mass in the universe.

The importance of the Nucleon Cluster Model to the field of nuclear physics, in general, and low temperature transmutations/low energy reactions, in particular, results from the discovery that low mass nuclei must contain antimatter clusters to various degrees, in addition to positive matter clusters. In addition, it is evident that any stable or radioactive isotope may be described by several different combinations of matter and antimatter NN, PP, NP, NPN and PNP clusters. Matter-antimatter clusters not only attract each other due to their opposite nature, but, when identical, annihilate when they come into contact.

Dr. Wolf's measurements of ^{103}Ru, ^{99}Rh, ^{101}Rh, ^{102}Rh, ^{105}Ag, ^{106m}Ag and ^{110m}Ag in palladium samples are the result of matter-antimatter reactions between palladium isotopes and normal hydrogen (Slide 3). ^{101}Rh, for example, is produced by hydrogen reacting with ^{104}Pd through a type of (p, α) reaction. In this case, ^{104}Pd can be considered to consist of 16 NP clusters, 18 NPN clusters, and 6 PNP clusters, along with other possible cluster combinations. Protium (the hydrogen nucleus) can be considered to consist of 5 NP clusters, 2 antimatter NPN clusters, and 1 antimatter PNP cluster. When these interact, ^{101}Rh is produced with 19 NP clusters, 16 NPN clusters, and 5 PNP clusters along with ^{4}He with 2 NP clusters. Again, other cluster combinations are evident for both ^{101}Rh and ^{4}He. Similarly, the NCM representation can be developed for the other isotopes measured in Dr. Wolf's experiments.

REFERENCES

1. F. William Walker, et al. Nuclides and Isotopes, Fourteenth edition, c 1989, available from General Electric Co., Nuclear Energy Operations, 175 Curtner Ave. m/c 397, San Jose, California 95125

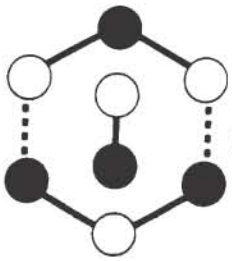

Clustron Sciences Corporation
1917 Upper Lake Drive
Reston, VA 22091
Phone: 703-476-8731
Fax: 703-827-4066

"General Explanation of Radioactivities
Reported by Dr. Wolf as Described by Dr. Passell (EPRI) at Monaco,"
by R.A. Brightsen.

Based on the Periodic Table of Beta-Stable Nuclides, the cluster structures of the six beta-stable isotopes of palladium can be represented as follows:

		NP	NPN	PNP	
46-Pd-102	→	18	16	6	
46-Pd-104	→	16	18	6	
46-Pd-105	→	15	19	6	Note constant PNP clusters
46-Pd-106	→	14	20	6	
46-Pd-108	→	12	22	6	
46-Pd-110		→	10	24	6

According to Dr. Passell, gamma ray spectrographs revealed no fewer than eight (8) radionuclides produced in the palladium cathode by low-energy Protons or deuterons:

47-Ag-110m, 45-Rh-99, 44-Ru-103, 47-Ag-106 m, 45-Rh-102, 46-Pd-100, 45-Rh-101, 47-Ag-105

Classical nuclear physics insists that, because of the "Coulomb barrier," these reactions can not take place. But experimental evidence proves, conclusively, that these radionuclides are produced. How can that possibly be? The Nucleon Cluster Model (NCM) provides the answer. Consider one reaction as an example:

Eq. 1 46-Pd-104 (proton, alpha) 45-Rh-101

In the NCM, the proton (1-H-1) structure requires the existence of antimatter clusters. Thus, the following five (5) structures can represent the proton:

NP	NPN	PNP
11	-4	-3
8	-3	-2
5	-2	-1
2	-1	0
-1	0	1

Let us examine Equation 1 in terms of clusters.

	NP	NPN	PNP
$^{104}Pd_{46}$	16	18	6
+			
$^{1}H_{1}$	5	-2	-1
	21	16	5
$^{101}Rh_{45}$	19	16	5
+			
$^{4}He_{2}$	2	0	0
	21	16	5

It is evident from these structures that the following reactions take place:

1) The 17th and 18th NPN in $^{104}Pd_{46}$ are annihilated by the two NPN antimatter clusters in the proton, and

2) The 6th PNP cluster in $^{104}Pd_{46}$ is annihilated by the one PNP antimatter cluster in the proton.

Since positives and negatives attract, there is no Coulomb Barrier for the reaction.

A comprehensive picture of this reaction follows:

$^{104}Pd_{46}$ + $^{1}H_{1}$ → $^{101}Rh_{45}$ + $^{4}He_{2}$

NP	NPN	PNP	NP	NPN	PNP	NP	NPN	PNP	NP	NPN	PNP
10	20	8	11	-4	-3	13	18	7	8	-2	-2
13	19	7	8	-3	-2	16	17	6	5	-1	-1
16	18	6	5	-2	-1	19	16	5	2	0	0
19	17	5	2	-1	0	22	15	4	-1	1	1
22	16	4	-1	0	1	25	14	3	-4	2	2

Similar analysis have been developed for the other observed radioisotopes.

NOTE: This paper appeared in the August 1995 issue of Infinite Energy. A copy of the definitive paper, entitled, "The Nucleon Cluster Model and the Periodic Table of Beta-Stable Nuclides," is available for $5.00, to cover copying and mailing costs, from Clustron Sciences Corporation.

Slide 1

APPLICATION OF NCM TO EXPERIMENTAL RESULTS

BACKGROUND

- CLUSTRON SCIENCES CORPORATION IS FAMILIAR WITH MANY OF THE MODELS PROPOSED TO EXPLAIN EXPERIMENTAL RESULTS THAT ARE INEXPLICABLE VIA CLASSICAL PHYSICS
- PURPOSE - TO PRESENT THE NCM EXPLANATION OF LOW ENERGY NUCLEAR REACTIONS
- CONSULTING ASSISTANCE IS AVAILABLE FOR APPLICATION OF THE NCM TO EXPERIMENTS

THE NUCLEON CLUSTER MODEL (NCM)

Mr. Ronald A. Brightsen
Clustron Sciences Corporation
1917 Upper Lake Drive
Reston, VA 22091
(703) 476-8731 VOICE
(703) 827-4066 FAX

TEAMS AVAILABLE TO SUPPORT GOVERNMENT DEFENSE PROGRAMS

Mr. Randolph R. Davis
44 Redding Ridge Drive
Gaithersburg, MD 20878
(301) 340-6052 VOICE
rhame@aol.com EMAIL
FAX available

Slide 2

NUCLEON CLUSTER MODEL

- IS A COMPLETELY SYSTEMATIC, PERIODIC AND SYMMETRIC DESCRIPTION OF ALL STABLE AND RADIOACTIVE ISOTOPES

- THE NCM "PERIODIC TABLE OF BETA STABLE NUCLIDES" FOR THE FIRST TIME IN THE HISTORY OF NUCLEAR PHYSICS INCORPORATES ALL KNOWN BETA-STABLE NUCLIDES
  (Ref. paper, "The Nucleon Cluster Model and the Periodic Table of Beta-Stable Nuclides," available from Clustron Sciences Corporation. The amount of $5.00 is requested to cover copying and postage)

- NCM DEMONSTRATES THAT ALL BETA-STABLE NUCLEI CAN BE DESCRIBED IN TERMS OF THREE CLUSTERS - NP, NPN, AND PNP

- NCM MAKES IT POSSIBLE TO EXPLAIN OTHERWISE INEXPLICABLE LOW-ENERGY NUCLEAR REACTIONS, SHORT-CIRCUITING THE COULOMB BARRIER

- OTHER APPLICATIONS OR IMPLICATIONS BEING PURSUED:
  - CONVERTING RADIOACTIVE WASTES TO SHORT-LIVED/STABLE ISOTOPES
  - CONVERTING Pu-239 TO U-235 OR TO NON-FISSIONABLE NUCLIDES
  - IMPROVING SILICON-BASED SEMICONDUCTORS
  - EXPLAINING ORIGIN OF THE ELEMENTS AND MISSING MASS

Slide 3

GENERAL EXPLANATION OF RADIOACTIVITIES REPORTED BY DR. WOLF AS DESCRIBED BY DR. PASSELL (EPRI) AT MONACO

- Ru-103, Rh-99, Rh-101, Rh-102, Ag-105, Ag-106m, Ag-110m OBSERVED IN PALLADIUM ELECTRODE (Ref. "Overview of the EPRI Program on Deuterated Metals," Thomas O. Passell, International Conference on Cold Fusion 5, Monaco, April 9-13, 1995)

- Pd-104 (11.4%) IS DEMONSTRATED BY THE NCM TO PRODUCE RH-101 THROUGH A LOW ENERGY (p,α) REACTION

46-Pd-104 + 1-H-1 ----------> 45-Rh-101 + 2-He-4

NP	NPN	PNP	NP	NPN	PNP	NP	NPN	PNP	NP	NPN	PNP
10	20	8	11	-4	-3	13	18	7	8	-2	-2
13	19	7	8	-3	-2	16	17	6	5	-1	-1
16	18	6	5	-2	-1	19	16	5	2	0	0
19	17	5	2	-1	0	22	15	4	-1	1	1
22	16	4	-1	0	1	25	14	3	-4	2	2

- SIMILAR ANALYSES HAVE BEEN DEVELOPED FOR OTHER RADIOACTIVE ISOTOPES

CORRESPONDENCE OF THE NUCLEON CLUSTER MODEL WITH THE CLASSICAL PERIODIC TABLE OF ELEMENTS

R.A. Brightsen
Clustron Sciences Corporation,
1917 Upper Lake Drive, Reston, VA 22091
Phone: 703-476-8731 Fax: 703-827-4066

The author has developed a new model of nuclear structure which is completely systematic, periodic and symmetric. This model is based on three "building blocks" for beta-stable nuclei: a neutron-proton cluster (NP), a neutron-proton-neutron cluster (NPN), and a proton-neutron-proton cluster (PNP). The author has been frequently asked questions by colleagues about how this new nuclear model relates to the Periodic Table of Elements, discovered by the Russian Mendeleev in 1869, and universally recognized by scientists throughout the world. This paper will deal with that relationship, and will demonstrate that there is a one-to-one relationship between the two models.

One of the first questions that must be asked is the following: Is there some commonality in the NCM that provides an explanation of the experimentally known stable isotopes of a given element? The answer lies in the relationship of NP clusters and NPN clusters. Let us, as an example, examine Fig. 1 giving nucleon cluster structures for the three stable isotopes of the element Magnesium (Z = 12), using NP = 3, 6 and 9 (a,b, and c).

Fig. 1 - Example: Nucleon Cluster Structures for Stable Isotopes of Magnesium

	a		b		c	
	(NP + NPN)	+ PNP	(NP + NPN)	+ PNP	(NP + NPN)	+ PNP
12-24	(3 + 3)	+ 3	(6 + 2)	+ 2	(9 + 1)	+ 1
12-25	(2 + 4)	+ 3	(5 + 3)	+ 2	(8 + 2)	+ 1
12-26	(1 + 5)	+ 3	(4 + 4)	+ 2	(7 + 3)	+ 1

Clearly, several key conclusions can be drawn from the above data:
1. Number of NP clusters decreases, the number of NPN clusters increases, and the sum of NP and NPN clusters is constant for each isotope of a given element.
2. The number of PNP clusters is constant for all isotopes of a given element.
3. The Z of an element is always given by (NP + NPN) + 2 x PNP.

One issue remains to be addressed - Does a systematic cluster relationship exist, for example, among cluster structures of the noble (rare) gases, as shown in the Periodic Table of Elements (He, Ne, Ar, Kr, Xe, and Rn)? For answers, let us examine Fig. 2.

Fig. 2 - Nucleon Cluster Description of He, Ne, and Ar

Z	Element	Symbol	(NP + NPN)	+ PNP	$= \Sigma_c$
2	Helium	He	2 +	0 = 2	
8			4	2 6	6
10	Neon	Ne	6 +	2 = 8	
8			4	2 6	6
18	Argon	Ar	10 +	4 = 14	

Let us also examine the cluster structures of some of the alkali elements, in Fig. 3.

Fig. 3 - Nucleon Cluster Description of Li, Na, and K

Z	Element	Symbol	(NP + NPN)	+ PNP = Σ_c	
3	Lithium	Li	3	+ 0 = 3	
8			4	2 6	6
11	Sodium	Na	7	+ 2 = 9	
8			4	2 6	6
19	Potassium	K	11 +	4 = 15	

The regular systematics of the data in these two figures, in turn, lead to the following:

Following the systematics, clearly indicated in Fig. 4, a complete "Atomic and Nuclear Periodic Table of Elements and Beta-Stable Isotopes of Each Element" has been completed. It is expected to be commercially available in wall-chart form in the near future.

*A comprehensive paper entitled, "The Nucleon Cluster Model and the Periodic Table of Beta-Stable Nuclides," is available from Clustron Sciences Corporation for a fee of $5.00 to cover reproduction and postage. This paper is also available on the world wide web at http://www.gslink.com/~ncmcn/Clustron/

Fig. 4 - Periodic Table - Atomic and Nuclear - Corresponding to Halides, Noble Gases, Alkalis and Alkaline Elements

		NP + + PNP = Σ_c NPN		NP + + PNP = Σ_c NPN		NP + + PNP = Σ_c NPN		NP + + PNP = Σ_c NPN
1	Hydrogen (H)	1 + 0 = 1	2 Helium (He)	2 + 0 = 2	3 Lithium (Li)	3 + 0 = 3	4 Beryllium (Be)	4 + 0 = 4
9	Flourine (F)	5 + 2 = 7	10 Neon (Ne)	6 + 2 = 8	11 Sodium (Na)	7 + 2 = 9	12 Magnesium (Mg)	8 + 2 = 10
17	Chlorine (Cl)	9 + 4 = 13	18 Argon (Ar)	10 + 4 = 14	19 Potassium (K)	11 + 4 = 15	20 Calcium (Ca)	12 + 4 = 16
35	Bromine (Br)	23 + 6 = 29	36 Krypton (Kr)	24 + 6 = 30	37 Rubidium (Rb)	25 + 6 = 31	38 Strontium (Sr)	26 + 6 + 32
53	Iodine (I)	37 + 8 = 45	54 Xenon (Xe)	38 + 8 = 46	55 Cesium (Cs)	39 + 8 = 47	56 Barium (Ba)	40 + 8 = 48
85	Astatine (At)	63 + 11 = 74	86 Radon (Rn)	64 + 11 = 75	87 Francium (Fr)	65 + 11 = 76	88 Radium (Ra)	66 + 11 = 77

Atomic and Nuclear
Periodic Table of Elements and Isotopes
(Based upon the Nucleon Cluster Model of the Atomic Nucleus)

No. of PNP clusters	No. of elements
0	4
1	4
2	4
3	4
4	4
5	14
6	4
7	14
8	4
9	14
10	14
11	4
12	14
13	4

ΔZ

	8	8	18	18	32
Halogen elements	1*	9	17	35	53	85
Noble Gas elements	2	10	18	36	54	86
Alkali elements	3	11	19	37	55	87
Alkaline elements	4	12	20	38	56	88

* new assignment

1 H 1+0=1	2 He 2+0=2	3 Li 3+0=3	4 Be 4+0=4														
5 B 3+1=4	6 C 4+1=5	7 N 5+1=6	8 O 6+1=7														
9 F 5+2=7	10 Ne 6+2=8	11 Na 7+2=9	12 Mg 8+2=10														
13 Al 7+3=10	14 Si 8+3=11	15 P 9+3=12	16 S 10+3=13														
17 Cl 9+4=13	18 Ar 10+4=14	19 K 11+4=15	20 Ca 12+4=16														
21 Sc 11+5=16	22 Ti 12+5=17	23 V 13+5=18	24 Cr 14+5=19	25 Mn 15+5=20	26 Fe 16+5=21	27 Co 17+5=22	28 Ni 18+5=23	29 Cu 19+5=24	30 Zn 20+5=25	31 Ga 21+5=26	32 Ge 22+5=27	33 As 23+5=28	34 Se 24+5=29				
					35 Br 23+6=29	36 Kr 24+6=30	37 Rb 25+6=31	38 Sr 26+6=32									
39 Y 25+7=32	40 Zr 26+7=33	41 Nb 27+7=34	42 Mo 28+7=35	+ 43 Tc 29+7=36	44 Ru 30+7=37	45 Rh 31+7=38	46 Pd 32+7=39	47 Ag 33+7=40	48 Cd 34+7=41	49 In 35+7=42	50 Sn 36+7=43	51 Sb 37+7=44	52 Te 38+7=45				
					53 I 37+8=45	54 Xe 38+8=46	55 Cs 39+8=47	56 Ba 40+8=48									
L 57 La 39+9=48	L 58 Ce 40+9=49	L 59 Pr 41+9=50	L 60 Nd 42+9=51	L + 61 Pm 43+9=52	L 62 Sm 44+9=53	L 63 Eu 45+9=54	L 64 Gd 46+9=55	L 65 Tb 47+9=56	L 66 Dy 48+9=57	L 67 Ho 49+9=58	L 68 Er 50+9=59	L 69 Tm 51+9=60	L 70 Yb 52+9=61				
L 71 Lu 51+10=61	72 Hf 52+10=62	73 Ta 53+10=63	74 W 54+10=64	75 Re 55+10=65	76 Os 56+10=66	77 Ir 57+10=67	78 Pt 58+10=68	79 Au 59+10=69	80 Hg 60+10=70	81 Tl 61+10=71	82 Pb 62+10=72	83 Bi 63+10=73	84 Po 64+10=74				
					85 At 63+11=74	86 Rn 64+11=75	87 Fr 65+11=76	88 Ra 66+11=77									
A 89 Ac 65+12=77	A 90 Th 66+12=78	A 91 Pa 67+12=79	A 92 U 68+12=80	A 93 Np 69+12=81	A 94 Pu 70+12=82	A 95 Am 71+12=83	A 96 Cm 72+12=84	A 97 Bk 73+12=85	A 98 Cf 74+12=86	A 99 Es 75+12=87	A 100 Fm 76+12=88	A 101 Md 77+12=89	A 102 No 78+12=90				
					A 103 Lr 77+13=90	104 Rf 78+13=91	105 Ha 79+13=92	106 Sg 80+13=93									

LEGEND

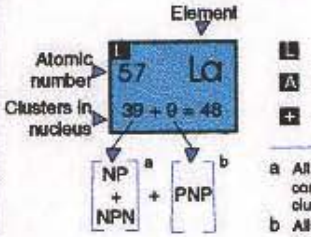

L = Lanthanide series
A = Actinide series
+ = All isotopes are beta-active

a All isotopes of an element have a constant number of (NP+NPN) clusters
b All elements have a constant number of PNP clusters

EXCESS HEAT EVOLUTION AND ANALYSIS OF ELEMENTS FOR SOLID STATE ELECTROLYTE IN DEUTERIUM ATMOSPHERE DURING APPLIED ELECTRIC FIELD

Tadahiko Mizuno, Tadashi Akimoto
Kazuhisa Azumi, Masatoshi Kitaichi, and
Kazuya Kurokawa
Hokkaido Univ., Kitaku, North 13 West 8, Sapporo 060 Japan

Michio Enyo
Hakodate National College of Technology, Tokuracho 14-1, Hakodate 042 Japan

ABSTRACT

A proton conductor, the solid state electrolyte, made from oxide of strontium, cerium, niobium and yttrium can be charged in a hot D_2 gas atmosphere to produce excess heat. Anomalous heat evolution was observed for 12 in 80 cases of the samples charged by alternating current for 5 to 45 Volts at temperatures ranging from 400 to 700°C. Several kinds of alkali metals, Ca, Mg, Bismuth, Lantanides and Aluminum were locally segregated and distributed around the melted and swelled parts of the samples that generated an excess heat.

INTRODUCTION

The alleged Cold Fusion reaction still has not been confirmed because of lack of data. It is very important to obtain precision relationships quantitatively between each reaction products that may cause the reaction. We understand that the most desirable parameter to analyze the reaction mechanism is to obtain simultaneously all the quantities such as heat evolution, neutron emission, tritium generation, and so on. However, unfortunately, this is very difficult due to difficulties to reproduce and control the phenomena. Even if it has been possible, usually the amounts of reaction products are very low and sometimes nearly or under the detection limit; it is difficult to calibrate quantitatively. Therefore, it is suitable to analyze the element in the sample before and after the experiment.

EXPERIMENTAL

Samples were made from a mixture of metal oxide of Sr, Ce, Y and Nb. The procedures were developed by Iwahara et al. [1-3]. These powdered oxides were first mixed, and then sintered in an electric furnace at 1,400° C in air for 16 hours. The samples were pulverized, and mixed, alcohol was added, and the samples were put in a pressing machine and formed into round plates of 20 mm in diameter and 1 mm thick. These plates were again sintered at 1,300-1,480° C in air for 16 hours. Sample densities ranged from 3.0 to 5.2; the theoretical density for perfectly sintered sample is 5.8. Both sides of the sintered sample were then coated with porous Pt film, by painting a Pt organic compound and deposition in 700° C or coated by Ar sputtered to Pt in vacuum. The resulting Pt film thickness was 0.15-0.3 μm. The film is porous and has a very rough surface; Hydrogen gas easily passes through the film and reaches to ceramic surface.

Experimental arrangement is shown in Fig. 1. The sample was heated to a constant temperature with an electric heater covered with stainless steel. Electric power was supplied from a stabilized power source. The electric fields of constant voltage (Electric power of proton driving: EPD) was supplied from a

function generator via a power amplifier. Pressure was measured by a capacitance manometer with 0.1 Torr accuracy. Temperatures were recorded with 0.1° C accuracy by three thermocouples that were coated by a thin stainless cover. All parameters, EPD (voltage and electric current), heater power, sample temperature, gas pressure and cylinder wall temperature were recorded through a data logger and computer to floppy diskette. The reaction cell is made by a stainless steel cylinder 40 cm long, 20 cm in diameter, with walls 5 mm thick.

Upper part of the cell is shown in Fig. 2. The sample is held on both sides by 0.3 mm thick Pt plates which are in turn sandwiched between 0.3 mm thick Pt plates. Three thermocouples with thin stainless steel are pressed directly on the upper Pt plate. The Pt plates make electrical and thermal contact with ceramic sample and thermocouples. This part is fixed on place of heater part. Spiral heater wire covered with ceramic insulator is also connected to the bottom part of the sample. EPD power was supplied through copper wires of 1.6 mm in diameter. The sample holder is surrounded by Ni plate reflectors. The holder is fixed with four supports made of 6 mm diameter stainless steel rods that were covered by alumina insulator. Four nuts attached under the support rods pressed Pt plate, alumina spacer and sample to make tight contact with thermocouples. These thermocouples have a spring action. The components are welded to the cell cover flange that have several electric connectors. The connectors introduce thermocouple, electric power lines for the heater and electric field supply for the sample.

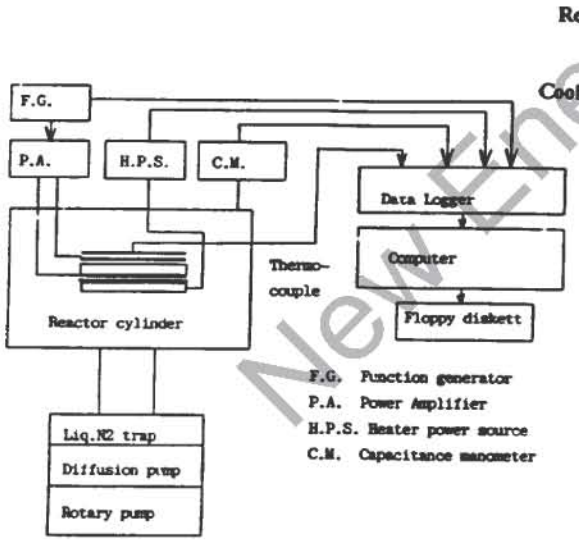

Fig. 1 Schematic representation of the measurement system.

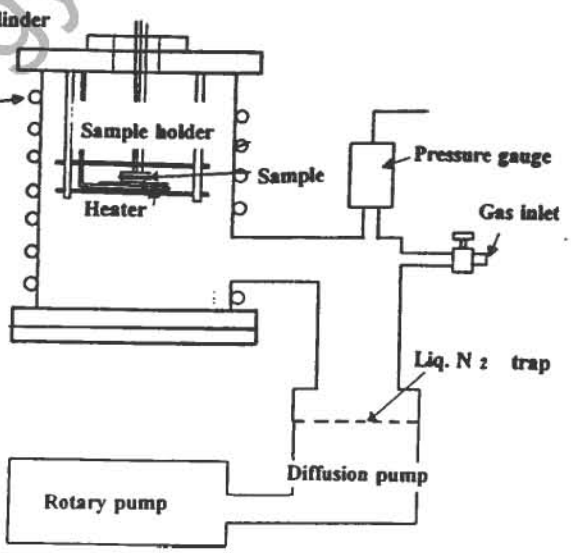

Fig. 2 Experimental set up.

Experimental procedures are described as follows: (1) The reactor cylinder is evacuated by a rotary and diffusion pump (with liq. N_2 trap) to 2 x 10^{-5} Torr. (2) Sample temperature is raised to 400-700° C. (3) Gas is introduced into the cylinder at 0.1-50 Torr. (4) The sample is charged with EPD power at 5-45 Volts alternating power, with frequency set between 10^{-4} and 1 Hz depending on the sample temperature and thickness. (5) All the samples were analyzed for element detection by EPMA, ICP and EDS analyzer.

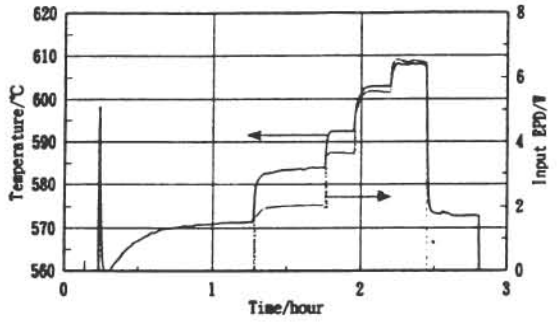

Fig. 3 Temperature change due to input EPD in H_2 gas.

RESULTS
HEAT MEASUREMENTS

The relationships between input EPD and temperature were calibrated with a dummy sample and a ceramic heater. Next relationship is obtained between temperature (T) and EPD (E) in the range from 400 to 700° C as follows:

$$E = A \exp BT \qquad (1)$$

A and B are constants that are caused from gas kinds, pressure and sample dimensions. We obtained, for example, 6.4 ° C temperature rise for one watt input EPD in 10 Torr of D_2 gas at 500° C with 2 cm diameter and 1 mm thickness of sample. The excess heat generation can be readily estimated from the relationship.

Fig. 3 is a typical result obtained in 13 Torr of H_2 gas; this has not shown any excess heat generation. All the temperature changes are caused with input EPD deviation. However, Fig. 4 shows a relation between temperature and EPD input (a) and estimating of typical excess heat evolved (b), in 12 Torr of D_2 gas. With only heater power supplied, the sample temperature rose to 50° C and almost stabilized. After 3 hour EPD input of + 26 V, 0.001 Hz was supplied. At 4.6 hours the sample temperature rose 625° C and excess heat was clearly generated after the time (Fig. 4b). Input EPD varied unstably and cannot be kept constant input power because the EPD currents are effected with temperature change. After the EPD power off, characteristic phenomena were seen; excess heats were evolved during an hour. Total excess heat evolution is estimated as 11 K joule.

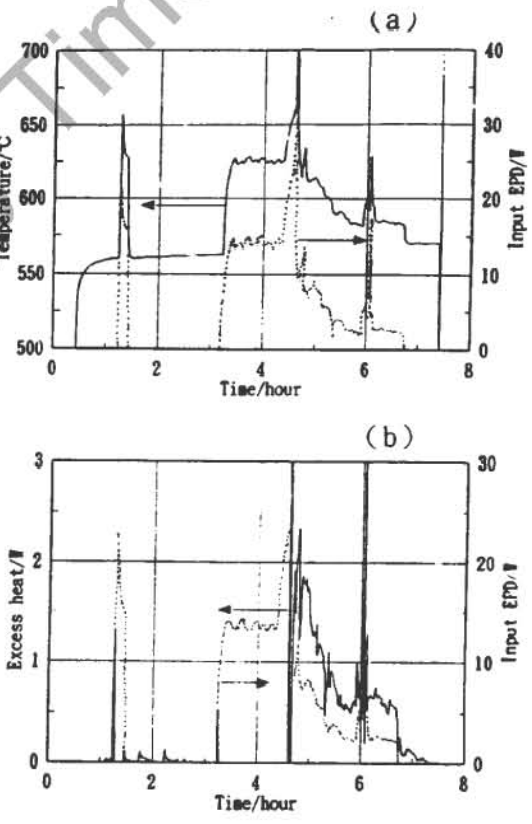

Fig. 4 Changes of temperature and EPD input in D_2 gas (a), changes of excess heat (b).

ANALYSIS OF ELEMENTS

All the samples, including no excess heat, were analyzed by EPMA, ICP, EDS and SEM observation. Fig. 5, for example, shows the sample surface observation by SEM; many holes and swelled parts can been seen. The EDS analysis shows the existence of Al, Sm and Gd elements around the parts. These elements exist locally near the changed parts of the sample. Fig. 6 shows the element mapping for the sample surface (a) and cross section (b) by EPMA.

Characteristic phenomenon can be seen for Sr and Ce concentrations; these concentration profiles show an opposite relation. High Sr concentration areas coincidences with low Ce concentration profile. They are a reverse profiles. Other additive elements, Nb and Y show no change and kept the same concentrations as before while Pt film is almost peeled off around the swelled and melted parts.

Aluminum exists around the changed parts at the sample and it also can be detected in the bulk layer. However, Ca is only found under the surface layer in the changed parts; it strongly segregates locally. Mg distributes widely around the changed parts and shows lower concentration than the Ca. Other lanthanides cannot be detected by the EPMA method because of their low concentration value.

Several samples were analyzed for element change by ICP method. Table 1 is the ICP result; Each case shows the average value of five for the before and the no excess heat samples and 10 of excess heat evolved samples. Significant increase can be seen for Mg, Ca, Al, Sr, Fe, Bi, Sm, Gd and Dy. Other impurities are also increased in each case; this phenomenon can be considered due to contamination from the surround. Ceramic samples are sintering material having many holes and porous; they are easily contaminated. However, former elements show clear increase after excess heat generation.

CONCLUSION

All previous attempts at Cold Fusion experiments can be classified as either wet or dry loading of hydrogen isotopes. Contrary to previous works, the initial attempts have been done by Granite et al. (4). They thought it would be useful to combine the wet and dry methods to apply electrochemical potential in the gas phase. They employed ß-alumina specimens for the study and sometimes observed few emission of neutrons as low as the background. The ß-alumina is unstable at high temperature up to 300° C and shows no proton conductivity. Meanwhile, lattice type proton conductors such as perovskite oxide kept steady proton conductivity high as the temperature region around 1000° C. Excess heat usually evolved certain time lag after applying the input power. Proton mobility at the temperature is easily obtained using the Nernst-Einstein relation as follows:

$$D/RT - \sigma/nZ^2e^2 \qquad (2)$$

Here, **Ze** is charge number as 1 for $\mathbf{D}^+$, n ion density in the sample that obtained from current density. Proton mobility 4 x 10^{-6} at 450° C and 1.05 x 10^{-5} at 540° C $cm^2/s \cdot V$ obtained by the relation are same as Yajima data (5). However, the time lag between the occurring excess heat evolution and the supply of input power is almost ten times larger than the time that obtained the relationship for the case of proton reach a side to another one. And the excess heats clearly decreased after ceased the input power supply. This phenomenon suggests that the excess heat evolution may be induced by deuterium flow in the conductor accelerated by an electric field. Only five samples in fifty showed the excess heat evolution. Also, the construction and composition of the proton conductor can be considered an important factor that decides the reaction of excess heat evolution. Clear increase of several element such as Al, Ca, Mg, Bi, Sm, Gd and Dy. It is still under consideration that the elements are reaction products of requisite existence for the Cold Fusion.

REFERENCES

1. H. Iwahara, T. Esaka, H. Uchida and N. Meda, *Solid State Ionics*, 3/4, 359 (1981).
2. H. Iwahara, H. Uchida, K, Kondo and K. Ogaki, *J. Electrochem. Soc.*, 135, 529 (1988).
3. T. Yajima, K. Koide, K. Yamamoto and H. Iwahara, *Denki Kagaku*, 58, 547 (1990).

4. E. Granite and J. Jorne, *J. Electroanal. Chem.*, 317, 285 (1991).
5. T. Yajima, Doctoral thesis (1992).

Table 1 ICP analysis for impurities in the samples.

Element	Before experiment	No excess heat	Excess heat evolved
Li	5 ± 0.7	5 ± 0.7	5 ± 1
Na	10 ± 1	10 ± 1	12 ± 1
Mg	5 ± 0.8	5 ± 1.2	10 ± 3
K	10 ± 0.9	10 ± 1.5	15 ± 1.8
Ca	20 ± 2	20 ± 0.8	40 ± 5
Ba	40 ± 5	40 ± 8	40 ± 10
Al	3 ± 0.2	5 ± 1	15 ± 5
Si	1.5 ± 0.1	3 ± 1	5 ± 1
Fe	0.5 ± 0.1	3 ± 1	5 ± 1
Ni	2 ± 0.1	3 ± 1	5 ± 1
Cu	0.3 ± 0.1	1 ± 1	1 ± 1
Cr	1 ± 0.1	2 ± 1	2 ± 1
Cd	0.5 ± 0.1	1 ± 0.5	1 ± 0.5
Pd	6.5 ± 1	6 ± 1	8 ± 2
Bi	0	0.1	5 ± 1
Zn	0.5 ± 0.1	1 ± 0.1	2 ± 0.2
Nd	2.5 ± 0.1	2.5 ± 0.1	4 ± 1
Sm	2.0 ± 0.1	2.0 ± 0.1	10 ± 1
Gd	0	0	5 ± 1
Dy	0	0	5 ± 1

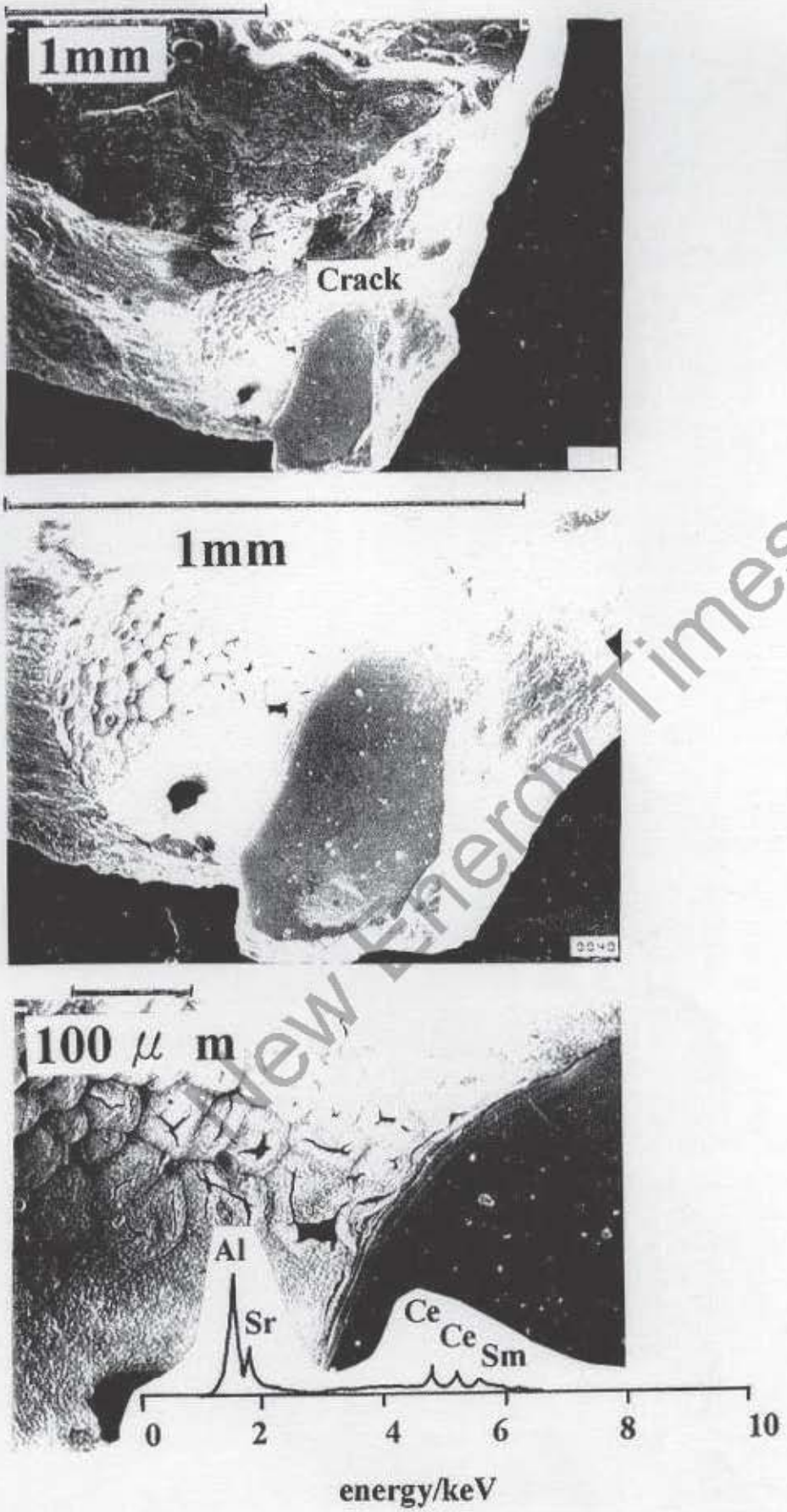

Fig.5 SEM and EDS spectroscopy observation for surface of excess heat evolved sample

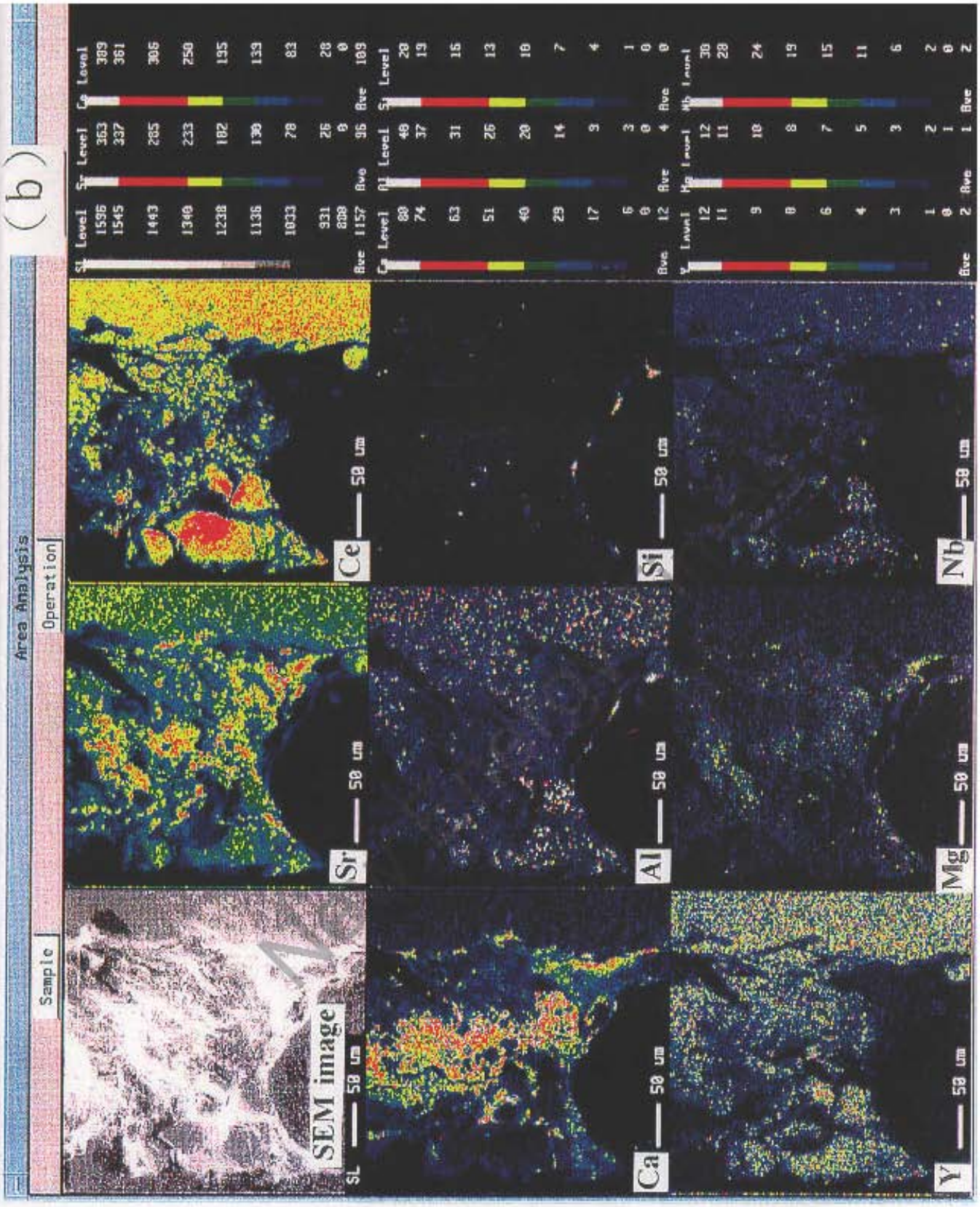

Fig.6 EPMA image of excess heat evolved sample, concentration scales for each elements are shown in right hand side at the photos, (a): surface; Sr, Ce, Nb, Al, Pt, and Y (b): cross section, right hand sides of each image show bulk layer; Sr, Ce, Ca, Al, Si, Y, Mg and Nb

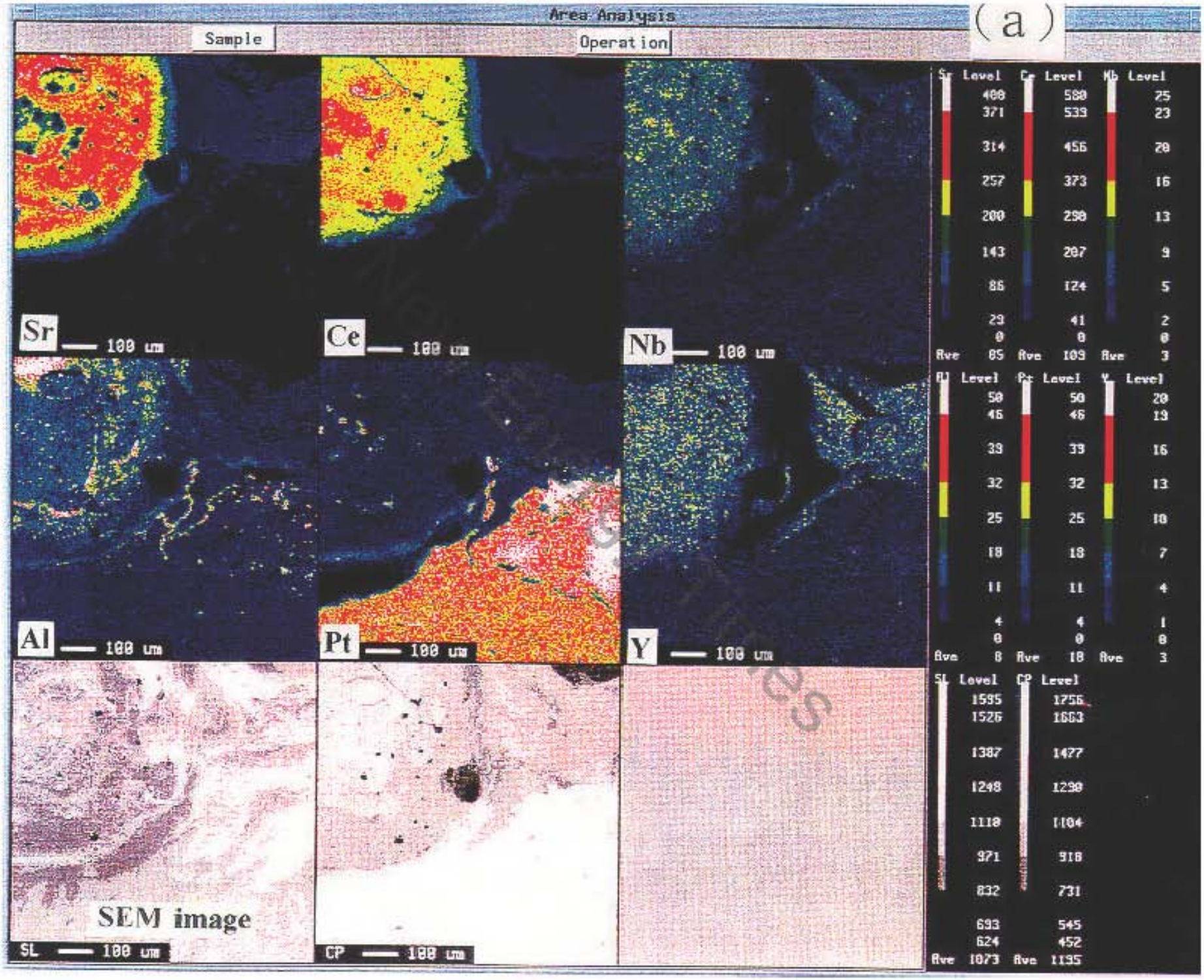
Area Analysis
(a)
Sample
Operation
Sr
Ce
Nb
Al
Pt
Y
SEM image
SL
CP
100 um
Sr Level
400
371
314
257
200
143
86
29
0
Ave 85
Ce Level
580
539
456
373
290
207
124
41
0
Ave 109
Nb Level
25
23
20
16
13
9
5
2
0
Ave 3
Al Level
50
46
39
32
25
18
11
4
0
Ave 8
Pt Level
50
46
39
32
25
18
11
4
0
Ave 18
Y Level
20
19
16
13
10
7
4
1
0
Ave 3
SL Level
1585
1526
1387
1248
1110
971
832
693
624
Ave 1073
CP Level
1756
1663
1477
1290
1104
918
731
545
452
Ave 1135

PLASMA SHAPING: AN ATOMIC TRANSMUTATION CONCEPT

Ronald J. Kovac
Mountain States Mine and Smelter, Boulder CO 80303
A.M. 303-444-5279, 24 hr. 303-449-3993, eves. 303-449-0579

A form of cold fusion, or elemental transmutation appears to have occurred when a vacuum tube containing only nitrogen (^{14}N) was exposed to electromagnetic force fields. Gas spectrometer analysis revealed that the contents in the tube after electromagnetic shaping included substantial amounts of helium (^{4}He) and lithium (^{5}Li). ^{5}Li is a "missing link" element in that mass spectrometer literature [2] indicates that there is no element of atomic weight 5, but its existence is theoretically predicted. [See Special Addition on page 103 for confirmation.] [Note: Nuclides and Isotopes show ^{5}Li with half life of 3 x 10^{-22} sec. Ed.]

The creation of this mass 5 element is offered as support for the notion that cold fusion, ultra subatomic particles, gravity, electricity, and magnetism are each a consequence of special interrelated geometric formations moving in microscopic space. If glass, rarefied nitrogen, and electricity/magnetism can cause cold fusion, and transmute or create an element with the missing atomic mass of 5, *then the geometry of motion in space appears to be an important factor in atomic transmutation*. This concept will hereafter be referred to as the "geometry of space bending."

SPACIAL CONCEPTS

First, I would like to indicate that the idea of producing ^{5}Li is not unprecedented. To do this, I refer to a quote from the physics Nobel laureate Julian Schwinger of UCLA in *Cold Fusion* magazine [3]. Schwinger's comment is important in that ^{5}Li is normally absent in mass spectrometer analyses.

To quote Schwinger:

"I note here the interesting possibility that ^{3}He produced in the pd (proton-deuteron) fusion reaction may undergo a secondary reaction with another deuteron of the lattice, yielding ^{5}Li (an excited state of ^{5}Li lies close by). The latter is unstable against disintegration into a proton and ^{4}He. Thus, protons are not consumed in the overall reaction which generates ^{4}He."

The metaphysician Walter Russell (1871-1963) perhaps supplies the motivation for certain experiments, with his hypotheses of spacial vortices and atomic structures. His work has been the focus of Tim Binder and Toby Grotz. But in a recent article, Laurence Hecht [4] pointed out the ramifications of the work of the German mathematician Karl Friedrich Gauss, which provided a spacial interpretation of the tractfix and catenary forms that appeared to describe the shapes observed in my experiment. The tractfix and catenary forms of Gauss are reminiscent, to some extent, of the spacial forms described by Russell [5].

POTENTIAL IN A SPACE OF NEGATIVE CURVATURE

To provide some background, Hecht points out the special properties of the tractrix-pseudosphere and the catenoid. Hecht compares the electrical potential of the sphere, a shape of constant positive curvature, and

the pseudosphere, a shape of constant negative curvature (to be explained later). He generalized the Newtonian concept of potential in a field of positive curvature to include spaces with negative curvature where potential surfaces consist of concentric pseudospheres. This leads to a geometric definition of the concept of mass, explaining the transformation of mass into energy in terms of a catenoid-helioic structure.

To quote Hecht:

"According to biographer Ralph W. Dunsington, Karl Friedrich Gauss first considered this surface (of the pseudosphere) in the period 1828-1830. But it was Eugenio Beltrami, the Italian collaborator of Gauss's famous student, Bernhard Reimann, who systematically elaborated the properties of the pseudosphere beginning about 1865 in order to examine more profoundly such physical phenomena as the propagation of waves in an incompressible elastic medium [4]."

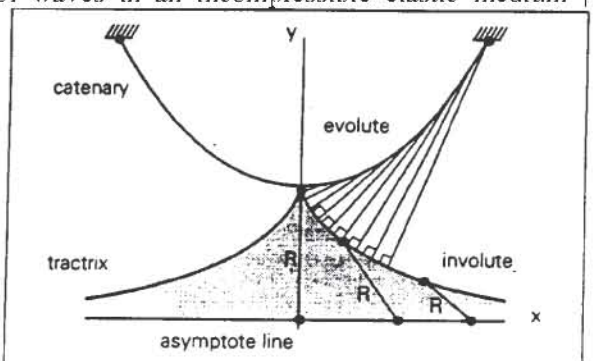

Fig. 1—Tractrix-Catenary As Involute And Evolute. If a taut string is unwound from the center of the catenary, the curve produced is the tractrix. The relationship is that of involute-evolute. If the thread is viewed at various points as it unwinds, it is always tangent to the catenary and normal to the tractrix.

A catenary is the shape formed by the curve of a loose string, under the influence of gravity, suspended by its two ends (see Fig. 1). For any catenary, another curve exists such that lines tangent to the catenary are normal lines to other curve. One of these other curves is one which intersects the catenary at exactly one point. It is called a tractrix (see Fig. 1). The tractrix, otherwise known as an equitangential curve, is defined as a curve such that a length (R) drawn from its point of tangency with the tractrix to its point of intersection with the curve's asymptote (x-axis), is constant.

The catenary and tractrix are related in that the catenary is the evolute of a tractrix, and the tractrix is the involute of the catenary. An evolute, or envelope of normals, is the curve which lies tangent to all the normals drawn to a curve, and the involute is a curve which lies normal to all the tangents drawn to another curve.

If rotated about the horizontal axis (x), the catenary becomes a catenoid, and the tractrix becomes a pseudosphere (see Fig. 2). The pseudosphere is of geometrical significance because, like the sphere, the pseudosphere possesses constant Gaussian curvature for all points on its surface. Gaussian may be determined by multiplying the reciprocals of the radii of the largest and the smallest circle which approximate a curve at a given point. If the circles are on the same side of the surface, the product is said to be positive, as in the case of the sphere; if they are on opposite sides, the product is negative, as in the case of the pseudosphere.

Another similarity between pseudospheres and spheres is that, integrated to infinity, the surface area of a pseudosphere is the same as that of a sphere of equal radius (R).

Hecht believes this is significant in understanding field potential geometries, and consequently mass-energy transformations:

"In the same way in which we represented the Newtonian potential by means of concentric spherical shells, we may represent the negative curvature potential by concentric pseudospheres... Physically, the

reversal of sign is interpreted as a reversal of the force from repulsion to attraction, or vice-versa. My interpretation is that the concept of point center of mass applies only to objects on the macroscopic scale in which the potential surface is a sphere, not to objects below the atomic level in which, I hypothesize, the potential surface is a pseudosphere...I suggest that the pseudospherical potential, in fact, represents the potential function of the nucleus and that by a transformation that leaves the curvature of the potential surface unchanged, it becomes the electromagnetic wave of zero rest mass [4]."

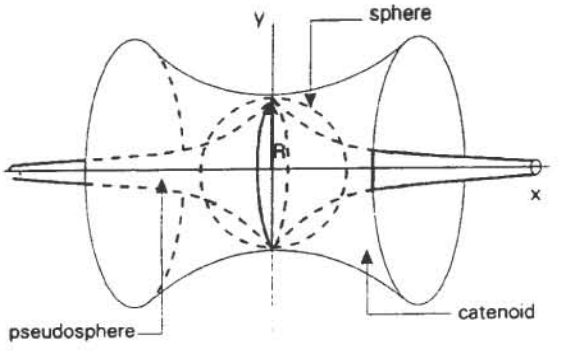

Fig. 2—Generation of Pseudosphere-Catenoid. The pseudosphere and its evolute, the catenoid, are generated by rotating the tractrix-catenary system about the x-axis.

The tractrix and the catenary are interconnected; one is descriptive of the other. Hecht points out that the catenoid structure can be cut and stretched along its central longitudinal axis to form an electromagnetic waveform (as in Meusnier's transformation, see Fig. 3). He also suggests that this was known by Christian Huygens in 1690. Huygens' principle of waves and refraction states that, "Rays of light are straight lines which intersect at right angles the waves which intersect them,.... ," which contradicts claims that Huygens did not understand the transverse nature of light.

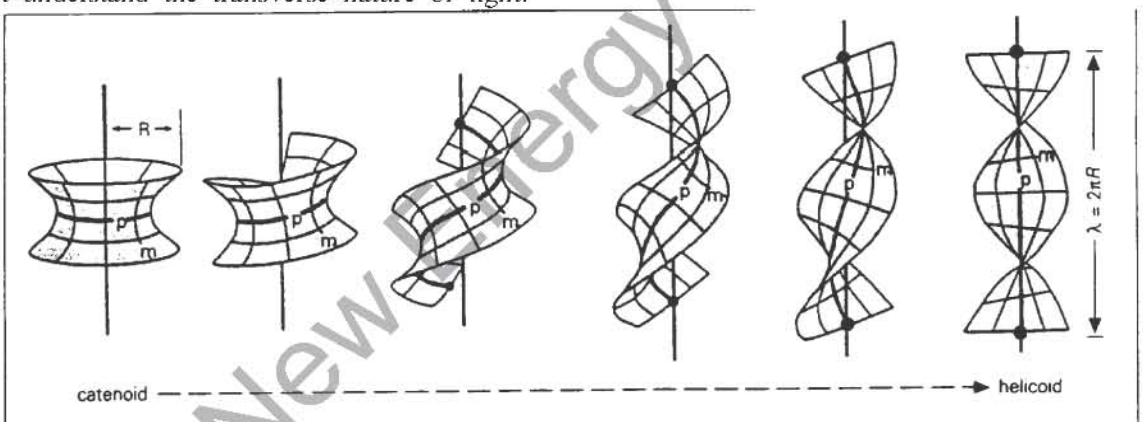

Fig. 3—Meusnier's Transformation. The catenoid is slit down one side and pulled apart, producing the helicoid. There is no change in the Gaussian curvature and both are minimal surfaces. The small circumference of the catenoid (p) becomes the length of the helicoid.

THE EXPERIMENTS

Empirically, the geometries described in the previous discussion were revealed in experiments wherein an electromagnetic catenoid could be generated and observed, and the energy associated with it measured. Fig. 4 shows the apparatus used to for the creation of a pseudospheroid, and the analysis of the matter which resulted from the process.

Initially, I chose to stress a vacuum (24 in. Hg) of ordinary air, using high voltage (see Fig. 5). Capillary boundaries were used to mold the catenoid. Since the application of electrical, magnetic, physical or

thermal stress to air usually results in the emission of light, I supposed the fluorescence would make visible any catenoids or pseudospheres that might have formed. Emission spectroscopy and residual gas analysis from a gas spectrometer were used to keep track of signs of transmutation and energy transformation.

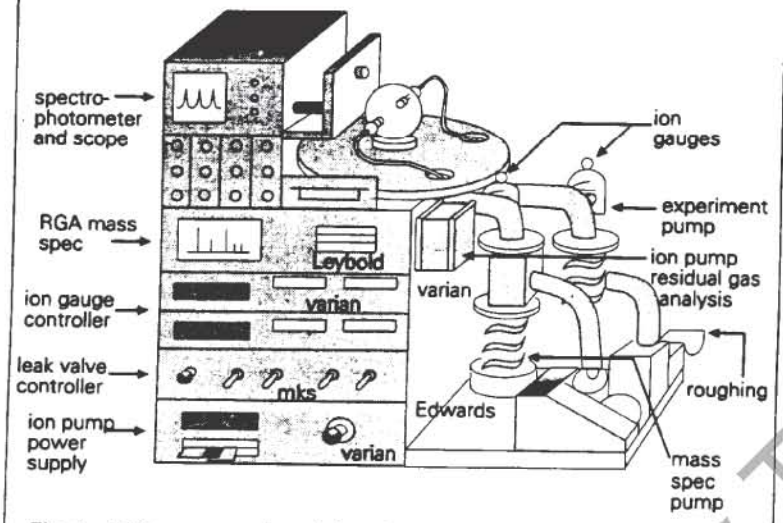

Fig. 4—Follow-up experimental equipment purchased and assembled to quantify results.

In the experiment, the orange-reddish glow normally found on and near the positive electrode was half-catenoid cone extending out from the surface of the glass frit (see Fig. 6). On the other side of the glass frit was the other half of the same catenoid. The other half of the catenoid had the blue glow normally found on or near the negative electrode. After only a few seconds of applying voltage, the capillary hole through the glass frit, which was the center of the blue/red catenoid, melted closed. The red and blue catenoid halves then jumped to a new, unused capillary hole through the frit. The heat required to melt the Pyrex glass frit capillary was a good preliminary indication of the catenoid temperature.

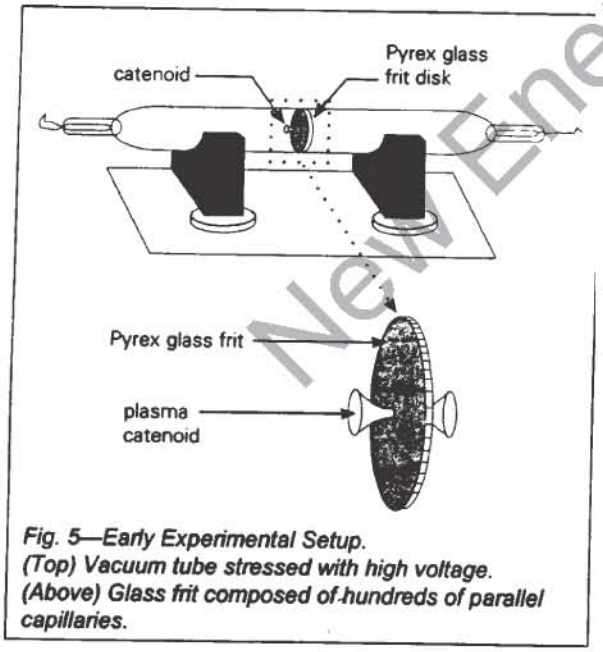

Fig. 5—Early Experimental Setup.
(Top) Vacuum tube stressed with high voltage.
(Above) Glass frit composed of hundreds of parallel capillaries.

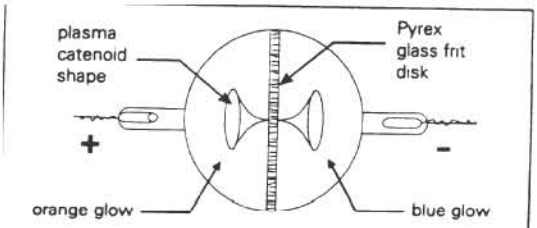

Fig. 6—High voltage sent through the capillary holes of a Pyrex frit partition forms a catenoid. The capillary fuses from the heat generated and the catenoid jumps to a new capillary hole.

With the pressure in the above arrangement at 24 in. Hg, I was able to generate the geometry of the pseudosphere in the plasma. With adjustment, a toroid of orange plasma was created inside the blue plasma cone. After many test runs, a buildup of clear plastic-like material appeared on the outside of the positive electrode (see Fig. 7). There also was a buildup of an organic-looking, gray, opaque material at the ends of the wire of the same electrode.

Because of the strange appearance and inaccessible location of this accumulation of new material. I have decided to delay its investigation. Subsequent experimentation using another glass ball with the same electrodes is planned. This repeat experiment will include residual gas analysis using a mass spectrometer and emission spectroscopy. The analytical system is illustrated in Fig. 4.

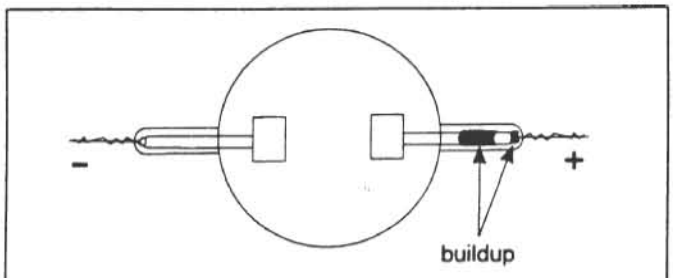

Fig. 7—A plastic-like buildup appeared around the positive electrode, and another type of buildup at the electrode wire junction in the pseudosphere tube.

In a later experiment, ^{4}He was shown to have formed at a 3.75% concentration of the parent gas, N_2; and ^{5}Li, at 2.5% (see Fig. 8). It is unlikely that the presence of ^{5}Li represents contamination form external sources; according to spectrometry literature ^{5}Li does not exist [2]. The cold fusion process that produced these results used only N_2 plasma and magnetic shaping. The plasma tube had no constrictions nor capillary fusion facilities, only two needle-point stainless electrodes (no platinum, nickel, nor palladium cathodes were involved).

INTERPRETATIONS

To explain the observed phenomena, I have applied Hecht's extensions of the ideas of Gauss and Russell, as well as my idea of the toroid knot. I believe that it would be fruitful to investigate how shaping plasma into the geometries explained by Gauss and Russell can be applied to cold fusion, assuming that the plasma bends in the likeness of the surrounding space in the process called the "geometry of space bending."

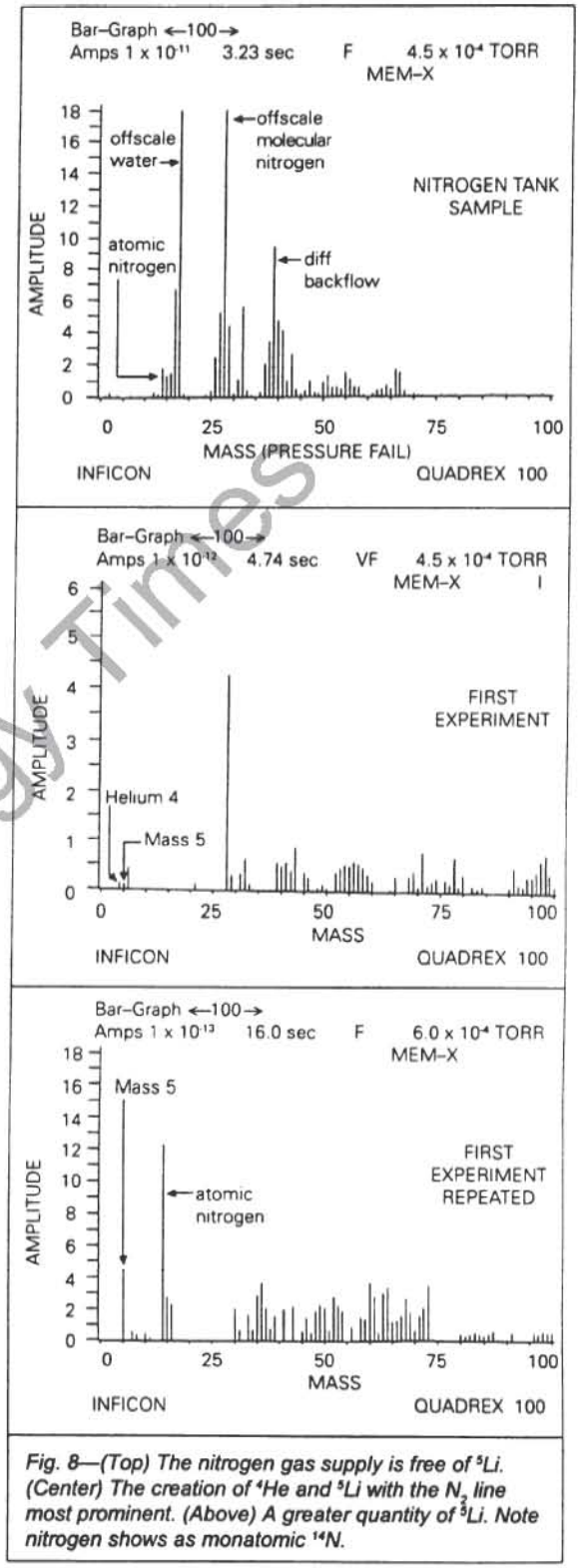

Fig. 8—(Top) The nitrogen gas supply is free of ^{5}Li. (Center) The creation of ^{4}He and ^{5}Li with the N_2 line most prominent. (Above) A greater quantity of ^{5}Li. Note nitrogen shows as monatomic ^{14}N.

Toroids may form in an electromagnetic field, as shown in Fig. 9. The compressed, repelling lines of force create a set of concentric shells of increasingly smaller size until the smallest is only the size of a subatomic particle. The cancellation of the electric field and the magnetic field, according to the right-hand vector rule, creates a hole, inside of which there is neither electricity nor magnetism on a macroscopic level. In this region, the atomic substructure may satisfy a special equilibrium, which maintains a small zone of toroid turbulence, enforced by the electric fields (see Fig. 10). Then, something as small as a subatomic particle could exist as a toroid for an instant at the center, but would collapse as it moved to the side, becoming a toroid without a hole (a sphere).

I postulate that the toroid forms as space bends, rotates and compresses like the rubber band of a toy airplane when the propeller is wound. If motion is continually applied to the system by winding the rubber band, the wound band will start to form knots in its windings (see Fig. 11). I think this knot is like a toroid at the center of the rubber band (catenoid), and that, by analogy, it represents the formation of subatomic particles which are able to either radiate their energy as electromagnetic force or coalesce into the subatomic particles recognized by modern classical atomic physics.

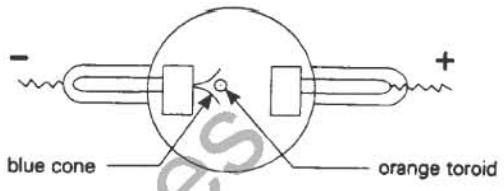

Fig. 9—With adjustment, a toroid of orange plasma is created inside a blue plasma cone at the negative electrode. The toroid is stable for a matter of minutes.

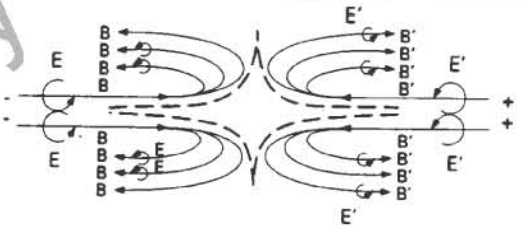

Fig. 10—Field lines of the pseudosphere anode and cathode of the previous experiment. Dotted lines represent a region inside of which a toroid supporting turbulence is achieved; i.e., heavy, slow, positive ions are trapped and spun by the E and B fields.

The toroids of fast-moving, compressed space have the option of axially radiating energy or continuing the toroid-forming motion (as mass). Either way, space is consumed by the compressive action at the toroidal location (the center of mass), and the surrounding space is subsequently stressed to fill the void left by the winding and compression. In other words, a flow of space to a center of mass is created.

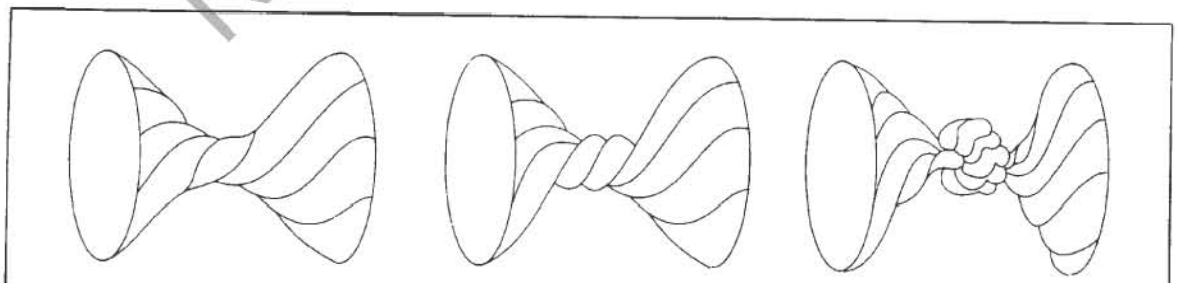

Fig. 11—An example of space bending, forming knots in its windings to create a toroid.

As this flow (stress) of space is shared with nearby mass objects, it forces the center of mass of the neighboring objects toward its center of mass. In this way, the flow of space toward centers of mass

becomes the gravitational force between objects. The weight of any atomic group per unit volume, then, would be related to the extent to which that group bends space (or consumes space motion).

COMMENTARY by Tim Binder

In closing, I would like to provide the following notes on the experiments from Tim Binder. Quoting from *Fulcrum* [1], pp. 32-36:

"Readers of *Fulcrum* are already familiar with the past demonstrations of transmutation that Ron Kovac, Toby Grotz and myself have achieved and here is a brief summary of that work:

"Working with one possible geometrical shape of the magnetic fields that Walter Russell described in A New Concept of the Universe [5], we were able to apparently demonstrate the transmutation of water vapor into fluorine and nitrogen as reported in *Fulcrum,* vol. 1, no. 2. In further, unreported experiments, we succeeded in transmuting nitrogen into hydrogen and several other elements.

Russell stated that by shifting the field arrangement and/or the polarity strengths he was able to prolate or oblate the oxygen nucleus into nitrogen or hydrogen and vice versa. We found by shifting the shapes of the magnetic fields with our "transmutator" (a special device used to manipulate magnetic field conditions like those created by Russell) after heating our gas samples in the emission photospectrometer by running an electric current through the plasma and then allowing the heated gas to cool down in our magnetic field arrangement, we were able to demonstrate transmutations as identified by photo emission spectroscopy.

As the experiments were being conducted, we had continuous monitoring of what was occurring in the computerized mass spectrometer (CMS) by printed readout as well as a video recording of the sequence (see Fig. 8). What Kovac later observed (while studying) the data was truly amazing. In our first run, we had transmuted the nitrogen gas plasma (^{14}N) into helium 4 (^{4}He) and lithium 5 (^{5}Li) in the amounts of 3.75% and 2.5%, respectively, from the parent nitrogen gas. The transmutation had occurred not when we expected it to; namely, after being heated and then allowed to cool down in the field, but simply as the plasma was sitting in the field before any heating.

Kovac's paper... describes the experiments we have done in terms of cold fusion and in terms of Karl Gauss' geometry. I will now comment on his descriptions and show the relationship between Gauss' and Russell's geometries as I understand them.

First, notice that the creation of lithium 5 from nitrogen was remarkable from two aspects: number one, it was a transmutation of nitrogen into lithium which by conventional science is impossible; and number two, ^{5}Li is proclaimed by standard literature and science to be nonexistent. Before our July experiments, this particular atomic structure and mass of lithium (^{5}Li) was one of the missing links in the nucleonic tables; its existence had been predicted but never demonstrated [3].

Transmutation of ^{14}N to ^{5}Li, a heretofore unseen and unknown isotope of lithium, is significant for this research team in that there is no way the experimenters would have seeded or contaminated their results. The results are indisputable and can be easily reproduced in any sophisticated laboratory.

Kovac cites the many different methods and materials that have been used to demonstrate cold fusion in several very prominent research facilities since Fleischman and Pons did their first cold fusion experiments in 1989 in Utah. He then makes the profound point throughout his article that all of these many different processes are all functioning because of a common fundamental feature; namely, the "geometry of space bending."

What Kovac is pointing out is that all the various cold fusion processes are in their own fashion working by engineering the bending of space or the formation of vortical motion focusing heat and light in the center of the system and radiating that intense, tightly wound up motion back out as energy (heat of cold fusion) or mass of elemental transmutation via the vortex equatorial plane.

In Kovac's toroid knot analogy, he says that energy is expressed by unraveling the knot back out the central (polar) axis and matte is expressed by leaving the knot system at 90° or right angles to the central axis.

This appears to me to be dissimilar to Russell's cosmogony in that (Kovac claims that) energy and mass increase by way of the polar central axis (through centripetal motion) and they both decrease by way of the equatorial axis through centrifugal motion. Russell says the knot is wound up by the north-south charging poles and unwinds via the east-west discharging equatorial poles. He does not allow the knot to unwind (using) the same axis that it (uses to) wind up. He says that the direction of winding when it reverses is now not the central axis anymore, but the equatorial axis that is at 90° to the central axis. When this unwinding process reaches its end at cube wave field boundaries it then reverses direction and potential and becomes a polar central winding up (process). Russell says that matter and energy turn inside-out and outside-in.

If we understand Kovac's unraveling of the knot through the central axis to mean what I have stated as Russell's cosmogony, only then are (the theories) congruent. This is why in Russell's diagrams of wave motion he shows both pairs of spirals winding and un-winding within each other, which Kovac has shown in his article in a similar way where he has a pseudosphere and catenoid super-imposed on each other. Here, I interpret the pseudosphere to be the windup spiral motion and the catenoid the unwinding spiral motion with the toroid knot representing the mass formation and the spirals of pseudosphere-catenoid geometry representing the space that is becoming matter or matter that is becoming space.

Kovac makes the salient point that none of the materials that the various researchers have used are essential. The only essential is what Kovac is calling "the bending of space geometry." The "bending of space geometry" is a vortex motion controlled by electric potential fields that science calls magnetic and electric fields that curve low potential motion in a centripetal direction to form density and high potential, and curve high potential motion in a centrifugal direction to form tenuity and low potential. This process is a focusing and unfocusing of light-motion. The point is to create a vortex and control it.

With our quartz plasma tube and electrodes at each end and externally focused magnetic fields, we were able to generate this geometry of space bending or vortex formation in such a way that we changed the vortex motion of nitrogen (^{14}N) to the vortex motion of ^{5}Li and ^{4}He. The final quantitative analysis (performed by measuring and comparing the relative peak heights on the CMS charts, Fig. 8) of the first processing showed 2.5% ^{5}Li, 3.73% ^{3}He and the remaining 93.75% (of the tube's contents were) untransformed nitrogen. When we reprocessed the same tube, the percentage of ^{5}Li went to 6.5%. This was done with little temperature change, and if temperatures were modified, we might have vastly increased the amounts of transmuted lithium and helium.

The vortex known as nitrogen was subject to an external magnetic field vortex (what Russell calls an electric field) that changed (the shape of) some of the nitrogen vortices from a gyroscopic motion spinning in the plane of nitrogen to spinning in the planes of ^{5}Li and ^{4}He. Kovac explains the cold fusion and transmutation processes in terms of Gauss' pseudosphere-catenoid geometry determining the bending of space to form what Kovac calls toroid knots.

Kovac goes on to describe that this tightly wound toroid (centripetally bound and compressed) mass can then either unwind back through its axis (as it turns inside-out) as energy production (heat, electricity and/or light), or it can unwind equatorially as a catenoid spiral in secondary mass formation to form various elements. Thus, we see mass-energy transformations occurring again as in Russell's descriptions of motion to and from wave field cube wall boundaries to and from mass spherical center boundaries.

REFERENCES

[1] Timothy A. Binder, "A Further Report on the Russell Science Research - The World Balance Through Free Energy Project," *Fulcrum*, vol 3, no 2 (1994): 32-36.

Ronald J. Kovac, "A Report on the Russell Science Research (RSR): Transmutation of Nitrogen to Lithium and Helium, Plasma Shaping Reveals New Atomic Transformation Technique and Cold Fusion at Chemical-Molecular Energy Levels," *Fulcrum* vol 3, no 2 (1994): 18-31. (*Fulcrum* is published by The Univ. of Science and Philosophy, Swannanoa, Waynsboro, VA 22980.)

[2] Inficon, Div. Leybold-Heraeus Co. Quyadrex 100 manual #074-099, Sec. 4, p 16, Table 4-3, Spectra interpretation Guide.

[3] Julian Schwinger, "Cold Fusion: A Brief History of Mine," *"Cold Fusion"*, vol 1, no 1 (1994): 14, 35. (*"Cold Fusion"*, Peterborough, NH 03458-1107)

[4] Laurence Hecht, "Potential in a Space of Negative Curvature," *21st Century* vol 5, no 4 (1992): 14-22. (*21st Century*, PO Box 16285, Washington, CD 20041)

[5] Walter Russell, A New Concept of the Universe, Univ. of Science and Philosophy, Swannanoa, Waynsboro, VA 22980.

APPENDIX 1

CATENOID, OPPOSING FIELD MAGNETOHYDRODYNAMIC TOROID MODEL

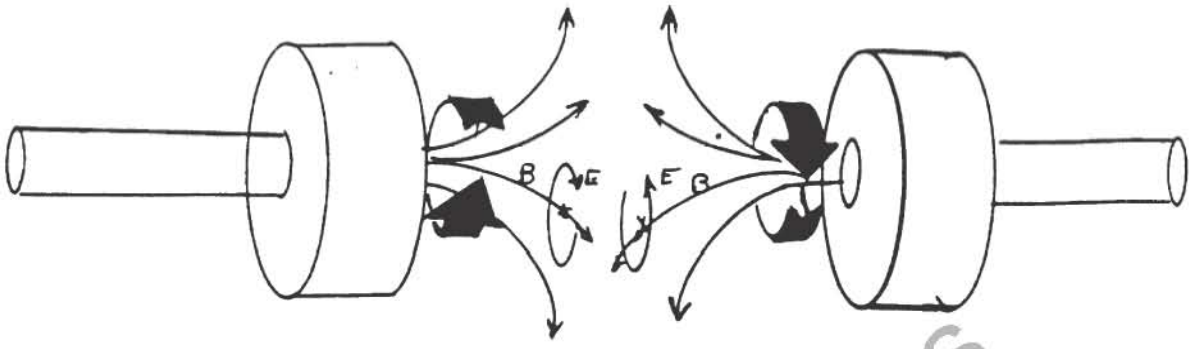

Fig. 1 Shows two cylindrical magnets at the ends of two hollow tubes (electrodes). The two magnets are opposed to each other as N-N or S-S. Because they are opposed to each other the field lines of magnetism at first race toward each other and then are deflected outward from the central axis at a curve which becomes right angle to the central axis. The right hand rule dictates that any magnetic field line also has an electric field counterpart which curls around it, as drawn. The direction of this electric field is similar in direction to the fingers of the right hand if the magnetic field is the thumb. This becomes interesting when you consider the same applies to the other magnet's field lines. It's electric field curves in the opposite direction, by the same rule. These two electric fields are then pushing in opposite directions against each other. This pushing causes the magnets to rotate opposite each other (the heavy black arrows).

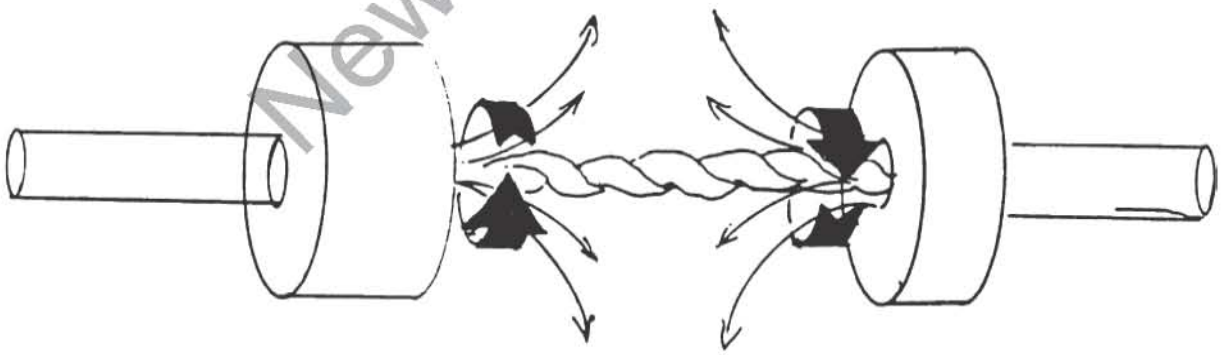

Fig. 2 Shows the same opposed magnets with a glow discharge plasma going from one hollow electrode to the opposite hollow electrode. It is important to review the fact that any "neon tube" type glow discharge is an equal population of + and - ions in a gas mixture. Because they are attracted to each other, individually, the total effect is an elastic bendable entity, somewhat like a rubber band in behavior. It is also necessary to remember that these plasmas are subject to respond to any nearby moving magnetic fields. For this reason the counter rotating fields just outside the plasma around the central axis cause the plasma to twist like the rubber band of a wind-up model airplane.

APPENDIX 2

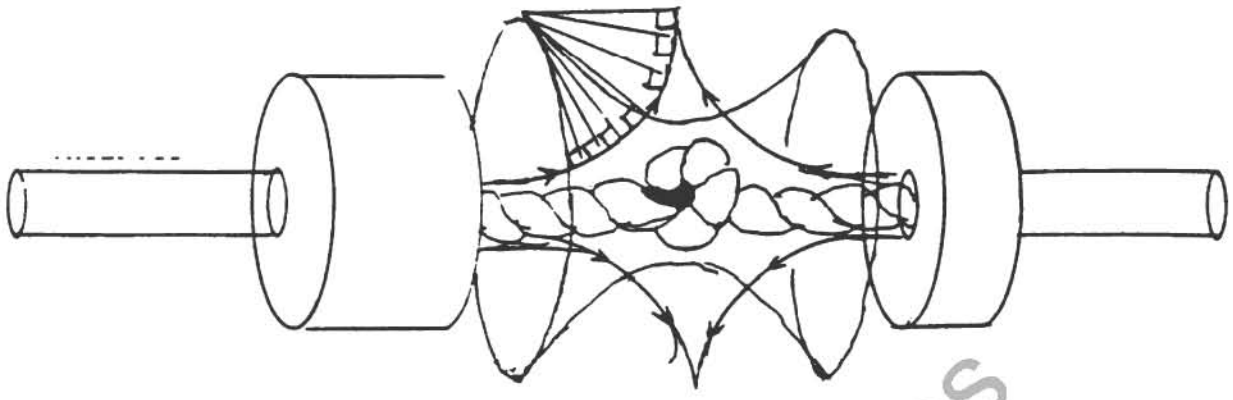

Fig. 3 Shows the plasma being twisted by the nearby rotating magnetic fields to such excess as to form a knot. This knot is real and has been experimentally demonstrated by myself, video taped and photographed. It results in forming a relatively stable toroid or doughnut suspended at the center of the equipotential magnetic field lines. These field lines form a geometric surface called a pseudosphere. A pseudosphere is like two funnels pressed together top to top. There exists a close geometric relationship between the pseudosphere and the catenoid. The catenoid is like two funnels pressed together point to point. For every pseudosphere there is a catenoid associated with it. If at every point on the surface of a pseudosphere a perpendicular line is extended from the surface at that point the total effect will be the generation of the associated catenoid surface. Most importantly, there are infinite co-axial pseudospheres and catenoids. These are arranged like the many layers of the skin of an onion. All the perpendiculars of all the coaxial pseudospheres intersect at either end of the catenoid to form the HALOS, as drawn in Fig. 3 and Fig. 4.

APPENDIX 3

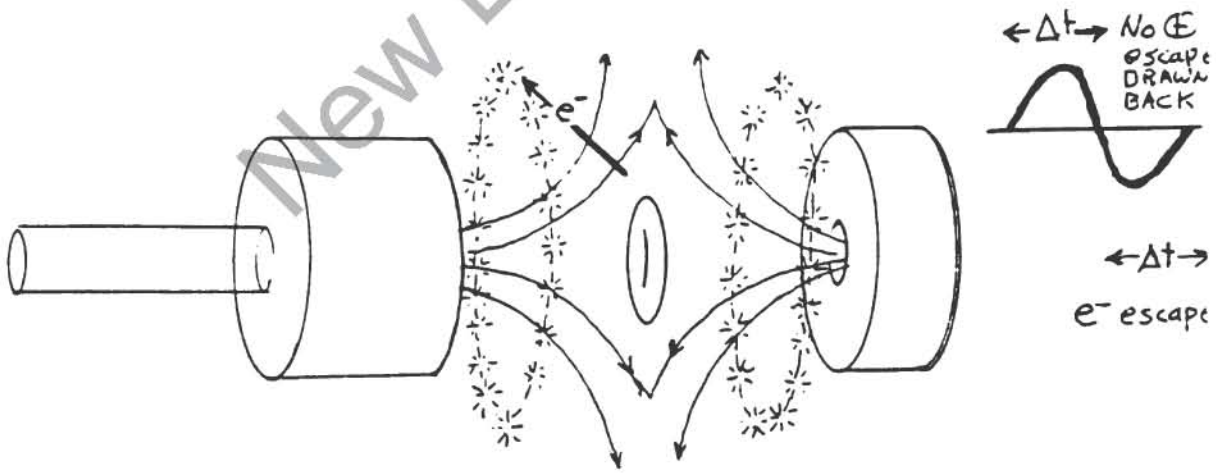

Fig. 4 Shows mass separation by electromagnetic oscillation. In the lab experiments I have demonstrated there occurs an electromagnetic oscillation (explanation of this oscillation is available in my other publications). During the positive cycle of this oscillation the positive ions are repelled and try to escape the confines of the magnetic pseudosphere. These ions are heavy and slow, relative to the mass and speed of their associated electrons. Before they move outside of the magnetic field the field has reversed to its negative cycle part and is pulling them back to the center. These large ions are doomed to become the stuff the toroid is made of. The electrons have an equally strange destiny. The electrons or negative particles are small and very fast. During the negative part of the oscillation they are easily repelled

outside the center of the magnetic pseudosphere. Most important: the right hand rule again dictates that all departing electrons must exit PERPENDICULAR to the magnetic field lines. This implies perpendicular to the surface of the pseudosphere. This, also means the negative particles not only create a real world negative surface, the catenoid, but even more profound, they create the two rings of greatest negative particle density per unit time, the HALOS. This model could explain the halos of the famous Hubble photograph of the nebula 1987-A. It could also explain the other "star birth" Hubble photos.

With this model I created stable toroid plasmas at will. The question was how small can these toroids be created by this technique? I tried to create them sub atomic in size. I hoped that they would give results in transmutation of nitrogen into another element. I obtained atomic mass 5 from atomic mass 14. (nitrogen) as measured by a quadrupole mass spectrometer and by emission spectroscopy.

APPENDIX 4

Table 1

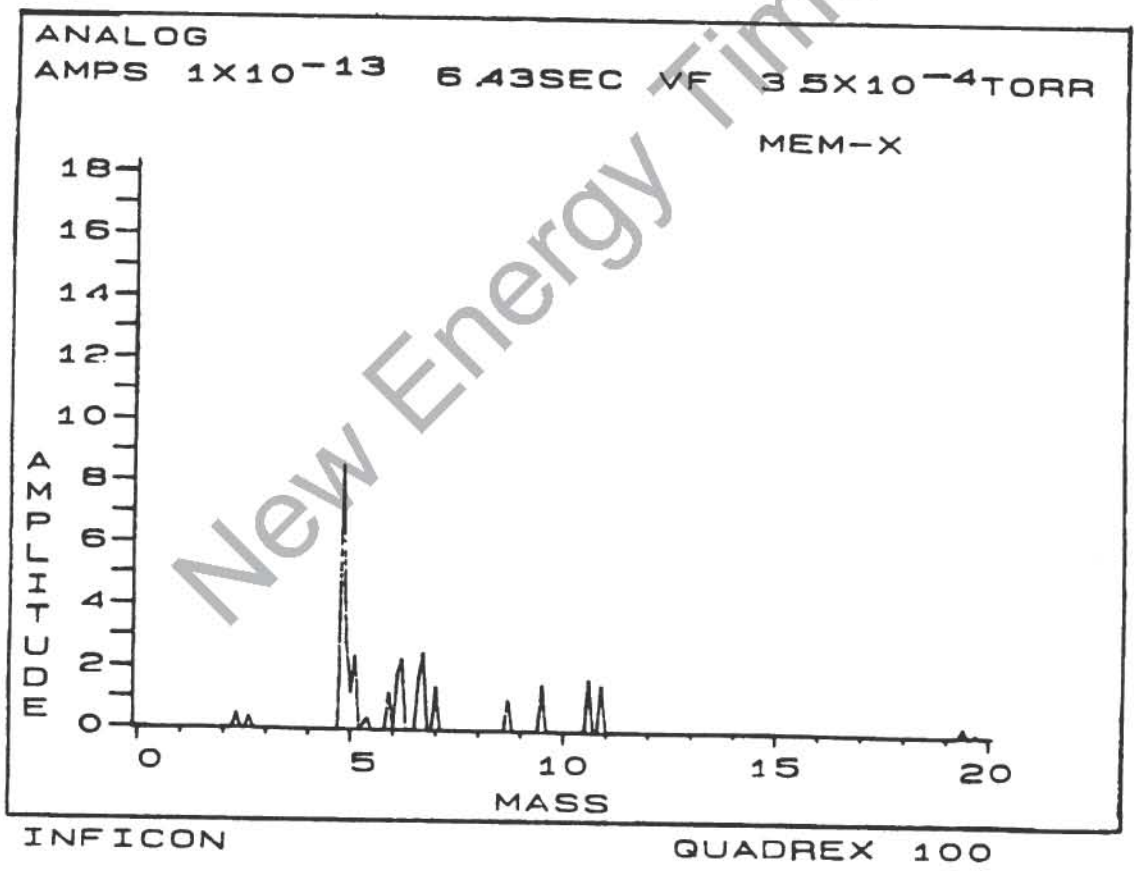

APPENDIX 5

Table 2

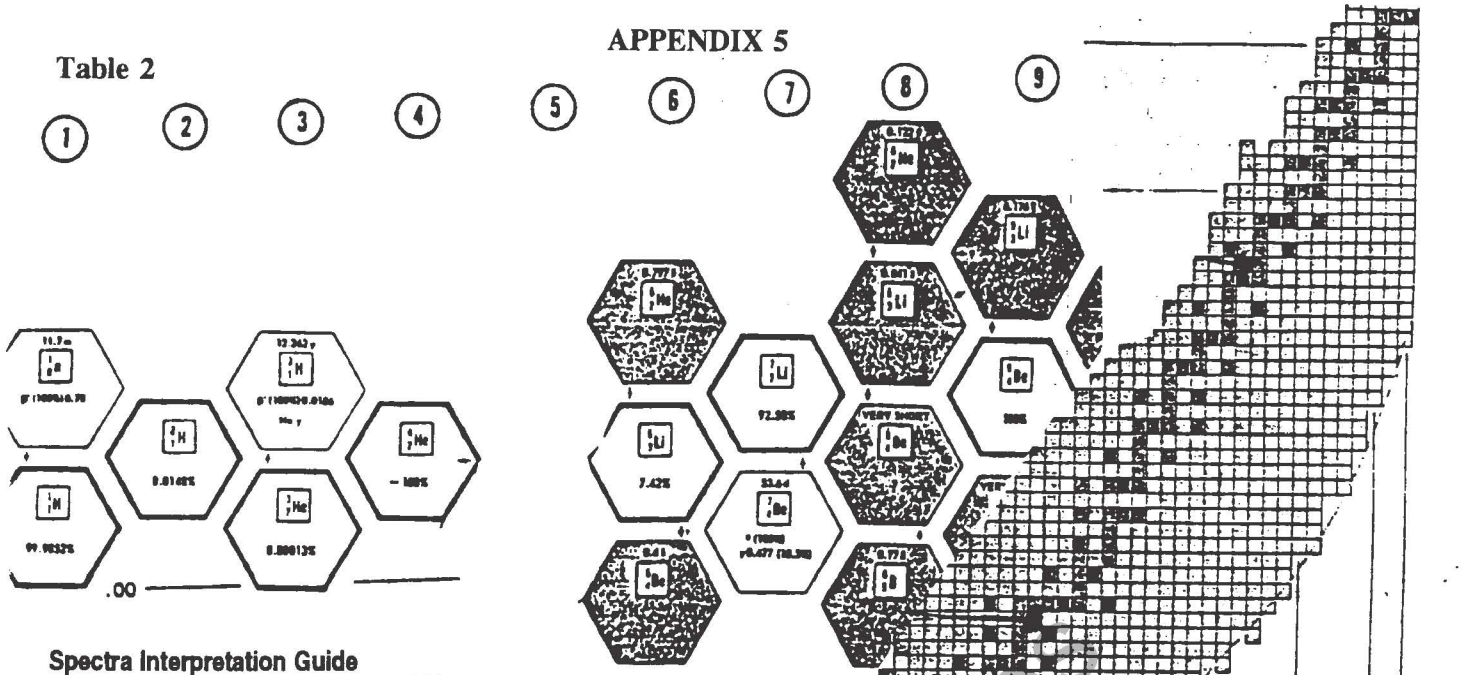

Spectra Interpretation Guide

F Fragment
P Parent Ion
DI Doubly Ionized

AMU NO.	CHEMICAL SYMBOL	SOURCES	
1	H	Water F or Hydrogen P	
2	H_2, D	Hydrogen, Deuterium (H^2)	
3	HD, H^3	Hydrogen, Deuterium, Tritium (H^3)	
4	He	Helium	
5		No known elements	
6	C^{++}	Doubly ionized C^{12}	Rare
7	N^{++}	DI N^{14}	Rare
8	O^{++}	DI O^{16}	Rare
9		No known elements	
10	Ne^{++}	DI Ne^{20}	Rare
11	Ne^{++}	DI Ne^{22}	Rare
12	C	Carbon, Carbon Monoxide F Carbon Dioxide F	
13	CH, C^{13}	Methane F, Carbon Isotope	
14	N, CH_2	Nitrogen, Methane F	
15	CH_3	Methane F	
16	O, CH_4, NH_2	Oxygen or Carbon Monoxide F Methane P, Ammonia F	

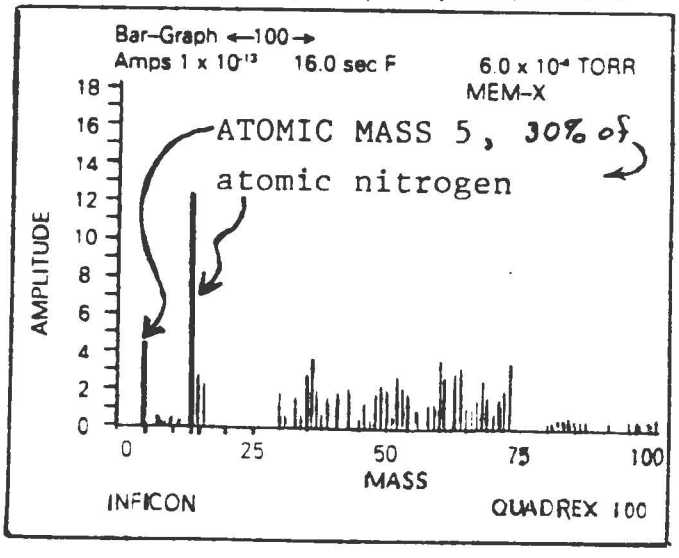

APPENDIX 6

WHAT IF YOU USE HELIUM INSTEAD OF NITROGEN? ---- TRITIUM?.... POSITRON? .....?

Table 3

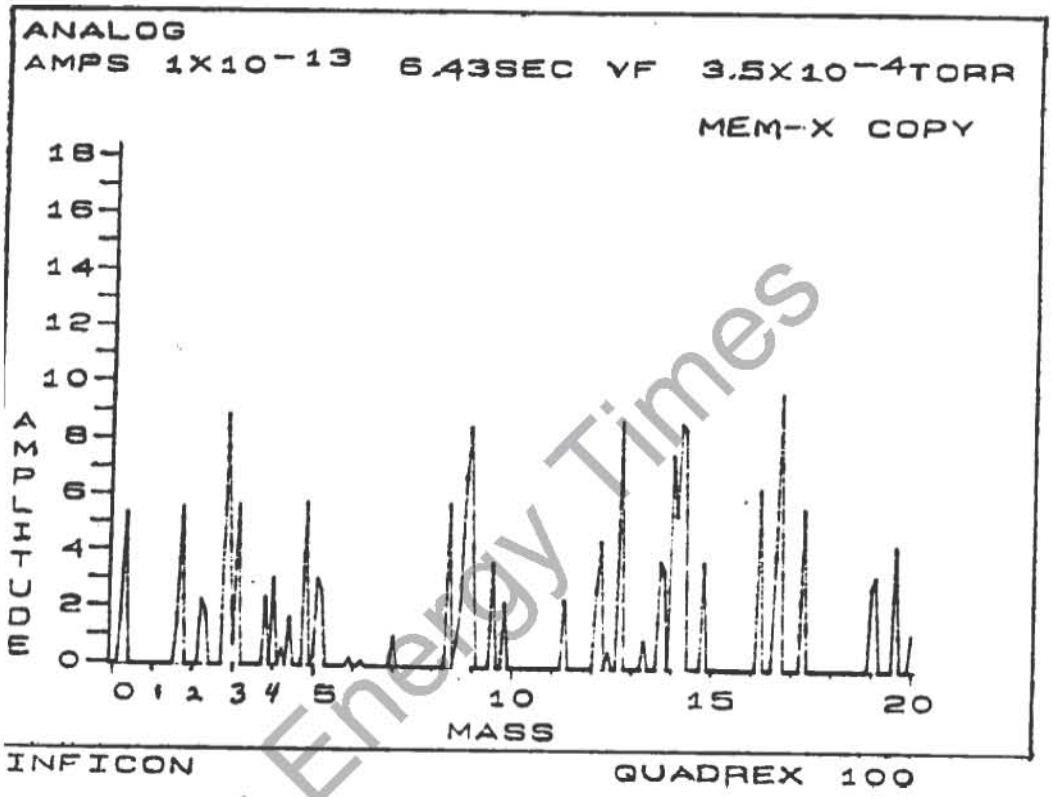

When I substituted Helium for nitrogen in the opposing magnetic field plasma tube I got the above results. Notice the positively charged atomic mass less than one and the atomic mass three. Helium gas leaked into the plasma tube after amu = 5 was created also created amu = less than 1, accompanied by a hugh pressure increase.

WHAT IF YOU SQUEEZE PLASMA THROUGH A CAPILLARY HOLE TO MAKE THE CATENOID INSTEAD OF THE MAGNETIC FIELD METHOD? same amu = 5 was obtained as measured by mass spec.

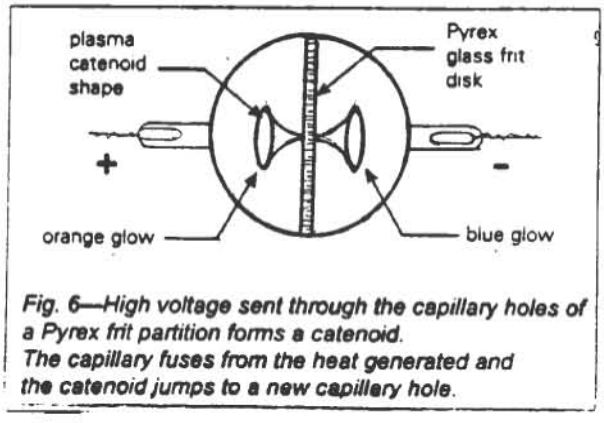

Fig. 6—High voltage sent through the capillary holes of a Pyrex frit partition forms a catenoid. The capillary fuses from the heat generated and the catenoid jumps to a new capillary hole.

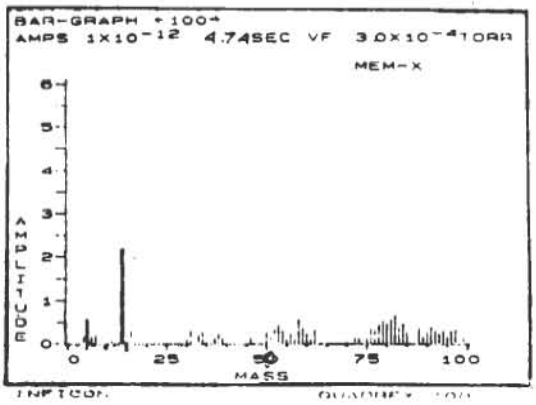

APPENDIX 7

CONGRATULATIONS WEIMAN AND CORNELL:

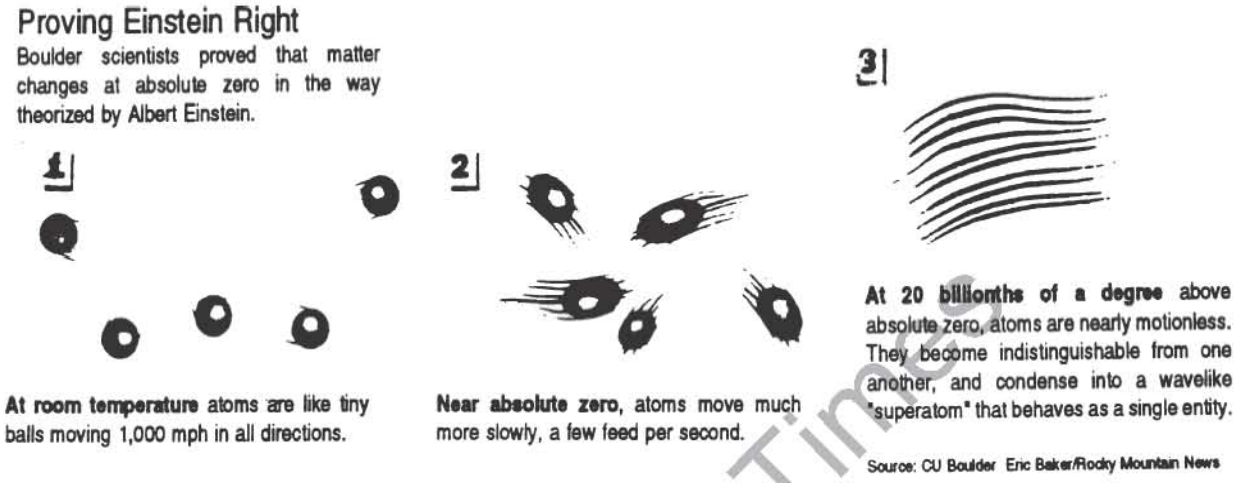

THE TOROID IS THE ONLY SELF SUSTAINING ELECTROMAGNETIC WAVE IN NATURE, SO THE ABOVE BOSE/EINSTEIN VERIFICATION MUST ALSO BE VERIFICATION OF WALTER RUSSELL, KARL GAUSS, AND RON KOVAC;

Consider that the Weiman / Cornell "wavelike super atom" to be the TOROID WAVE FORM (of atoms cooling to their toroid form, not just any wave form). Then toroid alignment occurs as the next colder energy conservative state, having a common dipole. If the atoms get colder, the toroids join in a helix configuration allowing even more energy conservation. As the system gets even colder the helix (which I call the toroid knot in previous pages) unravels as a catenoid by the reverse electromagnetics previously described for amu = 5. Absolute 0 would imply the atoms would become nondistinguishable from background. (THEY WOULD VANISH).

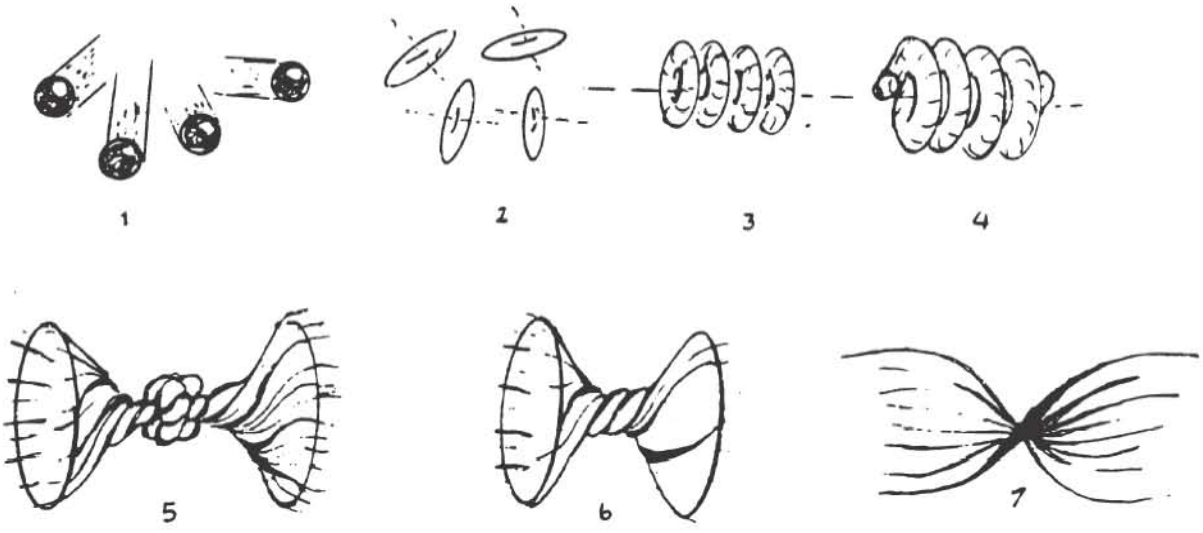

APPENDIX 8

MATHEMATICS V.S. TYPOLOGY

A literature search quickly yields great quantity of vortex, toroid mathematics, yet I must include a reference to one of the best of these:

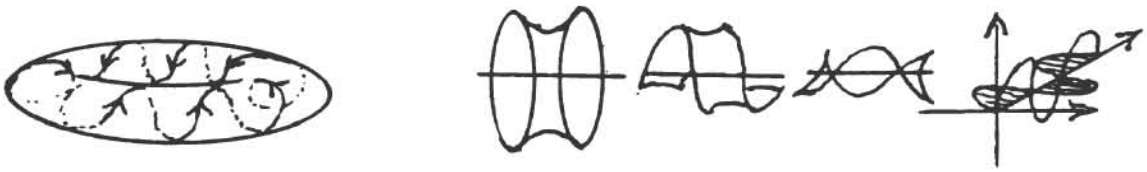

Dr. Wells, of the Dept. Physics, University of Miami through the Fusion Energy Foundation and the **trisops** Corporation did an elegant review of theoretical history and showed that the toroid dimensions for cosmology or the hydrogen atom were the **Eigen values of the appropriate Euler-Lagrange equation**, resulting from the variation of the free energy of the generic plasma. He even identified the "around the circumference of the toroid," helicity. **He did not identify that this helicity initially had to come from an external structure**, (a catenoid), [1].

Karl Gauss, by contrast as previously discussed, had good capture of the catenoid and pseudosphere relations but ignored the next closest relative, the toroid.

I would like to lay claim to the idea and associated math and typology of a toroid descending from the pseudosphere-catenoid by way of the twisting, the toroid knot model, and the associated amu = 5, 3, and <1 work.

"The creation of this mass 5 element is offered as support for the notion that cold fusion, ultra subatomic particles, gravity, electricity, and magnetism are each a consequence of special interrelated geometric formations moving in microscopic space. If glass, rarefied nitrogen and electricity/magnetism can cause cold fusion, and transmute or create an element with the missing atomic mass of 5, then geometry of motion in space appears to be an important factor. This is hereafter referred to as the "geometry of space bending."

[1.] IEEE Transactions on Plasma Sci., Vol. PS-14, No. 6, Dec. '86..

SPECIAL ADDITION

late addition from Texas A&M confirming **atomic mass 5.**

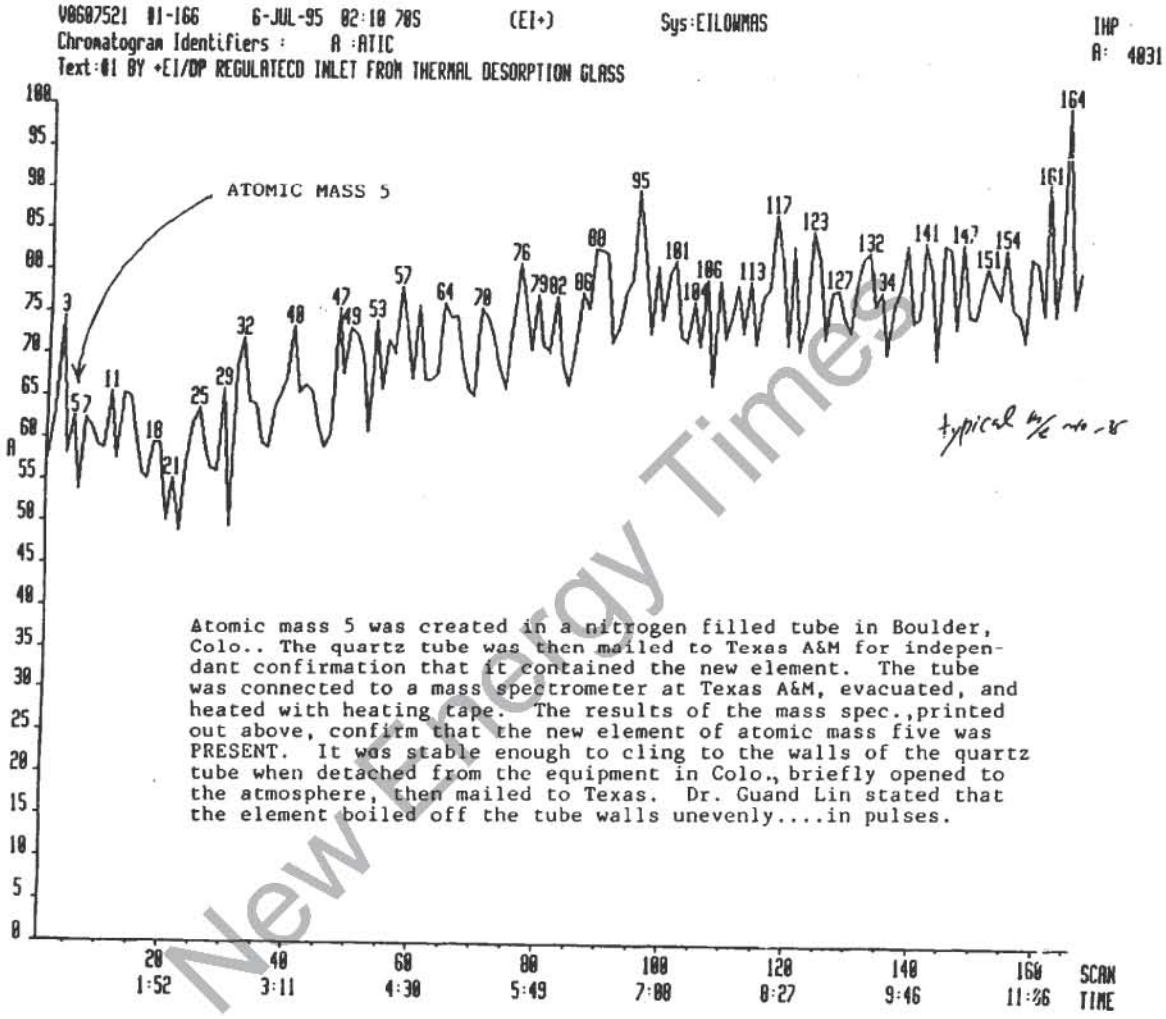

LOW TEMPERATURE NUCLEAR CHANGES USING MAGNETIC FIELDS AND DUAL POLARITY CONTROL

Toby Grotz
Wireless Engineering Inc.
760 Prairie Avenue
Craig, Colorado 81625
970.824.6834 Phone
970.824.7864 Fax

ABSTRACT

This paper is a report on an experimental re-examination of the data reported by Westinghouse Laboratories on the work of Walter Russell. Recent research has been conducted by the authors in order to verify Russell's theories and experiments. Attempts have been made to repeat the experiments that Russell conducted in 1927 at the Bloomfield New Jersey Laboratory of Westinghouse. Russell reported at that time that he had found a novel way to change the to ratio of hydrogen to oxygen in a sealed quartz tube containing water vapor (Russell, 1989). The use of magnetic fields was shown to produce this effect. The end result of the experiments was to demonstrate a cheap and efficient method of hydrogen production for a hydrogen fuel based economy. Experiments performed to repeat these results have met with some success. This paper will present the theory and results of experiments performed in an attempt to duplicate these tests.

Russell's work also involved the assembly of a device to produce energy from the background flux of fields designated by some researchers as zero point energy. (Bearden, Grotz, Hathaway, Puthoff) [2, 3, 4, 5]. The device was constructed to take advantage of the same forces that Russell maintained were necessary for the occurrence of low temperature nuclear changes. The author has uncovered experiments that were conducted by Walter and Lao Russell in conjunction with Raytheon Corporation in Colorado Springs and General Chapman of NORAD. The author recently discovered the original blue prints which were found to have been preserved in Colorado Springs and the "Russell Optical Dynamo Generator" was found in the fall of 1991 in a basement, intact after 30 years. Documents from the 1960s show that Russell reported over unity operation as a result of his circuit configuration and the operation of specially designed coils.

INTRODUCTION

The purpose of this paper is to outline the research conducted in attempts to verify the low temperature nuclear change theories and experiments of Walter Russell. Russell was President of the Society of Arts and Sciences in 1920. During this time he met many scientists and began to formulate theories concerning the nature of matter and energy (Clark), [6]. In 1926 Russell predicted the existence and characteristics of deuterium, tritium, neptunium and plutonium. He devised several unique periodic charts of the elements showing the position of these elements in relation to a universal Nine Octave Cycle. One of these charts is presented with this report (see Fig.).

On Russell's chart of the elements, the elements are placed along a continuous spectrum of increasing compression and resulting density and are organized into octaves. The inert gases act as the beginning and end of each octave. The chart organizes the elements in increasing order according to melting points

and other characteristics until it reaches carbon. Carbon, placed in the center of the forth octave, is seen to be the balance point for the full chart and the point of perfect stability. Elements up until carbon are, according to Russell, integrating or condensing until a maximum of pressure results in the formation of carbon. Elements past carbon on the chart are expanding or disintegrating leading to the phenomenon of radioactivity (Mann), [7].

The elements form according to what Russell called The Wave Of Creation. The wave consists of pairs of spiralling vortexes that join together at their apexes while another pair, joined at the bases, diverge from themselves at a common center. The wave is the precursor to matter. It is the fabric of sub space, if you will. It is non-material and exists in a dimension removed from view. The wave controls and results in the formation of matter which is detectable from our dimension. This is why we seem to see a duality of wave and particle like nature in atomic and photonic structure. This is not a paradox. The wave is a wave when it is a wave and the particle is a particle when it is a particle. The wave becomes the particle which then becomes the wave (Grotz), [3].

Russell's Description of the Wave of Creation

The wave is described by Russell as causing "the integration of matter at poles and disintegration at equators. Matter integrates by the contraction of one pair of spirals around the shafts which wind it into spheres by the way of its poles, and disintegrates it by the expansion of the other pair which unwinds it by the way of equators (Secret of Light, p. 251), [8].

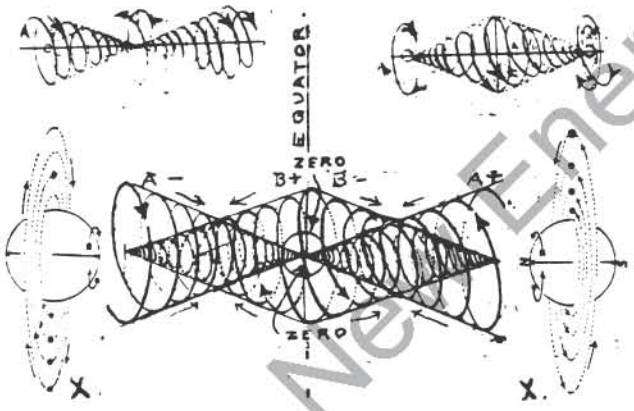

Fig. 1. Russell's "Wave of Creation"

The theory proposed by Russell, and later proven by experiment (see the following section of this paper), is that there is no such thing as transmutation from one element to another (Russell, 1939), [9]. One element can never become another for each is voided when another condition makes its continuance impossible and another one possible. Russell maintained that elements were not things, they are conditions. In order to prove this he set up a series of experiments which will be described below. In an attempt to verify these experiments, we have and are attempting to reproduce them as closely as possible. Our test data will be presented later in this paper.

INITIAL EXPERIMENTS

The experiments to prove the theory set forth by Russell were done in the laboratories of the Westinghouse Lamp Company at the Bloomfield, NJ facility. A laboratory was supplied and a number of senior research scientists acted as consultants to the project. In Russell's words, he "demonstrated [the] principle of dual polarity control by arranging two pairs of solenoids - one with more windings than the other - in such a manner that the dual polarity of nature was simulated. With a steel or glass disc for an equator and a steel rod for amplitude, I adjusted my solenoids approximately to a plane angle where I roughly calculated oxygen belonged in its octave. I improvised an adjustment apparatus which would enable me to fasten my adjustment securely at any angle I chose. I then inserted a few centimeters of water in an evacuated quartz tube which had electrodes at each end for spectrum analysis readings. Upon

heating the tube in an electric furnace, and inserting it into the solenoid with the electric current turned on until the tube cooled, the first spectrum analysis showed over **80% to be hydrogen and the rest practically all helium. There was very little oxygen**" (Russell, 1953), [10].

Each time the apparatus was reset for a different gas, a new spectrum analysis was obtained. The procedure was able to produce a preponderance of nitrogen, oxygen, or helium, depending on the settings of the coils and their angular relationship.

The test report reproduced here in the text is an example which was reported in "A Brief Treatise On The Russell Cosmogony" (Russell, 1953), [10]. It is clear that the experiment produced a significant change in the tube. **Where there had only been water vapor consisting of hydrogen and oxygen in the tube, nitrogen and inert gases in the amount of 69.1% were detected**. The analysis showed:

Oxygen 14.9
Hydrogen 16.0
Nitrogen
or inert gases . . . 69.1

Russell was convinced that the process could be refined by experiment and mathematically analyzed so that hydrogen, nitrogen, or oxygen could be obtained without the others.

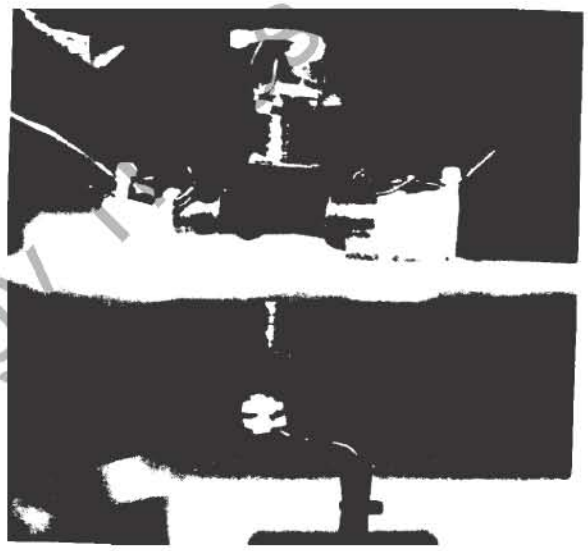

Fig. 2. 4-solenoid test fixture.

EXPERIMENTAL SETUP

The attempt to recreate the results reported by Westinghouse Laboratories used the equipment shown in photos accompanying this text. A fixture for holding four solenoids (Fig. 2) was designed to allow adjustment of the solenoids to the required angles. A power supply was built which allowed the current to each solenoid to be adjusted separately. This allowed individual control of the magnetic fields of each solenoid. The magnetic fields required for the experiment were generated by modified Guardian Electric A240 intermittent duty solenoids. The solenoids were modified only by removing the factory standard actuator and inserting a core of the same diameter, but cut to fit so that the core was flush at both ends. The magnetic fields were measured with a Thomas and Skinner model 7315 Gauss Meter. The field strength was measured at the center surface of the solenoid core. With a 600 ma current the field strength was 1450 gauss.

The spectral analysis was conducted with a Varian AA 175 Atomic Absorption Spectrometer setup for emission spectroscopy. The analog output from the spectrometer was recorded on an HP 7100B Strip Chart Recorder. Calibration of the spectrometer was done using spectrum tubes manufactured by Electro-Technic Products Company and supplied by Edmund Scientific Company. Charts for hydrogen, nitrogen, oxygen, and water vapor were run using the standard tubes. The results were found to be consistent with and matched data presented in standard tables (CRC Handbook of Chemistry and Physics).

EXPERIMENTAL PROCEDURE

The water vapor sample to be treated according to Russell's work at Westinghouse Laboratories, was produced by heating a small amount of distilled water placed in a sealed quartz tube. The quartz tube was scrubbed chemically with nitric acid, washed repeatedly, baked out and pumped down, to remove any contaminants before the sample was introduced to the tube. The tube was equipped with a T fitting which allowed the tube to be evacuated before it was back filled with water. Each end of the tube contained electrodes which served a dual purpose. The tube was heated to 300 °C using the electrodes to excite the water vapor with a 5 KV AC source.

After the gas was heated, an emission chart was made using the Varian Spectrometer. The tube was then inserted into the solenoid holding fixture and magnetic fields were applied as the sample cooled. A second emission chart was then made of the treated sample.

The experimental method described above by Russell, used solenoids "one with more turns than the other". Since this description does not give a definite explanation, the solenoids in this experiment were controlled using different currents, 500 ma on the vertical solenoids and 250 ma on the off-axis solenoids. This was an approximation at achieving the different field strengths that Russell obtained using turns ratio control.

The angles necessary to produce low temperature nuclear changes are described by Russell in a number of sources. (Russell, 1926, 1947, 1953,), [11, 8, 10]. Because the fixture designed for the experiment did not allow the tight angles used by Russell, it was decided to use angles that would allow the formation of Fluorine. (the physical size of the solenoids prevented them from use at the angles specified by Russell) According to the reference material, the angle necessary for the formation of fluorine is 44 degrees from vertical. Two of the solenoids were placed at this angle directly opposite one another. When the procedure for heating the tubes and allowing them to cool, as described above, was followed, the spectrum showed an increase in the spectral peak associated with fluorine (see chart with text).

ANALYSIS OF RESULTS

The fluorine peak was detected when the experiment was repeated. Each time the test was run, the sample tube was cleaned and a fresh sample of water was added. A spectrum was obtained of the new sample. The sample was then subjected to magnetic fields. The fluorine peak was again detected. These preliminary tests indicate that the Westinghouse Lab reports may be valid and that more tests are indicated.

FUTURE WORK

In order to duplicate the results described in the initial Westinghouse report, a new fixture will be designed and constructed. This fixture will allow the angles that Russell used for the formation of hydrogen and nitrogen to be reproduced. Results of these tests will be reported at a future date.

AN EXPERIMENT PRODUCING POWER WITH ZERO POINT ENERGY, THE RELATIONSHIP TO LOW TEMPERATURE NUCLEAR CHANGES

The energy of the vacuum has been analyzed and described by many researchers (Puthoff), [5]. Use of this energy is necessary for the creation of matter and low temperature nuclear changes (Russell). Walter

Russell reported to have found a means to harness this vacuum energy. In the fall of 1959, General Chapman, Colonel Fry, Major Sargent, Major Cripe, and others from NORAD in Colorado Springs, attended a meeting at Swannanoa, Virginia [14] at the invitation of Walter Russell (University of Science and Philosophy). At this meeting Russell explained the workings of a device he proposed to build to take advantage of the vacuum state energy, and the two directional movement of energy from gravitation, (generation), to radiation (degeneration). During the following year Russell, his wife, Lao, and their assistants built the device. General Chapman was advised of their progress on a routine basis.

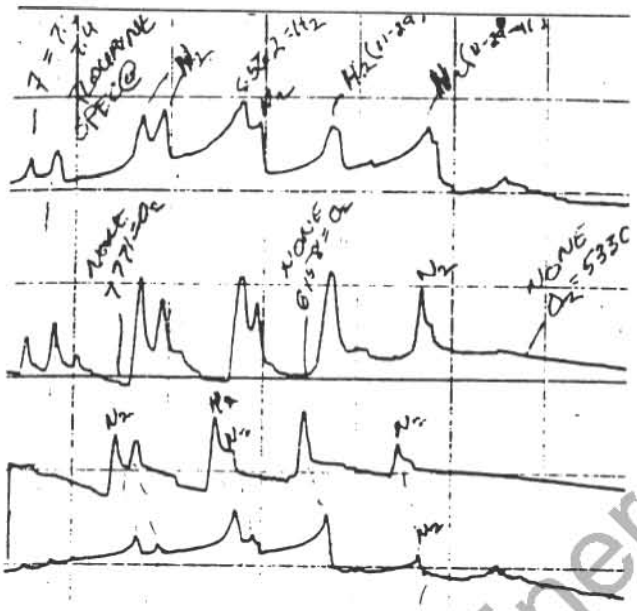

Fig. 3 Spectrum output with attracting magnetic fields. The solenoid configuration for this test was attracting mode (North to South). Two solenoids were in a vertical position, the second pair of solenoids was offset from the vertical by 44 degrees, the expected angle for fluorine based on the Russell charts. The two peaks on the left are fluorine at wavelengths of 7,311 and 7,398. The next two peaks to the right are representative of nitrogen. Note the relative amplitude of the nitrogen peaks with respect to the fluorine peaks.

Fig. 4 Spectrum output with opposing magnetic fields. The solenoid configuration for this test was opposing mode (North to North). Two solenoids were in a vertical position, the second pair of solenoids was offset from the vertical by 44 degrees, the expected angle for fluorine based on the Russell charts. The two peaks on the far left are fluorine at wavelengths of 7311 and 7398. Note the increase in fluorine amplitude relative to the next two peaks to the right which are representative of nitrogen.

The device was based on the "power multiplication principle" discussed in the many books Russell had written, many of which have been previously foot noted in this paper [see references]. From a memo dated March 16, 1961, the following description is given:

"This new power and light generator employs a power multiplication principle of nature...which multiplies gases of minus zero melting points into solids of over 3000 degrees; or multiplies the cold of space into hot stars and novas of incredibly high temperatures. The reason it has never been known is because of the false concept of gravity which assumes it to be a force of attraction which pulls inward from within instead of a cyclic force which controls the expansion of cold into heat, and the expansion of heat into cold...Nature's first principle of power production and the construction of matter is to produce heat from the cold of space. The heat thus generated radiates back into cold to complete the wave cycle which automatically repeats itself in this ageless sun universe of infinite continuity Every wave is a perfect

dynamo, but the very purpose of waves is to generate heat in its armatures at wave amplitude points. **That is the only way waves create matter"**.

According to Russell, the theory that was used to harness the zero point energy field also explains the process needed to effect low temperature nuclear changes.

The prototype that was built consisted of two sets of dual coils. The coils were wound to simulate the process shown in Fig. 1. The idea behind the coils is to simulate the life cycle of the electric current.

On September 10, 1961, Walter and Lao Russell reported to their contacts at NORAD, that the coils had worked and that the President of the United States could announce to the world that a "greater, safer power than atomic energy" could be provided for industry and transportation (University of Science and Philosophy).

The Russells were convinced that they had found and demonstrated a new source of energy and a conversion process for what is now known as the zero point energy.

REFERENCES

[1] Russell, Walter, "A New Concept Of The Universe", The University of Science And Philosophy, 1989, pp 129, 130.
[2] Bearden,T., Sweet, F., "Utilizing Scaler Electromagnetics To Tap Vacuum Energy", Proceedings of The 26th Intersociety Energy Engineering Conference, Vol. 4, p370.
[3] Grotz, T., "Working Models Of Free Energy Systems", Proceedings of the 1993 International Symposium On New Energy", April 16th - 18th, Radisson Hotel, Denver, Colorado.
[4] Hathaway, G.D., "Zero Point Energy: A New Prime Mover?", Proceedings of The 26th Intersociety Energy Engineering Conference, Vol. 4, p376.
[5] Puthoff, H. "Source Of Vacuum Electromagnetic Zero-Point Energy", Physical Review A, Vol. 40, #9, Nov. 1, 1989, p4857.
[6] Clark, G., "The Man Who Tapped The Secrets Of The Universe", University of Science and Philosophy, Swannanoa, VA, 13th edition, 1980.
[7] Mann, J.D., "The Genius Of Walter Russell", Solstice, No. 36, May/June, 1989.
[8] Russell, Walter, "The Secret Of Light", 1947, University of Science And Philosophy, Swannanoa, VA 22980
[9] Russell, Walter, "Space and the Hydrogen Age", Address to the Annual Convention of the Eastern Electronic Association, May 13th, 1939.
[10] Russell, Walter, "A Brief Treatise On The Russell Cosmogony", 1953, University of Science And Philosophy, Swannanoa, VA 22980
[11] Russell, Walter, "The Universal One", 1926, University of Science And Philosophy, Swannanoa, VA 22980
[12] Russell, Lao, from the Archives of the University Of Science And Philosophy, Swannanoa, Virginia 22980
[13] Russell, Walter, "The Russell Genero-Radiative Concept", L. Middleditch CO., 75 Varick Street, NY, 1930.
[14] University Of Science And Philosophy, Documents, letters, etc. from the Archives, Swannanoa, Virginia, 22980.
[15] Grotz, T., Binder, T., Kovac, R., "Novel Means Of Hydrogen Production Using Dual Polarity Control And Walter Russells Experiments with Zero Point Energy", Proceedings of the 27th Intersociety Energy Engineering Conference, August 3 - 7, 1992, Town And Country Hotel, San Diego, CA.

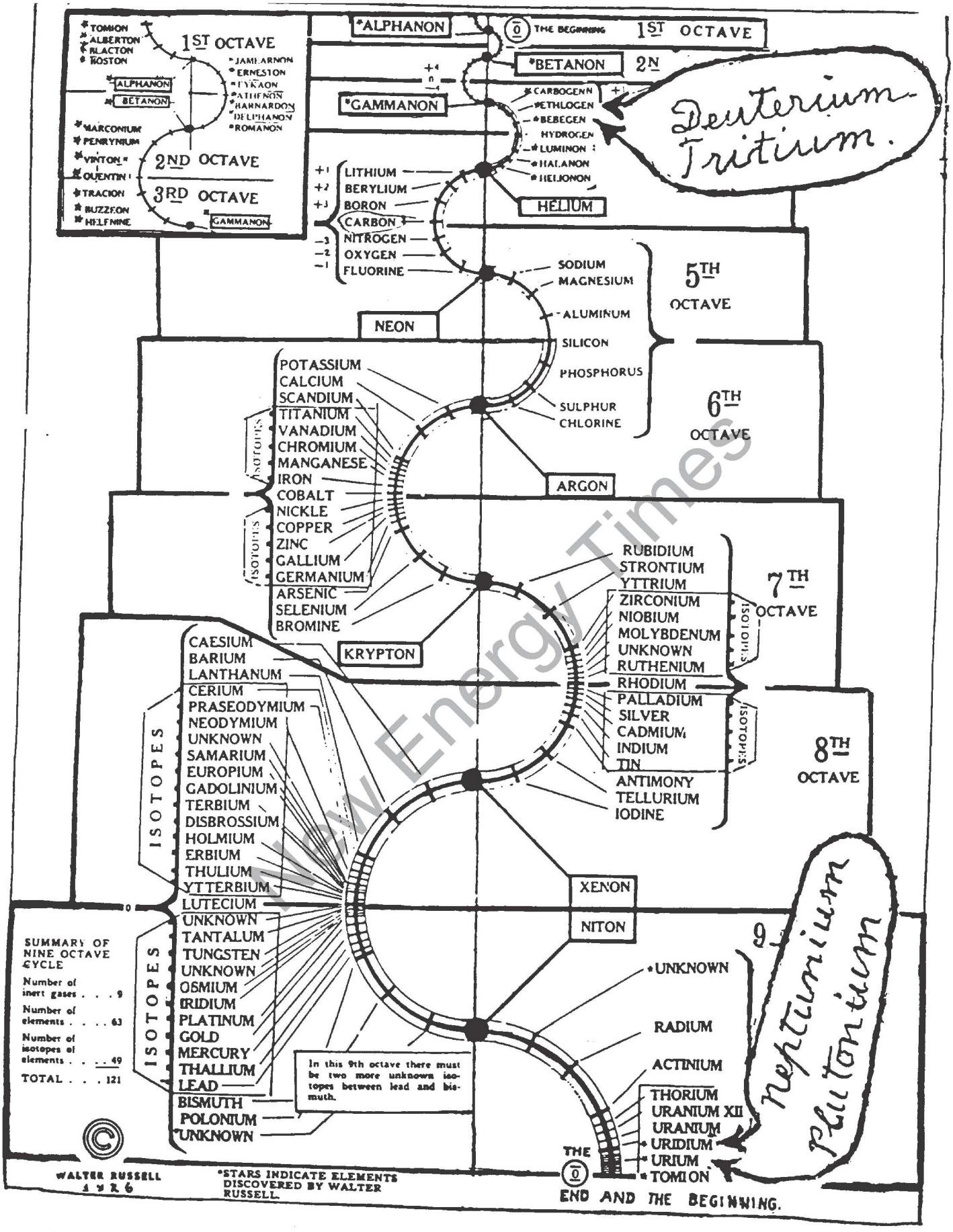

The Russell Periodic Chart of the Elements, No. 1

TRITIUM PRODUCTION FROM A LOW VOLTAGE DEUTERIUM DISCHARGE ON PALLADIUM AND OTHER METALS

T. N. Claytor, D. D. Jackson and D. G. Tuggle

Los Alamos National Laboratory
Los Alamos, NM 87545

ABSTRACT

Over the past year we have been able to demonstrate that a plasma loading method produces an exciting and unexpected amount of tritium from small palladium wires. In contrast to electrochemical hydrogen or deuterium loading of palladium, this method yields a reproducible tritium generation rate when various electrical and physical conditions are met. Small diameter wires (100 - 250 microns) have been used with gas pressures above 200 torr at voltages and currents of about 2000 V at 3-5 A. By carefully controlling the sputtering rate of the wire, runs have been extended to hundreds of hours allowing a significant amount (> 10's nCi) of tritium to accumulate. We will show tritium generation rates for deuterium-palladium foreground runs that are up to 25 times larger than hydrogen-palladium control experiments using materials from the same batch. We will illustrate the difference between batches of annealed palladium and as received palladium from several batches as well as the effect of other metals (Pt, Ni, Nb, Zr, V, W, Hf) to demonstrate that the tritium generation rate can vary greatly from batch to batch.

INTRODUCTION

We report on our tritium generation results from a palladium wire-plate configuration subjected to periodic pulsed deuterium or hydrogen plasma. This configuration is reproducible within a batch and produces a measurable amount of tritium in a few days. As in other work in this area, it has been found that the output is very batch dependent and sensitive to material impurities that prevent hydriding. As in our previous work [1,3], all tritium data was obtained from several batches of 100 or 250 micron wire and 250 micron thick plate from J&M or Goodfellow metals. In these experiments most of the tritium data was obtained with on-line tritium gas monitors. Several times, the gas was oxidized and tested with a scintillation counter.

Some have criticized the detection of tritium because the signals seem to be (a) insignificant, (b) tritium is ubiquitous, and (c) the palladium metal is subject to possible tritium contamination. The magnitude of the signals discussed in this paper are multi-sigma and are sometimes over a hundred times the tritium background in the supply gas. Furthermore, the rate of tritium evolution in the sealed system may be the most sensitive and rapid indicator of anomalous nuclear behavior in deuterided metals. As such, it is well suited for parametric investigations. We will briefly discuss the possible avenues for contamination and show that each is negligible, or not a factor, in the experiments described.

MATERIALS

For this work we used Cryogenic Rare Gases deuterium 99.995% that has 90 pCi/l of tritium, and research grade hydrogen with no detectable tritium (< 25 pCi/l). The major impurity in the deuterium is H_2 (0.005%) (He <1ppm). A total of 74.2 g of palladium wire/powder/foil was used in plasma experiments

described in this paper. Of that amount, 8.6 g was used in various hydrogen or deuterium control experiments. The palladium has been checked for tritium contamination by two independent methods (heating in hydrogen/deuterium and H_2 plasma).

Much of the palladium has been subjected to rigorous metallographic and impurity analysis. The impurity levels for the wires (Johnson Matthey Puratronic, Goodfellow) varied from the specification sheets and were in the 60-150 ppm range (mostly Cu, Fe, W and P) rather than the quoted values of 5-10 ppm. Most wires were used as received, but several wires were annealed in air (at 850°C for 2 hours) or stress relieved (600°C for 4 minutes) in air. Some of the wires (mostly J&M), when wrapped on a white macor ceramic spool and heated (to 600°C) left brown diffuse deposits (50 cm or more in length) or black diffuse spots (1-3 mm in length). The two batches that showed the most tritium did not yield the black spots but did leave light, small amounts of the brown deposits.

Three batches of palladium were used for the plate, the first batch of 220 micron thick foil was annealed at 850°C for 2 hours at 10^{-6} torr before use. A second batch had a different impurity analysis from the first, but was annealed in a similar manner; the third batch was used as received and had a different impurity level from the first two batches (although, all three plate batches had total impurities in the 350-500 ppm range, mostly Pt, Au, Cu and Fe). Wire from five batches (lots W13918, W06528, Z0114, NM 35680, Z0293, GF5140/6) was obtained from Johnson Matthey and Goodfellow Metals and one length of wire was supplied by Ben Bush. Only the Goodfellow batch and J&M (W13918) showed large (8 to 102 nCi) amounts of tritium although the other batches of J&M and Ben Bush wire produced small amounts (~1.5 to 6 nCi total per run).

Tritium contamination in the palladium wire and plate was tested by two independent methods: sputtering of the wire in a hydrogen plasma atmosphere and heating of the wire or plate to either 260 or 800°C in deuterium or hydrogen. No evidence of tritium (to within experimental error ~ 0.3 nCi) contamination was found in the heating experiments with hydrogen. The Goodfellow wire was tested for contamination (with null results ~ 0.3 nCi) by heating to 280°C sections (0.1 g) of wire taken between wire samples shown to produce tritium in the experiments. In our previous work [3] we were able to set a limit of 0.005 nCi/g obtained with ^{3}He detection of aged palladium samples from a different lot. Also, in an extensive independent [4] investigation of palladium wire, several hundred wire samples were tested and no tritium contamination was detected. The purity of the wire used in these experiments also weighs against, ubiquitous, intrinsic spot contamination, although the appearance of the black and brown deposits indicates that spot and distributed impurities can be present.

APPARATUS

Shown in Fig. 1 is one of two stainless steel gas analysis loops containing a 1.8 liter ion gauge and a 310.9 cc calibration volume. The atmospheric, ion gauge and sample pressure (0.2%), Femtotech and room temperatures (0.1°C) are recorded on a computer log at 60 s intervals. The pressure drop during hydriding of the wire and plate is used as an approximate indicator of the stoichiometry of the PdD**X**. Both loops have a heater to maintain the Femtotech (-0.03 nCi/l°C) at a constant temperature, an integral cold trap, and there are valves that allow the pressurization of the cell independent of the loop. A two micron filter is installed at the inlet of the ion gauge and at the outlet of the cell to eliminate spurious responses due to particulates. To eliminate the possibility of oil contamination, a molecular drag and diaphragm pump is used to evacuate the system.

The Femtotech ion gauge rejects pulse type radioactive events that effectively discriminate against radon and cosmic ray ionization. The initial background drift rate in the Femtotech was 0.002 nCi/h to 0.006

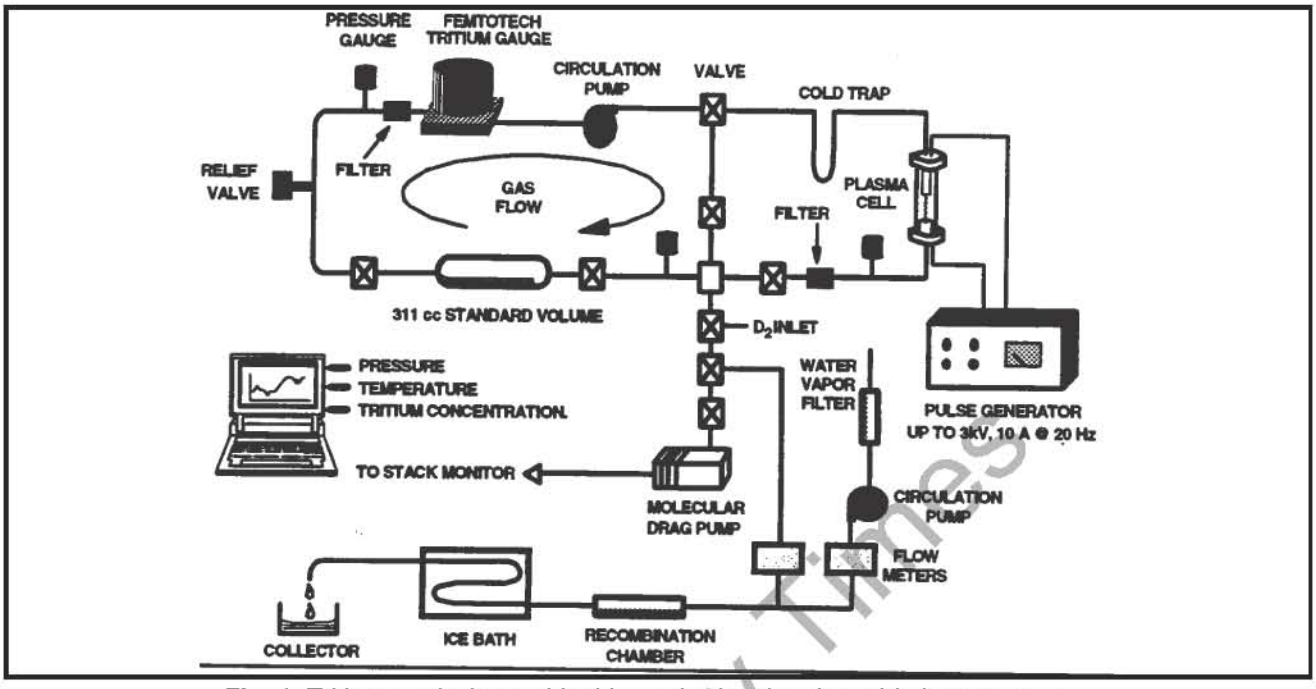

Fig. 1 Tritium analysis used in this study showing the oxidation apparatus.

nCi/h, but after exposure to the cells described in the paper, the drift rate increased, and could reach as high as 0.01 nCi/h. In order to return to the baseline rate, it was necessary to clean the loop tubing and Femtotechs halfway through the study.

A hydrogen oxidation system was built as a backup test for tritium using a scintillation counter (Packard 1600). Calibration D_2 gas with 25 nCi/l of tritium was used to test the two Femtotechs and the oxidation system. The two ionization systems agree to within 5% of each other while the scintillation results are within the experimental error (0.3 nCi) of the Femtotechs.

The typical arrangement of the cell allows a wire to sit perpendicular to and a few millimeters above a circular plate. In operation, the plasma is adjusted so that it envelopes the whole wire and contacts the plate at a small spot. Typically, the plasma is light blue (D_2^+) with areas of pink (D_3^+ or D^+). At high currents (> 5 A), a bright pink electron channel forms that extends parallel to the wire from the base of the wire to the plate. Initially, the Pd wire is 25 to 30 mm in length and about one mm from the plate. The plate diameter is 3.0 cm or 1.8 cm.

PROCEDURE

The procedure for a plasma run was to first fill the 3.1 liter loop with deuterium gas at 600 torr and obtain a measure of the initial background tritium concentration. With the loop drift rate measured, the deuterium was circulated through the cell to slowly hydride the sample. The pressure in the cell and the loop was then lowered to the operating pressure by pumping the excess deuterium out.

The wire was pulsed negatively, at 20 μs at 50 Hz, with currents between 2 and 5 A, voltages that varied from 1,500 to 2,500 V, and cell pressure of 300 torr. These conditions reduced the heating in the cell and maintained a cell to ambient temperature difference of less than 25°C to avoid gross dehydriding of the

wire and plate. It appeared important to avoid a plasma condition that resulted in either a bright pink electron channel or arcing at the tip of the wire. After a few hours of plasma operation the voltage-current stabilized, presumably due to the formation of small cones (10-20 microns high) all over the surface of the wire. After 20 hours, palladium was visibly sputtered onto the plate. The sputter rate at 300 torr, 3.5 A, was about ~2 Å/s. The cell pressure was monitored, and if it did not drop after 24 hours (indicating hydriding), then a small amount of CO_2 (0.75% by vol) was added, which would initiate hydriding.

At the end of a run the pressure was increased to 600 torr, the gas was circulated, and the system allowed to equilibrate for about 8 hours. If the reading was steady and CO_2 was added, then the gas was circulated through the liquid nitrogen cold trap to collect any water and determine if any tritiated water was present. The system was then pumped out, the cell closed off, and fresh deuterium added to the system after a couple of flushes with either fresh deuterium or air. The difference between the fresh deuterium and the deuterium reading after exposure to the plasma was used as the measure of the tritium content. In cases where more than 10 nCi were found, the palladium wire and plate were heated separately to over 250°C and the result admitted to the evacuated loop.

RESULTS

A total of 65 plasma wire experiments were performed, 12 of these were other than palladium wire and plate. Twenty experiments were run with multiple wires, usually 3 wires bundled together, and eight experiments used different thickness foils 25 to 125 microns thick. The balance of the tests were done with one 250 micron diameter wire and 250 micron thick plate. Three hydrogen plasma experiments were done with palladium plate and wire and two were done with platinum wire and plate. A summary of several background and foreground experiments is shown in Fig. 2. The best experiment, produced 102 nCi.

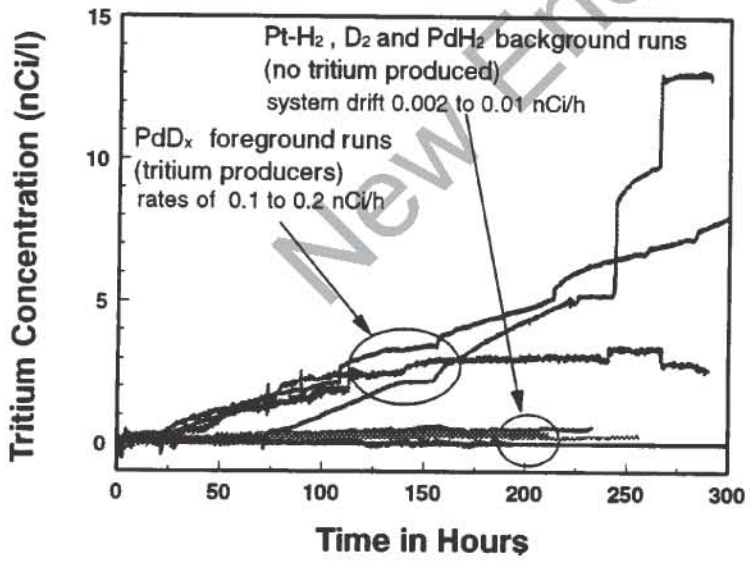

Fig. 2 Comparison of background and foreground results with a Pd wire-plate type plasma cell. A Pt wire-plate plasma and a flowing D_2 background is shown for comparison.

Plasma runs 3 and 4 deserve some detailed explanation since these produced the most tritium. First, (see Fig. 3) cell 3 was preheated in order to drive off any contaminants. The plasma was then started and the tritium generation rate was 0.15 nCi/h. Near the end of the run, the cell was twice flushed with deuterium, which caused the total tritium (as detected by the Femtotech) to jump up. At the conclusion of the experiment the plate and wire (from plasma 3) were heated, in situ, and released another 5.4 nCi. In order to resolve whether the tritium was originating in the plate or wire, they were separately heated after plasma 4. The wire released about 12.4 nCi of tritium while the plate had no measurable (< 0.3 nCi) release.

A number of Pt and Pd controls were run with D_2 or H_2. Most of these are shown in Fig. 2 in comparison with the foreground cells. In general, drift rates with the plasma on were in the 0.004 to 0.01 nCi/h range.

Not enough hydrogen and platinum blank experiments have been run to definitely conclude that tritium production is confined to the palladium-deuterium system. We believe, however, that because the hydrogen and non-hydriding metal experiments are low or null, that the rather large results with palladium are unique. We also ran several hydride forming metals other than palladium. In the case of Hf and Zr it was difficult to maintain the plasma, so for most of the run the background drift rate is similar to the cell with D_2 circulating (<0.003nCi/h). Tungsten, vanadium, niobium, and nickel-deuterium were on for about 100 hours, but their rates were still very close to background (0.007 to 0.009 nCi/h). Romodanov et al. [5] reported that Nb was more active than W, Zr, Ta or Mo in their gas discharge experiments. We also found small amounts of tritium in niobium (1.1 nCi), and observed a small rate with nickel-hydrogen (0.012 nCi/h). Both of these samples deserve further investigation.

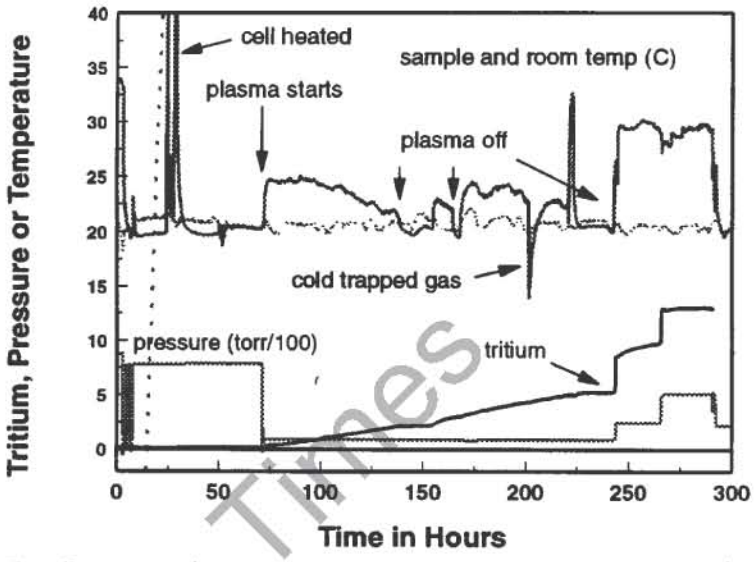

Fig. 3 The cell temperature, ambient temperature, tritium concentration, and pressure plotted to illustrate the operation of cell 3. When the sample temperature and the ambient temperature are close, the cell is off and the tritium concentration remains constant. Wehn the cell temperature drops below ambient, the cold trap is activated; no significant decrease in the tritium level was noticed.

The wire-plate plasma experiments have been very consistent but also very dependent on the exact batch of palladium that was used. We found that the batch, material and material condition are critical parameters. Our first batch of GF5140/6, for example, had an average rate of 0.4 nCi/h, with several rates greater than 0.1 nCi/h. Our second best results came from an arrangement with the second batch of the same wire in which three wires were bundled together. Their rates varied from 0.02 to 0.07 nCi/h.

At the conclusion of two of the experiments, about a third of the deuterium was oxidized and the heavy water and a control were submitted for scintillation counting. The results were 3400 to 213 dpm/ml and were in agreement (within experimental error) with the tritium activity calculated from the drop in reading of the Femtotech. Background activity from the D_2 gas prepared by this method is about 39 dpm/ml.

DISCUSSION

The basic premise that the detected ionizing material is tritium is indisputable because, (a) quantitative measurements agree with the scintillation counter, (b) the gas may be transported on a clean palladium bed between different ionization systems and produces an increased reading commensurate with the decrease in tritium concentration noted in the initial system, (c) as the pressure is decreased the tritium signal is seen to decrease (for dry gas) in a manner consistent with the calibration for a known level of

tritium in deuterium and finally, (d) the signal shows no diminution over a two week time period, consistent with the half life of tritium.

Three types of contamination of the wire are possible; the first is just surface contamination due to atmospheric or liquid exposure to tritium, the second type might be a distributed impurity, and the third would be a spot contamination. To avoid surface contamination, we thoroughly clean and polish the palladium surface prior to each run. If it were still present, a surface contaminant would be immediately evident when the wire was introduced to the analysis loop and deuterided, but we have not seen evidence for this type of contamination. We attribute the residue and smoke seen from some of the wires to entrained lubricant due to drawing the wire. This lubricant tends to be drawn out and smeared throughout the length of the wire, which implies tritium contaminated oil should be detected in long sections of the wire. However, wires that showed obvious high levels of oil contamination did not show tritium, and we did not observe a large tritium signal when the wire was heated and the oil suddenly evolved. Similarly, the dark spots are present after simply heating the wire to 600°C but there is no evidence for tritium release at temperatures as high as 850°C.

An indicator that the tritium originated in the cells is that the output was sensitive to the metallurgical condition of the palladium. Palladium wire annealed in air showed a lower output than as received wire. Likewise palladium wire stress relieved but not annealed showed a similar (about a factor of 3) reduction in output. This could be interpreted as a release of tritium if it was contamination, however, then the tritium would have been easily detected in the heating controls. In sample #4, that showed significant tritium output, post heating (250°C) of the palladium wire released 12.4 nCi of tritium. This amount of tritium would have been easily detected in the heating control of the same spool of wire (10 cm) taken from the next section of material. Furthermore, the tritium in the gas evolved from the wire during the post heating at 250°C was far (5340 nCi/l) above the equilibrium tritium concentration (31.4 nCi/l) in the gas after the run. The fact that such high concentrations can be left in the palladium suggests that the process is near but not at the surface. The pulse length is sufficient for the diffusion of 200 Angstroms (10 μs pulse length) into the palladium. Then the tritium may be sputtered (1 to 2 Å/s) out (along with the palladium) of the near surface layer by the energetic plasma. This would indicate that the tritium was in a 15 to 30 micron layer on the 250 micron in diameter wire. The fact that a significant amount of tritium shows up as (after the addition of CO_2) TDO is also indicative of a near surface reaction. Dendrites and aspirates (up to 20 microns high) on the surface of the palladium have been suggested [2] as possible tritium formation sites.

When palladium is hydrided it is stressed and, to some extent, work hardened. The wires after hydriding have always shown an increase in grain growth (to 50-100 microns) from the very fine (1-2 microns) microstructure initially observed with these materials. The observed reduction in stress relieved wires indicates that the dislocation density must play a very important role in the tritium production. However, since all as received wires were hard drawn but not all batches of wire showed production, there are other factors that are important, such as the purity and the hydriding.

The purity of the material varies from batch to batch, and within a batch sections of the wire are cleaner than other sections. Thus it could be that the lack of oil, iron or hydrogen impurities is critical or that there has to be an another atomic species present. We believe that the lack of oil or other impurities is important to help the material hydride efficiently. The key mechanism, however, may be associated with another impurity species that need be present only at the sub ppm level at the dislocations.

The importance of hydriding the palladium can be clearly observed in a plot (Fig. 4) of tritium output versus time for a sample from batch Z0293 that weakly hydrided. The tritium evolution rate was at the

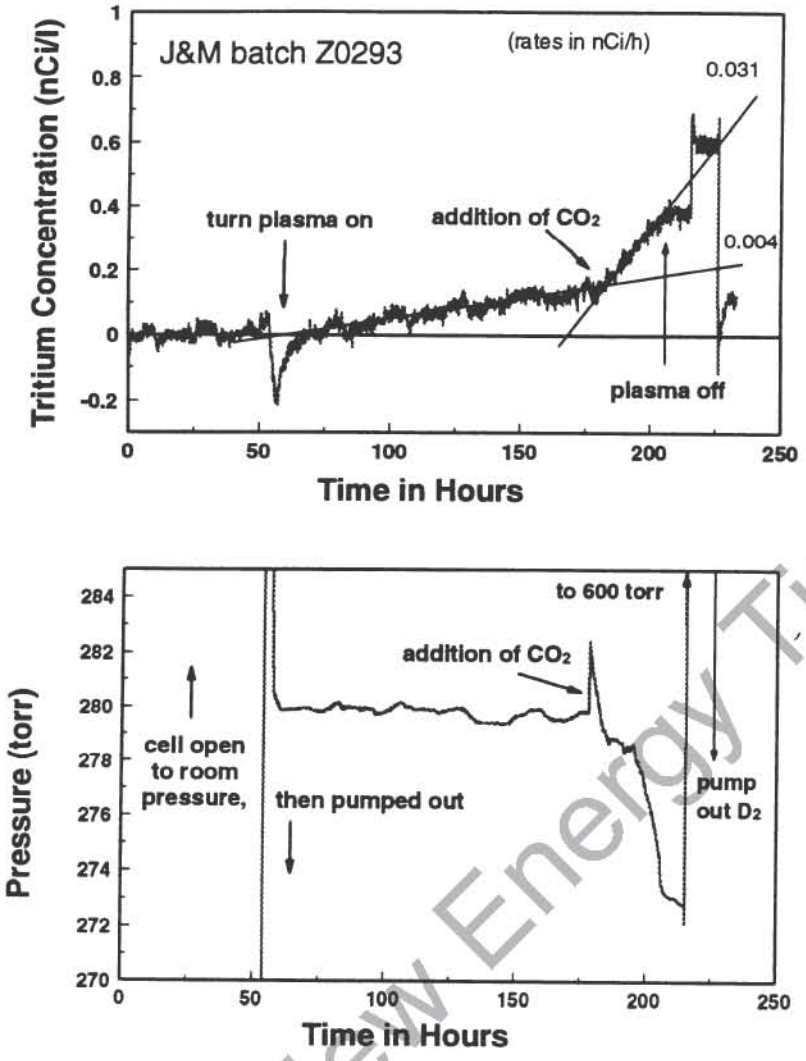

Fig. 4 Tritium output from a cell that appeared to be a non-producer until 2 torr of CO_2 was added to the deuterium. This caused the plate (and perhaps the wire) to hydride and a coincident rise in the tritium generation rate by a factor of ~7 was observed until the wire bent away from the plate.

background drift rate (0.004 nCi/l). When (0.75% by vol) CO_2 was added to the system the tritium rate increased to a rate some 7.7 times the background drift rate. Coincident with the tritium increase, the deuterium pressure dropped indicating the palladium plate was hydriding. This decrease in pressure is more than can be accounted for if the CO_2 is totally converted to D_2O. We confirmed this with a platinum control cell in which the pressure only decreased by 2 torr. In another experiment where the pressure immediately dropped, indicating that the palladium had initially hydrided, the tritium generation rate was ~0.02 nCi/h and an addition of CO_2 did not change the rate of tritium production.

The CO_2 may also make it feasible to run at lower pressures where a high loading is more difficult to achieve. An analysis of the ratio of tritiated water to tritium in the gas reveals that most (70%) of the tritium remains in the gas. Additions of CO_2 to Pt runs neither change the rate of drift (tritium) or exhibit large pressure decreases as shown in Fig. 4. The CO_2 and CO that is produced within the cell are known to be surface poisons that normally would not allow the palladium to hydride. However, in the presence of a reactive energetic plasma the surface is cleaned of these materials and deuterium is allowed to disassociate on the surface and diffuse in. When the plasma ceases, the surface poison reabsorbs inhibiting deuterium from recombining on the surface.

CONCLUSIONS

We have found that the tritium output depends on the temperature, pressure and current applied to the cells. Yet, the tritium yield is most sensitive to the purity and metallurgical condition of palladium used in the experiments. Various tests for tritium contamination confirm that there is no initial tritium contamination in the powder, foil, wire or other materials used in this study. CO_2 additions had a remarkable effect on the production of tritium by these cells and the effect seems to be related to and enhancement of the hydriding of the palladium.

It appears that very pure palladium is more effective than impure palladium in producing tritium. Based on our impurity analysis of the material we cannot identify a difference in concentration of a single impurity that is important to either include or exclude from the palladium. This is partially a morphological or metallurgical issue involving dislocations since we have seen a reduced output from annealed or stress relieved palladium when compared to as received palladium from the same batch. However, palladium that has been hydrided and dehydrided must always be annealed to reactivate it. The fact that most of the tritium is evolved promptly to the gas, yet significant amounts are found in the palladium suggest that the process is near but probably not at the surface.

ACKNOWLEDGMENTS

Many people were involved in a direct way with the experiments described here. Some of these were Ken Griechen, Roy Strandberg and Kane Fisher who were instrumental in the design and construction of the first few cells. Joe Thompson counted our tritiated water samples. Mike Hiskey and William Hutchinson were helpful in the analysis of contaminants in the vacuum system and on the samples.

REFERENCES

1. Tuggle, D. G., Claytor, T. N., and Taylor, S. F.; "Tritium Evolution from Various Morphologies of Deuterided Palladium.," Proceedings of the Fourth International Conference on Cold Fusion., December 6-9 1993, Maui, Hawaii., Ed. T. O. Passel, EPRI TR-104188-V1 Project 3170, July 1994, Volume 1, pp 7-2.

2. Bockris, J. O'M., Chien, C-C., Hodko, D., Minevski, Z., "Tritium and Helium Production in Palladium Electrodes and the Fugacity of Deuterium Therein," Frontiers Science Series No. 4, Proceedings of the Third International Conference on Cold Fusion., October 21-25 Nagoya Japan., Ed. H. Ikegami, Universal Academy Press Tokyo Japan., 1993, p 231.

3. Claytor, T. N., Tuggle, D. G., Taylor, S. F.; "Evolution of Tritium from Deuterided Palladium Subject to High Electrical Currents," Frontiers Science Series No. 4, Proceedings of the Third International Conference on Cold Fusion., October 21-25 Nagoya Japan., Ed. H. Ikegami, Universal Academy Press Tokyo Japan., 1993, p 217.

4. Cedzynska, K., Barrowes, S. C., Bergeson, H. E., Knight, L. C., and Will, F. W., "Tritium Analysis in Palladium With an Open System Analytical Procedure," *Fusion Technology*, vol 20, no 1, 1991, p108, and private communication.

5. Romodanov, V., Savin, V., Skuratnik, Ya. Timofeev, Yu., "Nuclear Fusion in Condensed Matter," Frontiers Science Series No. 4, Proceedings of the Third International Conference on Cold Fusion., October 21-25 Nagoya Japan., Ed. H. Ikegami, Universal Academy Press Tokyo Japan., 1993, p 307.

VARIATIONS OF THE HALF-LIVES OF RADIOACTIVE ELEMENTS AND ASSOCIATED COLD FUSION AND COLD FISSION REACTIONS

By Dr. R.A. Monti
Burns Developments Ltd.

INTRODUCTION

According to the Alpha-Extended model of the atom [1], heavier elements are made from lighter elements by Low Energy Transmutations (Cold Fusions). Conversely, lighter elements can be produced by Cold Fission of heavier elements.

Cold Fusion and Cold Fission are complementary and reversible processes [2], [3]. Some ordinary chemical reactions can cause Cold Fusion and Cold Fission of stable nuclei [4], [5]. This led me to test the effects of similar chemical reactions on unstable (radioactive) nuclei during early 1993 and a new series in March 1955 which is detailed herein.

OBJECTIVE

To achieve and observe Cold Fusion/Fission in radioactive elements by using a variety of proprietary formula Fusion/Fission Mixtures (FM's) and Collecting Elements (E's) and noting changes to radioactivity or evidence of significant changes to quantity of elements.

METHODOLOGY

It was decided to repeat the experiments conducted in 1993 which showed that a quick decay of radioactivity in Thorium (a few days) occurred within a metal bead resulting from the chemical reaction of Th with the FM's and E's.

The purpose was not only to simply repeat the experiments but also to test different FM's and E's in order to optimize radioactive decay.

The radioactive element tested was $90Th^{232}$ (half-life - 1.41×10^{10} years) which was readily available to us. The product was Thorium Ash.

Three different proprietary formula FM's were prepared initially in the quantity sufficient for the experiments devised (FM1, FM2, FM3). These were then discarded in favor of a variant of FM2 identified as FM 2N which was used for all the remaining experiments commencing with experiment 6.

Five different E's (E1, E2, E3, E4, E5) were used in the experiments.

I.C.P. tests ranging over 66 elements were made on the E's and the Thorium Ash to define their atomic composition and to establish experimental base lines. I.C.P tests ranging over 66 elements were made to all metal beads collected after the ignitions and analyzed for significant changes in elemental composition.

A specified quantity of Thorium ash was mixed thoroughly with different FM's and E's, with total weights ranging between 500g and 1200g. This mixture was then placed into a steel container and ignited. Observations and measurements for each experiment were noted in detail and are reproduced in summary form with this report.

OBSERVATIONS

The principal components of the Thorium ash were as follows:

Th	>20000	ppm, the test equipment was not calibrated to read greater concentrations.
Pb	10100	ppm
Mg	9300	ppm
Ce	6300	ppm
Al	2880	ppm
Fe	411	ppm
Au	5.41	ppm

The ignition resulted in smoke, orange-yellow flame, and a magma-like mass which, on cooling, become two components; being a collected metal bead at the bottom of the container and slag above it.

A Geiger counter held into the proximity of the smoke detected no radiation, a verification of tests of the smoke conducted during 1993 at the Southwest Research Institute in San Antonio, Tx., and elsewhere.

After separation, both the collected metal bead and the slag were radioactive, the bead reading approximately twice as much as the slag.

Radioactivity and radioactive decay was monitored on both the bead and the slag and in each case the radioactivity in the collected metal bead declined rapidly in a very short time, while the slag remained constant.

No effort was made during this sequence of tests to remove the remaining Th and other metals from the slag, except for experiments 12 to 15 which showed that the collected metal bead exhibited the same behavior as the bead from the initial ignition.

There were changes in the level of the base line metals. Changes considered to be significant had to be at least double the base line quantity or 10 ppm which-ever was the lower amount. These changes are noted on the attached summaries of the experiments.

CONCLUSIONS

The experiments revealed that I could devise a new Fusion/Fission Mix which gives fairly reproducible results and that I could make a selection among various different Collecting Elements.

The experiments have shown that

a) it is possible to cause accelerated decay (cold fission) of Thorium in metal surrounds, and

b) it is possible to cause a variety of different Cold Fusion and Cold Fission reactions by means of "ordinary" chemical reactions, and

c) it is possible to reduce radioactivity of slag by removing trace metals from the slag; more experiments are necessary.

The research field is now wide open.

REFERENCES

[1] R.A. Monti, "Cold Fusion and Cold Fission: Experimental Evidence for the Alpha-Extended Model of the Atom," communication to ICCF2, Como, Italy, 1991.
[2] R.A. Monti, "Low Energy Transmutations," communication to ICCF3, Nagoya, Japan 1992.
[3] R.A. Monti, "Experiments in Cold Fusion and Cold Fission," communication to ICCF4, Maui, Hawaii 1993.
[4] R.A. Monti, "Transmutation of Radioactive Elements by Atomic Chemistry," private communication to J.O'M. Bockris.
[5] J.O'M. Bockris, R.T. Bush, G.H. Lin, R.A. Monti, "Lattice Assisted Nuclear Transformations (LANT)." submitted to *Fusion Technology.*

SUMMARY OF R.A. MONTI EXPERIMENTS

number	1	2	3	4	5	6	7	8
radioactive materials used								
Th ash (grams)	20	20	20	10	10	10	10	10
fusion slag (grams)								
concentration								
-ppm	>20000	>20000	>20000	>20000	>20000	>20000	>20000	>20000
-cpm	>10000	>10000	>10000	>10000	>10000	>10000	>10000	>10000
collecting elements								
E1	x	x	x	x	x	x		x
E2	x	x	x	x	x	x	x	
E3	x	x	x	x	x			
E4						x	x	x
E5								x
fusion / fission mixes								
FM 1	x							
FM 2		x		x				
FM 3			x		x			
FM 4						x	x	x
Th post ignition radioactivity (note 1)								
start (day 1) - cpm	900	1000	765	740	1091	947	1455	638
end (day 10) - cpm	65	144	91	64	93	62	59	66
Th in metal bead - ppm	0.30	<0.10	0.42	0.10	0.10	<0.04	0.58	0.07
changes in other elements (note 2)								
Ni	x				x		x	x
Tl	x							
Bi	x	x	x	x	x		x	x
Au	(x)	(x)	(x)	(x)	(x)	x	(x)	x
Rh	x	x	x	x	x		x	
Pt		(x)					(x)	x
Be							x	
Sc							x	x
Cu							x	
Sb								x
Al								
Zn								
Mg								
Br								

Note 1: The background level of radioactivity was 60 cpm ± 10
Note 2: For changes to be reflected it had to be the lesser of 10 ppm or double. Parentheses indicate a decrease in ppm's.
Note 3: Experiments summarized herein were conducted during March 1995.

SUMMARY OF R.A. MONTI EXPERIMENTS (2)

number	9	10	11	12	13	14	15
radioactive materials used							
Th ash (grams)	10	10	10				
fusion slag (grams)				100	100	100	100
concentration							
-ppm	>20000	>20000	>20000	42.5	42.5	42.5	42.5
-cpm	>10000	>10000	>10000	750	750	750	750
collecting elements							
E1	x	x		x	x	x	x
E2	x	x					
E3							
E4	x		x	x	x	x	x
E5			x	x	x	x	x
fusion / fission mixes							
FM 1							
FM 2							
FM 3							
FM 2N	x	x	x	x	x	x	x
Th post ignition radioactivity (note 1)							
start (day 1) - cpm	713	586	1410	483	470	521	586
end (day 10) - cpm	67	57	60	66	54	63	53
Th in metal bead - ppm	0.07	<0.07	0.07	<0.03	<0.20	<0.09	<0.07
changes in other elements (note 2)							
Ni	x		x	x	x	x	x
Tl	x	x	x			x	x
Bi	x	x	x			x	x
Au	x	x	(x)	x	x	x	x
Rh			x				
Pt							
Be					x	x	x
Sc	x	x	x	x	x	x	x
Cu							
Sb			x	x	x	x	x
Al	x				x	x	x
Zn	x						
Mg				x			
Br					x		

Note 1: The background level of radioactivity was 60 cpm ± 10
Note 2: For changes to be reflected it had to be the lesser of 10 ppm or double. Parentheses indicate a decrease in ppm's.
Note 3: Experiments summarized herein were conducted during March 1995.

R.A. Monti Experiments - Graphs Depicting Radioacitve Decay

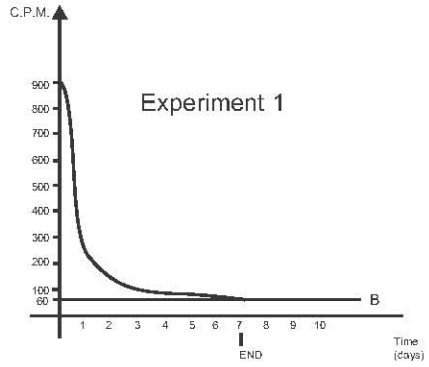

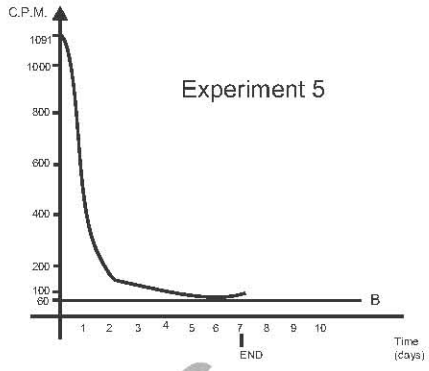

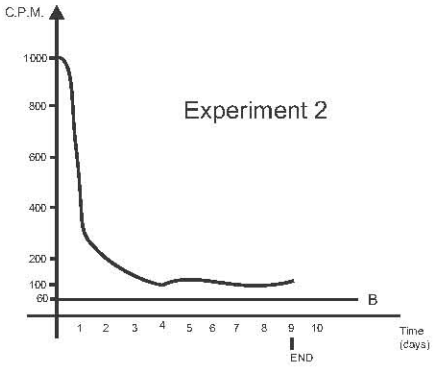

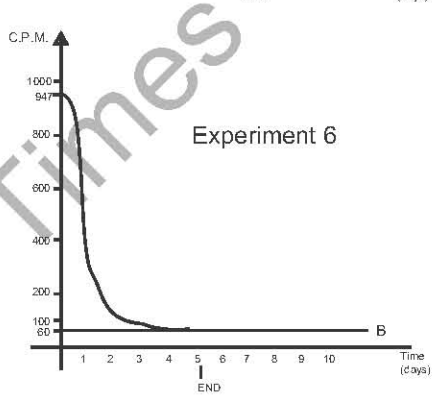

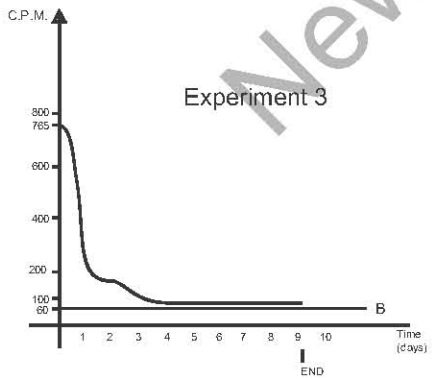

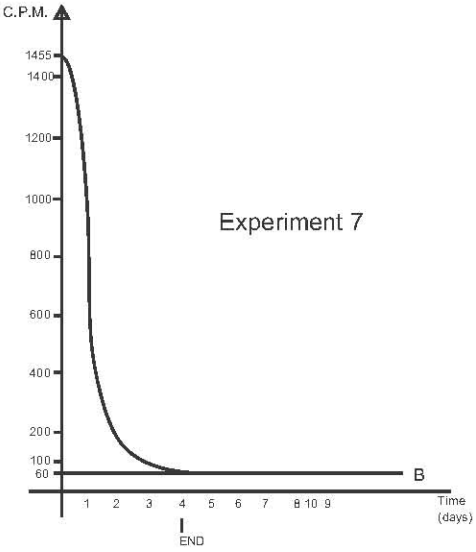

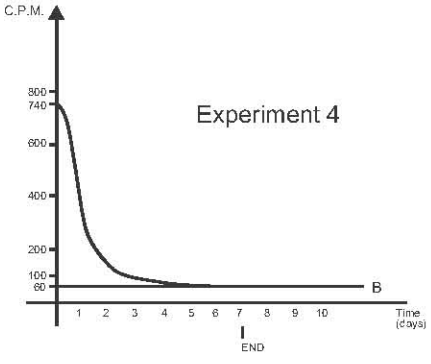

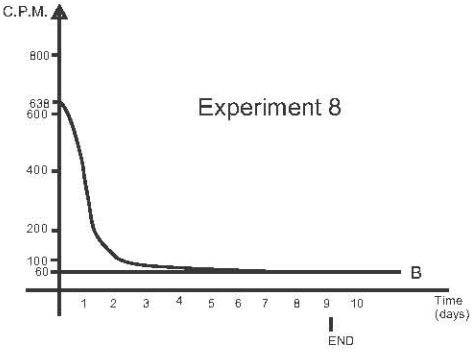

R.A. Monti Experiments - Graphs Depicting Radioacitve Decay

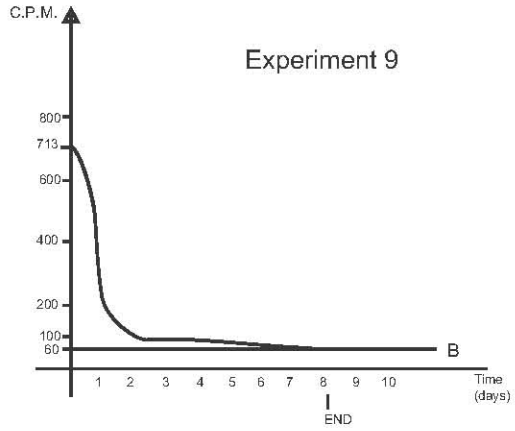

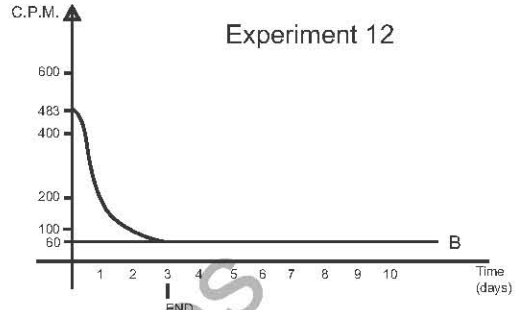

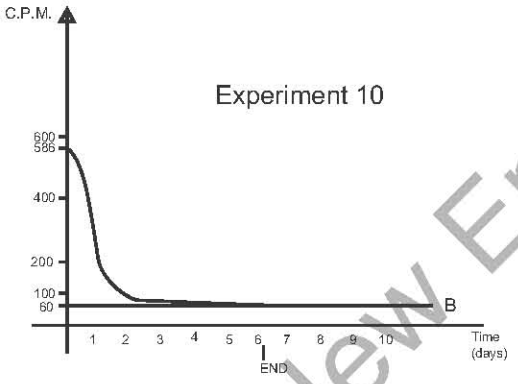

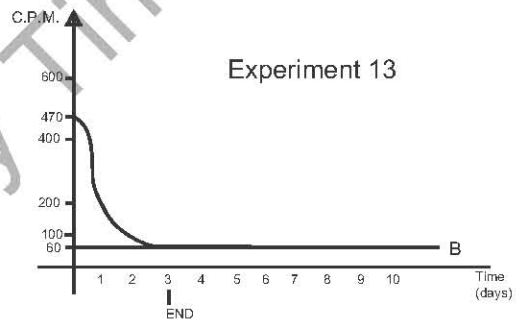

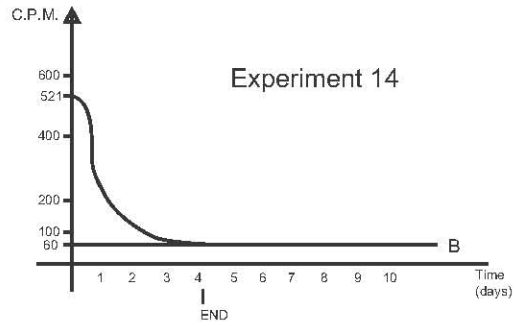

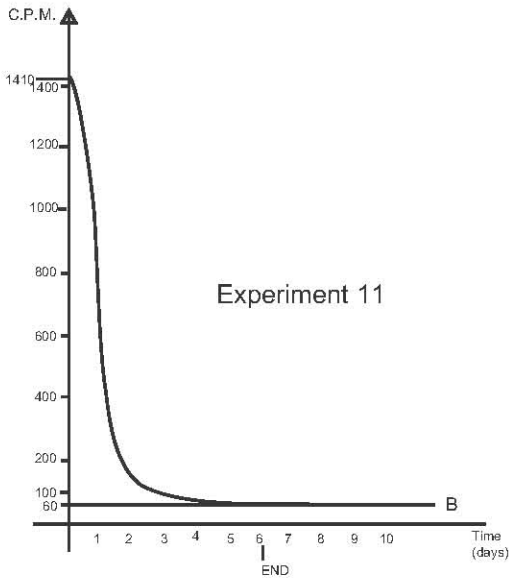

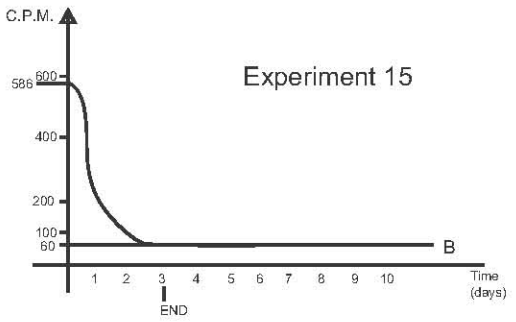

This paper is not a part of the foregoing conference.

POTENTIAL FOR POSITIONAL VARIATION IN FLOW CALORIMETRIC SYSTEMS

Mitchell Swartz
(c) JET TECHNOLOGY

February 10, 1996

Although many aspects of calorimeters have been discussed, including issues of potential problems with the thermometry (i.e. thermocouples, thermistors and thermometers, as well as electrical grounding and crosstalk, thermal mixing and sensor positioning problems), the potential impact of the positional effects of the flow calorimetry has not been mentioned. The positional orientation refers to the direction of the flow, and not to the orientation of any temperature probes therein. Despite the reported advantages for flow calorimetry in detecting enthalpy from putative fusion reactions, these studies theoretically suggest that there may be effects from positional variational in the calorimetry of such flow systems. Rather than 'ease of calibration' usually touted for such systems, it is suggested that calibration may be more complicated for vertical flow calorimetric systems. In the absence of additional calibration, it may be critical to keep semiquantitative calorimeters horizontal.

One recent series of reports using vertical flow calorimetry [1,2,3,4] involves the *CETI* microspheres, reported to use a few percentages of the metal of other systems. The microspheres have multilayer metallic coats and are used as a distributed electrode bed. The cell is 10 cm long, 2.5 cm in diameter, and contains 1 to 40 ml of beads. Electrolyte percolates through, removing the heat, and exits from the top. The flow causes a temperature gradient. The observed delta-T, between the top and bottom is in the range of 1.5 to 20C (flow rates is 1.0 - 1.5 liters per minute, with the water circulated by a magnetic impeller pump, total power consumption ~85 watts). At the ICCF5, the *CETI* cell was reported to have an input of 0.14 watts and a peak excess of 2.5 watts, a ratio of 1:18. At SOFE '95, the *CETI* cell had 0.06 watts input and 5 watts peak output, a ratio of 1:83. At Power-Gen, the ratio reportedly ranged from 1:1000 to 1:4000.

There have been several complaints regarding the *CETI* demonstrations in relation to recombination, flow measurement, and heat ejection [3]. Assuming the thermometry is correct, it is instructive to closely examine the calorimetry using a computer model representing heat and mass transfer. The equation used to derive the output, and therefore the presence of any excess heat involves the flow, the specific heat of the water, and temperature differential. Although this equation may be dimensionally correct, it may not be valid for low flow rates in certain cases discussed below. The role of the Bernard instability [5] has not been previously mentioned, even though it may have inadvertently impacted the calorimetry [4].

The following describes the result of a quasi-one-dimensional (Q1D) analysis which further examined the impact of the flow orientation, with respect to the gravitational field, during flow calorimetry. The model generated to test the hypothesis examined convection, conduction, and gravity-thermal instabilities. Figures 1 through 4 show four groups of curves which show the time-varying distribution of temperature

in such a quasi-one-dimensional model. The four groups of curves represent horizontal and vertical flow calorimetry, both with and without convection. In each graph, the spatial distribution of heat (in one dimension) is represented as a single curve. There is one curve for each point in time. There is heat input from a single point source - at midposition along the x-axis - during the entire time subtended by each series of curves. The earliest curves, in each group, are those closest to the x-axis where the heat arise out of the central point source. Thus the dynamics can be followed from the graphs generated for the model.

After the heat enters at the midposition along the x-axis it can be redistributed by thermal conduction, by convection and by redistribution secondary to the changes in specific gravity resulting from the temperature changes (as with the Bernard instability). Radiative loss is not considered in this simplified model. The first group of curves in Fig. 1, which is labeled "Horizontal Flow - Thermal Diffusion" to indicate that the flow is horizontal to the Earth's surface and that thermal diffusion is included. Fig. 1 shows both the midline exogenous heat component and a slow thermal diffusion away from the point-source of heat. The velocity is zero; that is, there is no convection. The second group of curves, Fig. 2, show the impact of convection upon the spatial distribution of heat. This figure shows how the redistribution of heat is used in typical flow calorimetry to generate a temperature gradient, from a sampling of which a calculation is made to determine the output heat (energy). The two groups of curves, Figs. 3 and 4, labeled "Vertical Flow" represent the output from a vertical system, both with and without the addition of upward convection. The extreme along the x-axis away from the point source of heat input, previously 'right' and 'left' in Figs. 1 and 2, are now 'top' and 'bottom' in Figs. 3 and 4. Upon examination of the curves on the lower left, gravity is observed to now play a role in the distribution of the warmed water. It is saliently obvious that because the thermal-driven buoyancy which also leads to the Bernard instability -- where hot water rises due to its lower specific gravity -- the curves in Fig. 3 do shift in position away from the symmetry exhibited by horizontal flow calorimetric systems even in the absence of convection (compare to Fig. 1). There may be, for such conditions, an apparent "signal" for zero flow because of the thermal instability, which simulates the effect of flow (the group of curves in Fig. 3; compare to the group of curves in Fig. 2). The addition of convection produces additional contribution to the heat shift in the vertical flow system (Fig. 4), quite similar to that which it does for horizontal systems (Fig. 2).

One observation from the model is that the boundary condition from zero to negligible flow conditions is different for the horizontal and vertical flow calorimetric systems. It is important to consider that generally, quoted efficiencies of energy generated from putative over-unity devices are calculated assuming the standard equation is always correct. Another salient observation resulting from this theoretical Q1D study is that simple equations which apply for horizontal calorimetric systems may not be strictly applicable for vertical flow calorimetric systems for low flow conditions. But which?

We now define η_B as the ratio of heat transported by the buoyant forces to the heat transported by solution convection.

$$\eta_B \equiv \frac{\text{heat transported by boyant forces}}{\text{heat transferred by solution convection}}$$

This Q1D model of heat and mass transfer has indicated that what is generally correct for horizontal calorimetric systems, may not be correct for vertical systems, when the non-dimensional number ($=\eta_B$) is significantly greater than zero. Any apparent amplification of the 'excess heat' (if any, and there does appear to be some) would be greatest at the low levels. Increased flow makes the positional error less important. As a corollary, any false excess heat, or excess heat magnification, should also reduce with increased flow.

In summary, thermometry may not be the only rate limiting factor for obtaining high-quality information from flow calorimeters if the non-dimensional number η_B {defined as the ratio of heat transfer by buoyancy to the heat transfer by convection} is greater than zero. η_B, in a real system where viscosity, turbulence, and other parameters play a role, depends upon other non-dimensional factors including the Archimedes non-dimensional number which is the ratio of the buoyant force to the viscous force, and possibly the Rayleigh non-dimensional number, which is the ratio of gravity to thermal conductivity. Studies are underway to explore this. It is also proposed that a simple test of the theory would be to build a rotatable flow cell with a resistive heat element, perhaps mounted on a goniometer for any system to check sensitivity. This hypothesis, and Q1D model of heat and mass transfer, do not imply that such systems do not exhibit 'excess heat.' But rather that any such reported 'excess heat' parameters may be inflated, if the information was indeed collected with a vertical flow calorimetric system, in the absence of confirmatory calibrations under low to moderate flow conditions where the non-dimensional number (η_B) is not trivial.

REFERENCES

[1] D. Cravens, "Flowing Electrolyte Calorimetry," Proceedings of 5th International Conference on Cold Fusion, 79-86 (1995).

[2] H. Fox, "Dramatic Cold Fusion Demonstration Seen By Hot Fusion Scientists," *Fusion Facts*, vol. 7, number 4, 1-4 (1995).

[3] M. Jones, "Some Simple Calculations Assuming 42 Cubic Feet per Minute," posted on sci.physics. fusion; excerpts in *Cold Fusion Times*, vol. 4, number 1, 6-8 (1996).

[4] M. Swartz, "Elementary Survey of CETI Microsphere Demo," *Cold Fusion Times*, vol. 4, number 1, 7-9 (1996).

[5] S. Chandrasekhar, "Hydrodynamic and Hydromagnetic Stability," Clarendon Press, Oxford, 9-75 (1961)

[6] J. Melcher, "Continuum Electromechanics," MIT Press, Cambridge, 10. 13-10. 18 (1981)

The author is most grateful to Gayle Verner, Hal Fox, Horace Heffner, Mark Hugo, Jed Rothwell, Barry Merriman and Profs. Louis Smullin and Keith Johnson of MIT and the staff of JET Technology and Fusion Information Center for helpful comments and assistance during the development of this model and the preparation of this manuscript.

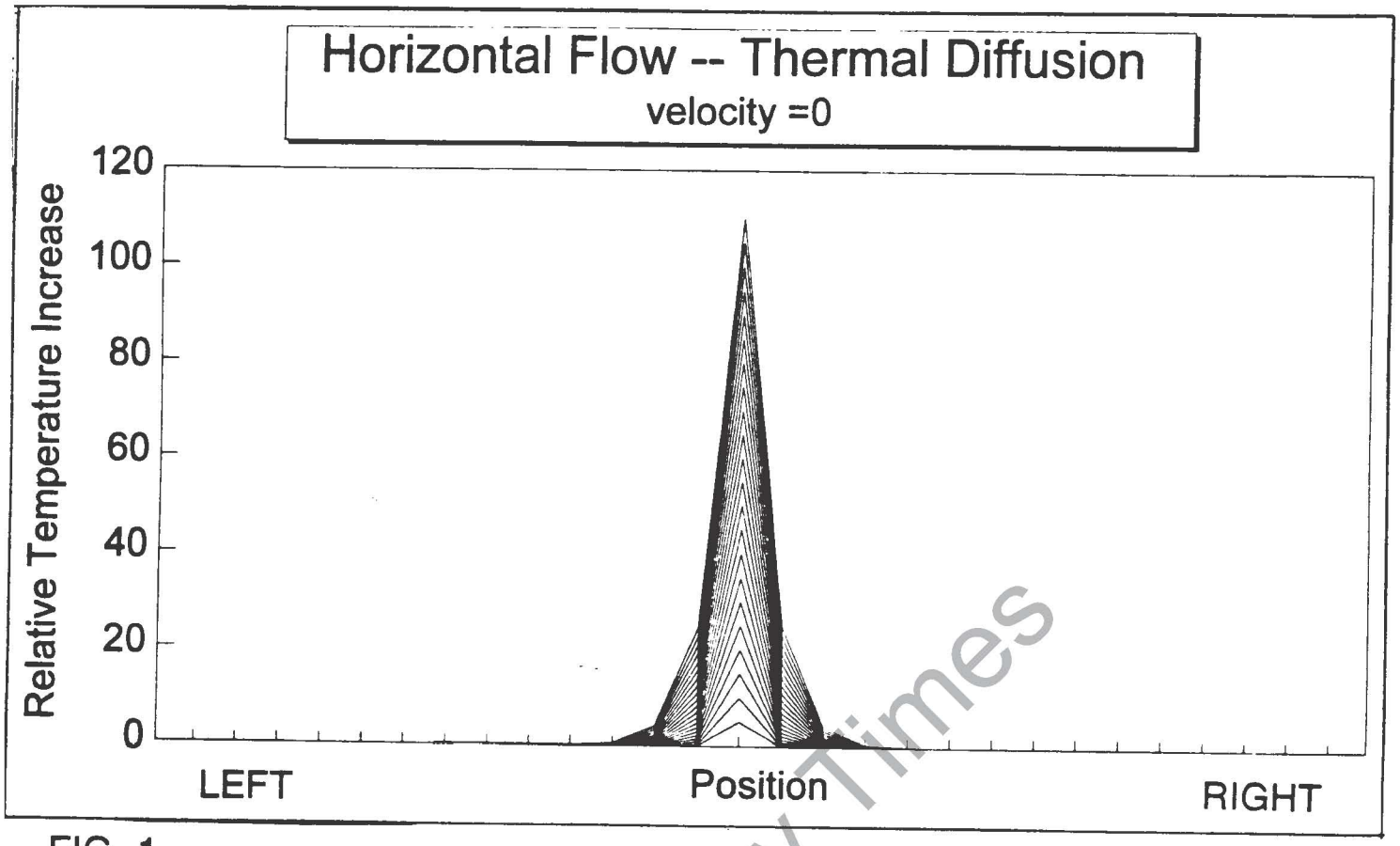

FIG. 1

FIG. 2

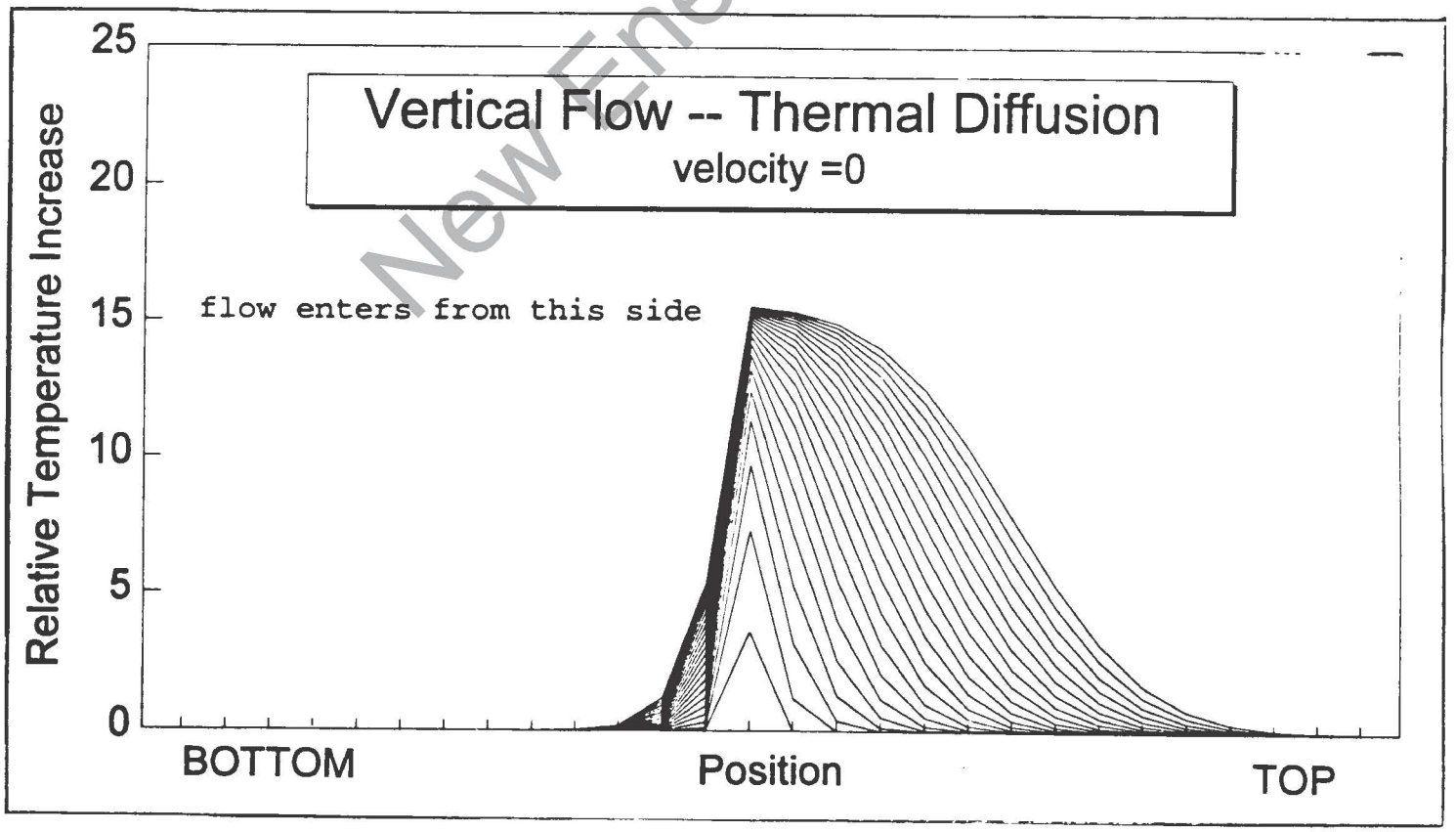

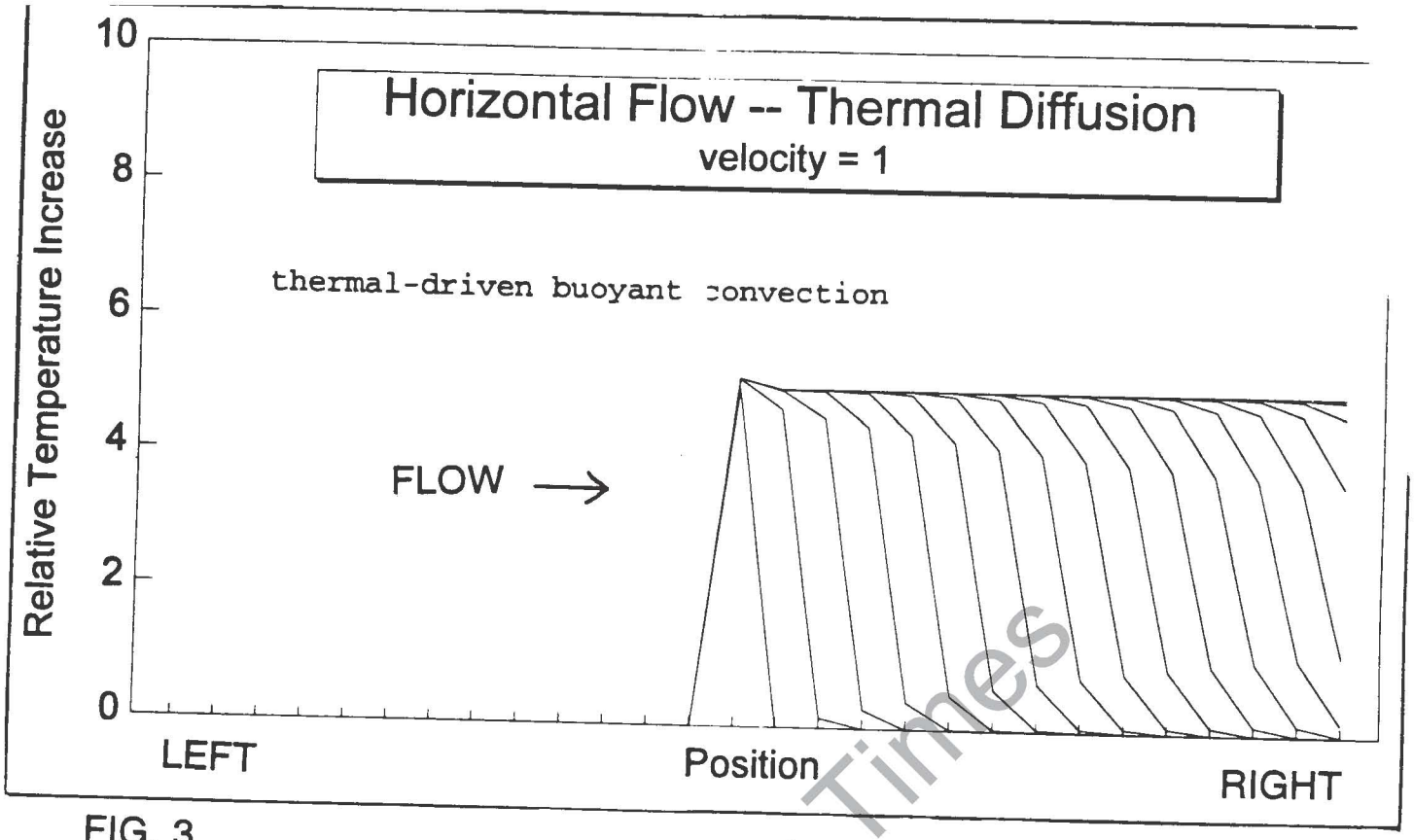

FIG. 3

FIG. 4

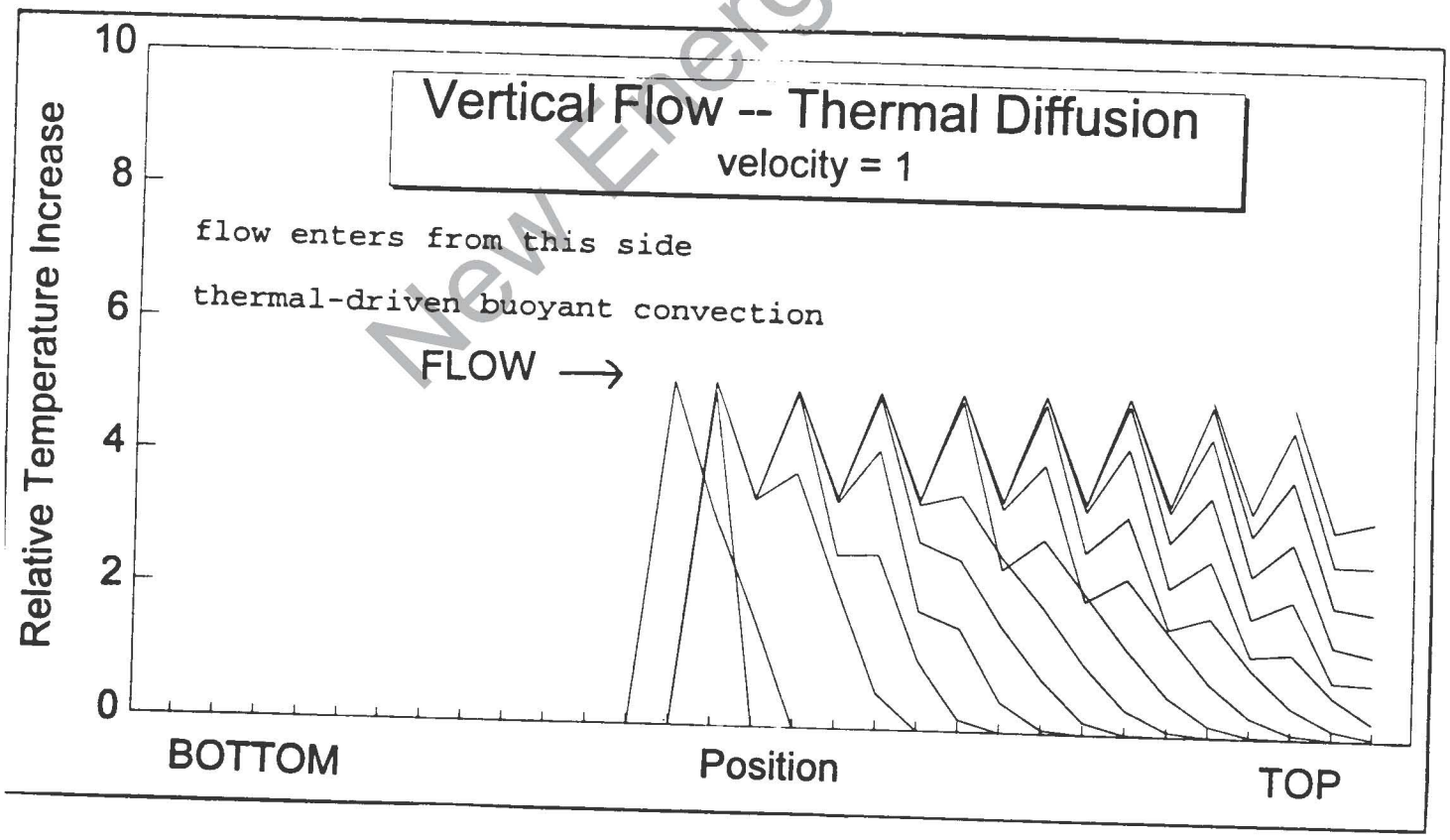

JOURNAL OF NEW ENERGY

A Journal of the Institute of New Energy Vol. 1, No. 1, 1996

Journal of JNE

January 1996
ISSN 1086-8259

The *FIRST* issue of JNE...
Contains the proceedings of the first conference on Low-EnergyNuclear Reactions held at Texas A&M University on June 19, 1995

January 1996 **Vol. 1, No. 1**

About the Editor
Hal Fox was the director of the first research laboratory at the University of Utah Research Park. Hal is also co-founder (with several U.S. cold fusion scientists) of ENECO, Inc., a Utah corporation dedicated to the commercialization of cold fusion.

Hal Fox is the leading founder of the Fusion Information Center which publishes both *Fusion Facts*, a monthly technical newsletter designed to keep subscribers informed of the latest developments in cold fusion, and *New Energy News*, a monthly newsletter for members of the Institute for New Energy and other world-wide subscribers.

Printed in the U.S.A

Journal of JNE

JOURNAL OF NEW ENERGY

A Journal of the Institute for New Energy

ISSN: 1086-8259

The Journal of New Energy is published quarterly by Fusion Information Center, Inc., with offices at the University of Utah Research Park, Salt Lake City, Utah.

Mailing address: Journal of New Energy
P.O. Box 58639
Salt Lake City, Utah 84158-0639
(801) 583-6232 FAX: (801) 583-2963

Instructions to Authors:
Professional papers on cold fusion and other enhanced energy systems are solicited from scientists, engineers, inventors, and students. Papers from recognized professionals may be published immediately with an invitation for peer-review comment. Other papers may be submitted for peer review. Names and addresses of any reviewers will be sent to authors with reviewers' comments.

The Journal of New Energy (JNE) is devoted to publishing professional papers with experimental results that may not conform to the currently-accepted scientific models. The topics to be covered in this journal include cold nuclear fusion, low-energy nuclear reactions, high-density charge cluster technology (including some plasma circuits where enhanced energy is produced), high-efficiency motors or generators, solid-state circuits that appear to provide anomalous amounts of output energy, and other new energy devices. Papers with experimental data are preferred over theoretical papers. Standard alternative energy topics such as hydrogen fuel, wind power, solar power, tidal power, and geothermal power are not solicited.

Authors should submit abstracts. If the abstracts are favorably considered for publication, the author will be sent an author's kit of instructions for the preparation of the paper. The editor and the editorial advisory board are responsible for making publication decisions.

Authors or their employers will be invoiced for production costs sufficient to cover the cost of publication in excess of subscription funds received. The JNE will try to match donors with authors from developing countries so that all acceptable manuscripts can be published. **Donors are requested to contact the JNE and they will be specially honored in the Journal.**

JOURNAL OF NEW ENERGY

A Journal of the Institute of New Energy Vol. 1, No. 1, 1996

Published by the
Fusion Information Center
P.O. Box 58639
Salt Lake City, Utah 84158-0638

A Quarterly Journal
Subscription: $150 for 4 issues
Single issues: $45

January 1996
ISSN 1086-8259

FUSION INFORMATION CENTER

The ***Fusion Information Center, Inc.*** (FIC) is a Utah Corporation founded in April 1989, with the goal of being a part of the new and exciting technology of cold fusion. The current president, Hal Fox, was the director of the first research laboratory at the University of Utah Research Park, Salt Lake City, Utah.

FIC is best known for its publication of two newsletters: ***Fusion Facts*** (monthly since July 1989) and ***New Energy News*** (monthly since May 1993). In addition to its publishing activities, FIC has been helping many inventors, scientists and authors with information and in some cases with funding.

Projected programs will expand FIC's scope of publishing and the commercialization of a few selected new-energy research & development projects. They continue to review new research as it appears.

FIC has the world's most complete collection of cold fusion papers and one of the best collections of new-energy papers and publications. We welcome the visit of authors, inventors, and scientists to our office in the University of Utah Research Park.

In some cases, we can help you find funding for your projects. Please call on us if you are involved in the development of new energy devices or systems.

Fusion Information Center, Inc.
P.O. Box 58639, Salt Lake City, UT 84158-0639
(801) 583-6232 FAX: (801) 583-2963

INSTITUTE FOR NEW ENERGY

The Institute for New Energy is an international organization to promote new and renewable energy sources. Its monthly newsletter is **New Energy News,** reporting worldwide on all facets of new and enhanced energy.

The Institute for New Energy
P.O. Box 58639
Salt Lake City, UT 84158-0639
Phone: 801-583-6232
FAX: 801-583-2963
E-mail: inc@padrak.com
Web Site: www.padrak.com/ine/

New Energy News

New Energy News (NEN) is the monthly newsletter for the Institute for New Energy,. containing 20 to 30 pages per issue.
It is *FREE* with your membership.

Membership

- Membership to the INE is $35.00 per year for individuals in the U.S.A.
- $40.00 for Canada, and Mexico
- $50.00 for all other countries, *and*
- $60.00 per year for Corporations and Institutions

Call the INE for additional information at the above address, *or*
Contact the INE President: Dr. Patrick G. Bailey — inc@padrak.com